



Università degli Studi di Milano
Facoltà di Scienze Matematiche, Fisiche e Naturali
Dipartimento di Chimica Inorganica, Metallorganica e Analitica "L. Malatesta"

DOCTORATE SCHOOL IN CHEMICAL SCIENCES AND TECHNOLOGIES
Ph.D. course - CHEMICAL SCIENCES (XXIV cycle)

DOCTORAL THESIS

**DEVELOPMENT OF INNOVATIVE ANALYTICAL PROCEDURES
FOR THE IDENTIFICATION OF ORGANIC COLORANTS
OF INTEREST IN ART AND ARCHAEOLOGY**

CHIM/01 - CHIM/12

Doctoral candidate:
Federica POZZI
R08330

Tutor:
prof. Silvia Bruni

Co-tutor:
dr. Marco Leona

Ph.D. course coordinator:
prof. Silvia Ardizzone

Academic Year 2010/2011

*Color is a power
which directly influences the soul.*

*Color is the keyboard,
the eyes are the hammers,
the soul is the piano with many strings.
The artist is the hand which plays,
touching one key or another,
to cause vibrations in the soul.*

W. Kandinsky

Table of contents

| | |
|---|----|
| Abbreviations | 7 |
| Introduction | 8 |
| Chapter 1 - Organic colorants in art and archaeology and their chemical characterization | 9 |
| Abstract | 9 |
| Organic colorants in art and archaeology | 10 |
| Chemical characterization of organic colorants | 14 |
| SERS enters the scene: history, chemistry and application to dye analysis | 16 |
| References | 19 |
| Chapter 2 - SERS spectral database of natural dyes on Ag nanoparticles aggregated by NaClO₄ | 22 |
| Abstract | 22 |
| Introduction | 23 |
| Natural organic dyes: history and chemistry | 24 |
| Anthraquinone dyes | 24 |
| Flavonol dyes | 25 |
| Flavone dyes | 26 |
| Chalcone dyes | 27 |
| Neoflavone dyes | 27 |
| Biflavonoid dyes | 28 |
| Neoflavonoid dyes | 28 |
| Naphthoquinone dyes | 29 |
| Carotenoid dyes | 29 |
| Curcuminoid dyes | 30 |
| Xanthone dyes | 30 |
| Indigoid dyes | 30 |
| Experimental | 31 |
| Chemicals | 31 |
| Analytical methods: extraction procedures, Ag colloid synthesis and sample preparation | 31 |

| | |
|---|-----------|
| Instrumentation | 32 |
| Results and discussion..... | 33 |
| Anthraquinone dyes..... | 34 |
| Flavonol dyes..... | 37 |
| Flavone and chalcone dyes..... | 42 |
| Neoflavonoid, neoflavone and biflavonoid dyes..... | 45 |
| Naphthoquinone and carotenoid dyes | 48 |
| Turmeric, gamboge and indigo..... | 51 |
| Conclusions..... | 53 |
| References..... | 54 |
| | |
| Chapter 3 - Identification of a yellow dye in ancient threads from the Libyan Sahara | 57 |
| Abstract | 57 |
| Introduction | 58 |
| <i>Rhus</i> and <i>Punica granatum</i> : long-history dye plants | 60 |
| <i>Rhus</i> or sumac (<i>Anacardiaceae</i>) | 60 |
| <i>Punica granatum</i> or pomegranate (<i>Punicaceae</i>) | 60 |
| Experimental | 60 |
| Chemicals and archaeological samples | 60 |
| Wool dyeing process | 61 |
| Analytical methods: extraction procedures, Ag colloid synthesis and sample preparation..... | 62 |
| Instrumentation | 62 |
| Results and discussion..... | 63 |
| Non-destructive analyses | 63 |
| Chromatographic analyses..... | 63 |
| SERS analyses | 66 |
| Conclusions..... | 70 |
| Acknowledgements..... | 70 |
| References..... | 71 |
| | |
| Chapter 4 - Identification of dyes in ancient Kaitag textiles from Caucasus | 73 |
| Abstract | 73 |
| Introduction | 74 |
| Experimental | 77 |
| Chemicals..... | 77 |
| Analytical methods: extraction procedures, Ag colloid synthesis and sample preparation..... | 77 |
| Instrumentation | 78 |

| | |
|--|------------|
| Results and discussion..... | 79 |
| Blues..... | 82 |
| Yellows..... | 84 |
| Greens..... | 86 |
| Reds..... | 88 |
| Browns and blacks..... | 91 |
| Conclusions..... | 94 |
| Acknowledgements..... | 94 |
| References..... | 95 |
| | |
| Chapter 5 - Comparative study of SERS methods for the detection of dyes in works of art..... | 96 |
| Abstract..... | 96 |
| Introduction..... | 97 |
| Experimental..... | 98 |
| Chemicals and art samples..... | 98 |
| Analytical methods: HF hydrolysis, Ag colloid synthesis and sample preparation..... | 98 |
| Instrumentation..... | 102 |
| Results and discussion..... | 103 |
| Analysis of reference dyes and HF hydrolysis optimization..... | 103 |
| Comparison of SERS spectra with and without HF hydrolysis..... | 110 |
| Conclusions..... | 123 |
| References..... | 124 |
| | |
| Chapter 6 - SERS and Raman study of watercolors from a historical Winsor & Newton handbook..... | 125 |
| Abstract..... | 125 |
| Introduction..... | 126 |
| Experimental..... | 127 |
| Chemicals..... | 127 |
| Analytical methods: HF hydrolysis, Ag colloid synthesis and sample preparation..... | 128 |
| Instrumentation..... | 128 |
| Results and discussion..... | 129 |
| Cochineal-based pigments..... | 132 |
| Alizarin-based pigments..... | 133 |
| Madder lake-based pigments..... | 135 |
| Synthetic pigments..... | 136 |
| Conclusions..... | 138 |
| References..... | 138 |

| | |
|---|-----|
| Chapter 7 - TLC-SERS study of the main components of Syrian rue dye (<i>Peganum harmala</i>) | 139 |
| Abstract | 139 |
| Introduction | 140 |
| Experimental | 142 |
| Chemicals..... | 142 |
| Analytical methods: extraction procedure, Ag colloid synthesis and sample preparation..... | 142 |
| TLC-SERS analytical method..... | 142 |
| Instrumentation | 143 |
| Results and discussion..... | 144 |
| Conclusions..... | 153 |
| Acknowledgements..... | 153 |
| References..... | 153 |
| | |
| Chapter 8 - Raman and DFT study of monobromoindigo | 154 |
| Abstract | 154 |
| Introduction | 155 |
| Experimental and theoretical methods | 157 |
| Chemicals..... | 157 |
| Synthesis of monobromoindigo..... | 157 |
| Instrumentation | 158 |
| Density functional theory (DFT) calculations..... | 158 |
| Results and discussion..... | 160 |
| Conclusions..... | 166 |
| Acknowledgements..... | 166 |
| References..... | 167 |
| | |
| Conclusions | 168 |
| | |
| Publications | 169 |

Abbreviations

ATR-FTIR = attenuated total reflection - Fourier transform infrared spectroscopy

ESI-MS = electrospray ionization - mass spectrometry

FTIR = Fourier transform infrared spectroscopy

FT-Raman = Fourier transform Raman spectroscopy

HPLC = high-performance liquid chromatography

HPLC-SERS = high-performance liquid chromatography coupled with surface-enhanced Raman spectroscopy

IRR = infrared reflectography

LC-MS = liquid chromatography - mass spectrometry

MALDI-MS = matrix assisted laser desorption ionization - mass spectrometry

NIR = near-infrared spectroscopy

SEM-EDX = scanning electron microscopy coupled with energy dispersive X-ray analysis

SERS = surface-enhanced Raman spectroscopy

TLC = thin layer chromatography

TLC-SERS = thin layer chromatography coupled with surface-enhanced Raman spectroscopy

UVF = ultraviolet fluorescence

UV-vis = ultraviolet-visible spectroscopy

Vis-RS = visible reflectance spectroscopy

XRD = X-ray diffraction

XRF = X-ray fluorescence

Introduction

Organic colorants obtained from natural sources such as plants and insects have been widely used as textile dyes or lake pigments for paintings, sculptures and other kinds of polychrome works of art since ancient times until the second half of the 19th century, when the industrial production of synthetic dyes had begun. The identification of these materials is of utmost importance for the conservation and long-term preservation of works of art and archaeological objects, and can provide valuable information about their historical context.

Several instrumental techniques have been employed for the detection of colorants over the years. In recent times, SERS has been also appreciated for its great potential in cultural heritage investigations, as the adsorption of the analyte on nanosized metal surfaces, resulting in a significant enhancement of the Raman scattering intensity and strong fluorescence quenching, leads to obtaining a specific fingerprint for many organic substances, markedly reducing the amount of sample that would be otherwise required for analysis.

The present doctoral thesis work aims to the improvement of pre-existing analytical methods as well as to the development of innovative procedures for the identification of organic dyes of artistic and archaeological interest, with special attention being devoted to SERS. The scientific results here reported are the fruit of a research activity carried out both at Università degli Studi di Milano and in the Department of Scientific Research of the Metropolitan Museum of Art (New York, USA).

First of all, an effective experimental protocol for SERS analyses on silver colloids was optimized and a wide spectral database of historical natural colorants was thus assembled, containing among the others the spectra of several dyes never studied before; their spectral patterns were carefully inspected and therefore discussed in connection with those of colorants belonging to the same molecular class. The same SERS procedure, in association with complementary analytical investigations of different kind, was then successfully applied to the identification of a yellow dye in ancient wool threads from an excavation site in the Libyan Sahara dating to the Garamantian time. Also, an extensive work for the scientific analysis of Kaitag textiles, a unique embroidered textile art form from Caucasus, was performed using non- and micro-destructive techniques of both chromatographic and spectroscopic type, allowing the detection of several red, yellow, brown, green and blue colorants as well as of the ink used for the underlying drawing, and suggesting possible reasons for a corrosion phenomenon often observed in brown and black areas of these precious artifacts.

Work carried out at the Metropolitan Museum of Art comprises a comparative study of the most relevant SERS approaches recently introduced in art analysis: results obtained from reference dyes were compared with those achieved on actual samples taken from a number of works of art and ancient objects, including masterpiece oil paintings, musical instruments, archaeological textiles and lake pigments. Watercolors from a Winsor & Newton handbook dating to 1887 were then characterized using SERS and ordinary Raman spectroscopies, and a database of original art materials was acquired. Also, coupling of TLC and SERS was investigated and tested as a tool for the separation and identification of the main alkaloid constituents of Syrian rue dye. Finally, a comprehensive Raman study of monobromoindigo, component of the historical colorant Tyrian purple, was performed, together with a detailed assignment of the spectral lines observed by comparison with density functional theory (DFT) quantum mechanical calculations.

Chapter 1

Organic colorants in art and archaeology and their chemical characterization

Abstract

This introductory chapter is intended to provide a quick overview of organic colorants and their use in textile dyeing, works of art and objects of cultural value over the centuries. Also, a brief outline is given about the analytical methods and chemical procedures that have been commonly employed and newly developed aiming to the identification of such materials. Among the different techniques, special emphasis is placed on the application of SERS, which has recently attracted increasing attention in this context thanks to its great potential in detecting minuscule amounts of colorants with very high sensitivity.

Organic colorants in art and archaeology

From prehistoric times, mankind has been fascinated by color and has left an imprint on his environment in the form of painted images, which both beautified his world and expressed his thoughts and feelings. In fact, color has always been a central element in the cultures of peoples all over the world, having been used throughout history for a great variety of purposes, not only, for instance, to produce artworks and embellish objects or individuals, but often to indicate importance and hierarchical status as well. In fact, at all times and locations, the quality and colors of fabrics were a clear sign of the social class which their owners belonged to; the more brilliant, vivid and striking the colors of the dyes, the more expensive, exclusive and precious they were.

Among the colored materials extensively employed since antiquity, natural organic colorants have played for millennia a key role as pigments to decorate objects and paint a wide range of polychrome works of art, to dye fabrics and also to manufacture functional items ordinarily used in everyday life (figure 1).



Figure 1. (a) Natural dyes. (b) Wool dyeing with natural colorants in a village in the mountains situated at the west of Isfahan, Iran.

First of all, definition of some of the most common terms that will be employed in the following is here provided^{1,2}, in order to avoid confusion and better understand the topics that will be henceforth discussed.

A **dye** or **colorant** is a water-soluble substance, mostly of organic origin, with which substrates are dyed directly or with the aid of another ingredient. The coloring component, reasonably stable to light, penetrates into the material to which it is being applied and binds itself sufficiently strongly that it is not removed, or otherwise affected, by washing or dry cleaning. On the other hand, a **pigment** is a colored compound which is not soluble in the vehicle. Pigments are often inorganic in origin, such as earth pigments, but can also be of organic origin, e.g. madder lake. They are bound onto the surface of textile or paper fibers by means of a binding medium such as oil, protein or gum.

As will be further discussed in this chapter, organic dyes are often incorporated into an inorganic substrate to produce a lake pigment or fixed to textile fibers by means of bridging inorganic ions called mordants.

Materials are colored when they absorb light selectively in the visible region of the electromagnetic spectrum. In particular, a **chromophore** is the part of a molecule responsible for its color, which usually consists of groups belonging to systems of conjugated double bonds, such as the vinylene group ($-C=C-$), the carbonyl group ($-C=O$) and the nitroso group ($-N=O$). A functional group that modifies the light absorbance, e.g. the hydroxyl group ($-OH$), the carboxyl group ($-COOH$) and the amino group ($-NH_2$), is called **auxochrome**.

It is well known that, prior to the introduction of synthetic colorants in the second half of the 19th century, all dyes were derived from a variety of natural sources. Roots, berries, wood, bark and leaves were definitely the main source of colorants in ancient times, but other organisms such as lichens, insects and sea snails have been widely employed by mankind over the centuries as well¹⁻³. Dyes deriving from natural sources were mainly blue, red, yellow and brown, while other hues could be achieved by the combined use of different dyestuffs; green shades, for instance, were traditionally obtained as mixtures of a blue and a yellow dye.

The chromophores contained in natural colorants, as will be further discussed in Chapter 2, are mainly anthraquinones, flavonoids and indigoids, even though different compounds belonging to other molecular classes such as carotenoids, curcuminoids, naphthoquinones and gallotannins are also frequently encountered^{4,5}. In particular, several blue and purple dyes, including indigo and Tyrian purple, owe their color to substances mostly related to indigotin which can be obtained from plants or shellfish, while other colorants producing similar shades, such as orchil, are extracted from different sources, e.g. lichens; reds are usually composed of anthraquinones and can be derived from insects, as in the case of cochineal, kermes and lac dye, or plants, among which madder was one of the most popular in antiquity (figure 2); the great majority of yellow colorants contain flavonoids, that occur in a wide variety of botanical sources as sugar derivatives, or glycosides¹⁻³. As also pointed out in Chapter 3, since many plants rich in flavonoids can be easily found all over the world in the vegetable kingdom, no individual source of yellow dye has become predominant over the centuries – as opposite to what happened with the red colorants madder and cochineal – and the choice of the dye source often depended on the species that were locally available.

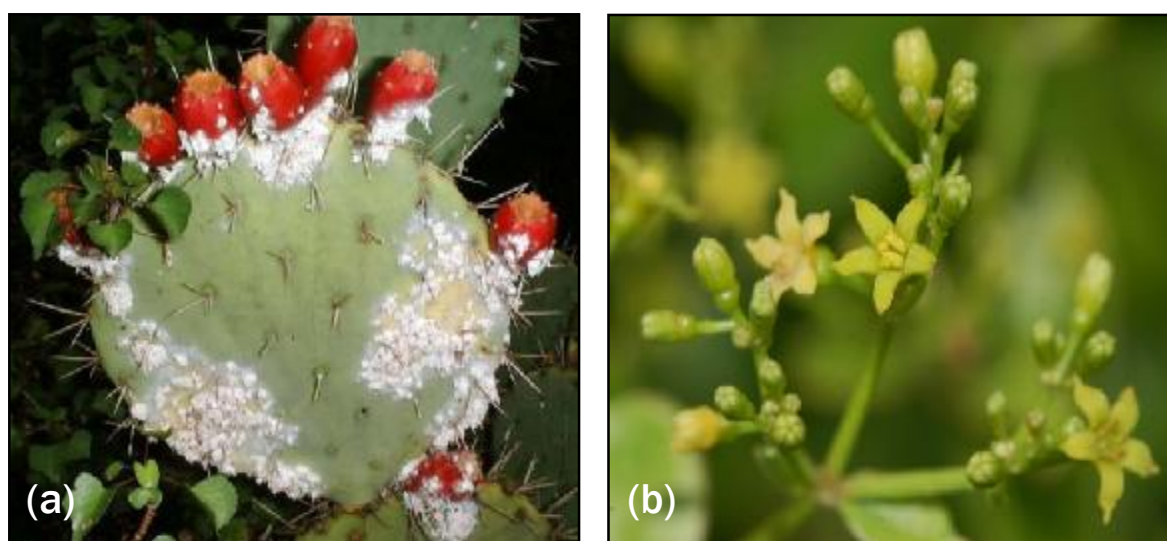


Figure 2. Examples of natural sources of organic colorants: (a) *Dactylopius coccus* scale insects, from which the red dye cochineal is extracted, living on the *Opuntia* cactus; (b) *Rubia tinctorum* plant, the roots of which are the source of a red colorant known as madder.

When used in painting, natural organic colorants have to be precipitated with an inert binder, usually a metallic salt, to create a lake pigment². In ancient times chalk, white clay and crushed bones were employed, being sources of calcium carbonate and calcium phosphate. The salts that are commonly used today include barium sulfate, calcium sulfate, aluminium hydroxide and aluminium oxide, all of which can be produced cheaply from inexpensive mineral ores.

Natural organic colorants used in textile dyeing can be divided into three different categories, depending on the procedure according to which they are applied to fabrics^{1,2,4,5}.

- **Vat dyes** - Colorants belonging to the present class are water-insoluble but, under reducing conditions, they can be converted into a "leuco" form, soluble in alkali deriving, in ancient times, from either wood ash, plant ash, lime or stale urine. Immersion of the textile into the dye solution allows the dissolved molecules of colorant to penetrate the fibers. After that, upon removal of the wet dyeing from the bath and exposure to atmospheric oxygen, these substances can be oxidized back to their colored forms which, by virtue of their insolubility in water, are trapped on the surface of the fiber. The best-known blue colorants, indigo and woad, as well as Tyrian purple, belong to this category. Vat dyes were named after the vats employed in the reduction of indigo plants through fermentation.
- **Mordant dyes** - Many colorants do not have a strong chemical affinity for the textile fibers, which therefore require to be treated prior to the dyeing stage, involving a two-step chemical reaction. A solution of a mordant, typically a metal salt, is first used to impregnate the fibers, allowing the metal ion to become complexed to appropriate functional groups in the structure of the textile. During the dyeing process, the colorant interacts with the mordant-fiber complex via ionic and coordinate covalent bonds to form insoluble brightly colored species. The complex thus formed within the fibers does not easily wash out of the textile and the resulting dyeing is therefore relatively fast. The term "mordant" comes from the Latin word *mordere*, "to bite": in the past, it was thought that a mordant helped the dye bite onto the fiber, so that it would hold fast during washing. Aluminium, iron, tin, chromium or copper ions, as well as tannins, are examples of mordants; one of the substances most commonly employed in ancient times for this purpose was potassium alum ($\text{KAl}(\text{SO}_4)_2 \cdot 12\text{H}_2\text{O}$), also known as potash alum or aluminium potassium sulfate, but iron sulfate ($\text{FeSO}_4 \cdot 7\text{H}_2\text{O}$) and tin chloride (SnCl_2) were often used as well. Alum occurs naturally in various minerals; potassium alum, in particular, is found in kalinite, alunite and leucite. Commonly employed in association with mordants are dye-assistants such as cream of tartar or oxalic acid, which brighten the colors, protect the fibers and help the absorption of the mordants. Mordant dyes can be used with wool, silk and protein yarns in general, while cellulose fibers such as linen and cotton have to be chemically modified before dyeing. The vast majority of natural colorants belongs to this category and yields different colors when combined with different mordants: a typical example is represented by madder lake, which can produce red, orange or violet shades when associated with aluminium, tin and iron mordants, respectively.
- **Direct dyes** - Also called substantive dyes, they are applied directly to the fiber without requiring any special treatment, but usually are less wash- and lightfast than vat or mordant dyes. Examples of direct dyes include turmeric and saffron, which can be fixed to all fibrous materials in aqueous solution.

The production of synthetic colorants, which started with the serendipitous discovery of mauveine by William Perkin in 1856 (figure 3), triggered a decline in the dominance of traditional natural dyes in world markets. Mauve had a short commercial lifetime, but its early success led to experimentation that produced within a relatively short space of time several improved coloring substances, offering a vast range of new colors at a lower price. In fact, only a few years after the discovery of the first synthetic dyestuff, a whole range of new colorants became available. Between 1870 and 1880 the large-scale market for natural dyes ended, indigo being one of the last to be replaced by its synthetic equivalent. In 1883 Adolf von Baeyer discovered the chemical structure of indigo, and by the end of the 19th century a commercially feasible manufacturing process had been developed^{1,2,5}.



Figure 3. Perkin's original bottle of mauveine dye, labelled "*Original mauveine prepared by Sir William Perkin in 1856*". Perkin accidentally discovered the formula for producing synthetic mauve dye while trying to synthesize quinine, a cure for malaria. The bottle is kept at the Science Museum of London.

Even today, natural and synthetic organic dyes are of great interest in the art conservation and forensic fields as ink and paint components, food colorants, cosmetic constituents and textile dyes. On the one hand, some of the most popular natural compounds employed in ancient times as dyestuffs have retained economic importance over the centuries as sources of colors in many foodstuffs and drinks: just to mention a few examples, anthocyanins play a crucial role in the purple-red shade of several wines, while flavonols and flavones are responsible for the color of many fruits and vegetables, as well as green teas. Also, a growing number of natural chromophores, such as carotenoids from saffron and annatto, anthraquinones from cochineal, curcumins from turmeric, as well as naphthoquinones from henna leaves, are being commercially produced and used as coloring agents in food, drugs and cosmetics⁶. On the other hand, synthetic dyes with improved properties have also found an increasing range of commercial applications over the years, even though their use is obviously restricted to those that could be tested as safe.

Chemical characterization of organic colorants

Paintings, sculptures and several other artifacts that are part of our cultural heritage, including textiles, books, furniture, archaeological objects and the organic residues found in association with them, often contain a great variety of both natural and synthetic coloring substances.

Chemical investigation of such materials is of great interest to art historians, restorers and art conservators. In fact, the analysis of ancient dyes can be of help in revealing what kind of substances were available in particular periods and geographical areas, providing valuable data about the historical context of a work of art, the lifestyle and the technical knowledge reached by a certain population in a given historical age, the provenance of textile materials, pigments, dyestuffs and colored artifacts, shedding light on the possible interactions between different cultures as well as the trade routes and commercial transactions which may have allowed the usage of a particular colorant far from its geographical source. Moreover, discovering the nature and the origin of the coloring substances employed in the production of a work of art can provide precious information regarding its original color and appearance, thus offering new insights into the artist's choices and original intention, the techniques used and the dates *ante quem* and *post quem* the art object was produced, possibly leading to the uncovering of falsifications and forgeries. Furthermore, scientific analysis applied to the study of art materials and, specifically, of pigments and dyes, may contribute to assess suitable conservation and restoration procedures to be applied to paint defects and degraded pigments in works of art of any kind; in fact, time, environmental conditions and several other circumstances unavoidably cause damage and deterioration to art objects and artifacts, which therefore require careful conservation to be safeguarded as important elements of our cultural heritage.

The identification of historical dyes is currently one of the most challenging tasks in the chemical investigation of art materials, for three main reasons. First of all, colorants in works of art and archaeological textiles are usually included in complex matrixes such as paint layers or cloth fibers, where they are present in mixture with other substances, e.g. binding media or mordants, and in very low concentrations due to their high tinting power. Besides, sampling of art objects is always limited to microscopic fragments, when at all allowed. An additional analytical challenge is posed by the remarkable susceptibility to deterioration of organic materials, which can undergo a number of chemical degradation processes leading to the formation of specimens with a different molecular structure in comparison to the primary organic dye. In this regard, a few cases reported in the literature are dealing, for instance, with the detection of products such as 2,4-dihydroxybenzoic acid and 2,4,6-trihydroxybenzoic acid deriving from morin in samples dyed with old fustic⁷ and from luteolin in weld and dyer's broom⁸; similarly, debromination upon ageing has been evidenced in indigoid components of purple^{9,10}. In particular, all colorants are prone to some degree of fading caused by many chemical oxidation processes when exposed to light¹¹. In this context, the recent identification of organic madder and cochineal-based purples and reds, in addition to inorganic vermilion and chrome yellow, in an important historical watercolor by the American master Winslow Homer was essential both to determine how the colorless appearance of the sky was actually the result of a fading process and to hypothesize how the painting most likely looked just after its completion¹².

As in the case of other organic substances of archaeological interest, also the analysis of historical dyes was significantly improved thanks to the introduction of instrumental techniques, both of chromatographic and spectroscopic types. In particular, many analytical methods have been exploited thus far for the detection of organic colorants in ancient fabrics and works of art.

Conventional techniques embrace, in the first place, UV-vis absorbance spectroscopy, which has allowed positive identification of several dyes including madder and indigotin on Anglo-Scandinavian textiles¹³; UV-vis reflectance spectroscopy was also evaluated as an alternative, sometimes leading to satisfactory results, as in the case of the detection of indigo used as a pigment or in Maya blue^{14,15}, without the need to take a sample. Nevertheless, in the majority of cases, electronic methods are strongly affected by matrix interference and show poor specificity, typically providing broad and featureless spectra that hardly allow specific identification. In the last few years, fluorimetry has also been successfully applied to the non-destructive study of pigments and colorants from medieval illuminations, paint cross sections, millenary textiles and wall paintings¹⁶⁻¹⁸.

However, if a sufficient amount of sample is available for analysis, chromatographic techniques are generally preferable, as they enable separation and reliable identification of individual components in dye mixtures. Among them, TLC was firstly applied to the investigation of madder lake samples from manuscripts dating to the 12th and 15th centuries in 1967¹⁹ and has thenceforth found increasing application in the analysis of organic colorants²⁰. Over the years, this separation technique has gradually been replaced by HPLC, which has become a well-established analytical tool for this sort of investigations and has to date allowed to identify the largest number of dyes in works of art and ancient textiles²¹⁻²⁵. Despite its great selectivity and specificity though, HPLC is a destructive tool and requires sizable sample, typically 1 mg of colorant or 5 mm of dyed fiber, which is obviously not always available from rare and priceless artifacts such as museum objects.

Among the vibrational spectroscopic techniques that have been evaluated for the analysis of organic colorants, e.g. FTIR^{26,27} and NIR²⁸ spectroscopies, Raman spectroscopy has the greatest potential for the analysis of minute amounts of dyes and has thus been used to characterize both natural and synthetic pigments²⁹⁻³². However, this technique has proven to be more suitable for the non-invasive analysis of inorganic coloring materials, as it suffers from inherently weak signals and strong molecular fluorescence from organic dyestuffs often precludes the measurement of Raman scattering; several organic colorants are in fact extremely fluorescent even when using relatively high wavelengths, namely 785 nm, for excitation, and the resulting background obscures their Raman spectrum^{1,5}. Furthermore, because only subnanogram levels of dyes are needed to achieve intense coloration, normal Raman spectroscopy is often not sensitive enough to probe these materials, especially when they are embedded in complex matrixes such as traditional artists' paints or historical textiles.

In recent years, the potential of SERS for the ultrasensitive detection of organic molecules used as artists' colorants has been widely appreciated and exploited. The introduction of this analytical tool in the field of cultural heritage investigations has significantly improved the chances of successfully identifying dyes, clearing the way for an enormous range of new possibilities of experimentation. A brief outline about the historical background and development of this technique, as well as its physicochemical principles and application to the analysis of organic colorants, is given in the following paragraph.

SERS enters the scene: history, chemistry and application to dye analysis

SERS is a surface-sensitive technique that allows to achieve significant enhancements of the Raman scattering intensity, as much as 10^{14} , for substances adsorbed on nanosized metal surfaces such as properly treated electrodes, colloidal particles and thin films (figure 4). Several articles, journal special issues and books are being published every year on this topic, which is currently at the center of a powerful renaissance, both in terms of a deepened fundamental understanding of the interactions between the nanostructured noble metal substrates and model analytes, and in terms of its applications; in this regard, comprehensive studies have been recently conducted by Aroca³³, Lombardi and Birke^{34,35}.

SERS effect has been firstly observed for pyridine adsorbed on electrochemically roughened silver in 1974 by Fleischman and coworkers³⁶. The discovery of such an enormous enhancement in the Raman intensity when a molecule is in the vicinity of metal nanoparticles, coupled with the suppression of fluorescence, generated considerable excitement and suggested the possibility that SERS could provide an invaluable tool as a reliable, high-resolution detection technique for extremely minute quantities of target molecules. Fleischman and coworkers justified the intense signals obtained for pyridine simply as a matter of the number of molecules that were scattering on the surface, not recognizing the occurrence of a major enhancement effect. In 1977 two research groups independently noted that the concentration of scattering species could not account for the enhanced signal and each proposed a mechanism for the observed phenomenon: Jeanmaire and Van Duyne³⁷ suggested an electromagnetic effect, while Albrecht and Creighton³⁸ hypothesized a charge-transfer effect. Their theories are generally still accepted as explaining the SERS effect.

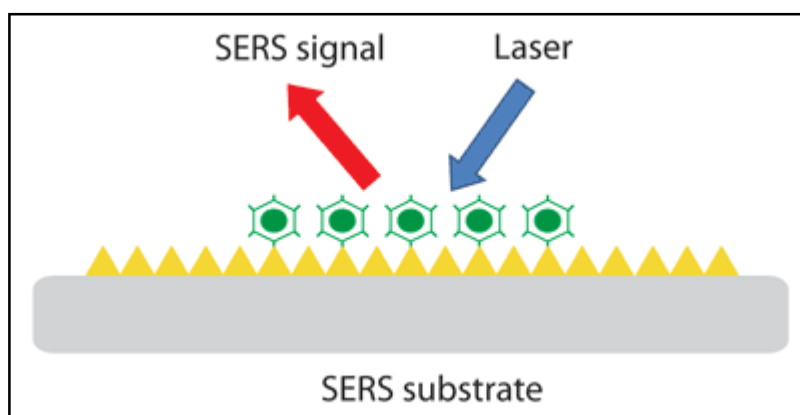


Figure 4. Conceptual illustration of SERS mechanism.

However, the exact mechanism of the enhancement effect of SERS is still a matter of debate in the literature. On the one hand, according to the electromagnetic theory, the increase in intensity of the Raman signal for adsorbates on particular surfaces is due to an enhancement in the electric field provided by the surface itself; this explanation can apply even in those cases where the specimen is only physisorbed to the surface, without chemical interactions. When incident light emitted by a laser strikes the surface, localized surface plasmons are excited, and the field enhancement is greatest when the plasmon frequency is in resonance with the radiation. In order for scattering to occur, the plasmon oscillations must be perpendicular to the surface; if they

are in-plane with the surface, no scattering will be observed. It is because of this requirement that roughened surfaces or arrangements of nanoparticles are typically employed in SERS experiments, as they provide an area on which these localized collective oscillations can occur. On the other hand, the chemical theory proposes charge-transfer effects between molecular orbitals of the target analyte and the conduction band of the noble metal substrate; it only applies for species which have formed a chemical bond with the surface, and as a result it does not fully explain the observed signal enhancement in all cases.

As far as selection rules are concerned, the term surface-enhanced Raman spectroscopy implies that this technique provides the same information as traditional Raman spectroscopy, simply with a greatly enhanced signal. However, while spectra deriving from most SERS experiments are similar to the non-enhanced ones, several differences in the number of modes are frequently observed: in fact, additional modes not found in the traditional Raman spectrum can be present in the SERS spectrum, while other modes can disappear. The modes observed in any spectroscopic experiment are dictated by the symmetry of the molecules and are usually summarized by selection rules. When molecules are adsorbed to a surface, the symmetry of the system can change, slightly adjusting the symmetry of the molecule, which can lead to differences in mode selection^{33,39}. One common way in which selection rules are modified arises from the fact that many molecules that have a center of symmetry lose that feature when adsorbed to a surface. The loss of a center of symmetry eliminates the requirements of the mutual exclusion rule, which dictates that modes can only be either Raman or infrared active. Thus, modes that would normally appear only in the infrared spectrum of the free molecule can appear in the SERS spectrum⁴⁰. The symmetry of a molecule can be changed in different ways depending on the orientation in which the molecule is attached to the surface. In some experiments, it is possible to determine the orientation of adsorption to the surface from the SERS spectrum, as different modes will be present depending on how the symmetry is modified⁴¹.

While the first experiments were performed on electrochemically roughened silver³⁶, the most widely used methods to prepare substrates for SERS experiments are now based on wet chemistry, i.e. chemical reactions in solution³³. Metal colloids can be synthesized by a number of different procedures, such as chemical reduction, laser ablation and photoreduction; among these, the first one mentioned has been the most popular thus far. The reaction is usually carried out by employing a starting metal salt, which is reduced by a chemical agent to produce colloidal suspensions containing nanoparticles with variable sizes, depending on the method of production. Generally, the size regime relevant to SERS experiments is between 10 and 80 nm. The shape and size of metal nanoparticles, which strongly affect the strength of the enhancement, can be partially controlled by appropriate choice of the preparation procedure; the most important parameters in this regard are the nature of the metal, the reducing agent, the temperature, the stabilizing agents and the metal ion concentration. Different kinds of nanoparticles support different plasmon resonances, depending on the size, shape and dielectric constant of the metal; the choice of surface metal is therefore dictated by the plasmon resonance frequency³³. Silver and gold are typical metals for SERS experiments because their plasmon resonance frequencies fall within visible and NIR spectral ranges, i.e. radiation used to excite Raman modes, and can thus provide maximal enhancement for these wavelength ranges. The absorption spectra of copper⁴², platinum and palladium⁴³ also fall within the range acceptable for SERS experiments.

Although the SERS technique has been discovered almost four decades ago, only in recent years sustained efforts have been devoted to its application to the study of cultural heritage objects. Guineau and Guichard first explored SERS to identify colorants of artistic and archaeological interest in 1987, demonstrating that significant enhancements could be obtained from the analysis of synthetic alizarin and extracts from an 8th century textile sample dyed with madder on a porous Ag electrode cooled with liquid nitrogen⁴⁴. However, because of the objective difficulties in achieving consistent and reproducible results with this technique, a considerable number of SERS studies started being published nearly twenty years later. In fact, as demonstrated by recent reviews and papers⁴⁵⁻⁴⁷, SERS has lately found increasing application for dye investigation in works of art and archaeological objects, thanks to its great potential in providing specific vibrational fingerprints even for extremely fluorescent colorants with high selectivity and sensitivity. Since it is not a separation technique, it suffers from a greatly reduced ability to resolve dye mixtures when compared to HPLC; nevertheless, it can be employed successfully with minute samples, as recent improvements have made measurements possible to be performed on a single pigment grain or a few-microns length of fiber.

Silver colloids synthesized according to the Lee-Meisel method⁴⁸, i.e. by citrate reduction of silver nitrate, have been to date the most popular substrate for SERS investigations of colorants in artworks, thanks to their easy preparation procedure; other kinds of supports, such as silver nanoparticles produced by laser photoreduction⁴⁹, silver island films and silver films over nanospheres^{50,51}, have been also tested as an alternative, and are worth further exploration in the future.

A lot of research carried out thus far in the field of SERS applied to art and archaeology is dealing with the characterization of reference substances: for years, alizarin, purpurin and anthraquinones in general have been the subject of most works available in the scientific literature⁵²⁻⁵⁹, even though a number of articles about flavonoids⁶⁰⁻⁶⁴, indigoid dyes^{65,66} and a few other chromophores have been published as well. In addition to providing valuable reference spectra, these papers have also investigated aspects such as complexation geometry, influence of pH and orientation of the analyzed molecules with respect to the metal substrate.

Because the orientation of the molecule with respect to the metal surface results in selective enhancement of certain signals, interpretation of the spectra can pose a real challenge, and therefore *ab initio* computational methods such as density functional theory (DFT) are sometimes used to assign the normal modes and interpret SERS data^{53,56,61,62,64}, even if comparison with reference spectral databases and a deeper understanding of the interactions of the dyes with various metal substrates are still required.

SERS experiments on historical artifacts, which all require that samples be removed from the work of art under investigation, initially employed harsh chemical extraction in strong acids in order to isolate the organic dye from the medium, invariably resulting in degradation of the host material; in recent years, the development of milder extraction procedures⁶⁷, non-extractive hydrolysis methods⁵⁵ as well as non-hydrolysis approaches^{51,68,69,70} has allowed positive identification of a number of organic pigments in tapestries, carpets, paintings and other valuable art objects.

Opportunities for future research include the extension of spectral databases of dyes already available in the literature to reference colorants that have not been characterized so far, as well as the development of non-invasive approaches which, combined with the use of robust nanofabrication techniques, will ultimately allow SERS to become an analytical tool of general applicability in the art conservation field.

References

- [1] J. H. Hofenk de Graaff, *The Colourful Past - Origins, Chemistry and Identification of Natural Dyestuffs*, Archetype Publications, London, **2004**.
- [2] A. Casoli, M. E. Darecchio, L. Sarritzu, *I Coloranti nell'Arte*, Il Prato Casa Editrice, Padova, **2009**.
- [3] D. Cardon, *Natural Dyes: Sources, Tradition, Technology and Science*, Archetype Publications, London, **2007**.
- [4] E. S. B. Ferreira, A. N. Hulme, H. McNab, A. Quye, *Chem. Soc. Rev.* **2004**; 33, 329.
- [5] J. S. Mills, R. White, *The Organic Chemistry of Museum Objects*, Butterworths, London, **1994**, p. 121.
- [6] H. Schweppe, *Handbuch der naturfarbstoffe*, Landsberg/Lech, Germany, **1993**.
- [7] E. S. B. Ferreira, A. Quye, H. McNab, A. N. Hulme, *Dyes Hist. Archaeol.* **2002**; 18, 63.
- [8] M. P. Colombini, A. Andreotti, C. Baraldi, I. Degano, J. J. Lucejko, *Microchem. J.* **2007**; 85, 174.
- [9] Z. C. Koren, *Photochemical vat dyeings of the biblical purple tekhet and argaman dyes*, paper presented at the 13th meeting of Dyes in History and Archaeology, Royal Museum of Scotland, Edinburgh, **1994**.
- [10] C. J. Cooksey, R. S. Sinclair, *Dyes Hist. Archaeol.* **2005**; 20, 127.
- [11] P. Cox Crews, *Stud. Conserv.* **1987**; 32, 65.
- [12] C. L. Brosseau, F. Casadio, R. P. Van Duyne, *J. Raman Spectrosc.* **2011**; 42, 1305.
- [13] G.W. Taylor, *Stud. Conserv.* **1983**; 28, 153.
- [14] M. Leona, J. Winter, *Stud. Conserv.* **2001**; 46, 153.
- [15] M. Leona, F. Casadio, M. Bacci, M. Picollo, *J. Am. Inst. Conserv.* **2004**; 43, 39.
- [16] A. Claro, M. J. Melo, S. Schafer, J. S. S. de Melo, J. S. S., F. Pina, K. J. van den Berg, A. Burnstock, *Talanta* **2008**; 74, 922.
- [17] C. Clementi, C. Miliani, A. Romani, U. Santamaria, F. Morresi, K. Mlynarska, G. Favaro, *Spectrochim. Acta, Part A: Mol. Biomol. Spectrosc.* **2009**; 71, 2057.
- [18] M. J. Melo, A. Claro, *Acc. Chem. Res.* **2010**; 43, 857.
- [19] L. Masschelein-Kleiner, J. Heylen, F. Tricot-Marckx, *Stud. Conserv.* **1968**; 13, 87.
- [20] H. Schweppe, *Handbuch der naturfarbstoffe*, Landsberg/Lech, Germany, **1993**.
- [21] J. Wouters, *Stud. Conserv.* **1985**; 30, 119.
- [22] J. Wouters, A. Verhecken, *Stud. Conserv.* **1989**; 34, 189.
- [23] L. Karapanagiotis, L. Valianou, S. Daniilia, Y. Chryssoulakis, *J. Cult. Herit.* **2007**; 8, 294.
- [24] M. R. van Bommel, I. Vanden Berghe, A. M. Wallert, R. Boitelle, J. Wouters, *J. Chromatogr. A* **2007**; 1157, 260.
- [25] M. V. Cañamares, M. Leona, M. Bouchard, C. M. Grzywacz, J. Wouters, K. Trentelman, *J. Raman Spectrosc.* **2010**; 41, 391.
- [26] S. A. Centeno, J. Shamir, *J. Mol. Struct.* **2008**; 873, 149.
- [27] R. D. Gillard, S. M. Hardman, R. G. Thomas, D. E. Watkinson, *Stud. Conserv.* **1994**; 39, 187.
- [28] S. Bruni, S. Caglio, V. Guglielmi, G. Poldi, *Appl. Phys. A: Mater. Sci. Process.* **2008**; 92, 103.
- [29] I. M. Bell, R. J. H. Clark, P. Gibbs, *Spectrochim. Acta Part A* **1997**; 53, 2159.
- [30] P. Vandenabeele, L. Moens, H. G. M. Edwards, R. Dams, *J. Raman Spectrosc.* **2000**; 31, 509.
- [31] G. Smith, R. J. H. Clark, *Rev. Conserv.* **2001**; 2, 92.

- [32] F. Schulte, K. W. Brzezinka, K. Lutzenberger, H. Stege, U. Panne, *J. Raman Spectrosc.* **2008**; 39, 1455.
- [33] R. Aroca, *Surface-Enhanced Vibrational Spectroscopy*, John Wiley & Sons, Chichester, UK, **2006**.
- [34] J. R. Lombardi, R. Birke, *J. Phys. Chem. C* **2008**; 112, 5605.
- [35] J. R. Lombardi, R. Birke, *Acc. Chem. Res.* **2009**; 42, 734.
- [36] M. Fleischmann, P. J. Hendra, A. J. McQuillan, *Chem. Phys. Lett.* **1974**; 26, 163.
- [37] D. L. Jeanmaire, R. P. van Duyne, *J. Electroanal. Chem.* **1977**; 84, 1.
- [38] M. G. Albrecht, J. A. Creighton, *J. Am. Chem. Soc.* **1977**; 99, 5215.
- [39] M. Moskovits, J. S. Suh, *J. Phys. Chem.* **1984**; 88, 5526.
- [40] E. Smith, G. Dent, *Modern Raman Spectroscopy: A Practical Approach*, John Wiley & Sons, Chichester, UK, **2005**.
- [41] A. G. Brolo, Z. Jiang, D. E. Irish, *J. Electroanal. Chem.* **2003**; 547, 163.
- [42] J. A. Creighton, D. G. Eadon, *J. Chem. Soc., Faraday Trans.* **1991**; 87, 3881.
- [43] C. Langhammer, Z. Yuan, I. Zorić, B. Kasemo, *Nano Lett.* **2006**; 6, 833.
- [44] B. Guineau, V. Guichard, *ICOM Committee for Conservation: 8th Triennial Meeting*, Preprints, Vol. 2, The Getty Conservation Institute, Marina del Rey, CA, **1987**, p. 659.
- [45] K. Chen, M. Leona, T. Vo-Dinh, *Sens. Rev.* **2007**; 27, 109.
- [46] K. L. Wustholz, C. L. Brosseau, F. Casadio, R. P. Van Duyne, *Phys. Chem. Chem. Phys.* **2009**; 11, 7350.
- [47] F. Casadio, M. Leona, J. R. Lombardi, R. Van Duyne, *Acc. Chem. Res.* **2010**; 43, 782.
- [48] P. C. Lee, D. J. Meisel, *J. Phys. Chem.* **1982**; 84, 3391.
- [49] M. V. Cañamares, J. V. Garcia-Ramos, J. D. Gómez-Varga, C. Domingo, S. Sanchez-Cortes, *Langmuir* **2007**; 23, 5210.
- [50] A. V. Whitney, R. P. Van Duyne, F. Casadio, *Proc. SPIE* **2005**; 117.
- [51] C. L. Brosseau, A. Gambardella, F. Casadio, C. M. Grzywacz, J. Wouters, R. P. Van Duyne, *Anal. Chem.* **2009**; 81, 3056.
- [52] I. T. Shadi, B. Z. Chowdhry, M. J. Snowden, R. Withnall, *J. Raman Spectrosc.* **2004**; 35, 800.
- [53] M. V. Cañamares, J. V. Garcia-Ramos, C. Domingo, S. Sánchez-Cortés, *J. Raman Spectrosc.* **2004**; 35, 921.
- [54] K. Chen, M. Leona, K.-C. Vo-Dinh, F. Yan, M. B. Wabuyele, T. Vo-Dinh, *J. Raman Spectrosc.* **2006**; 37, 520.
- [55] M. Leona, J. Stenger, E. Ferloni, *J. Raman Spectrosc.* **2006**; 37, 981.
- [56] A. V. Whitney, R. P. Van Duyne, F. Casadio, *J. Raman Spectrosc.* **2006**; 37, 993.
- [57] M. V. Cañamares, J. V. Garcia-Ramos, C. Domingo, S. Sánchez-Cortés, *Vib. Spectrosc.* **2006**; 40, 161.
- [58] M. V. Cañamares, M. Leona, *J. Raman Spectrosc.* **2007**; 38, 1259.
- [59] A. V. Whitney, F. Casadio, R. P. Van Duyne, *Appl. Spectrosc.* **2007**; 61, 994.
- [60] Z. Jurasekova, J. V. Garcia-Ramos, C. Domingo, S. Sánchez-Cortés, *J. Raman Spectrosc.* **2006**; 37, 1239.
- [61] T. Teslova, C. Corredor, R. Livingstone, T. Spataru, R. L. Birke, J. R. Lombardi, M. V. Cañamares, M. Leona, *J. Raman Spectrosc.* **2007**; 38, 802.
- [62] M. Wang, T. Teslova, F. Xu, T. Spataru, J. R. Lombardi, R. L. Birke, *J. Phys. Chem. C* **2007**; 111, 3038.
- [63] Z. Jurasekova, C. Domingo, J. V. Garcia-Ramos, S. Sánchez-Cortés, *Coalition* **2007**; 14, 14.

- [64] M. V. Cañamares, J. R. Lombardi, M. Leona, *e-Preserv. Sci.* **2009**; 6, 81.
- [65] I. T. Shadi, B. Z. Chowdhry, M. J. Snowden, R. Withnall, *Spectrochim. Acta Part A* **2003**; 59, 2213.
- [66] R. Withnall, I. T. Shadi, B. Z. Chowdhry, in *Raman Spectroscopy in Archaeology and Art History*, (Eds: H. G. M. Edwards, J. M. Chalmers), Royal Society of Chemistry, London, **2005**, pp. 152-165.
- [67] X. Zhang, R. A. Laursen, *Anal. Chem.* **2005**; 77, 2022.
- [68] E. Van Eslande, S. Lecomte, A.-S. Le Hô, *J. Raman Spectrosc.* **2008**; 39, 1001.
- [69] C. L. Brosseau, A. Gambardella, F. Casadio, C. M. Grzywacz, J. Wouters, R. P. Van Duyne, *Anal. Chem.* **2009**; 81, 7443.
- [70] L. H. Oakley, S. A. Dinehart, S. A. Svoboda, K. L. Wustholz, *Anal. Chem.* **2011**; 83, 3986.

Chapter 2

SERS spectral database of natural dyes on Ag nanoparticles aggregated by NaClO₄

Abstract

Several natural organic colorants used in antiquity in works of art and textile dyeing were characterized by SERS, in order to build a wide database that could integrate the data previously published in the literature, and the results of such scientific study are presented in this chapter. In particular, the SERS spectra of 11 dyes, namely dragon's blood, sandalwood, annatto, safflower yellow and red, old fustic, gamboge, catechu, kamala, aloe and sap green, were collected in this work for the first time. Silver colloids prepared according to the Lee-Meisel procedure, i.e. by reduction of a AgNO₃ aqueous solution with trisodium citrate dihydrate, were used as a metal substrate, while 1.8 M NaClO₄ was found to be the most effective electrolyte to be used as aggregating agent, giving the best results when added to the silver nanoparticles after the analyte.

Introduction

As discussed in Chapter 1, SERS has been more and more appreciated in the last few years for its great potential in cultural heritage investigations¹⁻³. Although the development of several micro-invasive analytical procedures has recently expanded the applicability of this technique in the art conservation field⁴⁻⁶, the necessity of obtaining a reliable match between spectra from unknowns and reference materials in a fast and convenient way is still to be fulfilled. In this context, the availability of extensive spectral databases would significantly increase the spectral recognition rate, making the entire identification process considerably easier. In the present study, a wide database of natural organic dyes used in antiquity for works of art and textile dyeing was created, containing SERS spectra for 25 colorants and 9 pure chromophores (table 1).

Table 1. Natural organic colorants included in the database acquired in the present work, divided into molecular classes and with indication of their main chromophores.

| Molecular class | Dyes | Main chromophores |
|-----------------|------------------|---|
| Anthraquinone | Aloe | Aloin, aloe emodin |
| | Cochineal | Carminic acid |
| | Lac dye | Laccaic acid A, laccaic acid B |
| | Madder | Alizarin, purpurin |
| Flavonol | Old fustic | Morin |
| | Stil de grain | Rhamnazin, emodin |
| | Sap green | Xanthorhamnin |
| Flavone | Weld | Luteolin, apigenin |
| | Dyer's broom | Luteolin, genistein |
| Chalcone | Safflower yellow | Hydroxysafflor yellow A |
| | Safflower red | Carthamin |
| | Kamala | Rottlerin |
| Neoflavone | Dragon's blood | 7,4'-dihydroxyflavylium, dracoflavylium |
| | Catechu | Catechin |
| Biflavonoid | Sandalwood | Santalinal A, santalin B |
| Neoflavonoid | Brazilwood | Brasilein |
| | Logwood | Hematein |
| Naphthoquinone | Alkanet | Alkannin |
| | Henna | Lawsone |
| | Walnut | Juglone |
| Carotenoid | Annatto | Bixin |
| | Saffron | Crocetin |
| Curcuminoid | Turmeric | Curcumin |
| Xanthone | Gamboge | Gambogic acid |
| Indigoid | Indigo | Indigotin |

In all cases, the dyes investigated were subjected to preliminary HPLC experiments, in order to assess their chemical composition and ascertain their purity. The interpretation of the collected SERS spectra was supported, when necessary, by the analytical results obtained for the colorants using subsidiary techniques, such as FT-Raman and micro-FTIR spectroscopies, HPLC and GC-MS.

Silver colloids, which are the most popular metal substrate for SERS, have been employed in many works thanks to their easy preparation procedure, mostly by using potassium nitrate to induce aggregation of the nanoparticles⁶⁻¹². Silver colloids synthesized according to the Lee-Meisel method were here used as substrates and sodium perchlorate was chosen as aggregating agent, due to its high efficiency tested in our laboratory on actual aged samples as well¹³ especially when added to the nanoparticles after the analyte.

In order to complete the data already available in the literature, the SERS spectra of 11 dyes, namely dragon's blood, sandalwood, annatto, safflower yellow and red, old fustic, gamboge, catechu, kamala, aloe and sap green, were collected in this work for the first time. The spectral patterns of such colorants were thus discussed in connection with those of the other dyes belonging to the same molecular class.

The database presented in this chapter contains reference SERS spectra of the most relevant colorants used in artistic production from ancient times until the 19th century and embraces a wide range of chromophores belonging to different molecular classes; for this reason, it may represent a useful and convenient resource for many spectroscopists interested in applying the SERS technique to investigate cultural heritage materials, and it could be easily employed for identification purposes when analyzing ancient dyed samples.

Natural organic dyes: history and chemistry

Several publications are dealing with the historical background of the most relevant natural dyes used in ancient times, among which the book written by Cardon is of primary importance¹⁴. A brief outline concerning the history and chemistry of the colorants that were here characterized by SERS is given in this section.

Anthraquinone dyes

Aloe

Aloe is obtained from the evaporated juice of the cut leaves of certain *Aloe* species, notably *A. vera*, from West Indies, *A. ferox* and *A. perryi*, from South and East Africa. Mentioned by Leonardo, it was used in paintings and decorative arts as a yellow or yellow-brown glaze especially by 16th century painters. During the 20th century, it was widely employed as a textile dye, providing different colors according to the mordant used. A major constituent of this colorant, up to 25%, is the anthraquinone aloin, a C-glycoside derived from aloe emodin, also present in aloe in smaller amounts¹⁵. According to Kremer, the supplier, our dye is obtained from the juice of thick leaves of different types of the *Liliaceae* group, to which *Aloe* species belong.

Cochineal

One of the main red colorants of animal origin, cochineal is obtained from the female insects of *Dactylopius coccus* and related parasite species of the *Opuntia* cactus family, indigenous to the New World and found in

Mexico, Central America and regions of South America. This pigment was used by the Aztecs for dyeing and painting, and only in the 16th century, following the Spanish conquest, was brought to Europe, where Canary Islands became one of the main suppliers. The major constituent of all cochineals is carminic acid, but the various species contain different amounts of other anthraquinone minor components which allow them to be distinguished in historical samples. Carmine is the currently accepted generic name for cochineal and another closely related colored substance, kermes, which was the principal insect dye in Europe before the discovery of America and, thus, of cochineal itself. Kermes mainly owes its color to kermesic acid and can be extracted from the female scale insect *Kermes vermilio*, which grows on Mediterranean oaks *Quercus coccifera* and *Quercus ilex*^{16,17}. Our colorant, commercially purchased from Zecchi (Florence, Italy), is reported to have been obtained from cochineal.

Lac dye

Lac dye is extracted from the eggs of the insect *Laccifer lacca*, also known as *Coccus laccae*, which develop in a resinous cocoon on the twigs of host trees in an arc from Northern India through to Indochina¹². Used in India and Japan since antiquity to dye silk, it has been found in Persian and Egyptian carpets of the 15th and 16th centuries¹⁵. It was not widely mentioned as a textile dye during the same period in Europe, where it was fully introduced only in the late 18th century^{12,15,18}. Lac dye was employed as an artists' pigment from the 13th century and enjoyed an extensive use in 15th century Italy and onwards¹⁸. The main coloring components of this colorant are laccaic acids A and B, belonging to the molecular class of anthraquinones.

Madder

Commonly used since antiquity for dyeing textiles, madder was mentioned by several Greek and Roman historians, such as Herodotus, Strabo, Dioscorides, Pliny the Elder, Vitruvius and Theophrastus, as well as in the Talmud^{19,20}. It can be extracted from the roots of *Rubia tinctorum* and related species, indigenous to India but widely cultivated in Europe and the Middle East too. Although madder has less tinctorial power than the scale insects above described, it has the advantage of producing shades from pink to black, purple and red when combined with different mordants¹⁶. The three main components of madder are alizarin, purpurin and pseudopurpurin; the chemistry of these and other quinonoid compounds is rather completely covered in a book by Thomson²¹. The first chemical investigations on madder date back to 1826. The identification of alizarin as the main chromophore of this colorant and its synthetic routes discovered in 1870 led to the industrial production of such coloring molecule, which largely displaced the natural dye in commercial use^{15,16,18}. Our pigment was purchased from Zecchi in the form of a lake.

Flavonol dyes

Old fustic

Extracted from the wood of *Chlorophora tinctoria*, typical of Cuba, Jamaica, Puerto Rico and other West Indian islands, old fustic was imported to Europe during the 16th century, becoming soon an important source for a yellow mordant dye. Although the colors obtained are not very lightfast, this colorant was widely used in

antiquity because of its low cost. Its main chromophore is the flavonol morin, which is present in the extract together with smaller amounts of kaempferol^{16,22}.

Stil de grain

The gold-yellow dye which constitutes stil de grain lake, also called Rhamno lake, Spincervino lake or buckthorn lake, can be obtained by extraction with hot water from the berries of *Rhamnus cathartica*, a wild plant diffused in the Northern hemisphere, in Brazil and Southern Africa. Known since ancient times and largely used from Middle Age to the 19th century for dyeing textiles, it was also employed in artistic techniques such as miniature, tempera and oil during the same period²³. It was used to produce orange and scarlet shades in mixture with cochineal, rather than for making pure yellows, because the color is very fugitive²⁴. Different glycosides of the flavonols quercetin, kaempferol, rhamnetin and rhamnazin are known components common to all these species, as well as the anthraquinone emodin. Our pigment is reported by Kremer to have been obtained by precipitating the extract of unripe buckthorn berries with alum.

Sap green

Sap green is also obtained from different kinds of *Rhamnaceae*, especially *Rhamnus cathartica*. To prepare the dye, the juice of the ripe buckthorn berries is squeezed out, mixed with alum, and allowed to thicken by evaporation to the consistency of honey²⁵. Used by itself, without mordant, the juice is yellow or green, depending on the ripeness of the berries, but its color is very deceptive. Recipes for its preparation were found in *De arte illuminandi*, a book written in the 14th century by an anonymous about the technique of manuscript illumination. It was employed from Medieval times to the 19th century in textile dyeing and miniatures²⁶. Our colorant was purchased by Kremer as the extract obtained from ripe buckthorn berries.

Flavone dyes

Weld

Extracted from *Reseda luteola*, weld grew wild in most Europe but was also cultivated. Frequently mentioned in ancient recipes for dyeing fabrics, it was used in European textiles and early Anatolian carpets. In the former case, it was always the main yellow colorant, even though following the discovery of America it was partially replaced by fustic and, after the 18th century, by quercitron as well¹⁵. Weld shows a superior light fastness compared to other yellow natural dyes; when employed in association with alum as a mordant, it gives bright and fast yellow colors thanks to the presence of the flavones luteolin and apigenin as major chromophores²². Weld was also frequently used with woad or indigo to give fast green dyes¹⁶. Our raw material, purchased from Zecchi, consists of cut pieces from *R. Luteola*.

Dyer's broom

Dyer's broom is obtained from *Genista tinctoria* species, which grows wild throughout Central and Southern Europe, across Russian Asia and northward to Sweden¹⁶. It is native to England, where it was the only yellow dye before importation of others in the Middle Ages¹⁵. It owes its color to the flavone luteolin and the isoflavone genistein. Dyer's broom was purchased from Kremer as cut pieces from *G. tinctoria*.

Chalcone dyes

Safflower

Obtained from *Carthamus tinctorius*, safflower has often been used since antiquity for dyeing textiles especially in Egypt, Persia, India and China, despite its low light fastness. Its application on fabrics, which began in Europe in the 18th century, further increased during the 19th century²⁷. It was also employed as a dyestuff for furniture, food additive and for medical purposes in China, mostly because of its anticoagulant properties²⁸. Petals of safflower can provide red and yellow colorants: the red pigment, carthamin, is water insoluble at neutral pH but can be brought into solution under alkaline conditions, while the yellow coloring matters can be extracted in water¹⁶. Safflower was purchased from Zecchi as ground petals of the plant.

Kamala

Kamala powder can be obtained from the fruits of *Mallotus philippinensis*, a small evergreen tree native to Southeast Asia, and has been extensively used in India and neighboring Southeastern countries since 1100 B.C. Mainly employed as a textile dye, with good wash fastness but quite low light fastness, it was also used as food and beverage coloring matter and for artworks, including Medieval illuminations. Its main chromophore is rottlerin, belonging to the molecular class of chalcones²⁹. Our colorant is described by Kremer as the red brown powder extract of *M. philippinensis* fruits, containing rottlerin, isorottlerin, homorottlerin and resin.

Neoflavone dyes

Dragon's blood

Red natural resin, historically employed in the Mediterranean basin as a dye and for medical purposes, dragon's blood was widely used for dyeing wool, gluing and decorating pottery, in alchemy and for magic rituals and ceremonies in India. This substance was also employed as a pigment in paint and for enhancing the color of precious stones and staining glass, marble and wood of 16th - 18th century Italian violins. The original source for this resin in ancient times was *Dracaena cinnabari* from the island of Socotra. By the Medieval and Renaissance periods, alternative genera were used, such as *Dracaena draco* (Canary Islands and Madeira), *Daemonorops* (Southeast Asia) and *Croton* (New and Old World tropical countries)^{30,31}. The chemical composition of dragon's blood changes according to the botanical sources: for instance, *D. draco* contains 50% of abietic acid besides the two chromophores, dracorhodin and dracorubin, while *D. cinnabari* is mainly composed of biflavonoids and dihydrochalcones such as cinnabarone, dracoresene and dracoresinotannol^{30,31}. In recent times, two different substances, called dracoflavylum and 7,4'-dihydroxyflavylum, were isolated and characterized from *D. draco* and *D. cinnabari*³². Most of the dragon's blood which is traded today is classified as *Daemonorops*. According to the supplier, Kremer, our colorant was extracted from that genus as well, but chemical analyses showed, as reported below, that it is most probably a mixture of resins from plants of the *Dracaena* genus.

Catechu

Extracted from *Acacia catechu* and related species indigenous to India, catechu was introduced into Germany around 1800 especially for dyeing cotton and printing calicos, and came into general use in Great Britain and America during the 1830s. Depending on the mordant, it produces different color hues from yellow-brown to brownish-black with acceptable fastness³³. Its main chromophore is the flavanol catechin, which, according to Kremer, is the only constituent of our colorant.

Biflavonoid dyes

Sandalwood

Representative of insoluble redwood dyes, sandalwood is extracted from *Pterocarpus santalinus* and related species, typical of tropical Asia. The dyes that are obtained from their woods have been widely used since antiquity especially in India for dyeing textiles, mostly with a mordant and in combination with other pigments in order to provide dark red and brown colors, while in Europe they are known from the middle of the 16th century²⁶. Their main coloring agents, santalins, belong to the molecular class of condensed biflavonoids¹⁶. Our colorant is described by Kremer as an extract obtained from *P. santalinus*, composed of a mixture of santalins A, B and C.

Neoflavonoid dyes

Brazilwood

Soluble redwood colorants are obtained from various species of the genus *Caesalpinia*, native of Brazil, Nicaragua and Southeast Asia and imported into Europe in the 13th century^{15,16}. In particular, brazilwood, which can be extracted from *C. brasiliensis*, was employed to dye silk and wool and for manufacturing red inks^{18,34}, and it is due to its abundance on the Brazilian coasts that this country is so called^{16,34,35}. Although more economical than carmine, this dye appears to have been applied less frequently in paintings probably because it has a less satisfactory hue and poor color permanence¹⁸. The major coloring compound of colorants obtained from *Caesalpinia* species is brazilein, which is formed by oxidation of its precursor, brazilin, upon exposure to air and light.

Logwood

Another example of soluble redwoods, logwood is obtained from *Haematoxylon campechianum*, native to Central America, and has been known in Europe since the 18th century³⁶. Although the dye itself is red, it produces a wide range of colors when used with different mordants. These include black with copper, iron or chromium, gray with iron, blue and purple with alum and tin mordants, all displaying good fastness properties¹⁶. The compound responsible for the dyeing properties of logwood is hematein, which is originated by oxidation of hematoxylin, present in the fresh wood, upon exposure to air.

Naphthoquinone dyes

Alkanet

The root of *Alkanna tinctoria*, found in Southeast Europe and Asia Minor, yields a red dye called alkanet, known from ancient times¹⁵. Mentioned by the Greek historian Theophrastus (4th - 3rd century B.C.) and by Pliny, who describes the blood-red dyestuff obtainable from its roots, this colorant has been used to dye textile fibers, food products and cosmetics¹⁹. The main coloring component of alkanna is the naphthoquinone alkannin. Our colorant was purchased from Zecchi as cut pieces of *Alkanna* roots.

Henna

Henna is a red-orange colorant which can be obtained from the leaves of *Lawsonia alba*, also known as *Lawsonia inermis*¹⁵. Historically used for the coloring of hair and body, it could have been employed as a textile dye as well¹⁹. Henna owes its color to the compound lawsone, belonging to the molecular class of naphthoquinones.

Walnut

The *Juglans* genus comprises several species and it is widely distributed throughout the world. The common walnut, or *Juglans regia*, is its best-known member, representing an important species of deciduous trees found primarily in the temperate areas and commercially cultivated in the United States, Western South America, Asia, Central and Southern Europe³⁷. Besides the intensive use of leaves and bark in traditional medicine, walnut husks were chopped and employed for producing inks and brown colorants for textile dyeing¹⁹. The main chromophore of walnut is reported to be juglone, the naphthoquinone structure of which is closely related to that of lawsone. Our raw material was purchased from Kremer in the form of walnut hulls from *Nucum juglandis*.

Carotenoid dyes

Annatto

Extracted from the seeds of *Bixa orellana*, typical of Central America, annatto was employed by Mayas and Aztecs in Mexico and Incas in Peru; it was introduced into Europe in the 16th century but never became commercially important, essentially because of its low light fastness. The main chromophore of this colorant is a carotenoid called bixin, which was used in ancient times as a direct dye for cotton, silk and wool¹⁶. Annatto was purchased from Kremer in the form of *B. orellana* seeds.

Saffron

Obtained from the stigmas of the flowers of *Crocus sativus*, when used as a direct dye saffron gives a beautiful orange-yellow color, but it can also be employed in association with alum mordants. In the long run, it is an unstable coloring agent, as the imparted vibrant hue quickly fades to a pale and creamy yellow. Known from antiquity, evidence of its use dates back to Egyptian times, and it was very popular in Persia in classical times as well. Despite its high cost, saffron has been employed as a textile dye, particularly in China and India. Clothing dyed with saffron was traditionally reserved for the noble classes, implying that this colorant played a

ritualized and status-keying role. It was later replaced by cheaper dyes like weld, with better fastness properties¹⁶. Saffron's bitter taste and spicy fragrance result from the chemicals picrocrocin and safranal. *Cis*- and *trans*-crocins, glucosides of crocetin belonging to the molecular class of carotenoid, are responsible for the rich golden yellow hue imparted to dishes and textiles.

Curcuminoid dyes

Turmeric

Natural colorant with poor fastness to light, turmeric is obtained from the ground roots of *Curcuma longa*, native to India and Southeast Asia, and enjoyed an extensive use as a direct dye for cotton, wool and silk, mainly in combination with other colorants¹⁶. Known in Mesopotamia and employed by ancient Greeks and Romans, this dye was imported into Europe in 1612, where it became a popular colorant for silk scarves. It has also been used for a long period of time as medicine and food additive in Asian countries³⁸. The coloring matter in turmeric is the hydroxyketone curcumin.

Xanthone dyes

Gamboge

Yellow gum resin which can be obtained from the bark of *Garcinia Hanburyi* and related species typical of Southeast Asia, gamboge was imported into England in the 17th century. It is composed by a resin which is acetone-soluble, while the remaining part that is water-soluble was widely used in paintings. Its main chromophore, called gambogic acid, can be easily isolated as a pyridinium salt¹⁵.

Indigoid dyes

Indigo

Indigotin is the main chromophore of indigo, one of the earliest and most popular dyestuffs known to man. Employed since 2000 B.C. in Egypt, it is one of the most stable organic colorants, which also explains its wide use in oil paintings by some of the greatest masters of the 17th and 18th centuries, such as Rubens³⁹. Two were the main natural sources for indigotin: besides indigo from *Indigofera tinctoria*, native of tropical Asia, *Isatis tinctoria* was also available in Southern and Central Europe, North Africa and West Asia, from which woad can be extracted¹⁶. In the Middle Ages woad was extensively cultivated in Europe and, at the same time, small amounts of indigo from *Indigofera* were imported from India. Over the years, the overland trade of indigo acquired increasing importance, until the successful circumnavigation of the Cape of Good Hope by Vasco de Gama in 1498, which opened a new trade route resulting in indigo becoming one of the major commodities imported¹⁶. Natural indigotin was displaced by the synthetic pigment first prepared by Von Baeyer in 1878³⁶. Our dye was purchased from Zecchi as a powdered extract from *Indigofera tinctoria*.

Experimental

Chemicals

Indigo, cochineal, lac dye, madder lake, dragon's blood, brazilwood, logwood, sandalwood, alkanet, saffron, safflower, turmeric, old fustic, weld and gamboge were purchased from Zecchi (Florence, Italy), walnut, henna, annatto, stil de grain lake, dyer's broom, catechu, kamala, aloe and sap green from Kremer (Aichstetten, Germany), while hexane, silver nitrate, sodium perchlorate monohydrate, trifluoroacetic acid, *N,O*-bis(trimethylsilyl)trifluoroacetamide (BSTFA) with 1% trimethylchlorosilane (TMCS), alizarin, purpurin and luteolin from Fluka. Methanol, trisodium citrate dihydrate, acetonitrile, ethyl acetate, potassium hydroxide, catechin, apigenin, quercetin and morin were obtained from Sigma-Aldrich, while hydrochloric acid from Riedel-de Haën. All the aqueous solutions were prepared using ultrapure water (Millipore MilliQ).

Analytical methods: extraction procedures, Ag colloid synthesis and sample preparation

Most of the colorants here studied were commercially purchased as a powder of the dye itself. However, when the colorant as such was not available, the setup of suitable extraction procedures was optimized; in detail, for madder and stil de grain lakes the organic chromophores had to be isolated from their inorganic support, while in the case of walnut, alkanet, annatto, safflower yellow and red, weld and dyer's broom the dyes had to be extracted from their vegetable sources (hulls, roots, seeds, petals, woods, etc.).

Madder and stil de grain lakes - Madder and stil de grain were purchased as aluminated lakes. In order to isolate the organic dyes from their inorganic support, in both cases 2 mL of a 10% aqueous solution of HCl were added to a few milligrams of the dye and heated at 70°C for 5 minutes. The mixture was extracted by 2 mL of hexane, which was then drawn off from the aqueous phase with a Pasteur pipette and dried under a gentle N₂ stream⁴⁰.

Walnut - A vial containing small pieces of walnut hulls together with 8 mL of ethyl acetate was heated at 70°C for 50 minutes; the resulting solution was filtered and dried under a gentle stream of N₂⁴¹.

Alkanet - Alkanet roots were extracted with *n*-hexane in an ultrasonic bath at room temperature; sonication was repeated with 10 mL aliquots of solvent for 30 minutes, until the resulting solution appeared to be colorless. The combined extracts were filtered and evaporated under a gentle stream of N₂⁴².

Annatto - Annatto seeds were placed into a vial with 8 mL of a 4% KOH aqueous solution; the suspension was kept at room temperature for 15 minutes, then heated at 60°C for 15 minutes, filtered and finally dried under vacuum⁴³.

Safflower - The yellow dye was extracted from the petals of the plant in water at room temperature for one night, then filtered and evaporated in a drying oven at 60°C⁴⁴. The red colorant, carthamin, was subsequently obtained by soaking the petals in a sodium carbonate solution at pH=10-11. This solution was filtered on a piece of filter paper, which then released the red dye upon immersion in methanol; the pigment was finally dried under a gentle stream of N₂⁴⁵.

Weld and dyer's broom - In both cases, the vegetable material was treated with 6 mL of MeOH and 200 μL of 37% HCl at 65°C for 60 minutes; the obtained solution was filtered and dried under a gentle stream of N_2 ⁴⁶.

Ag colloids were prepared according to the Lee-Meisel procedure⁴⁷, by reduction of silver nitrate with trisodium citrate dihydrate. All glassware was washed beforehand with diluted HNO_3 , deionized and ultrapure MilliQ water in an ultrasonic bath and accurately dried. 18 mg of AgNO_3 were then suspended in 100 mL of deionized water previously degassed under a gentle N_2 stream, and heated to boiling before 2 mL of a 1% solution of trisodium citrate were slowly dropped under vigorous magnetic stirring; the solution was held at boiling point for 60 minutes with continuous stirring. The resulting colloid could be kept in the refrigerator in the dark, wrapping the flask in an aluminium foil, and was characterized by determining the wavelength of the absorption maximum in the visible region on a Jasco UV/VIS/NIR V-570 spectrophotometer. All the Lee-Meisel colloids prepared had an absorption maximum between 425 and 435 nm⁴⁸.

Solutions of commercial colorants were prepared daily at a concentration of 10^{-4} M, in methanol or water according to the solubility properties of each dye. Whenever necessary, solutions were filtered through a 0.45 μm GHP Acrodisc membrane filter. The metallic colloid was activated by inducing a partial aggregation of the nanoparticles: for this purpose, 1.8 M NaClO_4 was added to the colloid after the analyte. The SERS spectra reported in this chapter were all collected by adding in a test tube 300 μL of the analyte solution to 3 mL of Ag Lee-Meisel colloid, with subsequent addition of 125 μL of 1.8 M NaClO_4 under magnetic stirring. SERS measurements were performed by focusing the laser beam on a drop of the dye-colloid system deposited on the surface of a glass slide.

Instrumentation

SERS spectra were collected with a portable micro-Raman spectrometer, equipped with a 1800 lines/mm grating, a notch filter, an Olympus 50x microscope objective and a Peltier-cooled charge-coupled device (CCD) detector, by using a back-scattering geometry. A Nd:YAG laser provided the exciting radiation at 532 nm, with a power at the sample of about 1.5 mW. All the SERS spectra were recorded between 2000 and 200 cm^{-1} by collecting 30 scans with an exposure time of 4 s. A resolution around 8 cm^{-1} was estimated in the examined spectral range.

FT-Raman spectra were recorded in the macro-sampling mode between 4000 and 200 cm^{-1} with an RFT-600 Jasco spectrometer, using the 1064 nm emission of a Nd:YAG laser as excitation wavelength and collecting different numbers of scans depending on each dye. The output laser power was kept between 30 and 150 mW, and optimized for each sample in order to obtain the highest intensity of the Raman signals.

Micro-FTIR spectroscopy was used to identify xanthorhamnin previously isolated from sap green by collecting the compound corresponding to the most intense HPLC peak. The residue obtained by evaporation of the solvent was placed in a diamond cell and the spectrum was acquired between 4000 and 600 cm^{-1} using an IRT-3000 Jasco spectrometer with 4 cm^{-1} resolution, as the average of 64 accumulations.

HPLC analyses were performed with an HPLC PU-1580 Jasco pump, equipped with an LG-1580-02 Jasco gradient valve and a GASTORR GT-103 solvent degasser, by using an MD 1510 Jasco photodiode array (PDA) detector in order to obtain spectral information between 200 and 600 nm. A 25 μ L injection volume of a methanolic solution of the analyte was used for the analysis, which was executed on a Supelco Discovery C18 column (25 cm x 4.66 mm, particle diameter 5 μ m), with (A) ultrapure water and (B) acetonitrile both with 0.1% of trifluoroacetic acid as solvents, setting the flow rate at 1 mL/min. The solvent gradient was as follows: 95-70% A in 0-25 min, 70-40% A in 25-30 min, 40-5% A in 30-38 min, 5-95% A in 38-65 min.

GC-MS was used to identify rhamnazin previously isolated from stil de grain extract, by collecting the compound corresponding to the most intense HPLC peak. The analysis was carried out with a Shimadzu GC-MS system consisting of a QP 5050 gas chromatograph coupled with a quadrupole mass spectrometer using electron impact ionization (acceleration voltage 1.5 kV). Chromatographic separation was performed on an Equity-5 Supelco column (length 30 m, internal diameter 0.25 mm, film thickness 0.25 μ m), using poly(5%diphenyl/95%dimethyl)syloxane as stationary phase and He as carrier gas (flow rate 0.7 mL/min, surge pressure 27.7 kPa). The ion source and interface temperature was 280°C, while the scan range was m/z 40-800. The chromatographic heating gradient was as follows: initial temperature 57°C, 2 min isothermal, then ramped at 10°C/min up to 200°C, 3 min isothermal, then ramped at 20°C/min up to 300°C and then isothermal for 20 min. Prior to the analysis, a total of 230 μ g of each sample was submitted to derivatization in 20 μ L of BSTFA + 1% TMCS and 50 μ L of ethyl acetate, heating at 70°C for 30 minutes. The injection volume was 1 μ L.

Results and discussion

In this section, the SERS spectra acquired from several natural organic colorants and pure chromophores are reported, and the so obtained spectral patterns are discussed in connection with those of the other dyes belonging to the same molecular class. The observed wavenumbers are both displayed in the spectra to help in inspection and listed in tables along with the corresponding relative intensities, as follows:

[vs = very strong; s = strong; m = medium; w = weak; vw = very weak; sh = shoulder]

All the SERS spectra reported in this chapter were obtained on Ag nanoparticles synthesized according to the Lee-Meisel procedure and aggregated by the use of 1.8 M NaClO₄; this particular electrolyte, indeed, was found to give better results in comparison with other aggregating agents, such as NaCl, HCl, HNO₃ and KNO₃, that have been tested. In most cases, the use of sodium perchlorate does not lead to different spectral profiles with regard to the dyes here investigated, but it has proven to be extremely efficient, as it allows to observe significantly higher enhancement factors for all the examined colorants and to obtain a SERS spectrum even for those dyes that showed a strong fluorescence when analyzed by using other kinds of electrolytes.

Anthraquinone dyes

The SERS spectra of anthraquinone dyes are reported in figure 1, with all the corresponding wavenumbers listed in table 2, while the main chromophores of these colorants are shown in figure 2.

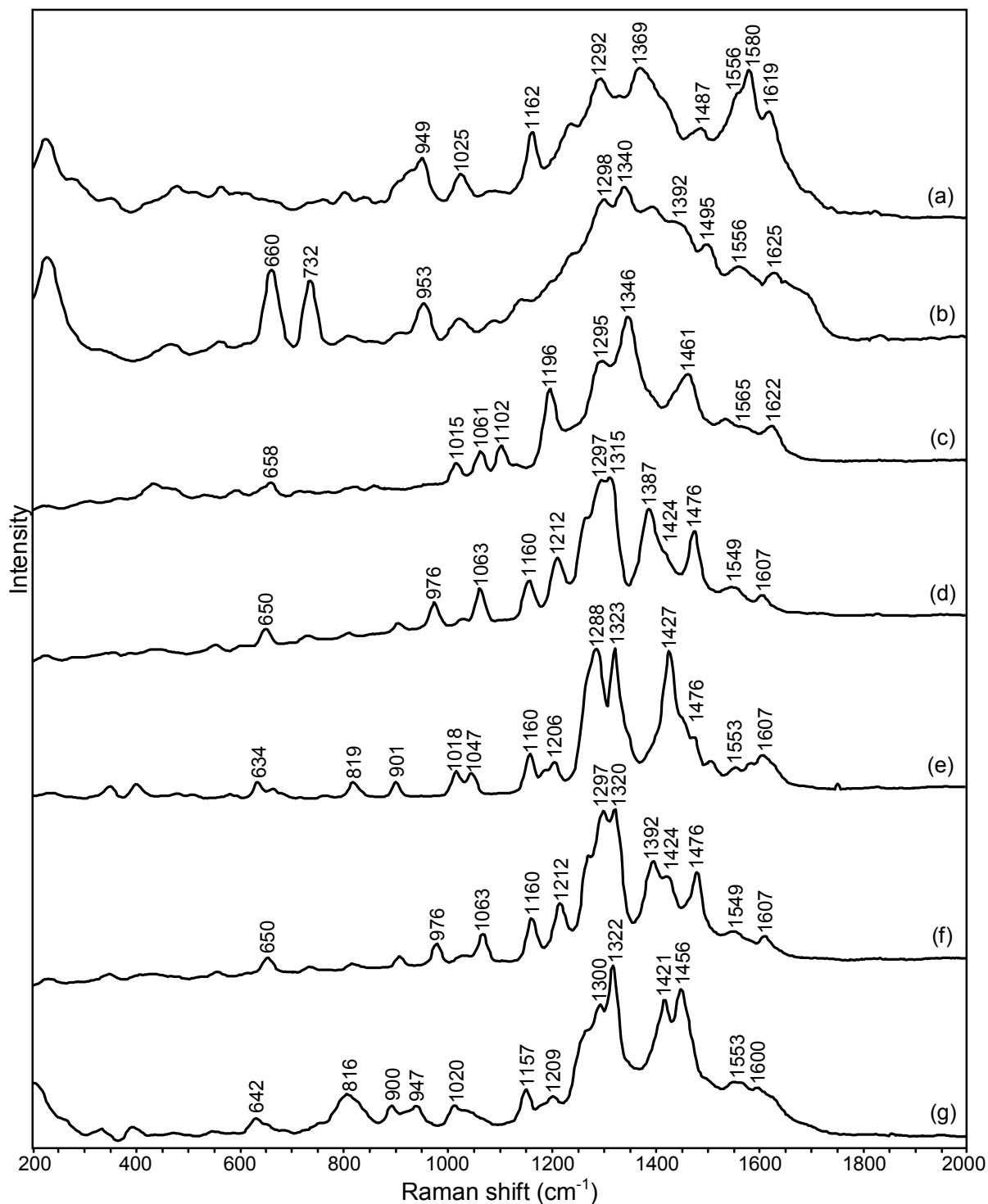
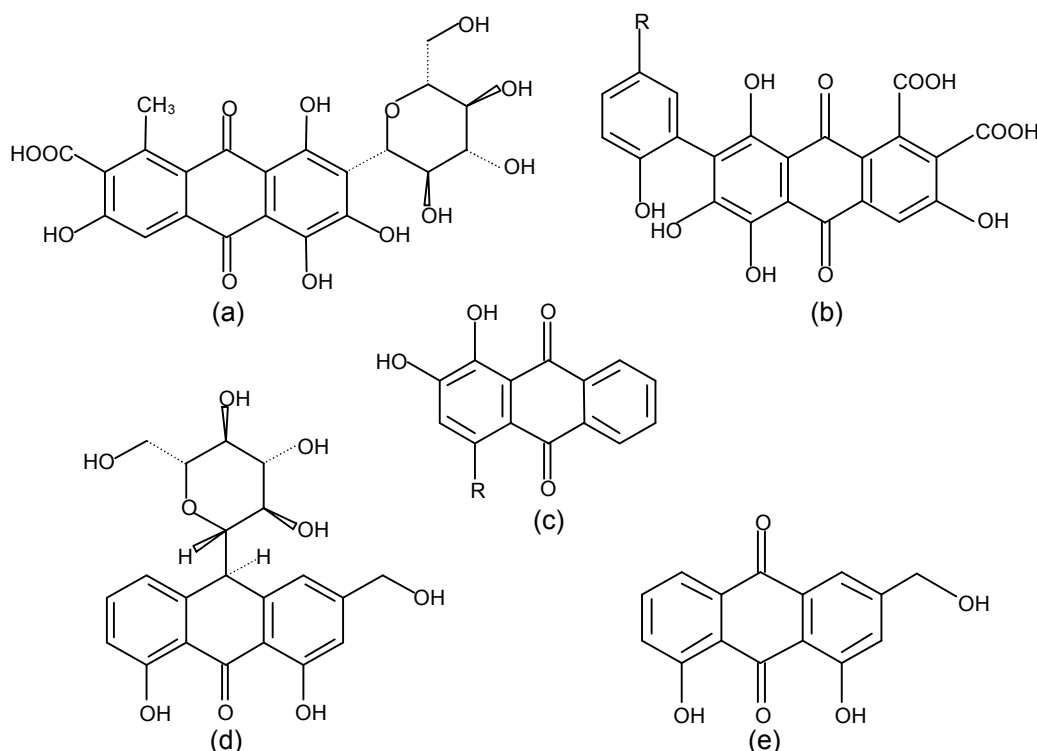


Figure 1. SERS spectra of anthraquinone dyes: (a) aloë, (b) cochineal, (c) lac dye, (d) purpurin, (e) alizarin, (f) madder upon extraction and (g) madder lake as such.

Table 2. Frequencies of SERS spectra of anthraquinone dyes with relative intensities.

| Anthraquinone dyes | SERS bands (cm ⁻¹) |
|--------------------------------------|---|
| Aloe Fig. 1 - Spectrum (a) | 1619s, 1580vs, 1556sh, 1487m, 1420sh, 1369vs, 1329s, 1292vs, 1236sh, 1162m, 1086vw, 1025w, 949m, 838vw, 801vw, 759vw, 561w, 476w, 352vw, 274sh, 224m |
| Cochineal Fig. 1 - Spectrum (b) | 1689sh, 1625m, 1556m, 1495s, 1431sh, 1392vs, 1340vs, 1298vs, 1237sh, 1194sh, 1140sh, 1088vw, 1020vw, 953w, 910vw, 806vw, 732m, 660m, 560vw, 469vw, 226s |
| Lac dye Fig. 1 - Spectrum (c) | 1622m, 1565sh, 1533m, 1461s, 1346vs, 1295s, 1196s, 1132vw, 1102m, 1061m, 1015m, 658w, 591vw, 471sh, 431w |
| Purpurin Fig. 1 - Spectrum (d) | 1607w, 1549w, 1476s, 1424sh, 1387s, 1315vs, 1297vs, 1267sh, 1212m, 1160m, 1063m, 1030vw, 976m, 906vw, 812vw, 732vw, 650w, 554vw, 429vw, 345vw, 227vw |
| Alizarin Fig. 1 - Spectrum (e) | 1607m, 1582w, 1553w, 1509w, 1476sh, 1453sh, 1427vs, 1323vs, 1288vs, 1206w, 1187sh, 1160m, 1047w, 1018w, 901w, 819w, 662vw, 634w, 402w, 348w, 236vw |
| Madder Fig. 1 - Spectrum (f) | 1607w, 1549w, 1476s, 1424sh, 1392s, 1320vs, 1297vs, 1267sh, 1212m, 1160m, 1063m, 1030vw, 976m, 906vw, 814vw, 732vw, 650w, 554vw, 429vw, 345vw, 227vw |
| Madder lake Fig. 1 - Spectrum (g) | 1600w, 1570w, 1553w, 1456s, 1421s, 1322vs, 1300s, 1273sh, 1209w, 1157m, 1041sh, 1020w, 947w, 900w, 816m, 642w, 557vw, 483vw, 405w, 345vw, 218m |

**Figure 2.** Anthraquinone dyes: (a) carminic acid, the main chromophore of cochineal; (b) laccaic acid A if R=CH₂CH₂NHCOCH₃ and laccaic acid B if R=CH₂CH₂OH, the main chromophores of lac dye; (c) alizarin if R=H and purpurin if R=OH, the main chromophores of madder; (d) aloin and (e) aloemodin, the main chromophores of aloe.

Colorants with chromophores having an anthraquinone structure exhibit rather similar SERS spectra. In particular, in the present experimental conditions, the following signals can be observed in all cases: a weak band around 1620 cm⁻¹, assigned to the stretching mode of the C-C bonds in the rings and of the C=O group

interacting with the Ag nanoparticles; a weak band around 1550 cm^{-1} , which can be attributed again to a ring C-C stretching mode; a medium band at about $1460\text{-}1470\text{ cm}^{-1}$, assigned to ring C-C stretching modes and to C-OH bending modes; a medium/strong band at a wavenumber ranging from $1390\text{ to }1420\text{ cm}^{-1}$ with a similar assignment; a strong band at $1290\text{-}1295\text{ cm}^{-1}$, assigned to C-OH bending modes^{11,12,49}.

Besides these lines that are common to all the examined dyes, some signals are characteristic of some of them. In detail: purpurin, alizarin and madder show additional bands of medium/weak intensity at 1212 and 1160 cm^{-1} and a strong band at $1315\text{-}1320\text{ cm}^{-1}$; cochineal and lac dye exhibit a strong signal at about 1340 cm^{-1} , assigned to the C-OH bending mode of carboxylic groups that are obviously present in the molecular structure of carminic and laccaic acids^{11,12}; cochineal gives rise to two rather intense bands at 732 and 660 cm^{-1} , the first of which is also reported in the literature¹¹ with medium intensity, irrespective of the pH value, and assigned to the rocking mode of the methyl group characterizing the structure of carminic acid and to the out-of-plane bending modes of C-H and C-OH bonds. It is interesting to notice that also the band at 953 cm^{-1} was here detected with medium intensity and is assigned as well in the above-cited reference to CH_3 rocking mode and to CCC bending mode. As far as the band at 660 cm^{-1} is considered, it is also reported in reference 11 for pH values from 6 to 9, but it was not assigned being rather weak, at variance with that observed in the present study but not unexpectedly due to different experimental conditions.

The SERS spectrum of madder lake as such was also acquired and compared with the spectrum of the corresponding extract. As shown in figure 1, while the latter is dominated by signals due to purpurin, the former has a closer similarity to the spectrum of alizarin, even though with different intensity ratios for some bands. Other authors have also reported SERS spectra of madder lake⁵⁰ or of alizarin/purpurin mixtures in the presence of Al^{3+} ⁵¹ substantially dominated by signals due to alizarin, a fact that is attributed to the higher detection limit that can be reached by SERS for purpurin. Nevertheless, it was demonstrated that, using the excitation wavelength of 514.5 nm - therefore not too different from the one adopted in this work - and acquiring the SERS spectrum at $\text{pH}=8$ - again a value similar to that measured for our colloid - detection limits comparable to or even better than those reached for alizarin could be obtained for purpurin by exploiting resonance conditions⁵². Indeed, in the experiment here conducted, the extract obtained from madder lake, which contains both chromophores as demonstrated by HPLC, gives a SERS spectrum that closely resembles that of purpurin. Therefore, it can be hypothesized, instead, that resonance conditions change upon Al^{3+} complexation, thus favoring alizarin over purpurin. Moreover, the SERS spectrum obtained for madder lake shows an increased intensity for those bands that are assigned to the monoanionic form of alizarin absorbed on the metal surface, in particular the band at 1456 cm^{-1} , while the SERS spectrum of free alizarin shows the pattern expected for the dianionic form, with the greatest intensity for the band at 1427 cm^{-1} ⁴⁹, different from that reported in the literature for madder lake analyzed without extraction directly on textile fibers⁵⁰ but in a similar way to that observed in solution for alizarin in the presence of Al^{3+} ⁵¹.

Among the colorants here investigated, the SERS spectrum of aloe is reported for the first time. This spectrum shares the features already described above, but is characterized by an additional very strong band at 1580 cm^{-1} , which is typical of the structure of 1,8-dihydroxy-9-anthrone⁵³ that can be recognized in the molecules of aloin and aloe emodin.

Flavonol dyes

The SERS spectra of flavonol dyes are reported in figure 3, with all the corresponding wavenumbers listed in table 3, while the main chromophores of these colorants are shown in figure 4.

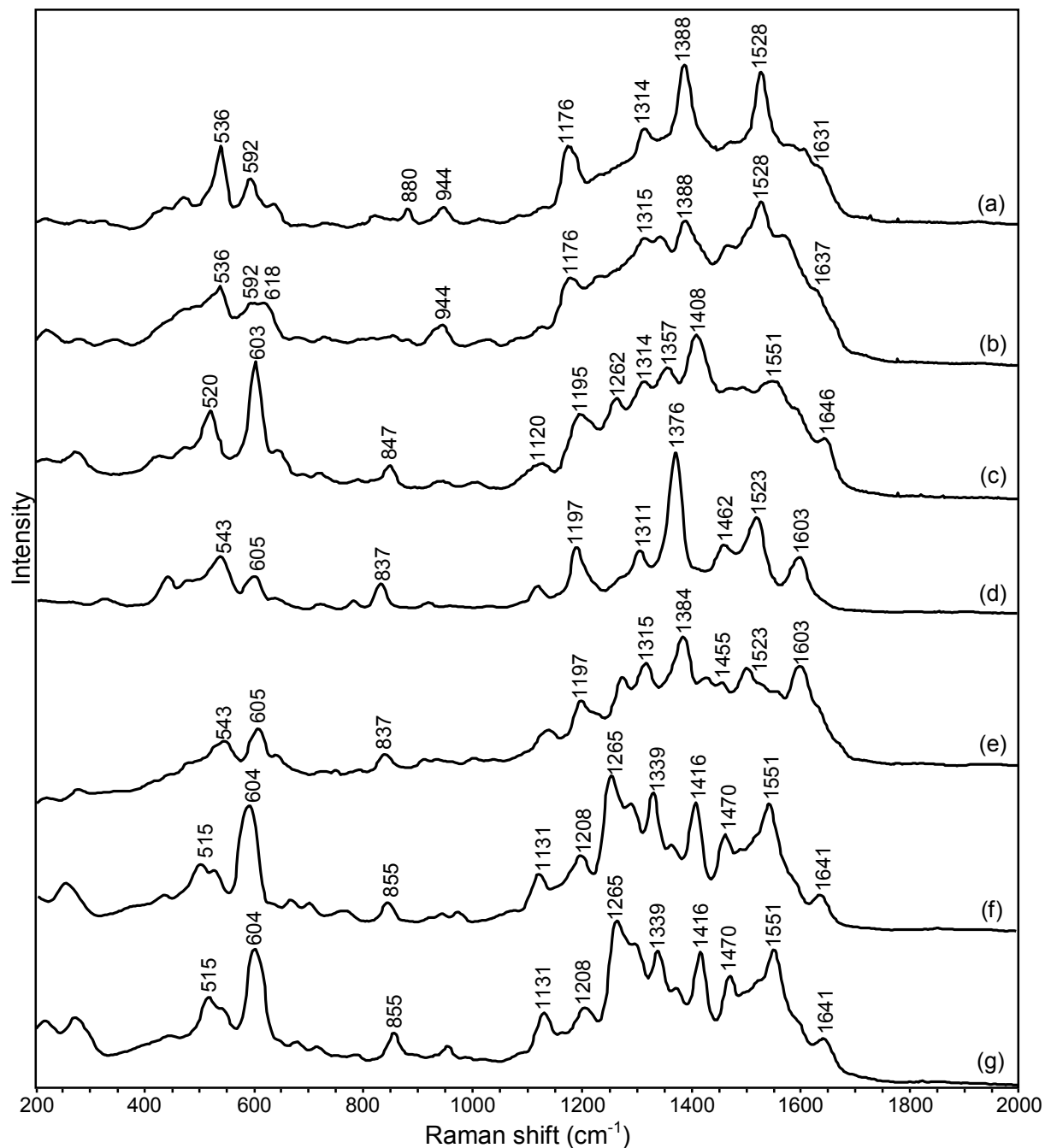


Figure 3. SERS spectra of flavonol dyes: (a) morin, (b) old fustic, (c) quercetin, (d) rhamnazin, (e) stil de grain, (f) xanthorhamnin and (g) sap green.

Table 3. Frequencies of SERS spectra of flavonol dyes with relative intensities.

| Flavonol dyes | SERS bands (cm ⁻¹) |
|--|---|
| Morin Fig. 3 - Spectrum (a) | 1631sh, 1607sh, 1582sh, 1528vs, 1470w, 1388vs, 1314s, 1176s, 1128vw, 1085vw, 1011vw, 944w, 880w, 820w, 728vw, 686vw, 633w, 592m, 536s, 465w, 434sh, 321vw, 278vw, 219vw |
| Old fustic Fig. 3 - Spectrum (b) | 1637sh, 1567sh, 1528vs, 1470w, 1388s, 1343m, 1315m, 1176m, 1128vw, 1085vw, 1029vw, 944w, 880vw, 728vw, 686vw, 618m, 592m, 536m, 465sh, 434sh, 342vw, 278vw, 219vw |
| Quercetin Fig. 3 - Spectrum (c) | 1646sh, 1590sh, 1551m, 1496w, 1472w, 1408vs, 1357m, 1314m, 1262m, 1195m, 1120w, 1005vw, 945vw, 847w, 717vw, 684vw, 643w, 603vs, 520m, 475w, 426w, 271w, 215vw |
| Rhamnazin Fig. 3 - Spectrum (d) | 1603m, 1523s, 1462m, 1376vs, 1311m, 1275sh, 1197m, 1122w, 958vw, 922vw, 837w, 784vw, 724vw, 640sh, 605w, 543m, 498w, 481w, 443w, 328vw, 270 vw |
| Stil de grain Fig. 3 - Spectrum (e) | 1603s, 1557sh, 1523sh, 1502s, 1455m, 1427m, 1384vs, 1315s, 1272s, 1197m, 1138m, 998vw, 909vw, 837w, 788vw, 717vw, 638sh, 605m, 543m, 275vw, 215vw |
| Xanthorhamnin Fig. 3 - Spectrum (f) | 1641w, 1596sh, 1551s, 1523sh, 1498sh, 1470m, 1416s, 1372w, 1339s, 1298sh, 1265vs, 1208m, 1131m, 955w, 855m, 789vw, 715vw, 678vw, 604s, 541sh, 515m, 448w, 271m, 217m |
| Sap green Fig. 3 - Spectrum (g) | 1641w, 1596sh, 1551s, 1523sh, 1498sh, 1470m, 1416s, 1372w, 1339s, 1298sh, 1265vs, 1208m, 1131m, 953w, 855m, 789vw, 715vw, 678vw, 602s, 541sh, 515m, 447w, 271m, 217m |

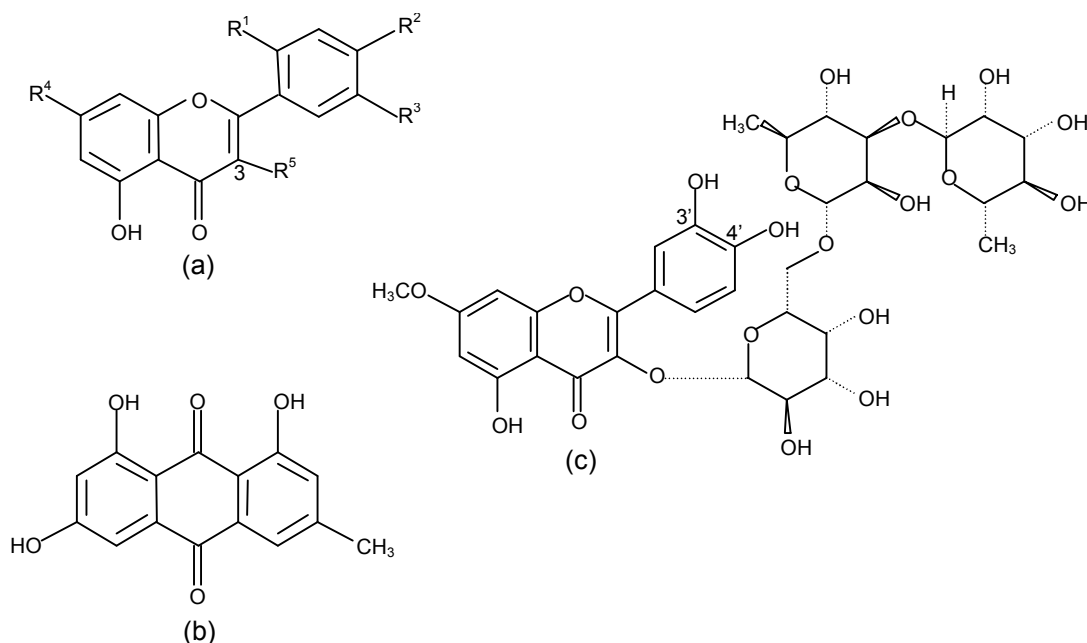


Figure 4. Flavonol dyes: (a) morin if R¹=R²=R⁴=R⁵=OH and R³=H, the main chromophore of old fustic; (a) rhamnetin if R¹=H, R²=R³=R⁵=OH and R⁴=OCH₃, rhamnazin if R¹=H, R²=R⁵=OH and R³=R⁴=OCH₃, quercetin if R¹=H and R²=R³=R⁴=R⁵=OH, kaempferol if R¹=R³=H and R²=R⁴=R⁵=OH, and (b) the anthraquinone emodin, the main chromophores of stil de grain lake; (c) xanthorhamnin, (a) rhamnocitrin if R¹=R³=H, R²=R⁵=OH and R⁴=OCH₃, and (b) the anthraquinone emodin, the main chromophores of sap green.

The SERS spectrum obtained for fustic is remarkably similar to that of its main chromophore, morin, for which the SERS vibrational wavenumbers have been previously published⁶. The observed spectral pattern, in which the intense bands located at about 1388 and 1315 cm^{-1} are assigned to the 3-OH bending as well as to aromatic ring vibrations^{8,54}, allows us to suggest for this molecule a coordination with the 3-hydroxy-4-keto-group to the metal surface. The proposed coordination mode of morin with respect to the metal surface is supported by structural studies of metal complexes involving such molecule⁵⁵. Moreover, the band at 1637 cm^{-1} , assigned to the C=O stretching, shows a significant decrease in wavenumber in comparison with the same signal situated at 1668 cm^{-1} in the FT-Raman spectrum (figure 5; the corresponding wavenumbers with relative intensities are listed in table 4), due to the lowering of the bond order upon coordination to the metal nanoparticles.

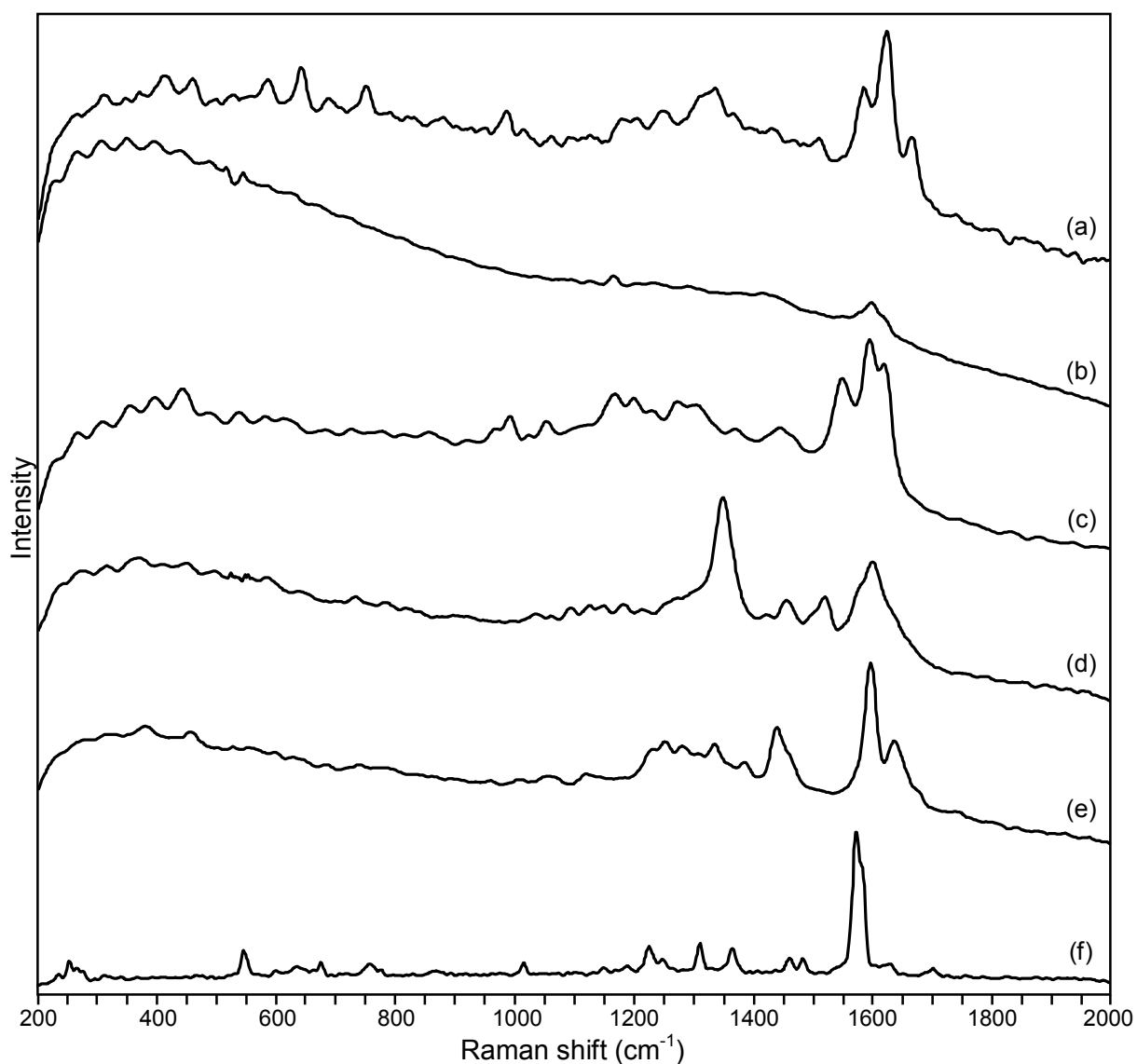


Figure 5. FT-Raman spectra of: (a) morin, (b) safflower, (c) kamala, (d) sandalwood, (e) gamboge and (f) indigo.

Table 4. Frequencies of FT-Raman spectra of morin, safflower, kamala, sandalwood, gamboge and indigo with relative intensities.

| Dyes | FT-Raman bands (cm ⁻¹) |
|-------------------------------------|---|
| Morin Fig. 5 - Spectrum (a) | 1668m, 1624vs, 1586s, 1511w, 1431w, 1367w, 1335m, 1311sh, 1247w, 1204w, 1178w, 1013vw, 986w, 750w, 686w, 642m, 585w, 459w, 411w |
| Safflower Fig. 5 - Spectrum (b) | 1621sh, 1600s, 1442sh, 1418w, 1312w, 1294w, 1234w, 1209w, 1170m |
| Kamala Fig. 5 - Spectrum (c) | 1621s, 1597vs, 1551m, 1496sh, 1448w, 1374vw, 1310w, 1276w, 1234vw, 1203w, 1172w, 1058w, 1028vw, 998w, 972sh |
| Sandalwood Fig. 5 - Spectrum (d) | 1600s, 1517m, 1455m, 1344vs, 1264sh, 1213vw, 1182vw, 1146vw, 1128vw, 1093vw, 1034vw |
| Gamboge Fig. 5 - Spectrum (e) | 1639s, 1597vs, 1439s, 1386w, 1335m, 1308w, 1281m, 1252m, 1231sh, 1120vw, 1058vw, 456vw, 380vw |
| Indigo Fig. 5 - Spectrum (f) | 1704vw, 1630vw, 1585sh, 1576vs, 1485w, 1463w, 1366w, 1312w, 1250vw, 1227w, 1190vw, 1151vw, 1017vw, 869vw, 779vw, 760vw, 678vw, 603vw, 547w, 279vw, 269vw, 256w, 238vw |

The SERS spectrum of quercetin shows a pattern that well corresponds to that reported in the literature for the same molecule on a citrate-reduced silver colloid with an excitation wavelength of 514.5 nm, i.e. experimental conditions similar to those employed in the present work⁵⁶. As shown by the literature data, if an excitation wavelength of 785 nm is used, a partly different spectrum is obtained^{6,56}. The observed spectral pattern is indeed similar to that of morin, and the most intense bands at 1408 and 1314 cm⁻¹, assigned to the 3-OH bending as well as to aromatic ring vibrations^{8,54}, allow us to suggest also for this molecule a coordination with the 3-hydroxy-4-keto- group to the metal surface. Moreover, as the signals at 1262 and 1120 cm⁻¹, attributed to the 3'- and 4'-OH in-plane bending^{8,57}, are only observed in the spectrum of quercetin, a second kind of coordination with the 3',4'-dihydroxyl group could be suggested for this latter molecule. Morin does not show such bands in the SERS spectrum, in accordance with the different structure of its dihydroxybenzenic ring. The proposed coordination modes of the examined molecules with respect to the metal surface are supported by structural studies of metal complexes involving flavonoids^{58,59}.

The SERS spectrum of stil de grain shows many bands that match well in wavenumbers with those observed for rhamnazin at 1603, 1523, 1315, 1197, 837, 605 and 543 cm⁻¹. Indeed, rhamnazin, together with the anthraquinone emodin, is the main chromophore detected by HPLC analysis in the examined dye. Other bands observed for the colorant are shifted in comparison with the spectrum of the flavonol, in particular from 1455 to 1462 cm⁻¹ and from 1384 to 1376 cm⁻¹. For rhamnazin, a coordination mode to silver particles analogous to that suggested for morin can be hypothesized on the basis of the close similarity of the corresponding SERS spectra. Finally, bands at 1427 and 1502 cm⁻¹ remain unassigned.

In contrast to madder lake, stil de grain lake without extraction did not give a SERS spectrum, probably due to the fact that the commercial product here examined also contained a significant amount of sodium sulfate as extender and was therefore considerably diluted.

The SERS spectrum of sap green corresponds perfectly with that of xanthorhamnin, the main chromophore of this dye according to HPLC-FTIR analysis (figure 6); this molecule could be identified by comparison with a reference FTIR spectrum from the IRUG (Infrared and Raman Users Group) database.

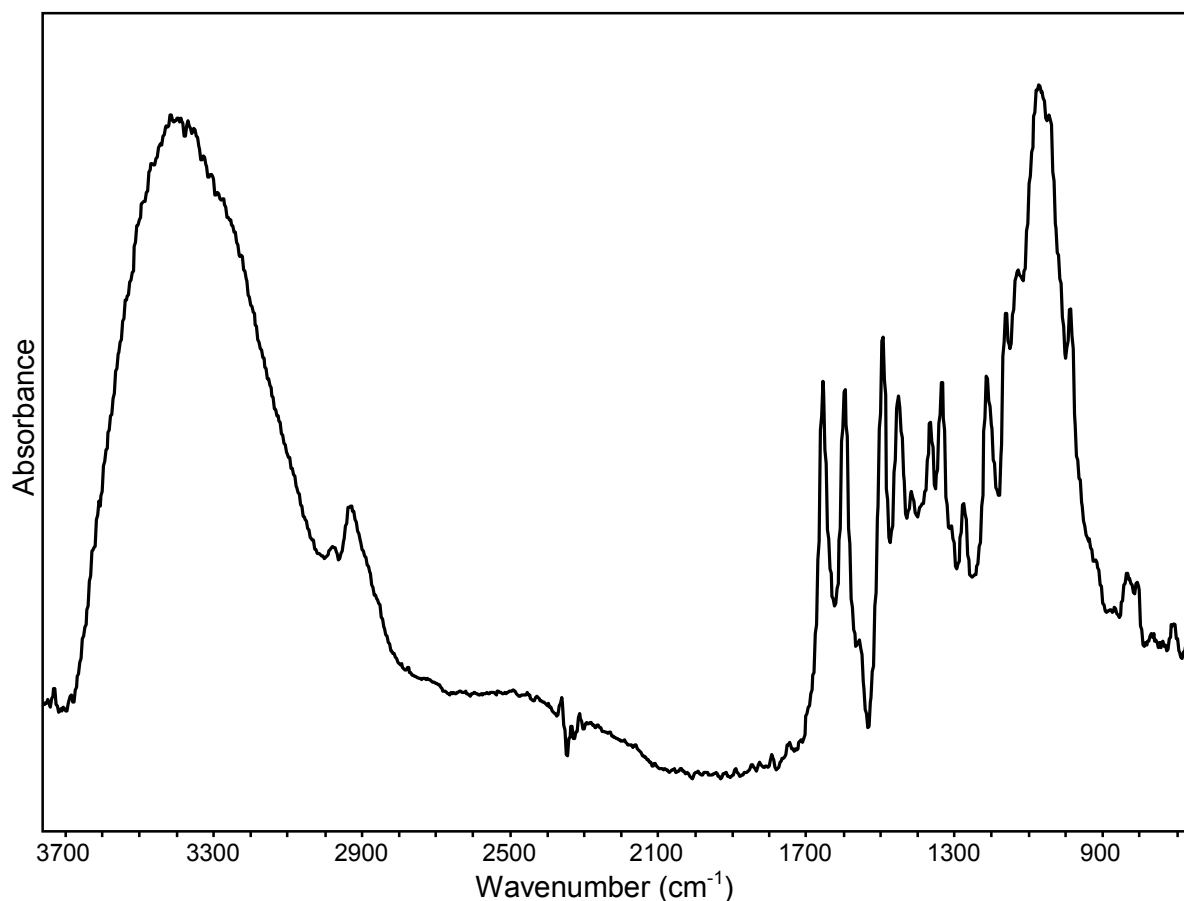


Figure 6. Micro-FTIR spectrum of xanthorhamnin, isolated from sap green by collecting the compound corresponding to the most intense peak in the HPLC chromatogram.

Some of the most prominent SERS bands of this molecule, at 1339, 1265, 1208, 1131 and 604 cm^{-1} , can be assigned according to literature data⁵⁷ to the in-plane bending modes of the 3'- and 4'-OH groups of the flavonol moiety, thus suggesting that the interaction of the molecule with the metal takes place through those groups. The remaining strong bands at 1551, 1470 and 1416 cm^{-1} are associated with vibrational modes of the aromatic ring, while the relatively high wavenumber of the C=O stretching mode at 1643 cm^{-1} allows us to rule out the involvement of the carbonyl group in the coordination to silver surface.

Flavone and chalcone dyes

The SERS spectra of flavone and chalcone dyes are reported in figure 7, with all the corresponding wavenumbers listed in table 5, while the main chromophores of these colorants are shown in figure 8.

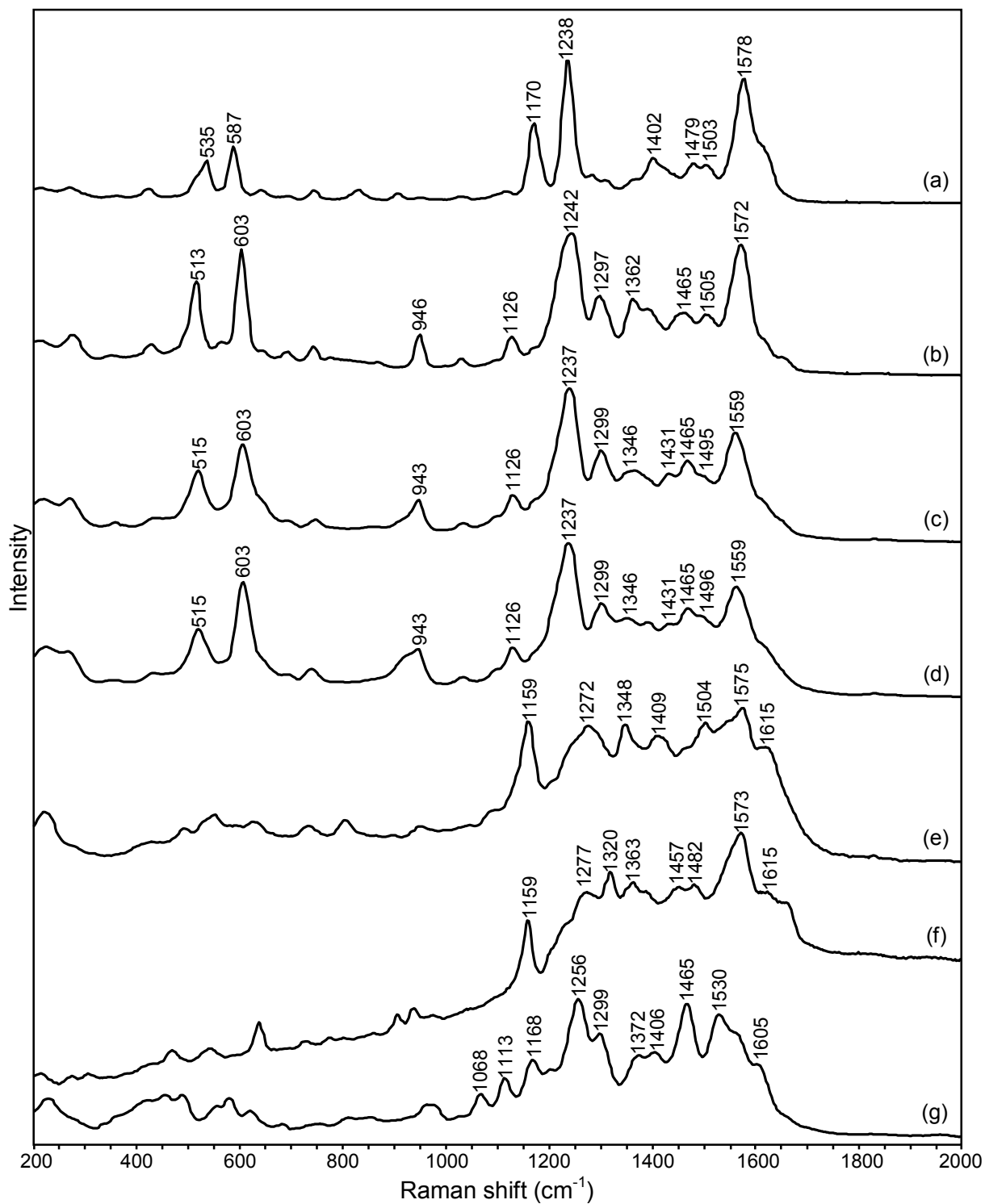
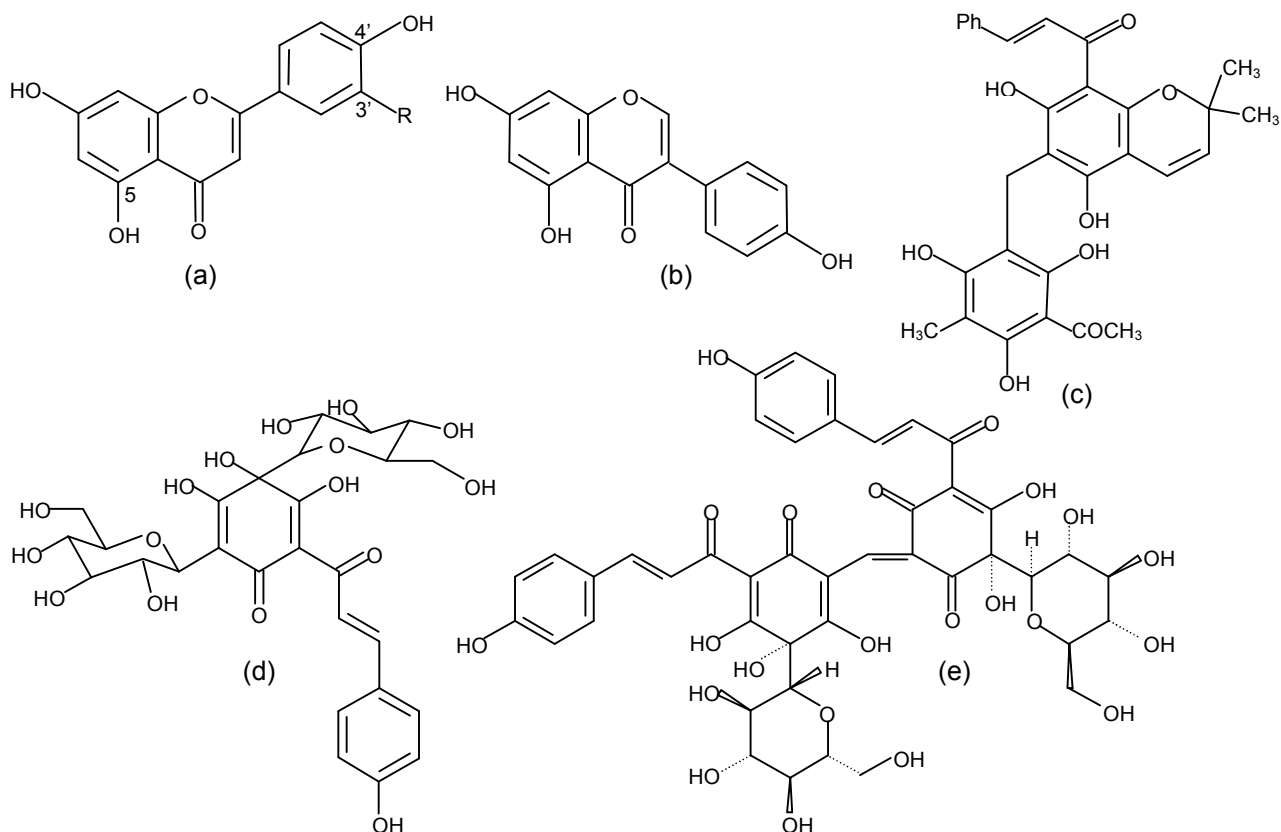


Figure 7. SERS spectra of flavone and chalcone dyes: (a) apigenin, (b) luteolin, (c) weld, (d) dyer's broom, (e) safflower yellow, (f) safflower red and (g) kamala.

Table 5. Frequencies of SERS spectra of flavone and chalcone dyes with relative intensities.

| Flavone and chalcone dyes | SERS bands (cm ⁻¹) |
|---|--|
| Apigenin Fig. 7 - Spectrum (a) | 1616sh, 1578vs, 1503w, 1479w, 1402w, 1362sh, 1310vw, 1285vw, 1238vs, 1170s, 1119vw, 1030vw, 950vw, 908vw, 832vw, 745vw, 693vw, 642vw, 587m, 536m, 517sh, 423vw, 363vw, 270vw, 214vw |
| Luteolin Fig. 7 - Spectrum (b) | 1651sh, 1615sh, 1572vs, 1505m, 1465m, 1448m, 1389m, 1362m, 1297m, 1242vs, 1174vw, 1126w, 1097vw, 1029vw, 948w, 772vw, 742vw, 692vw, 643vw, 602vs, 562vw, 513s, 426vw, 350vw, 273w, 212vw |
| Weld Fig. 7 - Spectrum (c) | 1651sh, 1615sh, 1559s, 1495sh, 1465m, 1431w, 1367w, 1346sh, 1299m, 1237vs, 1174sh, 1126w, 1097vw, 1029vw, 943w, 920sh, 742vw, 692vw, 643sh, 603s, 515m, 430vw, 356vw, 267w, 219w |
| Dyer's broom Fig. 7 - Spectrum (d) | 1651sh, 1615sh, 1559s, 1495sh, 1465m, 1431w, 1389w, 1346w, 1299m, 1237vs, 1174sh, 1126w, 1097vw, 1029vw, 943w, 920sh, 735vw, 692vw, 643sh, 603s, 515m, 430vw, 356vw, 267w, 219w |
| Safflower yellow Fig. 7 - Spectrum (e) | 1615sh, 1575vs, 1548sh, 1504vs, 1465sh, 1409s, 1348vs, 1272vs, 1206sh, 1159vs, 1092sh, 1048vw, 949vw, 803vw, 733vw, 625vw, 549w, 491vw, 425vw, 221w |
| Safflower red Fig. 7 - Spectrum (f) | 1658sh, 1615sh, 1573vs, 1482m, 1457m, 1389sh, 1363m, 1320s, 1277m, 1159m, 978vw, 938w, 907w, 860vw, 803vw, 775vw, 730vw, 640m, 546w, 473w, 311vw, 280vw |
| Kamala Fig. 7 - Spectrum (g) | 1605sh, 1565sh, 1530vs, 1465vs, 1406m, 1372m, 1299s, 1256vs, 1203w, 1168m, 1113m, 1068m, 975m, 963m, 851w, 809w, 752vw, 681vw, 620m, 578m, 555m, 488m, 456m, 420sh, 361sh, 228m |

**Figure 8.** Flavone and chalcone dyes: (a) luteolin if R=OH and apigenin if R=H, the main chromophores of weld; (b) luteolin if R=OH and (b) genistein, the main chromophores of dyer's broom; (c) rottlerin, the main chromophore of kamala; (d) hydroxysafflor yellow A, the main chromophore of safflower yellow; (e) carthamin, the main chromophore of safflower red.

First of all, a significant similarity was observed between the SERS spectra of weld and dyer's broom extracts and that of their main chromophore, luteolin, confirming the effectiveness of the well-known HCl:MeOH procedure^{46,60} which was applied in order to extract these two dyes from the corresponding plants.

Luteolin and apigenin presented comparable spectra, in accordance with the high resemblance of their molecular structures. The strong band around 1572 cm^{-1} , already attributed by density functional theory (DFT) calculations to the C=O stretching and 5-OH bending as well as to aromatic ring vibrations^{7,8}, indicates that such molecules are possibly attached to the metal surface by the C=O and the 5-OH groups. After all, this position is the unique chelation site for apigenin, while luteolin would be able to coordinate also with 3'- and 4'-OH: however, this latter possibility could be excluded as the signals corresponding to vibrational modes involving such groups are not very intense in the spectrum obtained for luteolin. This kind of coordination is also supported by spectrophotometric studies of metal complexes with luteolin and apigenin⁶¹.

As far as SERS spectra of safflower yellow, safflower red (carthamin) and kamala are considered, they show a rather similar pattern, probably due to a preferred interaction between the dye molecule and the metal surface through the 2-hydroxychalcone moiety of the molecule itself, i.e. the portion that allows chelation. In particular, the SERS spectra of all three colorants exhibit a band at about $1615\text{-}1605\text{ cm}^{-1}$, attributable to the C=O stretching mode and to the conjugated C=C bond, which is probably shifted upon coordination to lower wavenumbers when compared with normal FT-Raman spectra (figure 5; the corresponding wavenumbers with relative intensities are listed in table 4) where it is located at about 1620 cm^{-1} ^{62,63}. Moreover, in comparison with normal Raman spectra, the SERS spectra of the three dyes show a relative enhancement of bands due to ring vibrations, at 1575 and 1504 cm^{-1} for safflower yellow, at 1573 , 1482 and 1457 cm^{-1} for safflower red and at 1530 and 1465 cm^{-1} for kamala. Signals attributed to OH groups on the phenyl ring are also enhanced in the SERS spectra, as demonstrated in particular by bands at 1348 , 1272 and 1159 cm^{-1} for safflower yellow, at 1363 , 1320 , 1277 and 1159 cm^{-1} for safflower red and at 1372 , 1256 and 1168 cm^{-1} for kamala, assigned respectively to the stretching mode of the C-OH group in the ortho position to carbonyl⁶⁴ and possibly to the C-OH bending mode and the C-O stretching mode of hydroxyl groups on different ring positions.

Neoflavonoid, neoflavone and biflavonoid dyes

The SERS spectra of neoflavonoid, neoflavone and biflavonoid dyes are reported in figure 9, with all the corresponding wavenumbers listed in table 6, while the main chromophores of these colorants are shown in figure 10.

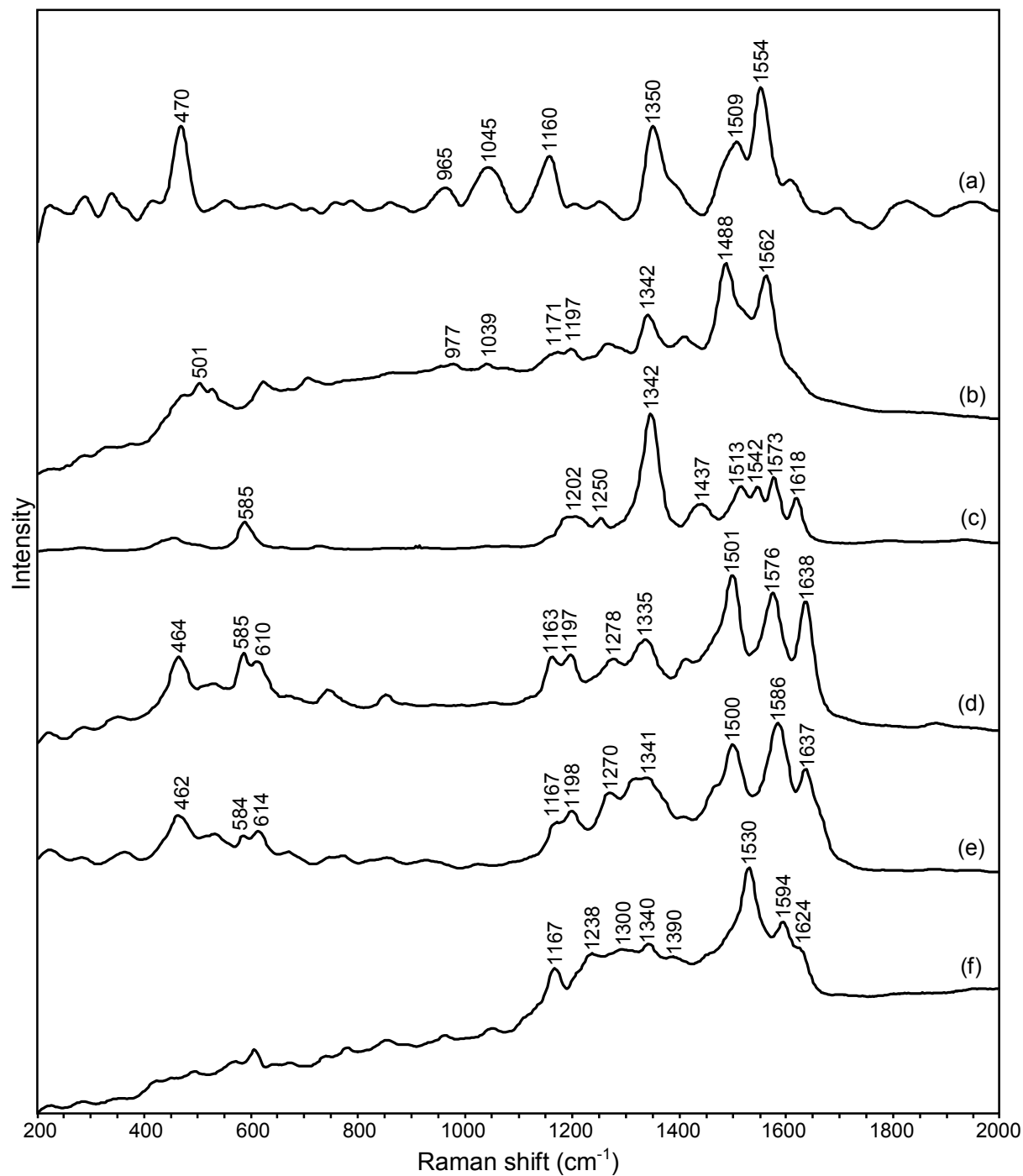


Figure 9. SERS spectra of neoflavonoid, neoflavone and biflavonoid dyes: (a) brazilwood upon baseline correction, (b) logwood, (c) sandalwood, (d) catechu, (e) catechin and (f) dragon's blood.

Table 6. Frequencies of SERS spectra of neoflavonoid, neoflavone and biflavonoid dyes with relative intensities.

| Neoflavonoid, neoflavone and biflavonoid dyes | SERS bands (cm ⁻¹) |
|---|--|
| Brazilwood Fig. 9 - Spectrum (a) | 1610w, 1554vs, 1509m, 1396sh, 1350s, 1254vw, 1207vw, 1160m, 1045m, 965w, 470s, 415sh |
| Logwood Fig. 9 - Spectrum (b) | 1562s, 1488s, 1409w, 1342m, 1266w, 1197w, 1171w, 1039vw, 977vw, 705w, 621w, 528w, 501m, 470w |
| Sandalwood Fig. 9 - Spectrum (c) | 1618m, 1573m, 1542m, 1513m, 1437m, 1342vs, 1250m, 1202m, 723vw, 585m, 503sh, 455w, 280vw |
| Catechu Fig. 9 - Spectrum (d) | 1638vs, 1576vs, 1501vs, 1414m, 1335s, 1278m, 1197s, 1163s, 852w, 745w, 610s, 585s, 531w, 464s, 347w, 286w, 219w |
| Catechin Fig. 9 - Spectrum (e) | 1637s, 1586vs, 1500vs, 1467sh, 1410w, 1341s, 1319s, 1270m, 1198m, 1169sh, 1021vw, 927vw, 853vw, 773vw, 744vw, 668vw, 614w, 584w, 531w, 462m, 362vw, 284vw, 221vw |
| Dragon's blood Fig. 9 - Spectrum (f) | 1624sh, 1594m, 1530vs, 1390m, 1340m, 1300m, 1238m, 1167m, 1048vw, 962vw, 852vw, 778vw, 737vw, 607w, 571vw, 490vw, 421vw, 347vw, 286vw, 219vw |

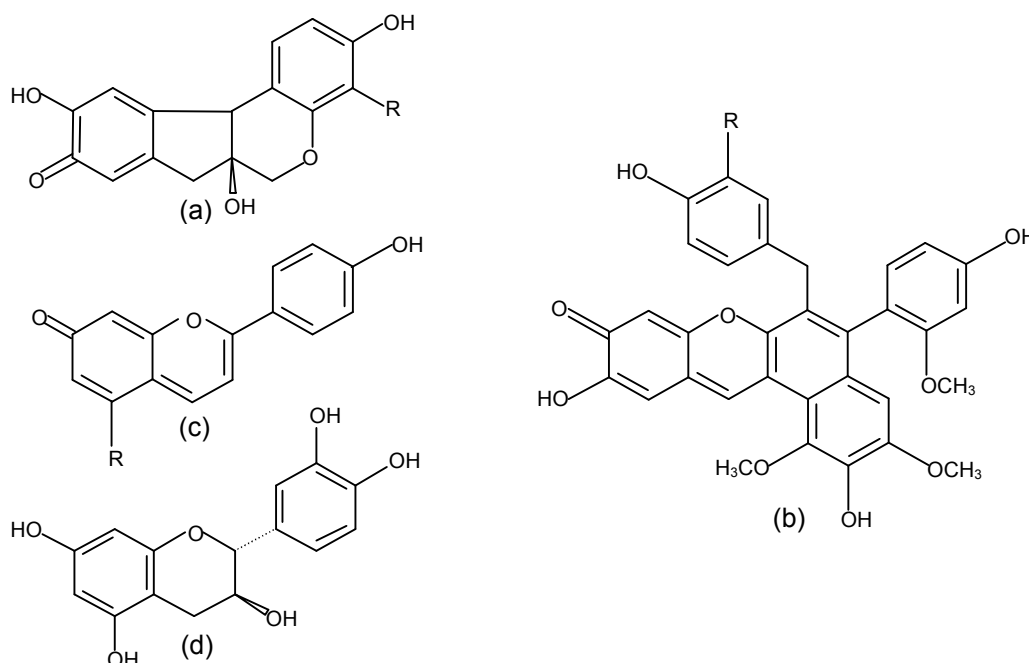


Figure 10. Neoflavonoid, neoflavone and biflavonoid dyes: (a) brazilin if R=H, the main chromophore of brazilwood, and hematein if R=OH, the main chromophore of logwood; (b) santalin A if R=OH and santalin B if R=OCH₃, the main chromophores of sandalwood; (c) 7,4'-dihydroxyflavylum if R=H and dracoflavylum if R=OCH₃, the main chromophores of dragon's blood; (d) catechin, the main chromophore of catechu.

The SERS spectra of the two neoflavonoid dyes studied in this chapter, brazilwood and logwood, display a remarkable similarity, notwithstanding the high fluorescence background shown by the spectrum of brazilwood, which indeed is presented here upon baseline correction. Such resemblance, also reported for the FT-Raman spectra of the same colorants³⁴, is expected on the basis of the molecular structures of the corresponding chromophores. The more characteristic bands observed in the spectra lie at 1560-1550 cm^{-1} and 1500-1490 cm^{-1} , both assigned to $\nu(\text{C}=\text{C})$ in reference 34; 1350-1340 cm^{-1} , attributed to $\nu(\text{C}-\text{O})$, $\delta(\text{OCC})$ and $\delta(\text{CH}_2)$; 1190-1160 cm^{-1} , assigned to $\delta(\text{C}-\text{H})$ and $\nu(\text{C}-\text{C})$; ca. 1040 cm^{-1} , due to in-plane $\delta(\text{CH})$; and 970 cm^{-1} , not observed and hence not assigned in the cited paper; 500-470 cm^{-1} , possibly due to ring deformation³⁵.

An exhaustive study of the FT-Raman spectra of dragon's blood from different botanical sources has been reported in the literature^{30,31}. HPLC analysis demonstrated that the main chromophores of the resin investigated here are dracoflavylum and 7,4'-dihydroxyflavylium, thus suggesting that probably our sample consists of a mixture of resins from *D. draco* and *D. cinnabar*³². In accordance with the molecular structures of such chromophores, the observed SERS spectrum, reported here for the first time, shows a good correspondence with the resonance Raman spectrum published in the literature for hydroxyflavylium derivatives⁶⁵ and also with the SERS spectrum obtained for sumac dye¹³ (see Chapter 3), the red color of which is due to anthocyanins. In particular, bands at 1624, 1594, 1530, 1390 and 1340 cm^{-1} are assigned to the ring stretching vibrational modes, while the broad signal around 1300 cm^{-1} and the band at 1167 cm^{-1} are attributed to the $\delta(\text{CH})$ modes; finally, the band at 1238 cm^{-1} can be assigned to the C-O stretching mode⁶⁵. Concerning catechu, the SERS spectrum of its major coloring molecule, catechin, was previously published¹⁰; however, it appears to be strongly affected by the spurious bands of the employed Ag colloid. In the present work, catechu exhibits a SERS spectrum very similar to that of catechin, characterized by strong signals at 1638, 1576 and 1501 cm^{-1} , attributable to C=C stretching modes, and a medium-intensity band at 1335 cm^{-1} that can be assigned to the C-O stretching vibration⁶⁶.

For sandalwood a spectral pattern similar to that of catechu is observed between 1620 and 1400 cm^{-1} , possibly related to the catechol moiety of the santalin A chromophore. Nevertheless, the strongest band lies at 1342 cm^{-1} , as observed also in the FT-Raman spectrum of sandalwood obtained with 1064 nm as excitation wavelength (figure 5; the corresponding wavenumbers with relative intensities are listed in table 4) and reported in the literature⁶⁷. This band is most probably due to the stretching vibration of the several C-O bonds characterizing the molecular structure of santalins.

Naphthoquinone and carotenoid dyes

The SERS spectra of naphthoquinone and carotenoid dyes are reported in figure 11, with all the corresponding wavenumbers listed in table 7, while the main chromophores of these colorants are shown in figure 12.

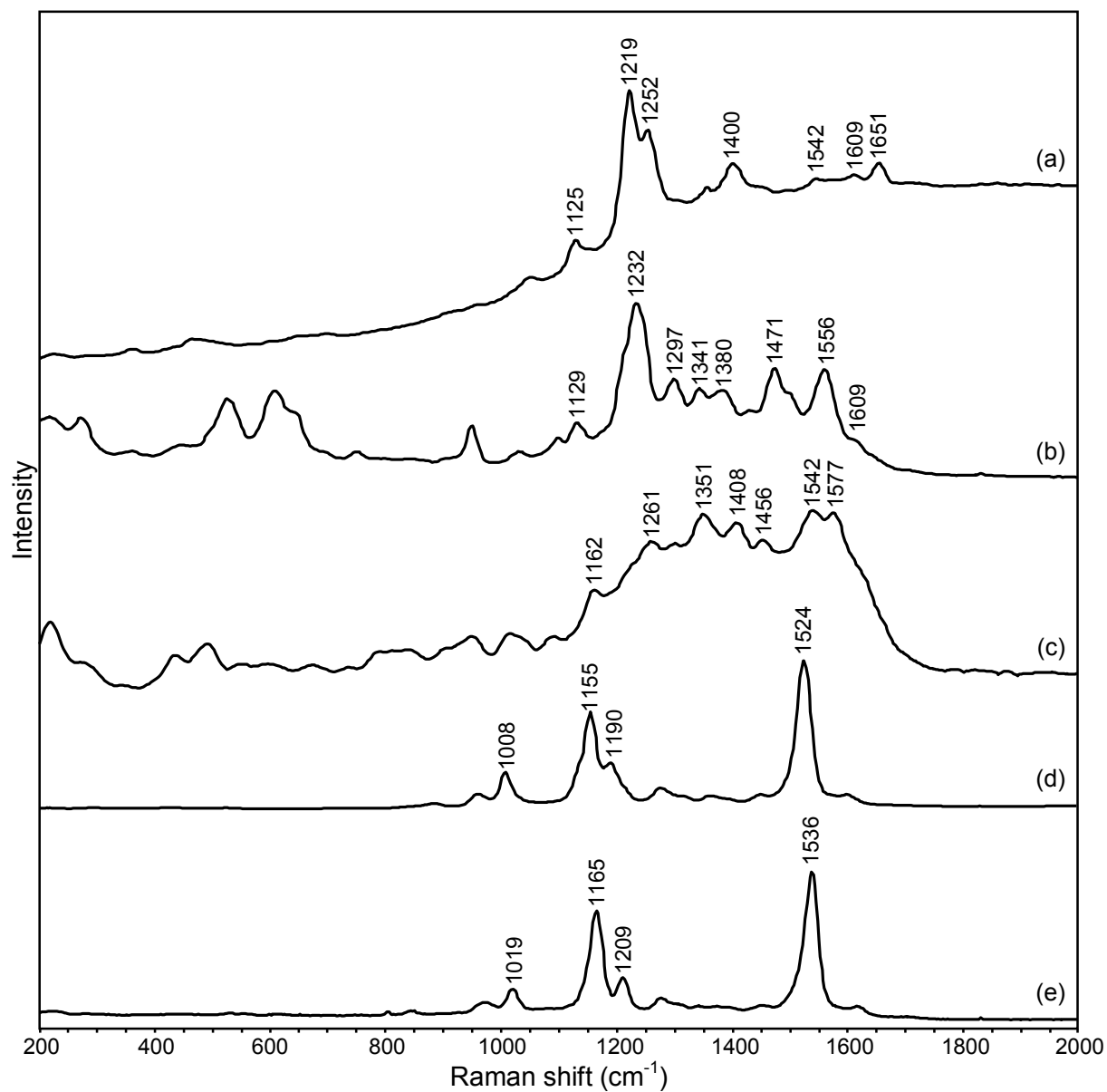


Figure 11. SERS spectra of naphthoquinone and carotenoid dyes: (a) alkanet, (b) henna, (c) walnut, (d) annatto and (e) saffron.

Table 7. Frequencies of SERS spectra of naphthoquinone and carotenoid dyes with relative intensities.

| Naphthoquinone and carotenoid dyes | SERS bands (cm ⁻¹) |
|------------------------------------|---|
| Alkanet Fig. 11 - Spectrum (a) | 1651w, 1609vw, 1542vw, 1456sh, 1400m, 1354vw, 1252s, 1219vs, 1125w, 1047vw, 461vw, 358vw, 222vw |
| Henna Fig. 11 - Spectrum (b) | 1609sh, 1556s, 1495sh, 1471s, 1428w, 1380m, 1341m, 1297m, 1232vs, 1129w, 1096vw, 1028vw, 948w, 749vw, 644sh, 606m, 522m, 445vw, 358vw, 272w, 216w |
| Walnut Fig. 11 - Spectrum (c) | 1577s, 1542s, 1456m, 1408m, 1351s, 1301w, 1261m, 1223sh, 1162w, 1016vw, 950vw, 492vw, 435vw, 219w, 172vw |
| Annatto Fig. 11 - Spectrum (d) | 1598vw, 1524vs, 1448vw, 1393sh, 1363vw, 1320sh, 1276w, 1190m, 1155s, 1008m, 963w, 887vw |
| Saffron Fig. 11 - Spectrum (e) | 1615vw, 1536vs, 1448vw, 1276w, 1209m, 1165s, 1019m, 969w |

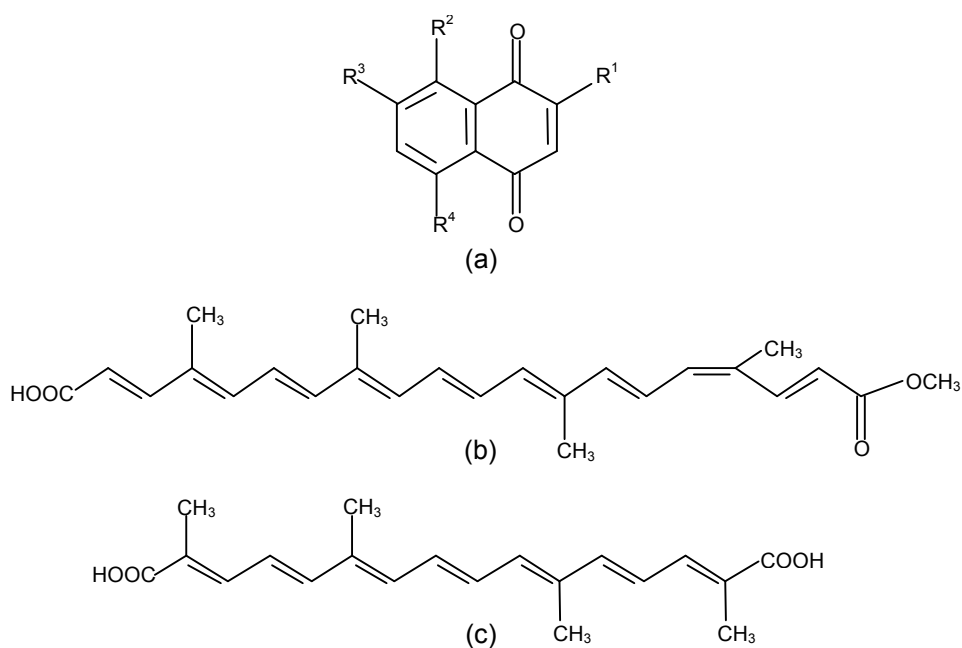


Figure 12. Napthoquinone and carotenoid dyes: (a) alkanin if $R^1=H$, $R^2=R^4=OH$ and $R^3=CH(OH)CH_2CH=C(CH_3)_2$, the main chromophore of alkanet; (a) lawsone if $R^1=OH$ and $R^2=R^3=R^4=H$, the main chromophore of henna; (a) juglone if $R^1=R^3=R^4=H$ and $R^2=OH$, the main chromophore of walnut; (b) bixin, the main chromophore of annatto; (c) crocetin, the main chromophore of saffron.

The SERS spectrum of alkanet shows bands at wavenumbers corresponding to those reported in the literature for the vibrational modes of naphthazarin⁶⁸. In detail, the strongest signal, lying at 1219 cm⁻¹, can be assigned to the deformation mode of the OH groups, but also other bands observed in the spectrum, namely at 1609, 1542 and 1400 cm⁻¹, can be attributed on the basis of the literature data⁶⁸ to vibrational modes comprising the bending of hydroxyl, obviously involved in the coordination to silver surface. However, the weak signal at 1609 cm⁻¹ could also involve the C=O stretching mode of coordinated carbonyl groups, while the band at 1651 cm⁻¹ can be assigned to the same vibrational mode for free carbonyl groups.

The chromophore of henna is lawsone, and indeed the strongest band in the SERS spectrum is observed at 1232 cm⁻¹, corresponding to the vibrational wavenumber reported in the literature for the C-OH group in iron(II) complexes of lawsone itself⁶⁹. The other group involved in coordination to the metal, i.e. the carbonyl group, gives rise to a weak shoulder at 1609 cm⁻¹.

The main chromophore reported for walnut is juglone, again a hydroxynaphthoquinone, but several other coloring molecules are contained in its extract, as reported in the literature⁷⁰. Among them, for example, also carotenoids are included, i.e. molecules that give a strong resonance Raman signal at the excitation wavelength of 532 nm used in the present work. Accordingly, the SERS spectrum of walnut is rather complex and does not allow a detailed assignment of the observed bands.

Annatto and saffron exhibit the typical Raman spectral pattern of carotenoids, with two strong bands at 1550-1500 cm⁻¹ and 1170-1150 cm⁻¹, attributed respectively to C=C and C-C stretching modes, and a medium intensity band at 1020-1000 cm⁻¹, assigned to in-plane rocking modes of CH₃ groups coupled with C-C stretching⁷¹. In detail, these bands are observed for saffron at 1536, 1165 and 1019 cm⁻¹, corresponding to wavenumbers reported in the literature for the Raman spectrum of crocetin, and for annatto at 1524, 1155 and 1008 cm⁻¹, corresponding to the values expected for *trans*-bixin⁷¹.

Turmeric, gamboge and indigo

The SERS spectra of turmeric, gamboge and indigo are reported in figure 13, with all the corresponding wavenumbers listed in table 8, while the main chromophores of these colorants are shown in figure 14.

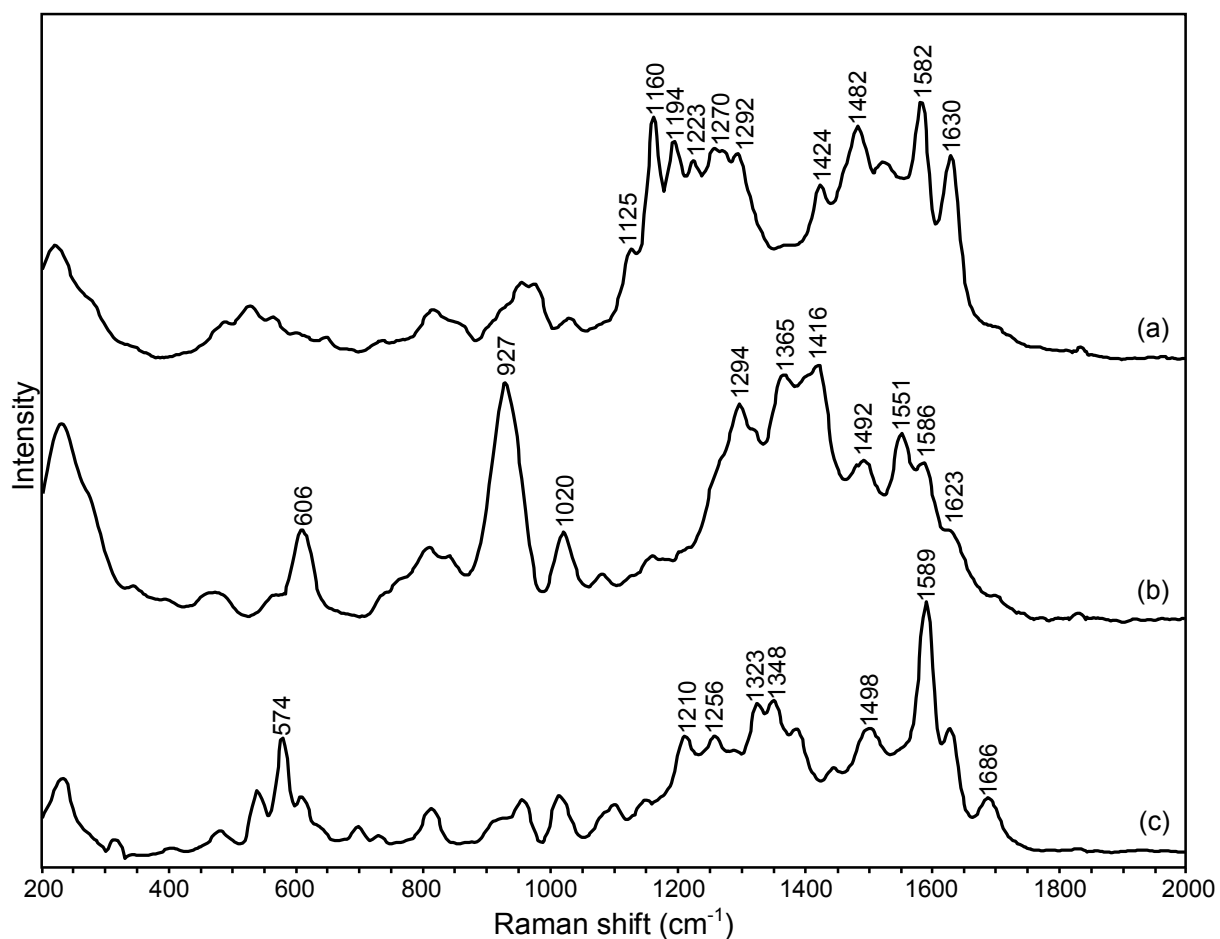


Figure 13. SERS spectra of (a) turmeric, (b) gamboge and (c) indigo.

Table 8. Frequencies of SERS spectra of turmeric, gamboge and indigo with relative intensities.

| Turmeric, gamboge and indigo | SERS bands (cm ⁻¹) |
|------------------------------------|--|
| Turmeric Fig. 13 - Spectrum (a) | 1630s, 1582vs, 1523s, 1482vs, 1424s, 1292s, 1270s, 1256s, 1223s, 1194s, 1160vs, 1125sh, 1025vw, 973w, 954w, 852sh, 816w, 735vw, 646vw, 603vw, 564w, 528w, 487w, 220m |
| Gamboge Fig. 13 - Spectrum (b) | 1623sh, 1586m, 1551s, 1492m, 1416vs, 1365vs, 1318sh, 1294s, 1201sh, 1159w, 1124sh, 1080vw, 1020w, 927vs, 838w, 806w, 761sh, 730sh, 606m, 559vw, 468vw, 340sh, 229s |
| Indigo Fig. 13 - Spectrum (c) | 1686w, 1625m, 1589vs, 1498m, 1443w, 1384m, 1348m, 1323m, 1287m, 1256m, 1210m, 1147w, 1098w, 1013w, 953w, 922sh, 811w, 729vw, 695vw, 638sh, 606w, 574m, 539w, 478vw, 402vw, 314vw, 232m |

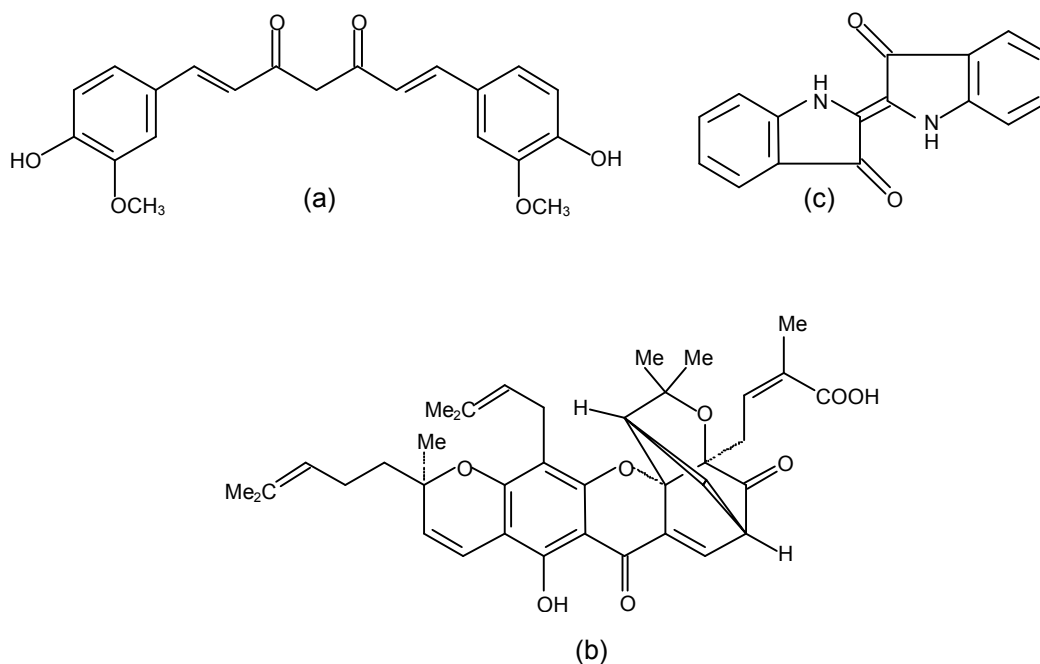


Figure 14. (a) Curcumin, the main chromophore of turmeric, (b) gambogic acid, the main chromophore of gamboge and (c) indigotin, the main chromophore of indigo.

In the present study, for turmeric a well-resolved SERS spectrum was obtained, which is similar to that reported in reference 61. The observed spectral pattern also shares some features of both SERS spectra reported in the literature³⁸ for curcumin on Ag citrate colloid with excitation at 514.5 nm at pH=6 and 12, that appears to be reasonable considering that the pH of the Ag colloid used in the present work is about 7.5. In the cited reference, some of the observed bands are related to a possible degradation of the molecule. However, the same authors also state that such a phenomenon should be in any case less pronounced at the considered excitation wavelength. Moreover, the observed bands agree in wavenumber with those reported in the literature for the vibrational spectra of solid curcumin, for which the following assignments have been indicated also on the basis of DFT calculations, considering that the molecule is predominantly in the enol form⁷³: $\nu(\text{C}=\text{C})$ and $\nu(\text{C}=\text{O})$ at 1630 cm^{-1} , $\nu(\text{C}=\text{C})$ and $\delta(\text{COH}^{\text{enol}})$ at 1582 cm^{-1} , ring vibrations of the phenyl groups at 1482 cm^{-1} , again ring vibrations and $\delta(\text{COH}^{\text{phenyl}})$ at 1424 cm^{-1} , $\delta(\text{C}=\text{CH})$ at 1292 cm^{-1} , $\delta(\text{CCH})$ and $\delta(\text{CCC})$ of phenyl rings and $\delta(\text{COH}^{\text{phenyl}})$ at 1270 and 1256 cm^{-1} , $\delta(\text{COH}^{\text{phenyl}})$ and $\delta(\text{COH}^{\text{enol}})$ at 1223 cm^{-1} , $\delta(\text{CCH})$ both of phenyl rings and skeletal bonds at 1194 , 1160 and 1125 cm^{-1} .

The SERS spectrum of gamboge is dominated by strong bands at 1416 , 1365 , 1294 and 927 cm^{-1} . Due to the complexity of the molecular structure of gambogic acid, a precise assignment of these bands is quite difficult. The three bands located at higher wavenumbers can be tentatively associated with vibrations of the aromatic ring substituted with the hydroxyl group, probably involved in the coordination to metal particles together with the adjacent carbonyl group. Indeed, the FT-Raman spectrum of the same dye (figure 5; the corresponding wavenumbers with relative intensities are listed in table 4) shows a signal attributable to the C=O stretching at 1639 cm^{-1} , which disappears in the SERS spectrum and is replaced by a shoulder at 1623 cm^{-1} thus

reinforcing the hypothesis of the participation of the carbonyl group in coordination to metal. The intense band at 927 cm^{-1} is possibly due the cyclic ether linkages characterizing the molecular structure⁷⁴.

The strongest signal in the SERS spectrum of indigo appears at 1589 cm^{-1} , while in the FT-Raman spectrum of the same dye a very intense band is observed at 1576 cm^{-1} with a shoulder at 1585 cm^{-1} (figure 5; the corresponding wavenumbers with relative intensities are listed in table 4). According to the literature⁷⁵, the second band, i.e. the one that is most probably enhanced in the SERS spectrum, is assigned to the stretching mode of C=C bonds, admixed with $\nu(\text{C}=\text{O})$ and $\delta(\text{N}-\text{H})$ vibrations. Moreover, the signal at 1498 cm^{-1} could be attributed, always on the basis of the above-cited literature data, to bending modes of C-H, N-H and C-C ring bonds, while three of the four medium-intensity bands located from 1350 to 1200 cm^{-1} , namely those at 1348 , 1323 , 1256 and 1210 cm^{-1} , can be assigned to vibrational modes that involve again the in-plane bending both of C-H and N-H groups. The strongest band observed at lower wavenumbers, i.e. the one at 574 cm^{-1} , can be attributed mainly to the out-of-plane deformation modes of C=C bonds. The weak band at 1686 cm^{-1} corresponds to the signal located at 1704 cm^{-1} in the FT-Raman spectrum (figure 5; the corresponding wavenumbers with relative intensities are listed in table 4) and is assigned to the stretching vibration of the carbonyl groups, which occurs at lower wavenumbers because of the coordination to silver.

Conclusions

25 natural organic dyes and 9 pure chromophores of interest in art and archaeology were analyzed by SERS spectroscopy on Ag colloids synthesized according to the Lee-Meisel procedure, in order to build a wide database, to be used for the identification of colorants in works of art and archaeological fabric samples. The highly efficient performance of 1.8 M NaClO_4 as aggregating agent was highlighted, especially when added to the silver nanoparticles after the analyte. The analytical data previously published in the literature were integrated by acquiring, for the first time, the SERS spectra of 11 additional natural dyes. Moreover, the SERS spectral patterns of the analyzed colorants were interpreted on the basis of the molecular classes to which the different dyes belong, highlighting the main analogies and common features.

The analyses here carried out on pure colorants and chromophores were also used as a reference for the identification of dyes in ancient Kaitag textiles from Caucasus, as discussed in Chapter 4, as well as in the development of a library search method which was applied to the second derivatives of FT-Raman and ATR-FTIR spectra of dyes previously fixed on fibers, aiming to evaluate the possibility of detecting natural colorants on textiles in a totally non-invasive way⁷⁶.

References

- [1] F. Casadio, M. Leona, J. R. Lombardi, R. Van Duyne, *Acc. Chem. Res.* **2010**; *43*, 782.
- [2] K. Chen, M. Leona, T. Vo-Dinh, *Sens. Rev.* **2007**; *27*, 109.
- [3] K. L. Wustholz, C. L. Brosseau, F. Casadio, R. P. Van Duyne, *Phys. Chem. Chem. Phys.* **2009**; *11*, 7350.
- [4] C. L. Brosseau, A. Gambardella, F. Casadio, C. M. Grzywacz, J. Wouters, R. P. Van Duyne, *Anal. Chem.* **2009**; *81*, 3056.
- [5] L. H. Oakley, S. A. Dinehart, S. A. Svoboda, K. L. Wustholz, *Anal. Chem.* **2011**; *83*, 3986.
- [6] M. Leona, J. Stenger, E. Ferloni, *J. Raman Spectrosc.* **2006**; *37*, 981.
- [7] C. Corredor, T. Teslova, M. V. Cañamares, Z. Chen, J. Zhang, J. R. Lombardi, M. Leona, *Vib. Spectrosc.* **2009**; *49*, 190.
- [8] T. Teslova, C. Corredor, R. Livingstone, T. Spataru, R. L. Birke, J. R. Lombardi, M. V. Cañamares, M. Leona, *J. Raman Spectrosc.* **2007**; *38*, 802.
- [9] Z. Jurasekova, J. V. Garcia-Ramos, C. Domingo, S. Sánchez-Cortés, *J. Raman Spectrosc.* **2006**; *37*, 1239.
- [10] Z. Jurasekova, C. Domingo, J. V. Garcia-Ramos, S. Sánchez-Cortés, *Coalition* **2007**; *14*, 14.
- [11] M. V. Cañamares, J. V. Garcia-Ramos, C. Domingo, S. Sánchez-Cortés, *Vib. Spectrosc.* **2006**; *40*, 161.
- [12] M. V. Cañamares, M. Leona, *J. Raman Spectrosc.* **2007**; *38*, 1259.
- [13] S. Bruni, V. Guglielmi, F. Pozzi, A. M. Mercuri, *J. Raman Spectrosc.* **2011**; *42*, 465.
- [14] D. Cardon, *Natural Dyes. Sources, Tradition, Technology and Science*, Archetype Publications, London, **2007**.
- [15] J. S. Mills, R. White, *The Organic Chemistry of Museum Objects*, Butterworths, London, **1994**, p. 121.
- [16] E. S. B. Ferreira, A. N. Hulme, H. McNab, A. Quye, *Chem. Soc. Rev.* **2004**; *33*, 329.
- [17] H. Schwappe, H. Roosen-Runge, *Artists' pigments*, Oxford University Press, New York, Vol. 1, **1986**, p. 255.
- [18] A. V. Whitney, R. P. Van Duyne, F. Casadio, *J. Raman Spectrosc.* **2006**; *37*, 993.
- [19] Z. C. Koren, *Archaeological Chemistry: Organic, Inorganic, and Biochemical Analysis*, **1996**, p. 269.
- [20] H. Schwappe, J. Winter, *Artists' pigments*, Oxford University Press, New York, Vol. 3, **1997**, p. 109.
- [21] R. H. Thomson, *Naturally Occurring Quinones* (2nd edition), Academic Press, London and New York, **1971**.
- [22] P. Cox Crews, *Stud. Conserv.* **1987**; *32*, 65.
- [23] A. Romani, C. Zuccaccia, C. Clementi, *Dyes and Pigments* **2006**; *71*, 218.
- [24] E. S. B. Ferreira, A. N. Hulme, H. McNab, A. Quye, *Dyes Hist. Archaeol.* **2003**; *19*, 19.
- [25] J. Wisniak, *Ind. J. History Sci.* **2004**; *39*, 75.
- [26] J. H. Hofenk de Graaff, *The Colourful Past - Origins, Chemistry and Identification of Natural Dyestuffs*, Archetype Publications, London, **2004**, p. 196.
- [27] A. Doménech-Carbó, T. Doménech-Carbó, C. Saurí-Peris, J. V. Gimeno-Adelantado, F. Bosch-Reig, *Microchim. Acta* **2005**; *152*, 75.
- [28] L. Fan, H.-Y. Zhao, M. Xu, L. Zhou, H. Guo, J. Han, B.-R. Wang, D.-A. Guo, *J. Chromatogr. A* **2009**; *1216*, 2063.

- [29] A. Casoli, M. E. Darecchio, L. Sarritzu, *I Coloranti nell'Arte*, Il Prato Casa Editrice, Padova, **2009**, p. 35.
- [30] H. G. M. Edwards, D. W. Farwell, A. Quye, *J. Raman Spectrosc.* **1997**; *28*, 243.
- [31] H. G. M. Edwards, L. F. C. de Oliveira, H. D. V. Prendergast, *Analyst* **2004**; *129*, 134.
- [32] M. M. Sousa, M. J. Melo, A. J. Parola, J. S. Seixas de Melo, F. Catarino, F. Pina, F. E.M. Cook, M. S. J. Simmonds, J. A. Lopes, *J. Chromatogr. A* **2008**; *1209*, 153.
- [33] R. J. Adrosko, M. Smith Furry, *Natural Dyes and Home Dyeing*, Dover Publications, New York, **1971**, p. 40.
- [34] H. G. Edwards, L. F. C. de Oliveira, M. Nesbitt, *Analyst* **2003**; *128*, 82.
- [35] L. F. C. de Oliveira, H. G. M. Edwards, E. S. Velozo, M. Nesbitt, *Vib. Spectrosc.* **2002**; *28*, 243.
- [36] K. Pawlak, M. Puchalska, A. Miszczak, E. Rosloniec, M. Jarosz, *J. Mass Spectrom.* **2006**; *41*, 613.
- [37] J. A. Pereira, I. Oliveira, A. Sousa, P. Valentão, P. B. Andrade, I. C. F. R. Ferriera, F. Ferreres, A. Bento, R. Seabra, L. Estevinho, *Food Chem. Toxicol.* **2007**; *45*, 2287.
- [38] M. V. Cañamares, J. V. Garcia-Ramos, S. Sánchez-Cortés, *Appl. Spectrosc.* **2006**; *60*, 1386.
- [39] J. Seixas de Melo, A. P. Moura, M. J. Melo, *J. Phys. Chem. A* **2004**; *108*, 6975.
- [40] M. A. Ackacha, K. Polé-Pawlak, M. Jarosz, *J. Sep. Sci.* **2003**; *26*, 1028.
- [41] N. Sharma, P. Ghosh, U. K. Sharma, S. Sood, A. K. Sinha, A. Gulati, *Anal. Lett.* **2009**; *42*, 2592.
- [42] G. Pekin, M. Ganzera, S. Senol, E. Bedir, K. S. Korkmaz, H. Stuppner, *Planta Med.* **2007**; *73*, 267.
- [43] R. Wissmann Alves, A. A. Ulson de Souza, S. M. de Arruda Guelli Ulson de Souza, P. Jauregi, *Sep. Purif. Technol.* **2006**; *48*, 208.
- [44] J. Gu, L. An, J. Liu, X. Chen, *Guangdong Weiliang Yuansu Kexue* **2005**; *12*, 61.
- [45] Z. C. Koren, *Dyes Hist. Archaeol.* **2001**; *16/17*, 158.
- [46] M. P. Colombini, A. Andreotti, C. Baraldi, I. Degano, J. J. Lucejko, *Microchem. J.* **2007**; *85*, 174.
- [47] P. C. Lee, D. J. Meisel, *J. Phys. Chem.* **1982**; *84*, 3391.
- [48] S. Bruni, V. Guglielmi, F. Pozzi, *J. Raman Spectrosc.* **2010**; *41*, 175.
- [49] M. V. Cañamares, J. V. Garcia-Ramos, C. Domingo, S. Sánchez-Cortés, *J. Raman Spectrosc.* **2004**; *35*, 921.
- [50] Z. Jurasekova, E. del Puerto, G. Bruno, J. V. Garcia-Ramos, S. Sánchez-Cortés, C. Domingo, *J. Raman Spectrosc.* **2010**; *41*, 1165.
- [51] E. Van Eislande, S. Lecomte, A. Le-Hô, *J. Raman Spectrosc.* **2009**; *39*, 1001.
- [52] I. T. Shadi, B. Z. Chowdry, M.-J. Snowden, R. Whitnall, *J. Raman Spectrosc.* **2004**; *35*, 800.
- [53] K. B. Andersen, M. Langgård, J. Spanget-Larsen, *J. Mol. Struct.* **1999**; *475*, 131.
- [54] M. Wang, T. Teslova, F. Xu, T. Spataru, J. R. Lombardi, R. L. Birke, *J. Phys. Chem. C* **2007**; *111*, 3038.
- [55] L. J. Porter, K. R. Markham, *J. Chem. Soc. C* **1970**; *344*, 1309.
- [56] Z. Jurasekova, A. Torreggiani, M. Tamba, S. Sánchez-Cortés, J. V. Garcia-Ramos, *J. Mol. Struct.* **2009**; *918*, 129.
- [57] M. V. Cañamares, J. R. Lombardi, M. Leona, *e-Preserv. Sci.* **2009**; *6*, 81.
- [58] J. P. Cornard, J. C. Merlin, *J. Inorg. Biochem.* **2002**; *92*, 19.
- [59] J. P. Cornard, J. C. Merlin, *J. Mol. Struct.* **2003**; *651*, 381.
- [60] M. P. Colombini, A. Carmignani, F. Modugno, F. Frezzato, A. Olchini, H. Brecoulaki, V. Vassilopoulou, P. Karkanias, *Talanta* **2004**; *63*, 839.

- [61] G. Favaro, C. Clementi, A. Romani, V. Vickackaite, *J. Fluoresc.* **2007**; 17, 707.
- [62] L. J. Bellamy, *The Infrared Spectra of Complex Molecules*, Methuen, London, **1966**, p. 162.
- [63] M. Palaniandavar, C. Natarajan, *Aust. J. Chem.* **1980**; 33, 737.
- [64] M. Muthukumar, P. Viswanathamurthi, K. Natarajan, *Spectrochim. Acta Part A* **2008**; 70, 1222.
- [65] J. C. Merlin, J. P. Cornard, *Spectrochim. Acta Part A* **1994**; 50, 703.
- [66] M. M. Ramos-Tejada, J. D. G. Durán, A. Ontiveros-Ortega, M. Espinosa-Jimenez, R. Perea-Carpio, E. Chibowski, *Colloids Surf. B: Biointerf.* **2002**; 24, 297.
- [67] C. M. Schmidt, K. A. Trentelmann, *e-Preserv. Sci.* **2009**; 6, 10.
- [68] M. Z. Tabrizi, S. F. Tayyari, F. Tayyari, M. Behforouz, *Spectrochim. Acta Part A* **2004**; 60, 111.
- [69] P. Garge, S. Padhye, *Inorg. Chim. Acta* **1989**; 157, 239.
- [70] F. Stampar, A. Solar, M. Hudina, R. Veberic, M. Colaric, *Food Chem.* **2006**; 95, 627.
- [71] H. Schulz, M. Baranska, R. Baranski, *Biopolymers* **2005**; 77, 212.
- [72] C. L. Brosseau, K. S. Rayner, F. Casadio, C. M. Grzywacz, R. P. Van Duyne, *Anal. Chem.* **2009**; 81, 7443.
- [73] T. M. Kolev, E. A. Velcheva, B. A. Stamboliyska, M. Spiteller, *Int. J. Quantum Chem.* **2005**; 102, 1069.
- [74] N. L. Colthup, L. H. Daly, S. E. Wiberley, *Introduction to Infrared and Raman Spectroscopy*, Academic Press, New York, **1964**.
- [75] M. Sánchez del Río, M. Picquart, E. Haro-Poniatowski, E. Van Elslande, V. H. Uc, *J. Raman Spectrosc.* **2006**; 37, 1046.
- [76] S. Bruni, E. De Luca, V. Guglielmi, F. Pozzi, *Appl. Spectrosc.* **2011**; 65, 1017.

Chapter 3

Identification of a yellow dye in ancient threads from the Libyan Sahara

Abstract

The real effectiveness of SERS on Ag colloids aggregated with NaClO_4 , discussed in Chapter 2, has been here successfully demonstrated for the identification of a yellow dye in two ancient wool threads found in the Royal Tumulus of In Aghelachem, Libyan Sahara, belonging to the Garamantian period (2nd - 3rd century A.D.). HPLC highlighted the presence of ellagic acid in the extracts from the threads, excluding other chromophores. This result, together with the high content of malic acid detected by GC-MS, suggested the possible use of pomegranate rind or sumac berries as source of the yellow dye, both plants being documented in the Fezzan area during the Garamantian period. HPLC analyses and SERS spectra acquired on the extracts of the ancient threads were therefore compared with those obtained from pomegranate and sumac extracts of the corresponding fruits and reference wool samples dyed in the laboratory, allowing us to identify the yellow dye as deriving from pomegranate (*Punica granatum*). SERS spectra of ellagic acid and dyes extracted from pomegranate rind and sumac berries were collected in this study for the first time.

Introduction

In the present study, SERS on Ag nanoparticles and HPLC were used to analyze two yellow-dyed wool threads (figure 1) from the Libyan Sahara, belonging to the Garamantian period (2nd - 3rd century A.D.). Besides these techniques, color analysis, SEM-EDX and GC-MS were also employed as complementary tools in order to gain preliminary information on the archaeological samples.

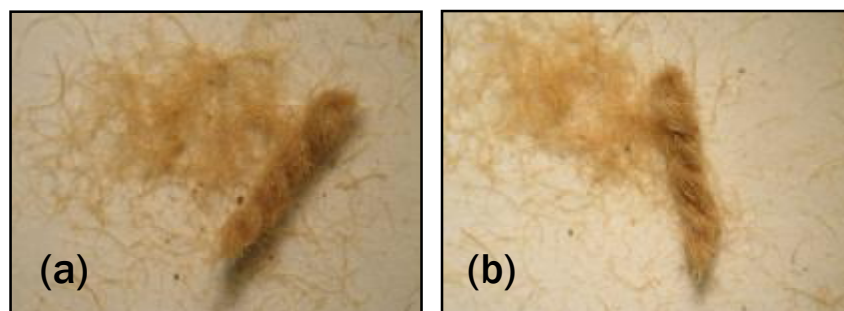


Figure 1. Yellow-dyed wool threads found in the Royal Tumulus of In Aghelachem, Libyan Sahara. The two fibers have an approximate length of 5 mm.

SERS on Ag colloids combined with the use of NaCl or poly-L-lysine and ascorbic acid as aggregating agents was already employed in a previous work¹ to identify Tyrian purple on a purplish bone fragment and madder on a red wool thread, the latter found at the same excavation site in the Libyan Sahara to which the samples here investigated belong. However, as discussed in Chapter 2, the use of a different electrolyte, namely NaClO₄, allowed us to obtain high quality SERS spectra for a number of commercial colorants and pure chromophores, and was therefore exploited again in the present study, giving rise to significantly improved spectral quality compared to other aggregating agents.

Among the various classes of natural dyes, yellows are often difficult to identify, as their plant sources are widely distributed in the natural world. In most cases, flavonoids are their main coloring matter, but a number of other brownish-yellow dyes are obtained from species which contain different chromophores, such as naphthoquinonoids, carotenoids, curcuminoids and tannins². Because of the great variety of plants producing yellow shades, the choice of the dye source often depends on the species that are locally available³.

Archaeobotanical remains from archaeological sites of the Fezzan area have demonstrated that an extended plant cover was present in the region, where a large number of species were used by local populations since the first millennia of the Holocene⁴. During Garamantian times, a number of seeds and fruits were found that could have been employed as sources for yellow colorants and tanning agents⁵ (table 1). Among them, based on the results of chromatographic analyses performed on the extracts obtained from the ancient threads, special attention has been paid to *Rhus* (sumac) and *Punica granatum* (pomegranate), which were considered the most probable sources of the yellow dye coloring the wool discovered at In Aghelachem.

Colorants were therefore extracted from the fruits of pomegranate and sumac, which were also used to dye wool samples in our laboratory, according to ancient recipes, in order to provide a reference for chemical analysis to be compared with the results obtained for the archaeological samples. Before extraction, the ancient threads were analyzed by vis-RS for color measurements as well as by SEM-EDX. Subsequently, the extracts obtained from the two samples, together with those of pomegranate and sumac fruits and reference dyed wool, were studied by GC-MS, HPLC and SERS.

Table 1. Dye plants found in Garamantian archaeological records from which yellow colorants can be obtained.

| Wadi | Wadi Al-Ajal | | | Wadi Tanezzuft | | Parts of the plants used to produce dyes (chromophores) |
|-----------------------------|-----------------|--------------|----------------------|----------------|-----------------------------|--|
| | Site | Zinkekra | Tinda | Jarma | Fewet | |
| Chronology | 900-400 B.C. | 370-110 B.C. | 400 B.C.-750 A.D. | 200-0 B.C. | 50 B.C.-1200 A.D. | |
| Garamantian phase | Formation phase | Late phase | Mature to Late phase | Mature phase | Classical phase to Medieval | |
| <i>Acacia</i> sp. | | | | + | + | Yellow dye from flowers of <i>A. dealbata</i> and pods of <i>A. nilotica</i> (flavonoids) |
| <i>Amaranthus</i> sp. | | | | | + | Yellow dye from whole plant of several species (betalains) |
| <i>Carthamus tinctorius</i> | | | + | | | Yellow dye from flower heads (flavonoids) |
| <i>Chenopodium</i> sp. | | | | | + | Gold/green dye from whole plant of <i>Ch. bonus-henricus</i> , <i>Ch. ficifolium</i> and some other species (flavonoids) |
| <i>Foeniculum vulgare</i> | + | | | | + | Yellow dye shoots, flowers and leaves combined (flavonoids) |
| <i>Gossypium</i> sp. | | | + | | | Orange/yellow dye from flowers of <i>Gossypium hopi</i> (flavonoids) |
| <i>Medicago</i> sp. | | | | | + | Yellow dye from seeds of alfalfa, <i>i.e.</i> <i>Medicago sativa</i> (flavonoids) |
| <i>Olea europaea</i> | | | + | | | Yellow/green dye from the leaves (flavonoids) |
| <i>Punica granatum</i> | | | + | + | | Dark gold dye from fruit rinds (tannins) |
| <i>Rhus tripartita</i> | + | | | | | A yellow dye is obtained from leaves and fruits of <i>Rhus coriaria</i> (tannins, anthocyanins) |
| <i>Vitis vinifera</i> | + | + | + | | + | Bright yellow to olive green dyes from leaves (tannins, flavonoids, anthocyanins) |
| References | 6, 7 | 7, 8 | | 5 | 9 | 10-16 |

***Rhus* and *Punica granatum*: long-history dye plants**

***Rhus* or sumac (*Anacardiaceae*)**

This genus comprises about 200 species from the temperate and tropical/subtropical regions. The leaves, bark, wood and fruits of many species are widely employed in dyeing and leather tanning. Phylogenetic studies and research on sumac extracts have shown that plants of different species have similar chemistry.

The Sicilian sumac *Rhus coriaria* has stems and bark rich in tannins. Leaves contain 20-35% tannins and yield a yellow dye; also, leaves can be collected as they fall in autumn and used as a brown colorant or as a mordant. Its fruit and bark are also employed^{12,13}: stem bark yields yellow, and root bark yields brown dyes¹⁷. *Rhus coriaria* and *Cotinus coggygria* have been known and used widely since Greek times, and sumac was among the genera described by Theophrastus (4th - 3rd century B.C.). *Rhus tripartita* can still be found in the Central Sahara, where the wild plant has a long and important history of local exploitation. Moreover, it was found as plant macro-remains in the archaeobotanical record from the Formation phase of Garamantian times (table 1) and also as pollen from earlier sites of the area¹⁸.

***Punica granatum* or pomegranate (*Punicaceae*)**

This species is native to Western Asia, most likely from Iran, Northeastern Turkey and the region of the South Caspian sea, and early became a spontaneous shrub in the Eastern Mediterranean regions¹⁹. Pomegranate has been cultivated from early antiquity for its valuable fruit throughout the Mediterranean and North African regions, including Central Saharan oases. Considering the locations and context of pomegranate representations and archaeobotanical evidence, this fruit has continued to maintain a long-time tradition of a luxury food²⁰. In Roman times, at the Villa Rustica in Oplontis, over a tonne of carbonized pomegranates was discovered²¹. Columella gave instructions on how to preserve pomegranate for over a year²², a knowledge that allowed its transport as goods.

Several parts of the plant were used as both a tanning agent and dye. In particular, the dried fruit rind yields a yellow colorant which was employed for dyeing clothes and for making a hair dye, or sometimes also as a mordant²³. The archaeobotanical record testifies that pomegranate was present in the Fezzan area at the Mature phase of Garamantian times (table 1). In the Fewet citadel, two seeds of *P. granatum* were found uncharred, suggesting a different depositional history compared with that of other seeds and fruits which were found in a charred state in the same context⁵.

Experimental

Chemicals and archaeological samples

Dried pomegranate rind was obtained from the herbalist's shop Kallidendria (Milan, Italy), while sumac berries were harvested in Palermo (Italy). Weld and dyer's broom vegetable cut pieces were purchased from Zecchi (Florence, Italy) and Kremer (Aichstetten, Germany), respectively. Acid potassium tartrate was obtained from

the pharmacy Dott. Ambreck (Milan, Italy). Ellagic acid, silver nitrate, sodium perchlorate monohydrate, trifluoroacetic acid and *N,O*-bis(trimethylsilyl)trifluoroacetamide (BSTFA) with 1% trimethylchlorosilane (TMCS) were purchased from Fluka. Methanol, trisodium citrate dihydrate, ethyl acetate and acetonitrile were obtained from Sigma-Aldrich. Hydrochloric acid was purchased from Riedel-de Haën and sodium chloride from Carlo Erba, while Na_2CO_3 and $\text{KAl}(\text{SO}_4)_2$ were obtained from Baslini. All the aqueous solutions were prepared using ultrapure water (Millipore MilliQ).

The two archaeological threads (figure 1), called “thread 1” and “thread 2”, were found in the Royal Tumulus of In Aghelachem in the Libyan Sahara. The site excavations were carried out within the Italian-Libyan Archaeological Mission in the Acacus and Messak (Central Sahara), Sapienza, University of Rome and Department of Archaeology of Tripoli (presently directed by S. di Lernia). The In Aghelachem area proved to be particularly rich in megalithic structures, mainly belonging to the Garamantian period. The Garamantes inhabited the Fezzan during the period from ca. 500 B.C. to ca. 400 A.D. and developed a network of sites controlling the Saharan caravan routes. Initially a sort of large tribal federation, the Garamantes had a true kingdom in the period between the last three centuries B.C. and the mid-4th century A.D. The Royal Tumulus of In Aghelachem, dating to the 2nd - 3rd century A.D., was the tomb of a person of relevant social status, as demonstrated by the remains of an originally rich votive deposition, including a bronze bracelet and a vessel. Moreover, a few fragments of dyed textiles were found, made with coarse and highly twisted threads, which can be cautiously interpreted as a kind of rigid small container²⁴.

Wool dyeing process

Washing - First of all, wool samples had to be washed in order to remove any lipidic residue which would make the interaction between the dye and the fabric rather difficult. For this purpose, 15 g of raw wool were immersed in a 10% aqueous solution of Na_2CO_3 , according to a partially modified procedure of the published protocol²⁵. The washing bath was slowly heated up to 40°C and then kept at this temperature for about 10 minutes and, after this, the wool was rinsed in distilled water and dried²⁶.

Mordanting - Alum, $\text{KAl}(\text{SO}_4)_2$, reported in the literature as the most common mordant used in ancient times²⁷, was employed to set the colorants on fabrics and increase their light fastness together with acid potassium tartrate, which was added to optimize the pH value. 15 g of washed wool were immersed in a solution obtained by mixing 3.6 g of $\text{KAl}(\text{SO}_4)_2$ in 150 mL of distilled water and 0.9 g of acid potassium tartrate in 720 mL of distilled water. After heating the resulting bath to 90°C in about 30 minutes and then cooling it to room temperature, the wool was rinsed in distilled water and dried²⁶.

Dyeing - Pomegranate and sumac dyes were extracted from 30 g of fruits in 150 mL of distilled water. The wool was then immersed in the resulting dyebath, which was heated at 90°C for 30 minutes. After cooling to room temperature, the wool was rinsed in distilled water and finally dried in the dark²⁶.

Moreover, wool samples were dyed according to the above-reported procedure but without mordanting, for comparison purposes. Indeed, the capability of tannins themselves to act as organic mordants also for other colorants is well known²⁸.

Analytical methods: extraction procedures, Ag colloid synthesis and sample preparation

Extraction of dyes from archaeological and reference wool samples was performed as follows. 0.5 mg of each thread were suspended in 200 μL of 4 M HF and placed in a polyethylene test tube which was kept at room temperature under magnetic stirring for 30 minutes. The resulting extracts were thus loaded onto a Discovery Supelco C18 SPE cartridge previously preconditioned by 5 mL of a 1:1 methanol:acetonitrile solution and 5 mL of milliQ water. Fluorides were washed from the cartridge with 5 mL of milliQ water with 0.01% trifluoroacetic acid, and the dyestuffs were then eluted using 3 mL of a 1:1 methanol:acetonitrile solution acidified with 0.01% trifluoroacetic acid. The so obtained solutions were finally evaporated under a N_2 gentle stream^{29,30}.

Extraction of dyes from plant sources was carried out as described in the following. Pomegranate and sumac fruits were suspended in 50 mL of deionized H_2O at room temperature overnight; the obtained solutions were then filtered and evaporated in a drying oven at 60°C ^{31,32}. Weld and dyer's broom vegetable cut pieces were treated with 6 mL of MeOH and 200 μL of 37% HCl at 65°C for 60 minutes; the obtained solutions were filtered and dried under a N_2 gentle stream²⁶.

Silver colloids prepared according to the Lee-Meisel procedure³³, i.e. by reduction of silver nitrate with trisodium citrate dihydrate, were used as a SERS metal substrate; their synthesis is described in detail in Chapter 2.

Solutions of pomegranate and sumac extracts obtained from fruits and reference dyed wool were prepared daily at a concentration of 10^{-4} M, while the yellow dye from the Libyan wool threads was dissolved in few drops of the solvent. The SERS spectra acquired from the samples were all collected by adding in a test tube 300 μL of a methanolic solution of the unknown analyte to 3 mL of Ag Lee-Meisel colloid, with subsequent addition of 125 μL of 1.8 M NaClO_4 under magnetic stirring, in order to induce aggregation of the nanoparticles. SERS measurements were performed by focusing the laser beam on a drop of the dye-colloid system deposited on the surface of a glass slide.

Instrumentation

Color measurements on the archaeological threads were taken by visible reflectance spectra using a Jasco UV-vis-NIR V-570 spectrophotometer equipped with an integrating sphere. A suitable software allowed to obtain the CIELab coordinates from the spectra.

SEM-EDX analyses were recorded with a Stereoscan Cambridge 360 scanning electron microscope equipped with an Oxford energy-dispersive electronic microprobe with LaB_6 filament; data acquisition was performed with 25 mm working distance and 20 kV accelerating voltage. Samples were covered with graphite in order to make them conductive for the observation and the microanalysis.

HPLC analyses were performed with an HPLC PU-1580 Jasco pump equipped with an LG-1580-02 Jasco gradient valve and a GASTORR GT-103 solvent degasser, by using an MD 1510 Jasco photodiode array (PDA) detector in order to obtain spectral information between 200 and 600 nm. A 25 μL injection volume of a

methanolic solution of the analyte was used for the analysis, which was executed on a Supelco Discovery C18 column (25 cm x 4.66 mm, particle diameter 5 μm), with (A) ultrapure water and (B) acetonitrile both with 0.1% of trifluoroacetic acid as solvents, setting the flow rate at 1 mL/min. The solvent gradient was as follows: 95-70% A in 0-25 min, 70-40% A in 25-30 min, 40-5% A in 30-38 min, 5-95% A in 38-65 min.

GC-MS analyses were carried out with a Shimadzu GC-MS QP 5050 gas chromatograph coupled with a quadrupole mass spectrometer using electron impact ionization (acceleration voltage 1.5 kV). Chromatographic separation was performed on an Equity-5 Supelco column (length 30 m, internal diameter 0.25 mm, film thickness 0.25 μm), using poly(5%diphenyl/95%dimethyl)siloxane as stationary phase and He as carrier gas (flow rate 0.7 mL/min, surge pressure 27.7 kPa). The ion source and interface temperature was 280°C, while the scan range m/z 40-800. The chromatographic heating gradient was as follows: initial temperature 57°C, 2 min isothermal, then ramped at 10°C/min up to 200°C, 3 min isothermal, then ramped at 20°C/min up to 300°C and then isothermal for 20 min. Prior to the analysis, a total of 230 μg of each sample was submitted to derivatization in 20 μL of BSTFA + 1% TMCS and 50 μL of ethyl acetate, heating at 70°C for 30 minutes. The injection volume was 1 μL .

SERS spectra were collected with a portable micro-Raman spectrometer, equipped with a 1800 lines/mm grating, a notch filter, an Olympus 50x microscope objective and a Peltier-cooled charge-coupled device (CCD) detector, by using a backscattering geometry. A Nd:YAG laser provided the exciting radiation at 532 nm, with a power at the sample of about 1.5 mW. All the SERS spectra were recorded between 2000 and 200 cm^{-1} by collecting 30 scans with an exposure time of 4 s. A resolution of around 8 cm^{-1} was estimated in the examined spectral range.

Results and discussion

Non-destructive analyses

Before extraction, the ancient wool threads were examined both by color analysis and SEM-EDX. The colorimetric coordinates ($L^* = 52.97$, $a^* = 7.93$, $b^* = 14.56$ for thread 1; $L^* = 66.37$, $a^* = 8.27$, $b^* = 24.60$ for thread 2) showed that the color of the threads can be more precisely defined as reddish-yellow, as also apparent from figure 1. The SEM-EDX analysis of the wool threads showed, besides the presence of sulfur due to amino acids, traces of metals such as Al, Fe and Cu, which could obviously be due to a contamination from the burial environment, even though a possible correlation with the mordant used in the dyeing process cannot be excluded³⁴. A similar result had been obtained for a red-dyed thread found in the same excavation site at In Aghelachem and investigated in our laboratory¹.

Chromatographic analyses

The application of a mild extraction method based on the use of HF at room temperature was essential in order to detect, in the HPLC chromatograms of the extracts obtained from the threads, a relevant amount of

ellagic acid (structure shown in figure 2), allowing us to rule out the presence of other chromophores such as flavonoids from weld or dyer's broom, reported in the literature as widely used in antiquity for dyeing textiles³⁵ (figure 3).

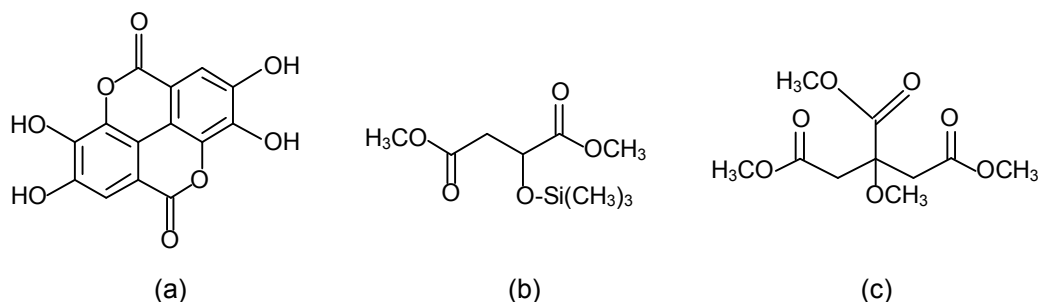


Figure 2. Molecular structures of (a) ellagic acid, (b) [(trimethylsilyl)oxy]dimethyl ester of butanedioic acid and (c) trimethyl ester of citric acid.

In previous studies, the detection of ellagic acid on ancient textiles which were supposed to be dyed with natural substances was not taken into account as a crucial indication of the employed colorant, as ellagitannins could also originate from the decomposition of plant fragments present in the environment, such as dead leaves and bark³⁶. However, in the present case, the possibility that ellagic acid could derive from a contamination is excluded, as previous analyses of a red-dyed thread from the Royal Tumulus showed the exclusive presence of madder without any trace of ellagic acid¹.

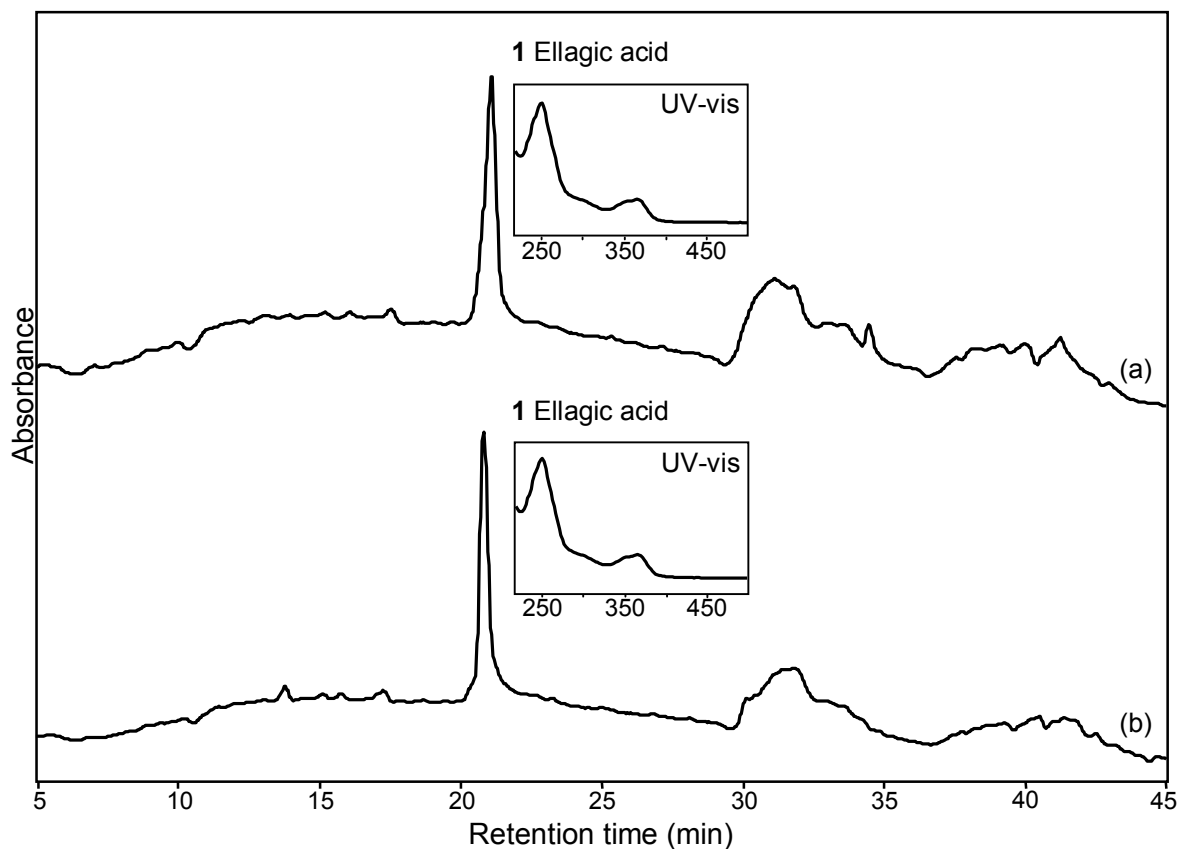


Figure 3. HPLC chromatograms of threads (a) 1 and (b) 2 HF extracts at $\lambda = 365$ nm. The only identified compound is (1) ellagic acid.

At the same time, in the extracts from the threads the presence of significant amounts of malic acid and a smaller quantity of citric acid (structures shown in figure 2) was highlighted by means of GC-MS (figure 4). Even though these substances are often detected in natural materials, their relative quantities in the samples investigated here are relevant and, moreover, they were not found in the red-dyed thread from the same excavation, thus suggesting that their presence is related to the dyeing process.

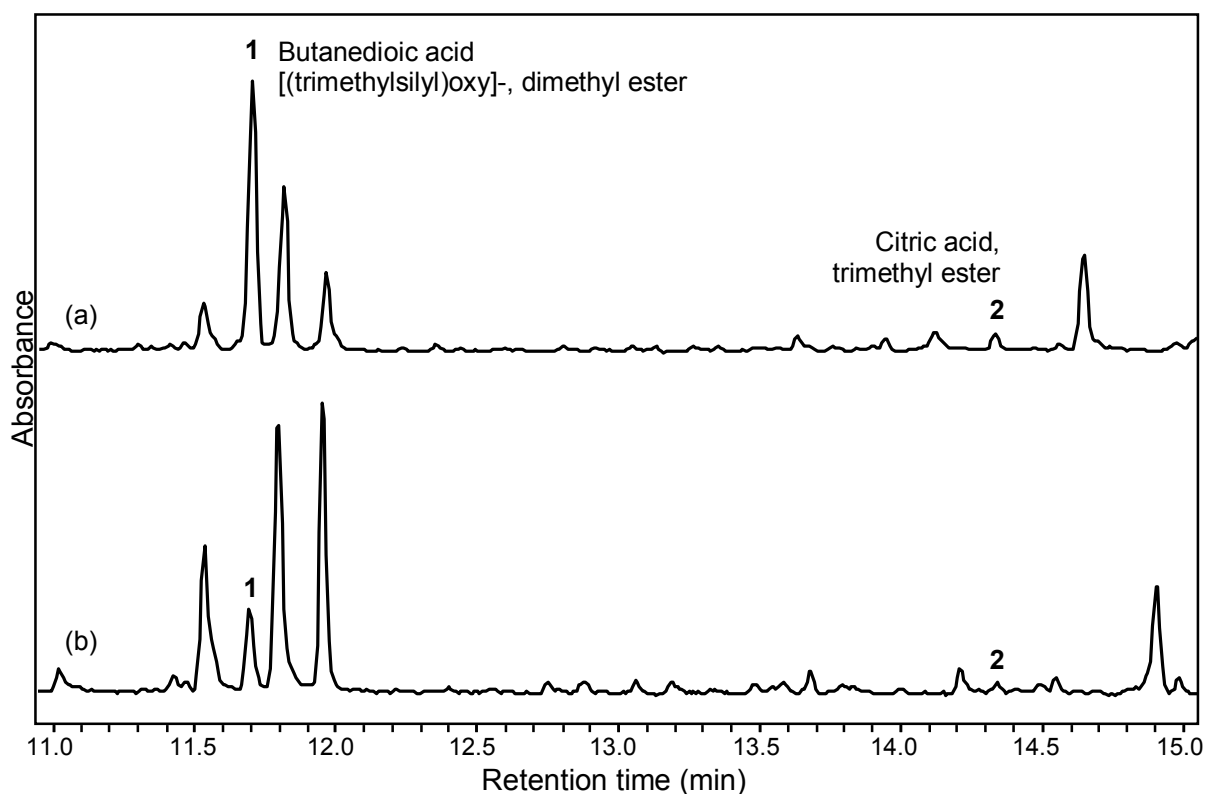


Figure 4. GC-MS chromatograms of threads (a) 1 and (b) 2 HF extracts. The identified compounds are (1) [(trimethylsilyl)oxy]dimethyl ester of butanedioic acid and (2) trimethyl ester of citric acid.

The results of chromatographic analyses hinted that, among the natural sources in the Fezzan area during the Garamantian period for reddish-yellow dyes³⁷, the most probable candidates were the fruits of pomegranate and sumac (table 1), i.e. plant parts that, besides containing tannins, could also be rich in malic acid (hydroxybutanedioic acid)^{2,38-40}.

Extracts from pomegranate rind and sumac berries, as well as from wool dyed with such colorants, were thus studied for comparison. Relevant amounts of ellagic and malic acids were found in both pomegranate and sumac extracts, ellagic acid being especially abundant in the pomegranate extract and malic acid in sumac extract. In the extracts from the freshly dyed wool threads, comparable amounts of ellagic, malic and citric acids with those detected for archaeological samples could be determined.

Hence, the above-discussed results of HPLC and GC-MS analyses supported the possible use of pomegranate or sumac dyes for the archaeological threads, but they were not decisive in order to point out which one of the two was really employed. However, HPLC analysis was useful, as it allowed us to detect in both cases other substances besides ellagic acid, which can be considered the real chromophores because of their absorption at higher wavelengths. Indeed, sumac was found to contain also anthocyanins, which could be

suggested as responsible for the intense red color of the extract, while high quantities of ellagitannins such as punicalagin were identified in the pomegranate extract and the reference dyed wool (figure 5), which are supposed to give rise to the yellow color thanks to their absorption at 380 nm. This latter observation, together with the detection of ellagic acid only in the ancient samples, allowed us to hypothesize that the yellow dye of the threads was from pomegranate. Indeed, ellagitannins were not found in the HPLC analysis of the archaeological samples, but this fact can be attributed to their complete hydrolysis to ellagic acid, which could have occurred over the centuries, and to an oxidative polymerization process which results in the formation of insoluble species⁴¹.

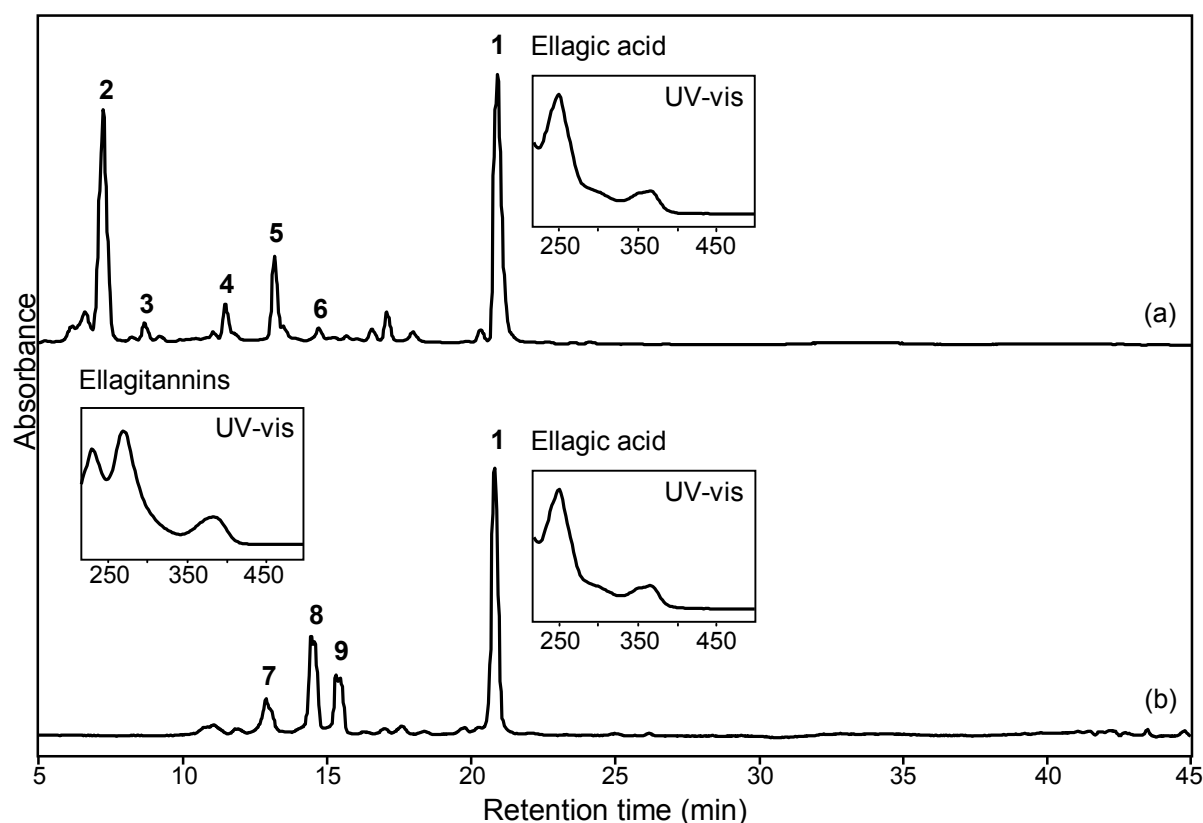


Figure 5. HPLC chromatograms of (a) pomegranate extract obtained from dyed wool and (b) pomegranate extract obtained from the fruit at $\lambda = 365$ nm. Identified compounds are (1) ellagic acid and (2)-(9) ellagitannins.

SERS analyses

SERS has proven to be an effective technique in validating the hypothesis put forward for the identification of the yellow dye on the basis of chromatographic analyses.

Our first attempt led to the collection of SERS spectra from the thread extracts by using 35 μ L of 1 M NaCl or 150 μ L of 0.01% poly-L-lysine together with 35 μ L of 1 M ascorbic acid as aggregants (figure 6), as this procedure previously allowed the identification of a red dye in a dyed wool thread from In Aghelachem¹. However, this method was not successful in the present case. The use of 1.8 M NaClO₄, already exploited in the construction of a SERS spectral database of colorants and discussed in Chapter 2, was found to be crucial to obtain from the samples good quality SERS spectra, especially when added to the colloid after the analyte, i.e. in an inverted order when compared to the most widely used procedure reported in the literature (figure 6).

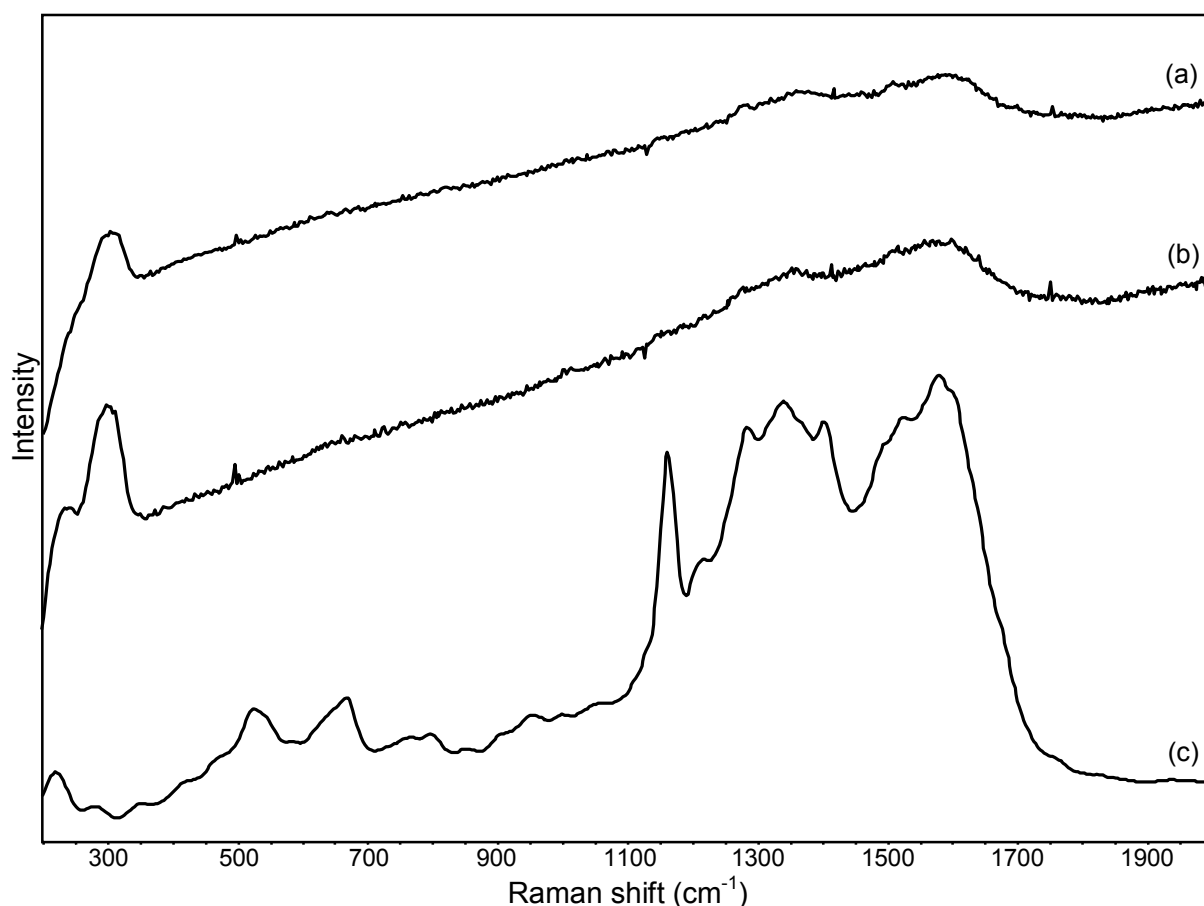


Figure 6. SERS spectra of extracts from thread 1 (a) on Ag Lee-Meisel colloid aggregated by adding 1 M NaCl, (b) on Ag Lee-Meisel colloid aggregated by the use of poly-L-lysine and ascorbic acid and (c) on Ag Lee-Meisel colloid aggregated by adding 1.8 M NaClO₄. Similar results were obtained for thread 2.

In accordance with the results acquired by HPLC, the SERS spectra obtained for the extracts from the archaeological samples were found to be clearly different from those of flavonoid dyes such as weld and dyer's broom (figure 7; the corresponding wavenumbers with relative intensities are listed in table 2), allowing us to exclude the possible use of this latter kind of substances as coloring matter for the ancient threads.

Comparing the results obtained from the SERS analysis of pomegranate and sumac reference dyes (Figure 7; the corresponding wavenumbers with relative intensities are listed in table 2), a greater similarity was observed between the spectra of the archaeological samples and those of pomegranate dye. The SERS spectrum of the sumac extract shows a very good correspondence with that of dragon's blood discussed in Chapter 2, as expected due to the similar molecular structure of their chromophores, as well as with the Raman and resonance Raman spectra of the hydroxyflavylium structure of anthocyanins reported in the literature. In particular, the bands at 1637, 1585, 1534, 1485, 1430 and 1357 cm⁻¹ are assigned to ring stretching vibrational modes, while the band at 1328 cm⁻¹ is attributed to the $\delta(\text{CH})$ modes; the band at 1247 cm⁻¹ is due to the C-O stretching mode and the medium intensity bands at 709 and 548 cm⁻¹ are assigned, respectively, to the $\delta(\text{CC})$ modes of the phenyl and benzopyrylium rings⁴². On the contrary, the SERS spectrum of the aqueous extract of pomegranate rind shows a similar, even if not identical, pattern to that of ellagic acid, indicating that the interaction between the Ag surface and the molecules of ellagitannins takes place through the polyphenolic moieties of the latter. The main difference between the spectrum of ellagic acid and that of

pomegranate extract lies in the relative intensities and exact wavenumbers of the bands assigned to stretching vibrations of the aromatic rings. Indeed, such signals are observed at 1603, 1560, 1492 and 1376 cm^{-1} for ellagic acid and at 1603, 1548, 1492 and 1359 cm^{-1} for ellagitannins from pomegranate.

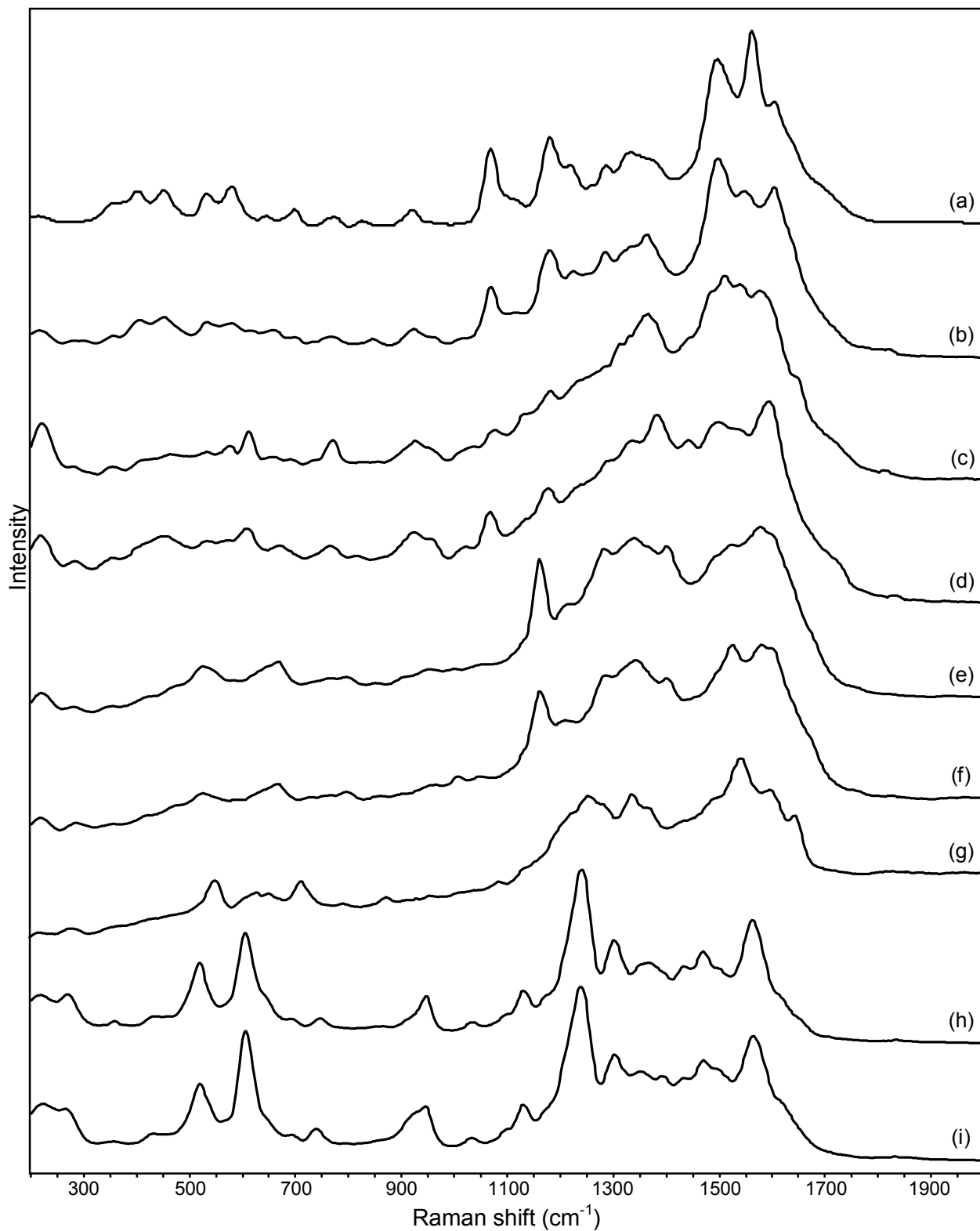


Figure 7. SERS spectra of (a) ellagic acid and extracts from (b) pomegranate rind, (c) mordanted and (d) unmordanted wool dyed with pomegranate, threads (e) 1 and (f) 2, (g) sumac berries, (h) weld and (i) dyer's broom vegetable cut pieces. All the spectra were obtained in MeOH solutions on Ag Lee-Meisel colloids aggregated by adding 1.8 M NaClO_4 to the nanoparticles after the analyte.

Table 2. Frequencies of SERS spectra reported in Figure 7 with relative intensities.

| Dyes | SERS bands (cm ⁻¹) |
|--|--|
| Ellagic acid Fig. 7 - Spectrum (a) | 1603m, 1560vs, 1492s, 1376sh, 1333m, 1285m, 1220m, 1178m, 1064m, 958vw, 921w, 827vw, 771vw, 699vw, 649vw, 580w, 531w, 450w, 405w, 355vw, 266vw, 222vw |
| Pomegranate rind Fig. 7 - Spectrum (b) | 1603m, 1548m, 1492s, 1359m, 1333sh, 1285m, 1220m, 1178m, 1064m, 1014vw, 958sh, 921w, 845vw, 771vw, 699vw, 657vw, 609vw, 580w, 531w, 450w, 405w, 352vw, 283vw, 222vw |
| Pomegranate-dyed mordanted wool Fig. 7 - Spectrum (c) | 1597s, 1544s, 1507s, 1359m, 1333sh, 1285sh, 1220sh, 1178w, 1064w, 1014vw, 958sh, 921w, 827vw, 771w, 699vw, 657vw, 609w, 580vw, 531vw, 450vw, 407vw, 352vw, 283vw, 222w |
| Pomegranate-dyed unmordanted wool Fig. 7 - Spectrum (d) | 1584s, 1544m, 1492m, 1381m, 1333m, 1285sh, 1220sh, 1178w, 1064w, 1014vw, 958sh, 921w, 819vw, 771w, 699sh, 668vw, 609w, 580vw, 531vw, 450w, 407vw, 352vw, 283vw, 222w |
| Thread 1 Fig. 7 - Spectrum (e) | 1603sh, 1578vs, 1522s, 1401s, 1335vs, 1285s, 1215m, 1159s, 1003vw, 954vw, 904vw, 802vw, 766vw, 725vw, 668w, 618sh, 582vw, 529w, 470vw, 412vw, 352vw, 283vw, 222w |
| Thread 2 Fig. 7 - Spectrum (f) | 1603sh, 1578vs, 1522vs, 1401s, 1335vs, 1285s, 1215m, 1159s, 1003vw, 956vw, 904vw, 802vw, 766vw, 725vw, 668w, 618sh, 582vw, 529w, 470vw, 412vw, 352vw, 283vw, 222w |
| Sumac berries Fig. 7 - Spectrum (g) | 1637s, 1585s, 1534vs, 1485sh, 1430sh, 1357sh, 1328s, 1275sh, 1247s, 1085vw, 960vw, 873vw, 794vw, 709m, 650w, 627w, 548m, 283vw, 222vw |
| Weld Fig. 7 - Spectrum (h) | 1562s, 1495sh, 1467s, 1430m, 1390sh, 1367m, 1300s, 1239vs, 1173sh, 1128w, 1094sh, 1029vw, 944w, 923sh, 745vw, 692vw, 645sh, 605s, 518m, 429vw, 359vw, 266w, 220w |
| Dyer's broom Fig. 7 - Spectrum (i) | 1562s, 1495sh, 1467s, 1430m, 1390m, 1351m, 1300s, 1239vs, 1173sh, 1128w, 1094sh, 1029vw, 944w, 923sh, 737vw, 692vw, 645sh, 605s, 518m, 429vw, 359vw, 266w, 220w |

As reported in table 2, the remaining bands are located at the same wavenumbers in both spectra. The most prominent ones have been assigned to the combination of C-O stretching and O-H deformation vibrations (1333 and 1178 cm⁻¹)⁴³ and to the breathing of the lacton and aryl rings (1064 cm⁻¹)⁴⁴. For comparison, figure 7 also reports the SERS spectra obtained from the acid extracts of mordanted and unmordanted wool dyed with pomegranate rind. Both spectra show a remarkable similarity with the pattern observed for the fruit extract, as also evidenced by the wavenumbers reported in table 2. As already stated, the spectra obtained for the extracts from the archaeological threads have a pattern similar to that of pomegranate dye, even though some differences can be observed. The most evident change is associated with the disappearance of the band at 1064 cm⁻¹, previously assigned to the lacton rings. Indeed, the opening of such rings is evident in oligomeric ellagitannins⁴⁵. Moreover, the intensity of the bands attributed to the combination of C-O stretching and O-H deformation modes, located at 1335 and 1159 cm⁻¹ (shifted in comparison with those observed for the pomegranate extract), is significantly increased. At the same time, in the region where the ring stretching vibrations are observed, the strongest band appears at 1578 cm⁻¹ and can be considered characteristic of highly substituted phenolic structures⁴⁶. The global enhancement of bands involving phenol groups supports

again the hypothesis of the formation of polymeric ellagitannins due to oxidation upon ageing of pomegranate dye⁴¹. Therefore, the results reported above support again the use of pomegranate for dyeing the archaeological samples.

Conclusions

The analytical results reported in this chapter allowed the characterization of two natural sources of yellow dyes, i.e. sumac berries and pomegranate rind, which have not been examined in detail so far from the point of view of their dyeing properties for historical textiles. In the context of a multi-technique approach for the identification of such colorants, special attention was paid to SERS: the good performance of 1.8 M NaClO₄ as aggregating agent was highlighted in comparison with that of other electrolytes employed in previous works on different dyes, especially when added to the silver colloid after the analyte, in an inverted order when compared to the most widely used procedure. By using this method, good quality SERS spectra of ellagic acid and colorants extracted from pomegranate and sumac fruits were obtained in this study for the first time.

From the archaeological point of view, the present work sheds new light on the dyeing technology in the Libyan Sahara during the Garamantian period and, more generally, on the use of pomegranate extract in antiquity to obtain yellow-dyed textiles. In particular, even though *P. granatum* was part of the archaeobotanical record of Garamantian sites, its seeds/fruits or pollen were not discovered in such great amounts to demonstrate its use as a dyeing plant, which instead could be ascertained in the present study. As a consequence, the pomegranate remains discovered in the area were likely to be part of the new Mediterranean/Near Eastern luxury goods exchanged by the Garamantian merchants.

Acknowledgements

A special thank to dr. Eleonora De Luca (Dipartimento di Chimica Inorganica, Metallorganica e Analitica “L. Malatesta”, Università degli Studi di Milano) for dyeing the reference wool samples and to professor Anna Maria Mercuri (Laboratorio di Palinologia e Paleobotanica, Dipartimento di Biologia, Università di Modena e Reggio Emilia) for giving us essential information about the archaeobotanical context of the Fezzan area in Garamantian times. Dr. Tommaso La Mantia (Università di Palermo) is also acknowledged for collecting sumac fruits and for giving us useful information regarding this plant, and dr. Lucia Mori for providing us with the archaeological samples.

References

- [1] S. Bruni, V. Guglielmi, F. Pozzi, *J. Raman Spectrosc.* **2010**; *41*, 175.
- [2] Z. C. Koren, in *Archaeological Chemistry*, ACS Symposium Series 625, (Ed: M. V. Orna), American Chemical Society, Washington DC, **1996**, p. 269.
- [3] J. S. Mills, R. White, *The Organic Chemistry of Museum Objects*, Butterworths, London, **1994**, p. 121.
- [4] A. M. Mercuri, *J. Archaeol. Sci.* **2008**; *35*, 1619.
- [5] A. M. Mercuri, G. Bosi, L. Olmi, L. Mori, E. Gianassi, A. Florenzano, *Boccone* **2009**; *23*, 379.
- [6] C. Ward, *World Archaeol.* **2003**; *34*, 529.
- [7] R. Pelling, *J. N. Afr. Stud.* **2005**; *10*, 397.
- [8] R. Pelling, in *Food, Fuel and Fields: Progress in African Archaeobotany*, Monographs on African Archaeology and Environment, vol. 15, (Eds: K. Neumann, A. Butler, S. Kahlheber), Heinrich-Barth Institut, Köln, **2003**, p. 129.
- [9] A. M. Mercuri, G. Trevisan Grandi, G. Bosi, L. Forlani, F. Buldrini, in *Aghram Nadharif. The Barkat Oasis (Sha'abiya of Ghat, Libyan Sahara) in Garamantian Times*, AZA Monographs, vol. 5, (Ed: M. Liverani), All'Insegna del Giglio, Firenze, **2005**, p. 335.
- [10] J. Cannon, M. Cannon, *Dye Plants and Dyeing*, Timber Press, Portland, **2003**, p. 128.
- [11] R. Corti, *Flora e Vegetazione del Fezzan e della Regione di Gat*, Reale Società Geografica Italiana, Firenze, **1942**, p. 505.
- [12] K. Fern, *Plants For A Future: Edible & Useful Plants For A Healthier World*, Permanent Publications, Clanfield, **2007**, p. 300.
- [13] M. Grieve, *A Modern Herbal*, Harcourt Brace, New York, **1931**, p. 919.
- [14] I. Grae, *Nature's Colors - Dyes from Plants*, MacMillan Publishing Co., New York, **1974**, p. 229.
- [15] P. C. M. Jansen, D. Cardon (Eds), *Plant Resources of Tropical Africa 3. Dyes and Tannins*, PROTA Foundation, Backhuys Publishers, Leiden, **2005**, p. 216.
- [16] J. C. Th. Uphof, *Dictionary of Economic Plants*, Hafner Publishing, New York, **1959**, p. 400.
- [17] P. M. Guarrera, *J. Ethnobiol. Ethnomed.* **2006**, *2*, 9.
- [18] A. M. Mercuri, *J. Arid Environ.* **2008**, *72*, 1950.
- [19] D. Zohary, M. Hopf, *Domestication of Plants in the Old World* (2nd ed.), Clarendon Press, Oxford, **1994**, p. 279.
- [20] G. Bosi, A. M. Mercuri, C. Guarnieri, M. Bandini Mazzanti, *Veg. Hist. Archaeobot.* **2009**; *18*, 389.
- [21] W. F. Jashemski, F. Meyer, *The Natural History of Pompeii*, Cambridge University Press, New York, **2002**, p. 528.
- [22] L. J. M. Columella, *De Re Rustica*, Book 12 (trans. R. Calzecchi-Onesti), Ramo Editoriale degli Agricoltori, Roma, **1947-1948**.
- [23] J. F. Dastur, *Useful Plants of India and Pakistan*, D.B. Taraporewala & Co. Pvt Ltd, Bombay, **1964**, p. 260.
- [24] S. Di Lernia, G. Manzi (Eds), *Sand, Stones and Bones*, AZA Monographs, vol. 3, Firenze, **2002**, pp. 102, 160, 165.
- [25] J. H. Park, B. M. Gatewood, G. N. Ramaswamy, *J. Appl. Polym. Sci.* **2005**; *98*, 322.
- [26] M. P. Colombini, A. Andreotti, C. Baraldi, I. Degano, J. J. Lucejko, *Microch. J.* **2007**; *85*, 174.

- [27] F. M. Helmi, O. M. El-Feky, E. H. Salib, *Egypt. J. Anal. Chem.* **2008**; 17, 53.
- [28] W. Novik, S. Desrosiers, I. Surowiec, M. Trojanowicz, *Archaeometry* **2005**; 47, 835.
- [29] J. Sanyova, *Microchim. Acta* **2008**; 162, 361.
- [30] M. Leona, J. Stenger, E. Ferloni, *J. Raman Spectrosc.* **2006**; 37, 981.
- [31] M. A. Khan, M. Khan, P. K. Srivastava, F. Mohammad, *Colourage* **2005**; 52, 53.
- [32] H. Bozkurt, *J. Sci. Food Agric.* **2006**; 86, 849.
- [33] P. C. Lee, D. J. Meisel, *J. Phys. Chem.* **1982**; 84, 3391.
- [34] M. Müller, B. Murphy, M. Burghammer, I. Snigireva, C. Riekkel, J. Gunneweg, E. Pantos, *Appl. Phys. A* **2006**; 83, 183.
- [35] E. S. B. Ferreira, A. N. Hulme, H. McNab, A. Quye, *Chem. Soc. Rev.* **2004**; 33, 329.
- [36] W. Nowik, S. Desrosiers, I. Surowiec, M. Trojanowicz, *Archaeometry* **2005**; 47, 835.
- [37] A. J. Thompson, K. A. Jakes, *Southeast. Archaeol.* **2002**; 21, 252.
- [38] S. Kurucu, M. Koyuncu, A. Güvenç, *J. Essent. Oil Res.* **1993**; 5, 481.
- [39] P. Legua, P. Melgarejo, M. Martínez, F. Hernández, *Options Méditerr.* **2000**; 42, 99.
- [40] S. M. Mavlyanov, S. Y. Islmbekov, A. K. Karimdzhanov, A. I. Ismailov, *Chem. Nat. Comp.* **1997**; 33, 279.
- [41] N. Vivas, M. F. Nonier, N. Vivas de Gaulejac, I. Pianet de Boissel, *C. R. Chim.* **2004**; 7, 945.
- [42] J. C. Merlin, J. P. Cornard, *Spectrochim. Acta A* **1994**; 50, 703.
- [43] A. Edelman, B. Lendl, *J. Am. Chem. Soc.* **2002**; 124, 14741.
- [44] E. Vogel, W. Kiefer, *Fresenius J. Anal. Chem.* **1998**; 361, 628.
- [45] U. Vrhovsek, A. Palchetti, F. Reniero, C. Guillou, D. Masuero, F. Mattivi, *J. Agric. Food Chem.* **2006**; 54, 4469.
- [46] R. A. Alvarez-Puebla, J. J. Garrido, R. F. Aroca, *Anal. Chem.* **2004**; 76, 7118.

Chapter 4

Identification of dyes in ancient Kaitag textiles from Caucasus

Abstract

Kaitag textiles, named after the Kaitag district of Southwest Daghestan, Russia, where they were manufactured, are a unique embroidered textile art form. They were used by families on special occasions such as the birth, marriage or death of one of their members and were thus passed down from generation to generation as family heirlooms. Today, only a few hundreds of these precious antique specimens can still be found, and surviving examples are mostly from the 17th and 18th centuries.

An extensive work for the scientific analysis of Kaitag textiles was here carried out as the logical continuance and updating of a previous study performed by TLC almost two decades ago. A multi-technique approach involving the combined use of micro-invasive tools, such as HPLC, SERS and SEM-EDX, and non-destructive techniques suitable for *in situ* analyses, such as vis-RS and XRF, aimed to identify the colorants used to dye Kaitag textiles. IRR and UVF were also employed to visualize underlying drawings and possible restorations. Corrosion phenomena observed in brown- and black-dyed areas were also investigated.

Introduction

The so called Kaitag textiles belong to the artistic production of Daghestan, presently a region of Russia situated in the Northern Caucasus with a mainly mountainous landscape. About 2.5 million inhabitants are distributed among 700 villages and 31 ethnical groups, one of them named Kaitag, with different languages and religious beliefs, from Christian and Jewish to Zoroastrian and Islamic¹. This great variety of traditions was also reinforced by the particular location of Daghestan on the ancient silk road that passed near the town of Derbent.

As described by Robert Chenciner, who first brought Kaitag textiles to the knowledge of the Western world, they were intended for ritual purposes, and particularly for protecting babies in a cradle from the devil eye, wrapping bridal dowry jewellery and covering the face of dead people². Kaitag textiles are usually cotton squares with silk embroideries, having an average size of 90 x 60 cm and decorative patterns mainly formed by abstract elements such as swastikas, ovals, rosettes and meanders, often deriving from the stylization of phyto- or zoomorphic subjects. The earliest examples are dated to the 16th and 17th centuries², and this production continued until the 19th century.

An extensive work for the scientific analysis of Kaitag textiles was promoted by the MATAM (Museum of Ancient Textile Art of Milan) association and carried out as the logical continuance and updating of the investigations performed by means of TLC by H. Bohmer and R. Karadag almost two decades ago³. On the one hand, this project was inspired by the need to determine, for a given artefact, the execution technique and the materials used, not only for the sake of knowledge but also for practical conservation purposes; from a methodological point of view, it was a convenient way of validating several micro- and non-destructive techniques which were used to gain knowledge about these precious artifacts, trying at the same time to safeguard the integrity of the objects studied. The most representative tints were selected for analysis in order to gain a wider knowledge of the dyes, and their combinations, employed over the centuries in Daghestan. A special attention was paid to those shades for which the identification of colorants is notoriously more difficult, especially yellows, and to cases of suspected alteration of the dye or evident damage to the thread.

In this chapter, the analytical results of the scientific study of 23 Kaitag textiles mostly dating from the 17th to the 18th century (figure 1) are presented, with special focus on the identification of colorants. A preliminary imaging campaign was performed on all of them using IRR and UVF, in order to better understand the technique used, study the underlying drawing and highlight any later integrations of the textiles. Thereafter, the dyes were analyzed by Gianluca Poldi (Dipartimento di Lettere, Arti e Multimedialità, Università degli Studi di Bergamo) using non-invasive techniques such as vis-RS, and colorimetric data were acquired on each of the points studied during the vis-RS measurements. Also, XRF was performed on two of the fabrics using a portable handheld spectrometer, while SEM-EDX was applied to the possible detection of mordants and to the investigation of corrosion phenomena observed in brown- or black-dyed areas of several among the examined Kaitag textiles. After that, several extraction procedures, based on the use of HF, HCl or pyridine in different experimental conditions, were applied to 65 dyed threads from Kaitag textiles typically less than 0.5 mm in length, which were then subjected to micro-destructive analyses by HPLC and SERS. A number of natural colorants could be thus identified by comparison with reference spectra belonging to a database previously acquired and discussed in Chapter 2.



Figure 1 (to be continued). Northeast Caucasian Kaitag textiles studied in the present work. Kaitag textiles 2 and 10 are dating to the 17th century, Kaitag textiles 1, 3, 4, 5, 6, 8, 11, 13 and 14 to the 18th century, while Kaitag textile 7 to the first half of the 19th century.



Figure 1 (continued). Northeast Caucasian Kaitag textiles studied in the present work. Kaitag textiles 20 and 21 are dating to the 17th century, while Kaitag textiles 16, 17, 18, 19, 24, 25, 26, 27 and 30 are dating to the 18th century.

Experimental

Chemicals

Silver nitrate, sodium perchlorate monohydrate, trifluoroacetic acid, hydrofluoric acid and pyridine were purchased from Fluka, methanol, trisodium citrate dihydrate and acetonitrile from Sigma-Aldrich, while hydrochloric acid was obtained from Riedel-de Haën. All the aqueous solutions were prepared by using ultrapure water (Millipore MilliQ).

Analytical methods: extraction procedures, Ag colloid synthesis and sample preparation

Several extraction procedures, based on the use of HCl, HF or pyridine in different experimental conditions depending on the dye color, were applied to 65 thread fragments of Kaitag textiles, typically less than 0.5 mm in length. The extracts thus obtained were then subjected to micro-destructive analyses by HPLC and SERS in order to identify the colorants.

HCl extraction - Red samples were treated with 6 mL of methanol and 200 μ L of 37% HCl at 65°C for 30 minutes, filtering the obtained solution through a 0.45 μ m GHP Acrodisc membrane filter and drying it under a N₂ gentle stream⁴.

HF extraction - Yellow, green, brown and black samples were suspended in 200 μ L of 4 M HF and placed in a polyethylene test tube which was kept at room temperature under magnetic stirring for 30 minutes. The resulting extracts were thus loaded onto a Discovery Supelco C18 SPE cartridge previously preconditioned by 5 mL of a 1:1 methanol:acetonitrile solution and 5 mL of milliQ water. Fluorides were washed from the cartridge with 5 mL of milliQ water with 0.01% trifluoroacetic acid, and the dyestuffs were then eluted using 3 mL of a 1:1 methanol:acetonitrile solution acidified with 0.01% trifluoroacetic acid. The so obtained solutions were finally evaporated under a N₂ gentle stream⁵.

Pyridine extraction - Blue samples were treated with a 1:1 pyridine:water solution at 90°C for 15 minutes, filtering the obtained suspension through a 0.45 μ m GHP Acrodisc membrane filter and drying it under a N₂ gentle stream⁶.

Silver colloids prepared according to the Lee-Meisel procedure⁷, i.e. by reduction of silver nitrate with trisodium citrate dihydrate, were used as a SERS metal substrate; their synthesis is described in detail in Chapter 2.

The SERS spectra acquired from Kaitag samples were all collected by adding in a test tube 300 μ L of a methanolic solution of the unknown analyte to 3 mL of Ag Lee-Meisel colloid, with subsequent addition of 125 μ L of 1.8 M NaClO₄ under magnetic stirring, in order to induce aggregation of the nanoparticles. SERS measurements were performed by focusing the laser beam on a drop of the dye-colloid system deposited on the surface of a glass slide.

Instrumentation

HPLC analyses were performed with an HPLC PU-1580 Jasco pump equipped with an LG-1580-02 Jasco gradient valve and a GASTORR GT-103 solvent degasser, by using an MD 1510 Jasco photodiode array (PDA) detector in order to obtain spectral information between 200 and 600 nm. A 25 μ L injection volume of a methanolic solution of the analyte was used for the analysis, which was executed on a Supelco Discovery C18 column (25 cm x 4.66 mm, particle diameter 5 μ m), with (A) ultrapure water and (B) acetonitrile both with 0.1% of trifluoroacetic acid as solvents, setting the flow rate at 1 mL/min. The solvent gradient was as follows: 95-70% A in 0-25 min, 70-40% A in 25-30 min, 40-5% A in 30-38 min, 5-95% A in 38-65 min.

SERS spectra were acquired with a portable micro-Raman spectrometer, equipped with a 1800 lines/mm grating, a notch filter, an Olympus 50x microscope objective and a Peltier-cooled charge-coupled device (CCD) detector, by using a back-scattering geometry. A Nd:YAG laser provided the exciting radiation at 532 nm, with a power at the sample of about 1.5 mW. All the SERS spectra were recorded between 2000 and 200 cm^{-1} as the average of 30 scans with an exposure time of 4 s. A resolution around 8 cm^{-1} was estimated in the examined spectral range.

SEM-EDX analyses were performed by means of a Hitachi-TM 1000 scanning electron microscope covering a magnification range between 20x and 10000x. The instrument was equipped with an energy-dispersive electron microprobe, a pre-centered cartridge filament and a high-sensitive semiconductor backscattered electron (BSE) detector. An accelerating voltage of 15 eV was employed for measurements.

Vis-RS measurements were carried out with a Minolta CM-2600d portable and compact spectrophotometer equipped with an internal integrating sphere and three Xenon pulsed lamps (52 mm diameter, d/8 geometry, standard black and white calibration), using a wavelength range of 360-740 nm, a wavelength pitch of 10 nm, a half bandwidth of 10 nm, with specular component included and excluded (SPIN and SPEX modes), and UV component included. Colorimetric data in the CIELab* space were also collected. Areas of 3 mm in diameter were studied, keeping the spectrophotometer in contact with the sample. For each color, 2 or 3 measurements were taken to assess reproducibility. This analytical technique⁸, mainly applied to the identification of pigments⁹, appears to be useful to distinguish some classes of dyes, like indigo and some reds, as sometimes pointed out in the literature^{10,11}.

XRF analyses were performed on scanning areas of 3 mm in diameter with a Thermo Scientific Niton XL3t 900s GOLDD energy dispersive portable spectrometer provided with an Ag anode (maximum voltage 50 kV, current 35 μ A), 4 built-in filters (6 kV no filter; 20 kV Cu filter; 40 kV Fe filter; 50 kV Mo filter), and an SDD detector. The acquisition time was 30 s for each filter. The possibility of operating at low voltages, i.e. 6 and 20 kV, is of utmost importance to allow the identification of light elements, such as Si, S and K.

IR reflectographic inspections were performed using a modified digital camera (Si-CCD detector, 5 Mpx, image maximum resolution 20 lines/mm) with a 850 nm high-pass filter and a 1000 W halogen lamp. The same camera, with a 415 nm high-pass, was used to record UV-induced fluorescence produced by a UV lamp (gas-discharge bulb, MPXL technology, maximum emission peak 356 nm). This kind of investigations are normally underestimated in respect to textiles, while they are particularly useful to acquire conservative information¹².

Results and discussion

In this section, a general outline concerning the dyes identified as responsible for the different hues observed on Kaitag textiles is offered. A detailed description of the results obtained is presented in table 1¹³.

Table 1. Analysis of dyes in Kaitag textiles. For each dye the analytical techniques that allowed identification are indicated. Unidentified dyes are marked with “n.d.” (not detected), while “?” means uncertain characterization. Iron amount is defined abundant for relative percentages from 20 to 40% and very abundant for relative percentages from 40 to 60% (referred to the total amount of elements detected by SEM-EDX).

| Kaitag textile | Color | Dyes identified | Analytical techniques |
|----------------|---------------------------|--|-----------------------|
| 1 | blue (background) | indigo | vis-RS |
| | red | madder | vis-RS |
| 2 | golden green (background) | luteolin (weld) + indigo | vis-RS, HPLC, SERS |
| | golden yellow | n.d. (not luteolin) | vis-RS, HPLC |
| | red | madder | vis-RS |
| 3 | red-brown (background) | madder + tannins | vis-RS, HPLC, SERS |
| | dark blue | indigo | vis-RS |
| | dark brown | tannins? | vis-RS |
| 4 | yellow | n.d. yellow (+ small amounts of indigo) | vis-RS, HPLC, SERS |
| | light blue | indigo | vis-RS |
| | red and salmon pink | madder | vis-RS |
| | brown (corroded) | tannins? | vis-RS |
| 5 | dark brown | weld + redwood? | vis-RS, HPLC, SERS |
| | light green | indigo + n.d. yellow | vis-RS |
| 6 | brown (background) | tannins? (abundant iron) | vis-RS, SEM-EDX |
| | red | madder | vis-RS, HPLC, SERS |
| | yellow | weld | HPLC, SERS |
| | blue | indigo | vis-RS, HPLC, SERS |
| | green | weld + indigo | vis-RS, HPLC |
| 7 | dark blue (background) | indigo | vis-RS |
| | red | madder | vis-RS |
| | red-pink | madder + n.d. dye | vis-RS |
| | blue-gray | indigo + n.d. yellow | vis-RS |
| 8 | brown | tannins | vis-RS, HPLC |
| | red | madder | vis-RS |
| 10 | green (background) | weld + indigo | vis-RS, HPLC, SERS |
| | red | madder | vis-RS |
| | black (corroded) | tannins (very abundant iron) | vis-RS, HPLC, SEM-EDX |
| 11 | gray ink | carbon based ink (no significant amounts of iron detected) | vis-RS, SEM-EDX |

| | | | |
|----|-----------------------|---|----------------------------|
| | green and white-green | indigo + n.d. yellow | vis-RS |
| 13 | red | madder | vis-RS |
| 14 | wine-red | madder + tannins (abundant iron) | vis-RS, HPLC, SERS |
| | red (various) | madder | vis-RS |
| | brown (corroded) | tannins | vis-RS, HPLC |
| 16 | dark brown (corroded) | tannins | vis-RS, HPLC |
| | green | indigo + n.d. yellow | vis-RS |
| | red | madder | vis-RS |
| 17 | light green | indigo + n.d. yellow | vis-RS |
| | red | madder | vis-RS |
| 18 | red | madder | vis-RS, HPLC, SERS |
| | blue | indigo | vis-RS |
| 19 | pink | redwood? | vis-RS, HPLC, SERS |
| | green-yellow | weld + indigo | vis-RS, HPLC, SERS |
| | blue | indigo | vis-RS |
| 20 | red (background) | madder | vis-RS, HPLC, SERS |
| | light green | weld + indigo | vis-RS, HPLC, SERS |
| | light yellow | weld | vis-RS, HPLC, SERS |
| | ochre yellow | weld + ? | vis-RS, HPLC, SERS |
| | blue | indigo | vis-RS, HPLC, SERS |
| | black (corroded) | tannins | vis-RS |
| 21 | red (background) | madder | vis-RS, HPLC, SERS |
| | yellow | weld | vis-RS, HPLC, SERS |
| | blue | indigo | vis-RS, HPLC, SERS |
| | green | weld + indigo | vis-RS, HPLC, SERS |
| | brown | tannins (abundant iron) | vis-RS, HPLC, SEM-EDX, XRF |
| | dark ink | carbon based ink (iron amounts detected comparable to background) | vis-RS, XRF, IRR |
| 24 | black | tannins (abundant iron) | vis-RS, SEM-EDX |
| | dark brown | tannins (abundant iron) | vis-RS, HPLC, SEM-EDX |
| | brown (corroded) | tannins? (very abundant iron) | vis-RS, SEM-EDX |
| | red | madder | vis-RS, HPLC, SERS |
| | yellow | n.d. | vis-RS, HPLC, SERS |
| 25 | black (background) | indigo + tannins (abundant iron) | vis-RS, HPLC, SEM-EDX |
| | red | madder | vis-RS, HPLC, SERS |
| | dark blue | indigo | vis-RS, HPLC, SERS |
| | blue | indigo | vis-RS |
| | light yellow | weld + ? | vis-RS, HPLC, SERS |
| | golden yellow | <i>Rhamnus</i> specie dye? | vis-RS, HPLC, SERS |

| | | | |
|----|--|----------------------------------|-----------------------------|
| | green | indigo + n.d. yellow | vis-RS, HPLC |
| 26 | dark red | madder | vis-RS |
| | blue | indigo | vis-RS |
| | light green | indigo + n.d. yellow | vis-RS, HPLC |
| | golden yellow | n.d. | vis-RS, HPLC, SERS |
| | dark ink | carbon based ink | vis-RS, XRF, IRR |
| 27 | dark brown (background) | indigo + tannins (abundant iron) | vis-RS, HPLC, SEM-EDX |
| | light brown (2 nd background) | tannins? | vis-RS |
| | yellow-brown | weld? + tannins (abundant iron) | vis-RS, HPLC, SERS, SEM-EDX |
| | yellow | n.d. | vis-RS, HPLC, SERS |
| 30 | brown-gray | indigo + tannins (no iron) | vis-RS, HPLC, SEM-EDX |
| | blue (background and embroideries) | indigo | vis-RS |
| | red | madder | vis-RS |



Figure 2. Visual inspection of a Kaitag textile.

Blues

The detection of indigotin (structure shown in figure 3) by both SERS and HPLC analyses (figures 4 and 5) on the whole range of blue tints for all the Kaitag textiles here studied, from lightest to darkest shades, regardless of the kind of yarn - silk or cotton, clearly suggested the use of indigo or woad, two of the most popular blue colorants widely employed for dyeing fabrics since antiquity. Such dyes can be extracted from *Indigofera tinctoria* and *Isatis tinctoria* respectively, the former being originally from tropical and temperate Asia, as well as parts of Africa, and the latter native to the steppe and desert zones of the Caucasus, Central Asia to Eastern Siberia and Western Asia. It is not possible to distinguish which one of the two colorants was actually used, as indigotin is the main chromophore of both of them. The identification of indigotin was made possible by comparison with reference data from a spectral database of natural dyes previously acquired and presented in Chapter 2¹⁴.

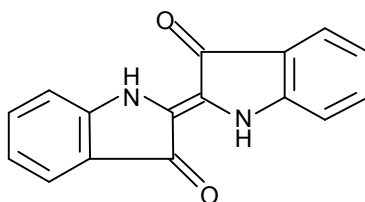


Figure 3. Molecular structure of indigotin, the main chromophore of both indigo and woad.

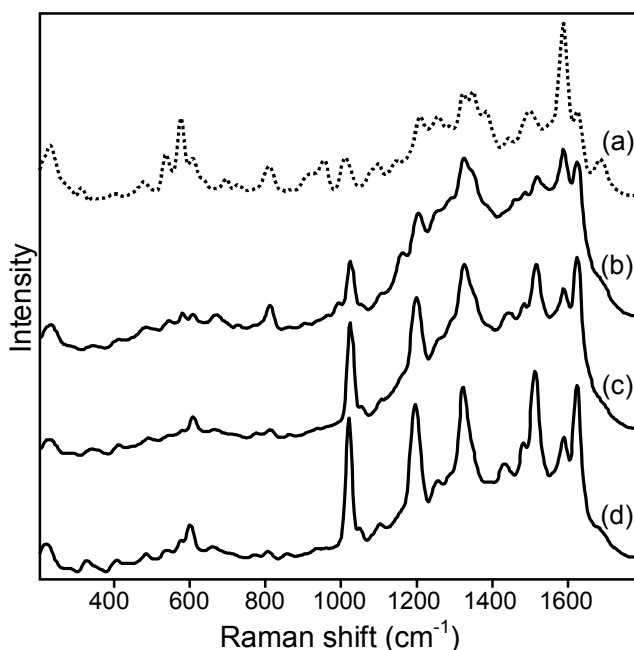


Figure 4. (a) SERS spectrum of reference indigo compared to those of extracts from blue embroideries of (b) Kaitag textile 6, (c) Kaitag textile 21 and (d) Kaitag textile 25.

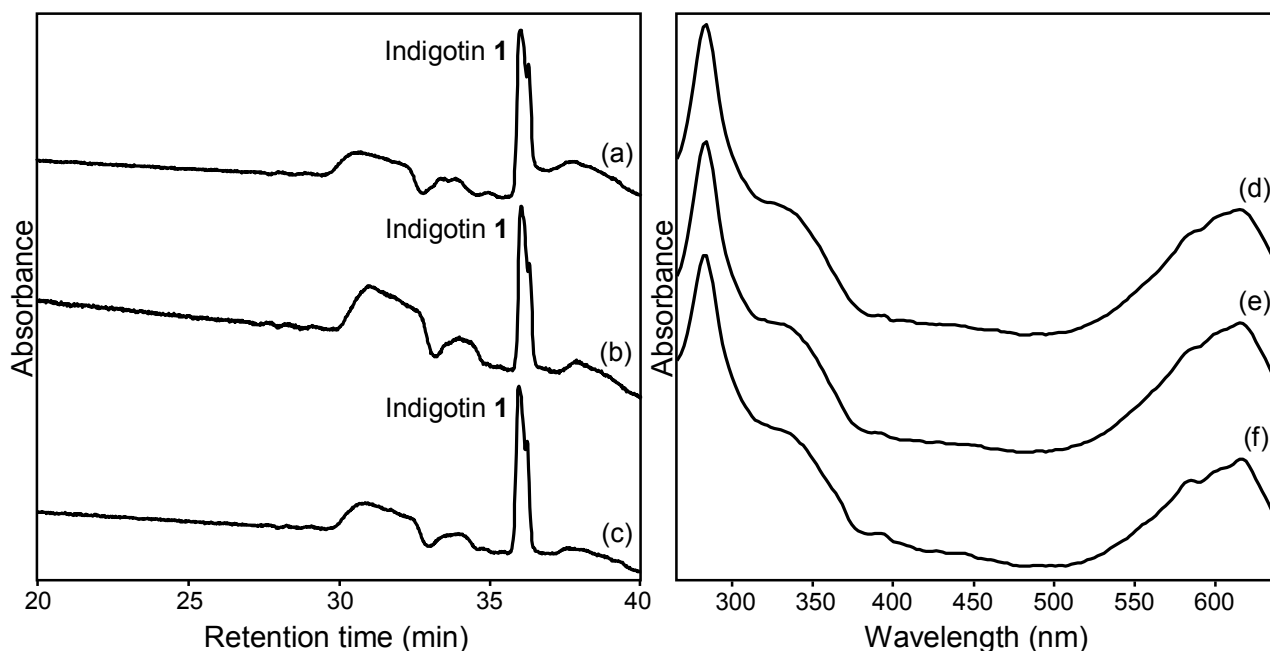


Figure 5. On the left, HPLC chromatograms of extracts from blue embroideries of (a) Kaitag textile 6, (b) Kaitag textile 21 and (c) Kaitag textile 25 at $\lambda = 600$ nm; the only identified compound is (1) indigotin. On the right, UV-vis spectra of indigotin from blue embroideries of (d) Kaitag textile 6, (e) Kaitag textile 21 and (f) Kaitag textile 25.

Preliminary hypotheses concerning the identification of the unknown blue dyes as indigo or woad had been put forward on the basis of vis-RS data, as indigotin exhibits a distinctive absorption band showing a reflectance minimum between 650 and 600 nm. Indigotin was detected not only in all the different shades of blue, but also in some gray, brown and black colors (figure 6).

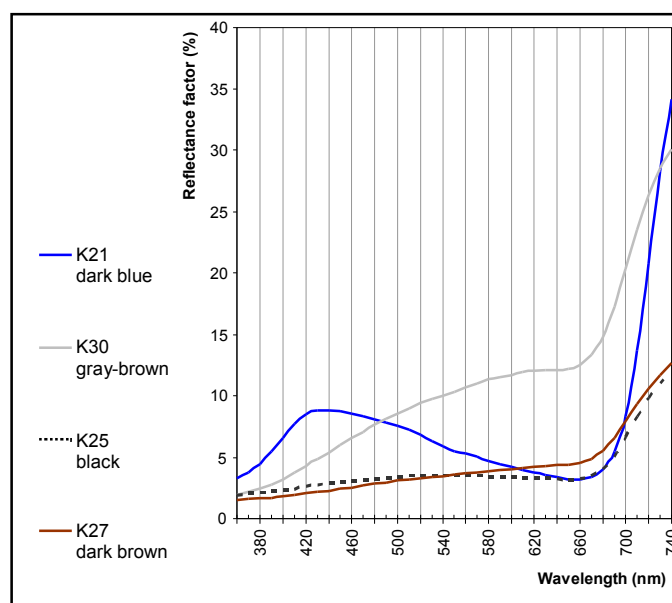


Figure 6. Vis-RS spectra of dark blue, gray-brown, black and dark brown areas of Kaitag textiles 21, 30, 25 and 27 containing indigotin.

Yellows

Yellow colorants are a wide class of substances, often flavonoids, that can be extracted from a number of natural sources the availability of which considerably varies depending on the geographical area, reason that makes their identification a challenging task to be accomplished.

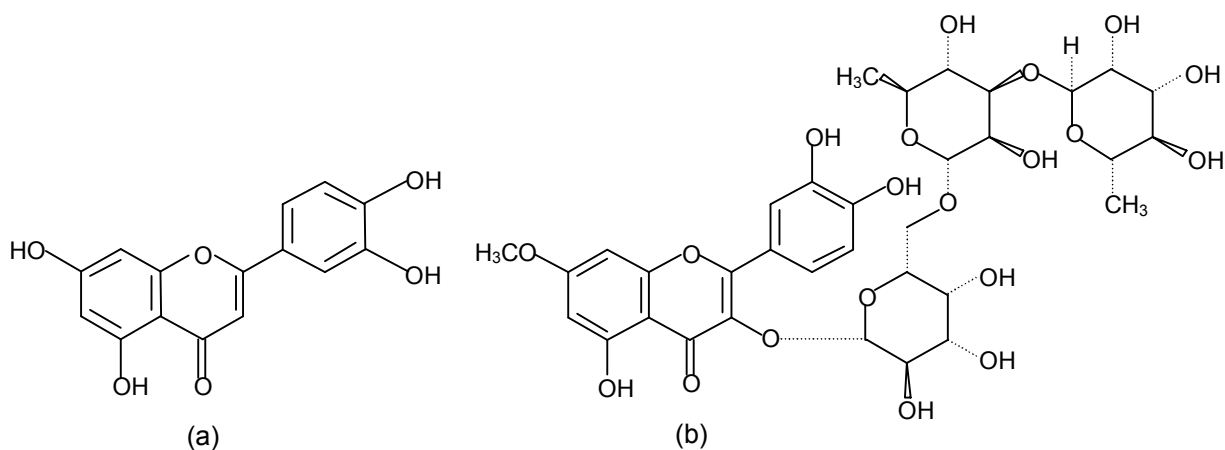


Figure 7. Molecular structures of (a) luteolin, the main chromophore of weld, and (b) xanthorhamnin, the main chromophore of the *Rhamnus* dye sap green.

For light yellow shades of Kaitag textiles 6, 20, 21 and 25, luteolin (structure shown in figure 7), the major chromophore of a few dyes from tinctorial plants such as weld, *Reseda luteola*, was detected by HPLC together with its 7-glucoside (figure 8); consistently, SERS spectra taken from such samples showed a remarkable resemblance with the spectral patterns obtained for reference luteolin and weld extract from the database of natural organic colorants previously acquired and presented in Chapter 2¹⁴ (figure 9).

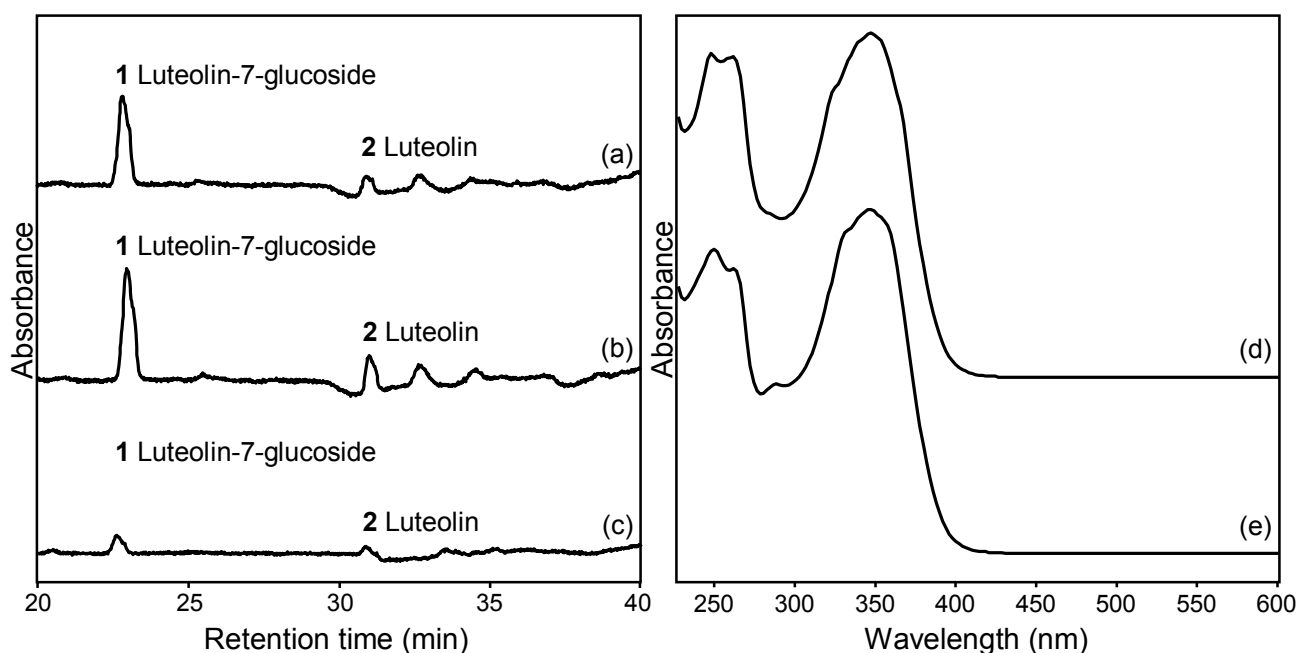


Figure 8. On the left, HPLC chromatograms of extracts from yellow embroideries of (a) Kaitag textile 6, (b) Kaitag textile 20 and (c) Kaitag textile 25 at $\lambda = 365$ nm; identified compounds are (1) luteolin-7-glucoside and (2) luteolin. On the right, UV-vis spectra of (d) luteolin-7-glucoside and (e) luteolin from yellow embroideries of Kaitag textile 6.

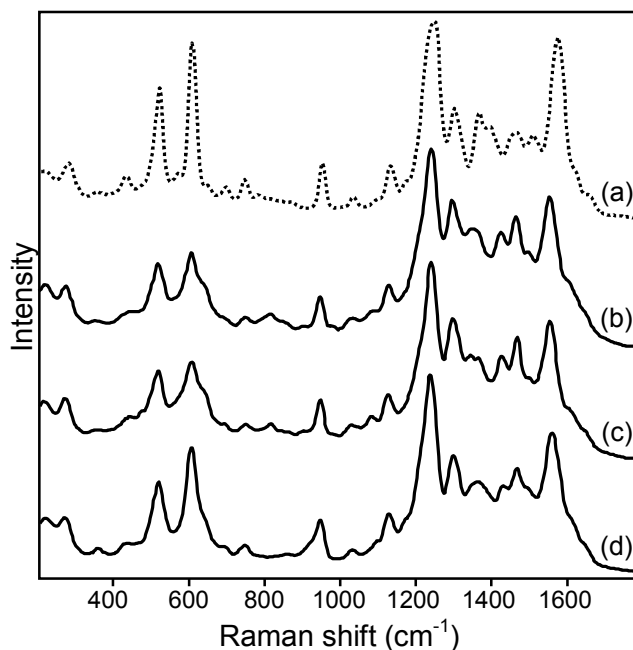


Figure 9. (a) SERS spectrum of reference luteolin compared to those of extracts from yellow embroideries of (b) Kaitag textile 6, (c) Kaitag textile 20 and (d) Kaitag textile 25.

An interesting exception is represented by the golden yellow embroidery of Kaitag textile 25, for which scientific analyses suggested the use of a dye belonging to the *Rhamnus* genus, possibly sap green (figure 10; structure of xanthorhamnin, the main chromophore of sap green, shown in figure 7).

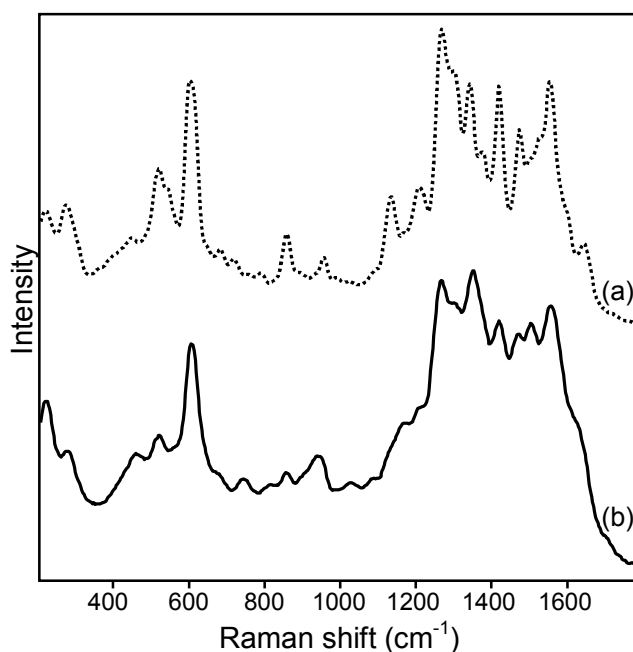


Figure 10. (a) SERS spectrum of the reference *Rhamnus* dye sap green compared to (b) that of the extract from a golden yellow embroidery of Kaitag textile 25.

Different hues of yellow, observed for instance in Kaitag textiles 2, 4, 24, 26 and 27, resulted in HPLC and SERS data which did not allow a certain identification of the corresponding colorants, that however turned out to differ from the previous ones mentioned. Due to the notorious difficulty for vis-RS in discriminating among several yellow dyes which do not exhibit characterizing bands, in this case we opted for taking into account electronic spectra just to accomplish a preliminary distinction among different classes of colorants, which can also be of help when interpreting data obtained from vibrational spectroscopic analyses: indeed, vis-RS spectra of many yellow dyes typically show an inflection point around 450 nm without any further remarkable feature. A number of colorants such as weld, safflower and Persian berries belong to this category, but not, for example, pomegranate, dyers' broom, saffron, turmeric, gamboge, and yellow-beiges such as alkanet and old fustic. As discussed below, the detection of a weak band at 540 nm in gold-yellow areas could be related to the presence of a small amount of madder added to the yellow tint, to which vis-RS is particularly sensitive.

Greens

Because of their poor light and wash fastness, green tints have been produced for long time as mixtures of blue, mainly indigo, and yellow colorants, as it is well documented in Europe and Middle Eastern countries. Consistently, in all the Kaitag textiles here examined, green colors were found to have been obtained by overlapping indigo with a yellow dye which, in most cases, appeared to be the same luteolin-based colorant, possibly weld, above discussed. Such samples invariably exhibited HPLC chromatograms dominated by the peak of indigotin together with that of luteolin-7-glucoside, while their SERS spectra matched all the main features of reference luteolin and weld extract (figure 11).

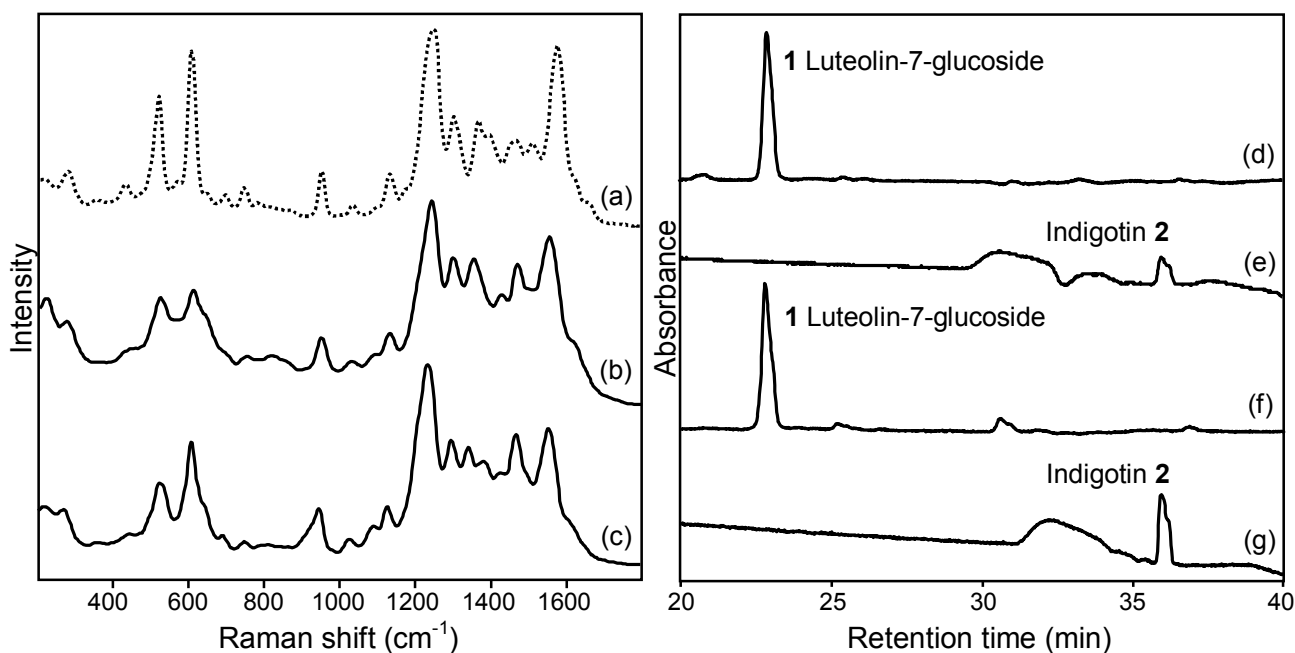


Figure 11. On the left, (a) SERS spectrum of reference luteolin compared to those of extracts from green embroideries of (b) Kaitag textile 20 and (c) Kaitag textile 21. On the right, HPLC chromatograms of extracts from green embroideries of Kaitag textile 20 (d) at $\lambda = 365$ nm and (e) at $\lambda = 600$ nm, and Kaitag textile 21 (f) at $\lambda = 365$ nm and (g) at $\lambda = 600$ nm; identified compounds are (1) luteolin-7-glucoside and (2) indigotin.

Different is the case of Kaitag textile 25, for which a dye belonging to the *Rhamnus* genus was detected as responsible for yellow shades: similarly, a yellow colorant different from weld seemed to have been employed in mixture with indigo to obtain greens as well, even though HPLC analysis was not able to ascertain whether or not such dye was the same used to achieve yellow tints in this Kaitag textile. Vis-RS measurements showed that the typical absorption band of indigo can be still recognized around 650 nm for green areas, while only in a few cases, when dealing with certain kinds of yellow colorants, it is shifted towards lower wavelengths, namely 630 nm, or again, when the main contribution is from yellow, it looks distorted, although the characteristic slope over 660-670 nm remains unchanged. Despite the fact that for vis-RS the identification of yellow dyes used in mixtures with blues to produce green shades is even more complex than the recognition of pure yellows, visible spectra obtained from green areas generally offer useful information if compared with those collected from yellow embroideries of the same Kaitag textiles: indeed, if the same yellow dye is employed both for yellow and green tints, spectra will exhibit the inflection point at the same wavelength in the blue region and similar ascending slopes within 460-470 nm (figure 12). In extremely rare cases, for instance Kaitag textile 20, the concave shape of the whole spectrum obtained from dark greens indicates that this particular shade did not arise from a mixture of indigo together with a yellow dye, but a brown colorant is present, possibly together with yellows compatible with weld or safflower (figure 12).

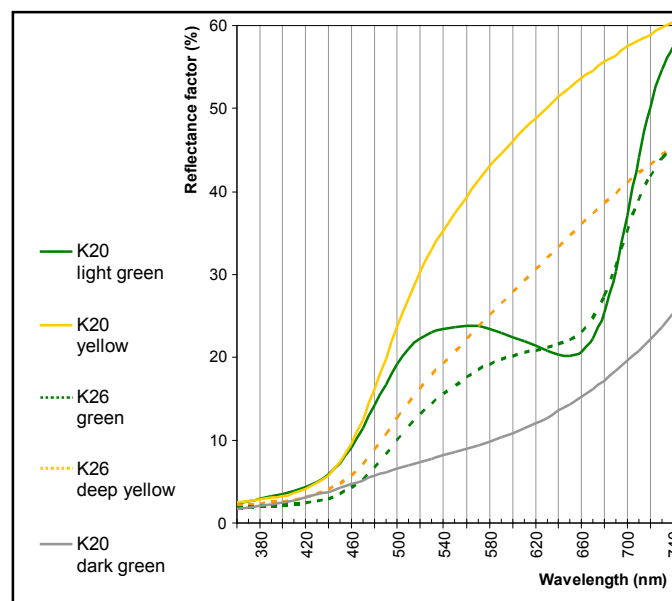


Figure 12. Vis-RS spectra of green areas of Kaitag textiles 20 and 26 containing indigotin and a yellow dye are compared to those of luteolin-based yellows from the same textiles. In the dark green of Kaitag textile 20 a brown dye is detected, while indigotin is absent.

Reds

Madder, the main chromophores of which, namely alizarin and purpurin, are shown in figure 13, is a well known textile dye obtained from the roots of *Rubia tinctorum* and related species.

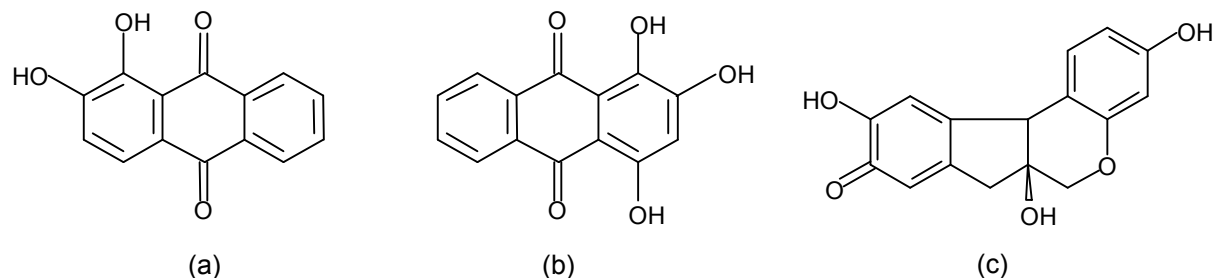


Figure 13. Molecular structures of (a) alizarin and (b) purpurin, the two main chromophores of madder, and (c) brazilin, the main chromophore of brazilwood.

This colorant was detected both on red silk embroideries and cotton backgrounds of almost all the 23 examined Kaitag textiles by vis-RS, thanks to the bands located around 510 and 550 nm, which are mostly due to the contribution of purpurin (figure 14). Specifically, the first band is usually stronger and placed between 490 and 510 nm, while the 550 nm band appears to be sometimes shifted to 560 nm; a weak band around 480 nm can be related to alizarin content (figure 14). Cochineal, kermes and lac dye, widely used in the past as well and generally identifiable using such analytical technique because of absorption bands at 520-530 nm and 560-580 nm (with some differences between the three dyes), never occurred in our investigations. The identification of madder on the majority of Kaitag textiles was also supported by micro-destructive analyses: indeed, both alizarin and purpurin were detected by HPLC, while SERS spectra perfectly correspond to those of the reference dye from our database¹⁴ (figure 15 and 16).

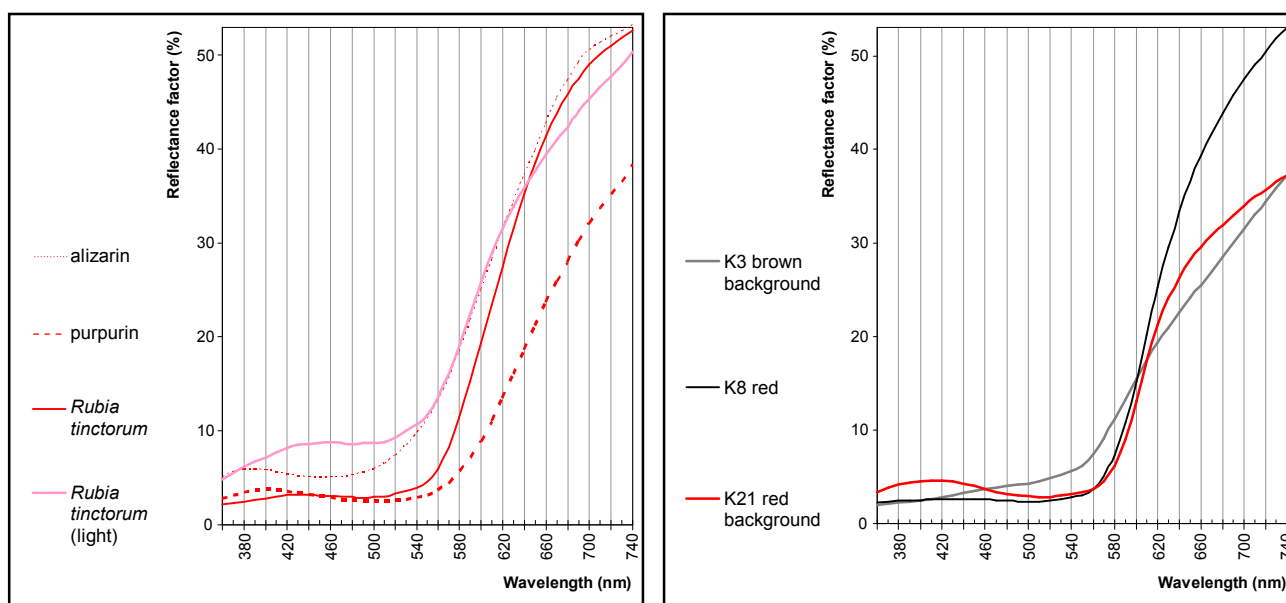


Figure 14. On the left, vis-RS spectra of reference samples dyed in the laboratory with madder from *Rubia tinctorum* (solid curves, where the weak bands at about 510 nm and 550 nm are diagnostic features) compared to spectra of alizarin and purpurin. On the right, vis-RS spectra of red, pink and brown areas of Kaitag textiles 3, 8 and 21 containing madder from *Rubia tinctorum*.

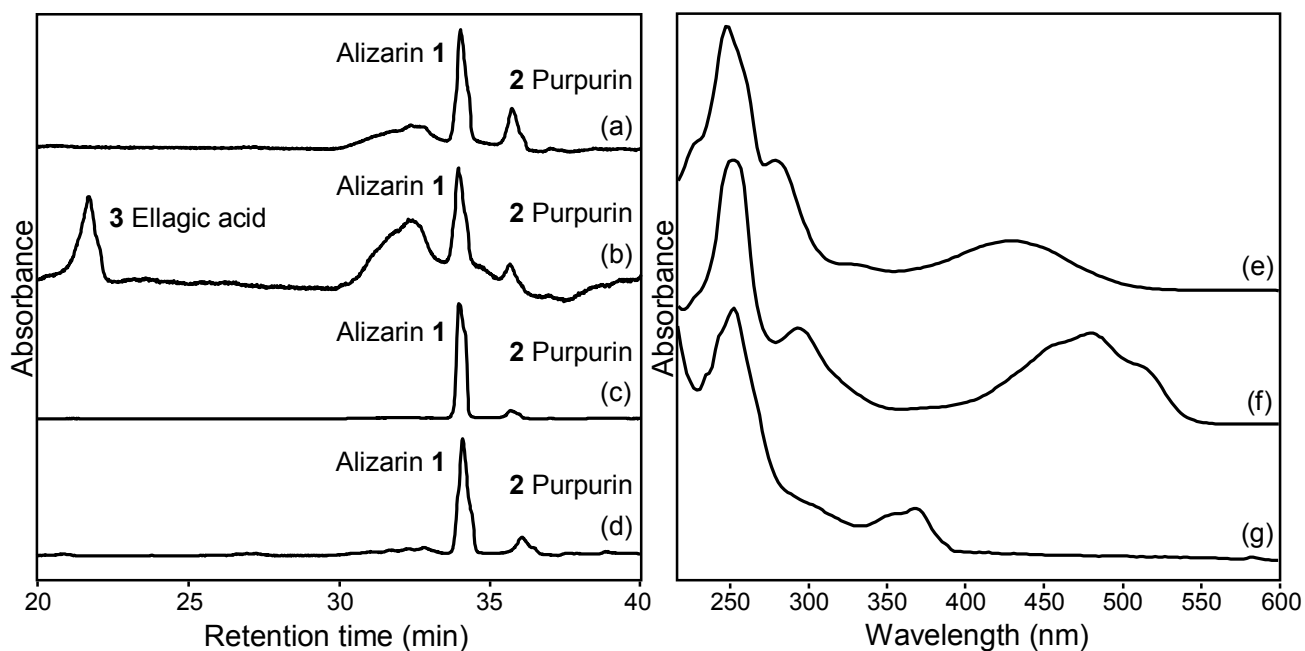


Figure 15. On the left, HPLC chromatograms of extracts from a purplish embroidery of Kaitag textile 14 (a) at $\lambda = 440$ nm and (b) at $\lambda = 365$ nm, (c) the red background of Kaitag textile 20 at $\lambda = 440$ nm and (d) a red embroidery of Kaitag textile 24 at $\lambda = 440$ nm; identified compounds are (1) alizarin, (2) purpurin and (3) ellagic acid. On the right, UV-vis spectra of (e) alizarin, (f) purpurin and (g) ellagic acid from a purplish embroidery of Kaitag textile 14.

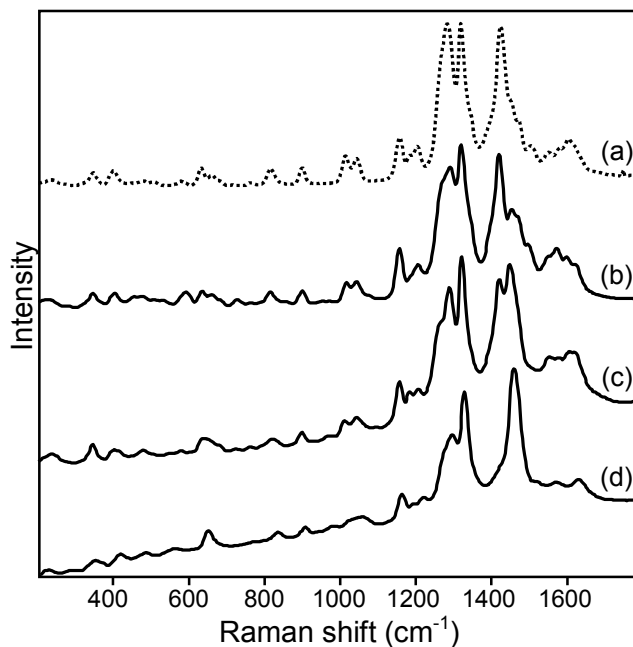


Figure 16. (a) SERS spectrum of reference alizarin compared to those of extracts from (b) a purplish embroidery of Kaitag textile 14, (c) the red background of Kaitag textile 20 and (d) a red embroidery of Kaitag textile 24.

Only exception is a pinkish hue observable in a few embroideries of Kaitag textile 19, for which scientific analyses suggested the use of a colorant belonging to the family of redwoods, such as brazilwood (figure 17; structure of brazilin, the main chromophore of brazilwood, shown in figure 13).

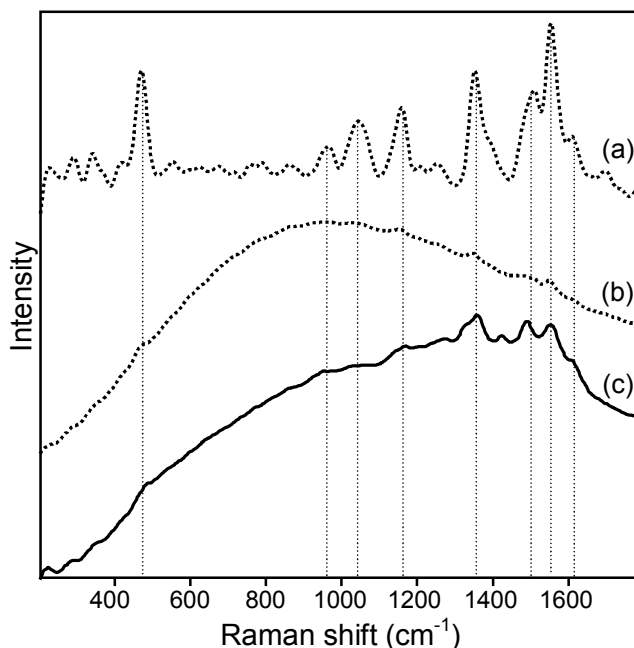


Figure 17. SERS spectra of (a) reference brazilwood upon baseline correction and (b) reference brazilwood as such compared to (c) that of the extract from a pinkish embroidery of Kaitag textile 19.

Moreover, it is remarkable that, in some cases, particular red tints were found to have been obtained as unusual mixtures of different dyes. With regard to this, interesting examples are offered by some purplish embroideries of Kaitag textile 14 as well as by the dark red background of Kaitag textile 3, for which the characteristic peaks of alizarin, purpurin and ellagic acid appeared in HPLC chromatograms, indicating the simultaneous use of madder and tannins (figure 15); in such cases, SERS spectra are still dominated by the signals of madder (figure 16).

Browns and blacks

Tannins, the use of which was highlighted by the detection of ellagic acid (structure shown in figure 18) in HPLC chromatograms (figure 19), turned out to be the main components of several brown shades found on the Kaitag textiles here examined, where they often appear in combination with remarkable amounts of iron, as confirmed by both XRF and SEM-EDX analyses.

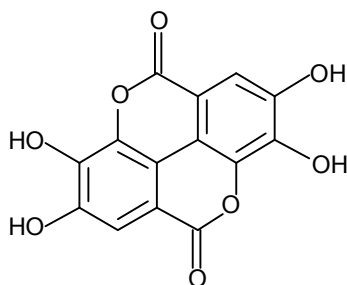


Figure 18. Molecular structure of ellagic acid, a marker for the presence of tannins.

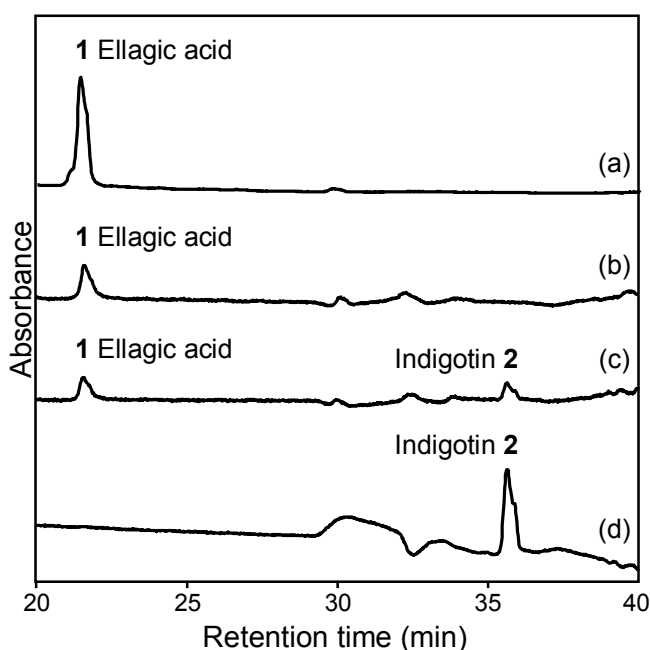


Figure 19. HPLC chromatograms of extracts from (a) a black corroded embroidery of Kaitag textile 10 at $\lambda = 365$ nm, (b) a brown embroidery of Kaitag textile 21 at $\lambda = 365$ nm, and a grayish brown embroidery of Kaitag textile 30 (c) at $\lambda = 365$ nm and (d) at $\lambda = 600$ nm; identified compounds are (1) ellagic acid and (2) indigotin.

The photograph of a corroded area of Kaitag textile 24 and the results obtained from EDX analyses are shown in figure 20 as an example; an iron content around 55% is estimated. It is interesting to notice that a high percentage of iron is frequently accompanied by corrosion of the dyed thread. Indeed, iron ions were usually employed in the form of ferrous sulfate, or vitriol, to form complexes with tannins which are responsible for particularly dark tints. Residual sulfates left on top of the substrate could lead, in the presence of humidity, to the formation of sulfuric acid that chemically attacks the substrate itself, giving rise to a corrosion phenomenon well known for causing damage to parchment- or cellulose-based supports of ancient manuscripts edited with iron-gall inks.

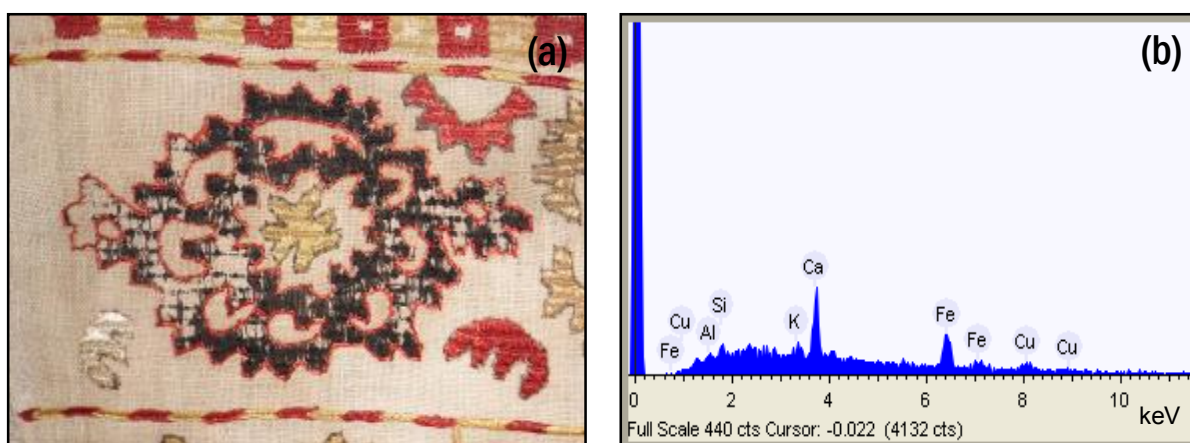


Figure 20. (a) Photograph of a black corroded area of Kaitag textile 24 and (b) results obtained from EDX analysis. An iron content around 55% is estimated for this sample. As in this case, a high percentage of iron is often accompanied by corrosion of the dyed thread.

For browns and blacks, vis-RS measurements were only indicative of the class which such dyes belong to, as the corresponding spectra exhibit a concave shape without other characterizing features (figure 21).

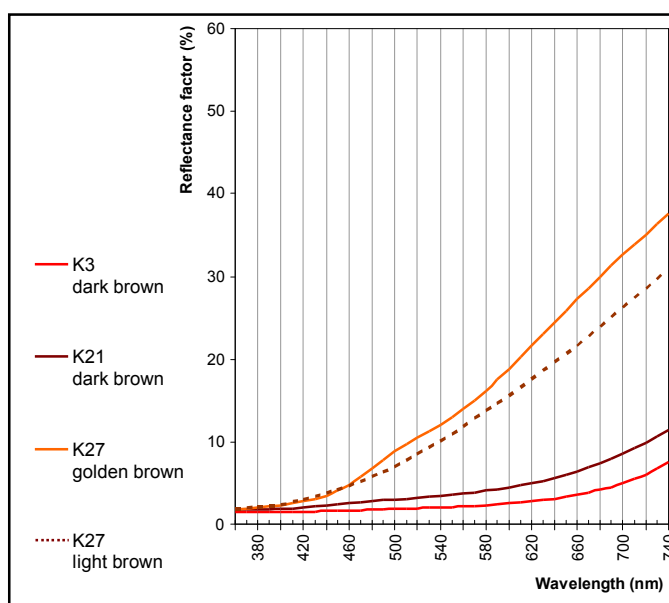


Figure 21. Vis-RS spectra of dark, golden and light brown areas of Kaitag textiles 3, 21 and 27 containing ellagic acid.

As already pointed out for red colorants in the previous paragraph, brown shades were involved in interesting cases of dye mixtures, too. In detail, tannins in combination with indigo were detected on dark brown and black parts of Kaitag textiles 25 and 27, as well as on grayish brown details of Kaitag textile 30. Indeed, HPLC analyses highlighted the presence of ellagic acid together with indigotin (figure 19), and the hypothesis of such overlapping was confirmed by vis-RS data. The chemical composition remains unknown for the bronze hue of Kaitag textile 19, the analogous but lighter tint of Kaitag textile 5 and the dark brown shade found on the same piece. For this latter tint, in particular, HPLC analysis supported the possible use of a luteolin-containing yellow colorant, even if no evidences were found concerning the other coloring components responsible for giving rise to the final tint. With regard to browns and blacks, it is worth mentioning the gray ink used for the underlying drawing in Kaitag textiles 8, 11, 21 and 26, which SEM-EDX and XRF analyses indicated to be free of iron and therefore classified as a carbon ink, consistently with what vis-RS spectra and high opacity in IR reflectograms suggested. Areas of Kaitag textile 11 with ink traces are shown in figure 22, while a SEM photograph of a thread with ink traces taken from this artifact is displayed in figure 23 along with the results obtained from EDX analysis.



Figure 22. Areas of Kaitag textile 11 where traces of ink are visible.

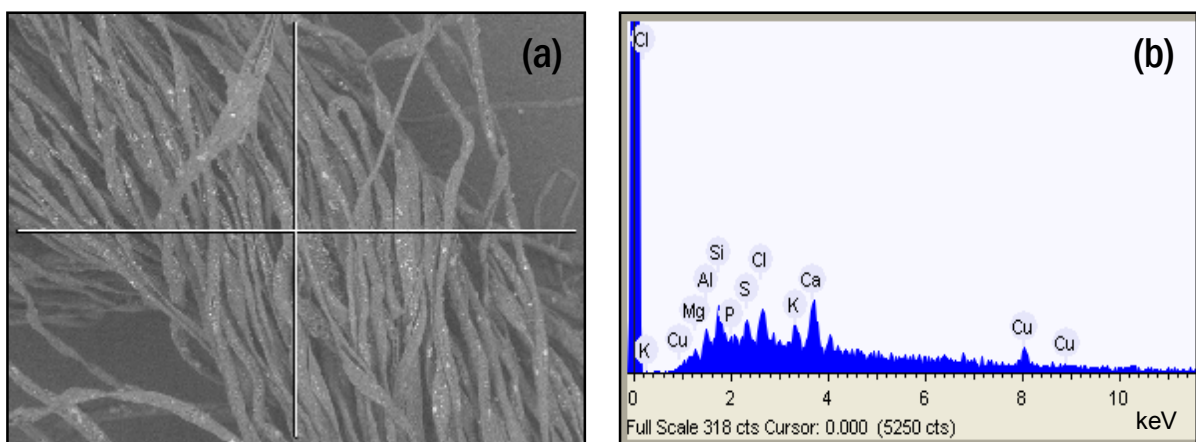


Figure 23. (a) SEM photograph of a thread with ink traces from Kaitag textile 11 and (b) results obtained from EDX analysis. The ink is found to be free of iron and is therefore classified as a carbon-based ink.

Conclusions

A total of 23 Kaitag textiles were examined, mostly dating from the 17th to the 18th century. First of all, the objects were examined by IR reflectography and UV fluorescence, then the dyes were analyzed using non-invasive techniques such as vis-RS on 250 measurement points. Vis-RS allowed a preliminary classification of colorants, particularly madder, indigo and its mixture with yellows to obtain green colors, and also tannins in brown tints; this technique, as expected, was not useful to characterize yellow dyes. After that, several extraction procedures, based on the use of HF, HCl or pyridine in different experimental conditions, were applied to 65 tiny portions of Kaitag textiles, which were then subjected to micro-destructive analyses by HPLC and SERS in order to identify the colorants. The dyes detected, which were all of natural origin, include: madder for red; madder in association with ellagic acid for pinkish hues; indigo for dark and light blue; weld for yellow; weld, or sometimes a different yellow dye, in combination with indigo for green; tannins mordanted with iron for dark brown; again tannins, sometimes with the addition of indigo, for black. As evidenced by SEM-EDX, a high content of iron is often accompanied by corrosion of the dyed thread; XRF confirmed that a significant amount of iron is present in brown and dark tints and highlighted that corroded areas are also characterized by high quantities of potassium, sulfur, calcium, titanium and, significantly, manganese, that can be considered as an impurity of vitriol-deriving minerals. Finally, the ink used for the underlying drawing was carefully examined and identified as a carbon-based ink.

Acknowledgements

A special thank to dr. Eleonora De Luca (Dipartimento di Chimica Inorganica, Metallorganica e Analitica “L. Malatesta”, Università degli Studi di Milano) for performing SEM-EDX analyses and to dr. Gianluca Poldi (Dipartimento di Lettere, Arti e Multimedialità, Università degli Studi di Bergamo) for carrying out IRR, UVF, XRF and vis-RS measurements.

References

- [1] C. Scaramuzza, *Kaitag, arte per la vita. Tessuti ricamati dal Daghestan*, Silvana Editoriale, Cinisello Balsamo, **2010**.
- [2] D. Hunt, R. Chenciner, *Optics and Laser Technology* **2006**; 38, 458.
- [3] R. Chenciner, *Kaitag. Textile art from Daghestan*, Textile Art Publications, London, **1993**.
- [4] M. P. Colombini, A. Andreotti, C. Baraldi, I. Degano, J. J. Lucejko, *Microch. J.* **2007**; 85,174.
- [5] J. Sanyova, *Microchim. Acta* **2008**; 162, 361.
- [6] P. Walton Rogers, in *Hochdorf IV, Die Textilfunde aus dem späthallstattzeitlichen Fürstengrab von Eberdingen-Hochdorf (Kreis Ludwigsburg) und weitere Grabtextilien aus hallstatt- und laténezeitlichen Kulturgruppen. Forschungen und Berichte zur Vor- und Frühgeschichte Baden-Württembergs 70*, (Ed: J. Banck-Burgess), Theiß, Stuttgart, **1999**, pp. 240-245.
- [7] P. C. Lee, D. Meisel, *J. Phys. Chem.* **1982**; 86, 3391.
- [8] G. Körtum, *Reflectance Spectroscopy. Principles, Methods, Application*, Springer Verlag, Berlin-Heidelberg-New York, **1969**.
- [9] M. Bacci, in *Modern analytical methods in Art and Archaeology*, (Eds: E. Ciliberto, G. Spoto), Springer Verlag, New York-Chichester-Weinheim-Brisbane-Singapore-Toronto, **2000**, pp. 321-360.
- [10] M. Leona, J. Winter, *Studies in Conservation* **2001**; 46, 153.
- [11] G. Poldi, in *Intrecci cinesi. Antica arte tessile (XV-XIX secolo)*, Moshe Tabibnia, Milano, **2011**, pp. 82-99.
- [12] G. Poldi in *Crivelli e l'arte tessile*, (Eds: M. Tabibnia, T. Marchesi, E. Piccoli), Electa, Milano, **2010**, pp. 155-179.
- [13] S. Bruni, E. De Luca, V. Guglielmi, G. Poldi, F. Pozzi in *Kaitag, arte per la vita. Tessuti ricamati dal Daghestan*, (Ed: C. Scaramuzza), Silvana Editoriale, Cinisello Balsamo, **2010**, pp. 121-143.
- [14] S. Bruni, V. Guglielmi, F. Pozzi, *J. Raman Spectrosc.* **2011**; 42, 1267.

Chapter 5

Comparative study of SERS methods for the detection of dyes in works of art

Abstract

Over the last few years, various SERS analytical methodologies for the identification of organic colorants in works of art have been developed, including many types of metal substrates as well as several procedures of sample pretreatment. In this chapter, the effect of pretreating samples by exposing them to HF vapor prior to analysis, a step designed to increase sample adsorption on the nanosized metallic support and enhance SERS signals, is evaluated. Materials studied include commercial pure colorants and lake pigments, fibers from textiles dyed in the laboratory, as well as actual aged samples, such as microscopic fragments of lakes on paper, ancient pigments and glazes from a number of works of art, representative of several cultures and belonging to different historical periods, i.e. from the 2nd century B.C. to the late 1800s. In each case, SERS spectra obtained with or without HF hydrolysis were critically compared. The pretreatment with HF vapor generally resulted in fast analysis and increased sensitivity, with only a few exceptions, as in the case of dyed silk fibers, where silk protein hydrolyzates were found to interfere with SERS analysis.

Introduction

As widely pointed out in the previous chapters, SERS has recently found increasing application for the analysis of organic colorants in works of art¹⁻³, as the adsorption of molecules on nanosized metal substrates significantly enhances their Raman signals and quenches their fluorescence.

Several SERS approaches combined with different procedures of sample pretreatment have been so far developed for the identification of dyes in ancient textiles and art objects, as discussed in the following.

Silver colloids obtained according to the Lee-Meisel procedure⁴, i.e. by chemical reduction of silver nitrate with sodium citrate, have been the most popular substrate for SERS investigations applied to cultural heritage materials thus far and have been regularly employed in this doctoral research work as well, as described in Chapter 2, 3 and 4, thanks to their easy preparation and use. Silver nanoparticles produced by photoreduction of a silver nitrate solution by using a laser/micro-Raman coupled system have been also tested as an alternative substrate for the *in situ* SERS detection of flavonoid and anthraquinonic colorants both in reference and ancient samples^{5,6}. Nevertheless, most of the work recently carried out at the Metropolitan Museum of Art on mordant dyes and lake pigments was based on a monodisperse silver colloid synthesized by microwave-supported glucose reduction of silver sulfate in the presence of sodium citrate as a capping agent⁷. Experiments have demonstrated that these nanoparticles have a narrow particle size range and show higher reproducibility and stability over the time in comparison with traditional Lee-Meisel colloids.

While SERS analyses have been recently carried out directly without any pretreatment steps on a range of materials⁸⁻¹¹, it could be expected that an increase in sensitivity would be obtained by acid treating the sample prior to analysis. As already discussed in Chapter 1, most natural colorants are in fact mordant dyes, fixed to the fabric by bridging metal atoms, called mordants, bound to charged groups in the dye molecule and in the textile fiber, and a similar situation is found with lake pigments, where the dyes are complexed to metal ions to form insoluble pigments^{12,13}. In HPLC analysis (the preferred, albeit more sample intensive technique for dye analysis) colorant extraction is usually performed by treatment with hydrochloric acid and methanol¹⁴. This procedure results in excellent dye removal but often causes extreme degradation of the substrate itself, thus giving rise to remarkable interferences in the SERS spectra, as also documented in our laboratory for the identification of a red colorant in ancient wool threads from the Libyan Sahara¹⁵. As an alternative, a non extractive gas-solid hydrolysis procedure, suitable for the analysis of microscopic fragments of textiles, lake pigments, glazes and performed by exposing the sample to hydrofluoric acid vapor in a closed microchamber, was developed specifically for SERS analyses at the Metropolitan Museum of Art¹⁶.

In the present work, the HF hydrolysis method has been first assessed and applied to the identification of dyes from archaeological textiles, sculptures, watercolors and oil paintings by SERS. After that, a systematic study has been here carried out to evaluate the performances of SERS on Ag colloids with and without HF hydrolysis when applied to the ultrasensitive detection of red organic colorants. In this context, a number of works of art and ancient samples representative of several cultures and belonging to different historical periods, i.e. from the 2nd century B.C. to the late 1800s, have been analyzed, including lakes from an original Winsor & Newton catalogue of watercolors on paper, colorants from dyed fabrics, an ancient pink lake pigment from Greece, as well as glazes from oil paintings and musical instruments.

Experimental

Chemicals and art samples

Silver nitrate, sodium citrate, sulfuric acid, glucose and hydrofluoric acid were purchased from Fisher Scientific, alizarin, purpurin, carminic acid, laccaic acid, ethanol and potassium nitrate from Sigma-Aldrich, while madder lake and carmine naccarat (alumina lake of carminic acid) were obtained from Kremer Pigments. All the aqueous solutions used for the nanoparticle synthesis were prepared using 18 M Ω ultrapure water (Millipore Simplicity 185 water purification system).

Microscopic fragments of equivalent size were taken from several works of art and ancient objects and subsequently investigated. Samples studied include: a tunic (Peru, South highlands, Pucara, ca. 135-525, private collection); a tasseled tunic (Peru, North coast, 1100-1250, The Metropolitan Museum of Art, accession number L.2010.17); a cap with feathers (Chile, 10th - 14th century, The Metropolitan Museum of Art, accession number 1994.35.133); a feathered bag (Peru, 15th - early 16th century, The Metropolitan Museum of Art, accession number 1994.35.101); Jan Lievens' *The card players* (oil on canvas, ca. 1624, private collection, New York); Arthur Dove's *Silver ball, barge, and trees* (watercolor, gouache, ink and charcoal on paper, New York, 1930, The Metropolitan Museum of Art, accession number 49.70.85); a marble statue of Caligula (Roman, 1st century, Virginia Museum of Fine Arts, accession number 71.20); a crucifix (Spain, Palencia, ca. 1150-1200, The Metropolitan Museum of Art, accession number 35.36a,b); a reliquary bust of Saint Barbara (Germany, Strasbourg, ca. 1465, The Metropolitan Museum of Art, accession number 17.190.1735); an original Winsor & Newton handbook of watercolor pigments dating to 1887; a pink pigment sample found in the excavation of a 2nd century B.C. site in Corinth, Greece; reference textiles dyed in the Department of Textile Conservation at the Metropolitan Museum of Art, i.e. wool dyed with Turkish madder, wool dyed with lac dye, silk dyed with cochineal and silk dyed with lac dye; Cézanne's *The card players* (oil on canvas, 1890-1892, The Metropolitan Museum of Art, accession number 61.101.1); Rembrandt's *Aristotle with a bust of Homer* (oil on canvas, 1653, The Metropolitan Museum of Art, accession number 61.198); a laboratory reproduction of a panel from the Nur al-Din room, the original version of which is on display at the Metropolitan Museum of Art (Damascus, Syria, 1280-1924); a mandolin made by Antonio Vinaccia (Naples, Italy, 1781, The Metropolitan Museum of Art, accession number 89.4.2140); a painted cloth depicting the celebration of the festival of cows (India, late 18th - early 19th century, The Metropolitan Museum of Art, accession number 2003.177).

Analytical methods: HF hydrolysis, Ag colloid synthesis and sample preparation

In this study, two SERS methodologies have been evaluated for comparison purposes:

- 1) SERS on Ag colloids upon HF hydrolysis;
- 2) SERS on regular and concentrated Ag colloids without any pretreatment.

Particular attention was dedicated to developing a safe HF hydrolysis procedure for sample pretreatment¹⁶. The reaction is carried out in a microchamber fashioned out of a BEEM size 00 polyethylene vial (8 mm I.D. x 20 mm H.). A 10 μ L drop of HF is placed in the bottom of the vial: the drop is naturally confined there due to the pyramidal shape of the cavity. A capsule thus prepared can be used for over a week without refilling with

HF. The sample holder is obtained by removing the cap from a BEEM size 3 vial (5.6 mm I.D. x 14 mm H.). Due to its smaller size when compared to the 00 vial, the cap fits snugly within the microchamber. The sample is placed in the sample holder, introduced into the microchamber, which is then closed by snapping the lid shut, and exposed to the HF saturated atmosphere for 5 minutes. Following removal from the chamber, the sample is left to stand in air under a fume hood for a while to allow any HF absorbed on it to evaporate, before being treated with the Ag nanoparticles: this step is a precaution against damage to the microscope optics rather than a health safety measure, as the amount of HF absorbed by the microscopic samples under investigation is deemed to be too small to pose any health hazard. The colloid is then deposited directly on the sample in the sample holder, which is then transferred to the Raman microscope for the analysis (figure 1).

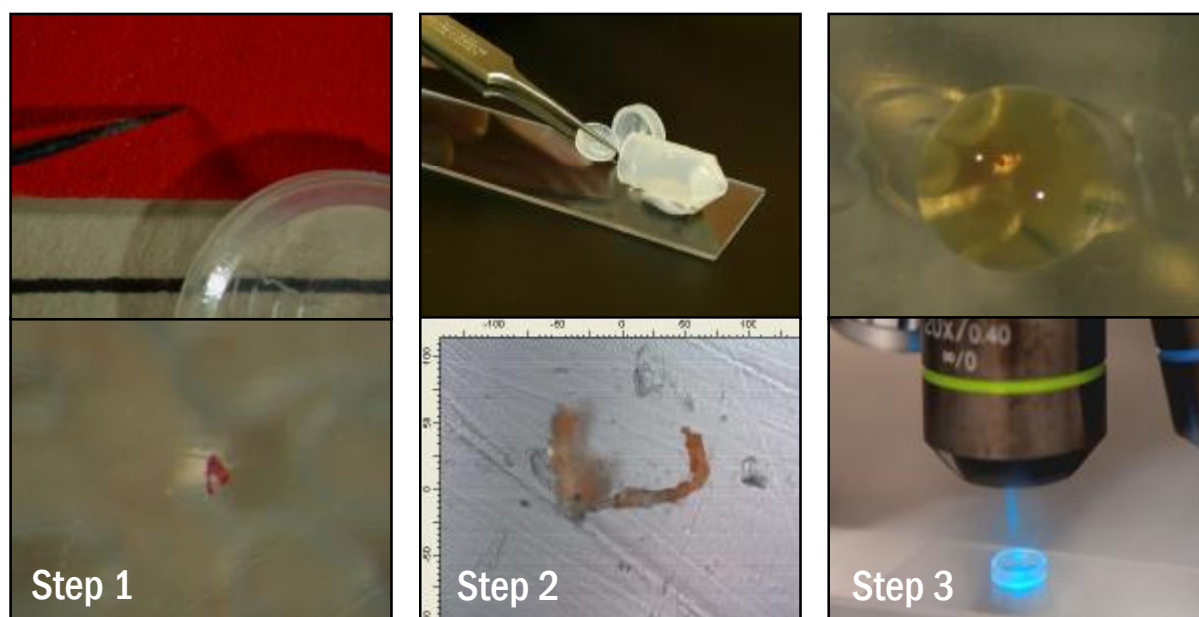


Figure 1. SERS analysis of a sample upon HF treatment. Step 1: a sample of about 20x20 μm in size is taken from the art object using a tungsten needle and placed in the sample holder. Step 2: the sample holder is introduced into the microchamber and the sample is thus exposed to HF vapors for 5 minutes. Step 3: Ag nanoparticles are deposited directly on the sample in the sample holder, which is then transferred to the Raman microscope for the analysis. Photographs taken by dr. Marco Leona.

Silver colloids synthesized by microwave-supported glucose reduction of silver sulfate in the presence of sodium citrate as a capping agent were chosen as a metal substrate for SERS analyses and prepared according to a previously published recipe⁷. In detail, 100 mg of AgNO_3 were dissolved in 5 mL of cold ultrapure water and 10% H_2SO_4 was added dropwise to precipitate Ag_2SO_4 . The precipitate was washed twice with ultrapure water, allowed to dry on a piece of filter paper and then dissolved in ultrapure water to give a 5×10^{-4} M solution. 25 mL of the silver sulfate solution were added to a pressure resistant Teflon microwave vessel (CEM Ultimate Digestion Vessel UDV 10, CEM Corporation), together with 2 mL of a 1%w solution of glucose and 1 mL of a 1%w solution of sodium citrate. The resulting mixture was shaken vigorously for a few seconds to mix the reagents, and heated to 120°C for a total of 60 s using a CEM MDS-2100 microwave digestion system with temperature and pressure monitoring (figure 2). The stock colloid was wrapped in an aluminium foil and kept refrigerated.

To reduce the amount of citrate in competition with the analyte for adsorption on the nanoparticles and prepare this colloid for use, 1 mL was centrifuged for 5 minutes at 16,060 x g RCF (relative centrifugal force) with a Fisher Scientific Accuspin 400 centrifuge, and 900 μ L of the supernatant were then removed and replaced with the same amount of 18 M Ω ultrapure water (Millipore Simplicity 185 water purification system). These nanoparticles will be henceforth referred to as microwave colloid.

A 5 times concentrated colloid, which will be referred to as 5x microwave colloid from now on, was also prepared for non-hydrolysis experiments by centrifuging the colloidal suspension and replacing 900 μ L of the supernatant with 100 μ L of ultrapure water.



Figure 2. On the left, the Ag colloid obtained by microwave-supported glucose reduction of silver sulfate in the presence of sodium citrate as a capping agent. On the right, the CEM MDS-2100 microwave digestion system with a pressure resistant Teflon microwave vessel where the nanoparticle synthesis is carried out. Photographs taken by dr. Marco Leona.

Silver nanoparticles synthesized by microwave-supported reduction of silver sulfate were chosen as a substrate for SERS analyses for two main reasons. First of all, as pointed out by Leona⁷, the use of microwave radiation can alleviate heat transfer and reagents mixing issues, as the solution is heated at a fast rate without temperature gradients, and this is crucial to achieve a better control of the reaction. As a consequence, the resulting colloid is characterized by a narrower absorption band and a considerably lower particle size dispersion in comparison to the traditional citrate-reduced nanoparticles obtained according to the Lee-Meisel procedure (figure 3). In detail, previous experiments gave rise to the following results: FWHM (full width at half maximum) of microwave colloid \sim 50 nm versus FWHM of Lee-Meisel colloid $>$ 120 nm; size distribution of microwave colloid = 3-10 nm versus size distribution of Lee-Meisel colloid = 3-50 nm. Sequential UV-vis measurements of the colloid absorption over time (figure 3) and SERS analyses of probe molecules such as 4-methylpyridine (figure 4) showed that microwave nanoparticles, unlike Lee-Meisel colloids, are stable and efficient over several months, thus leading to more reproducible SERS performances.

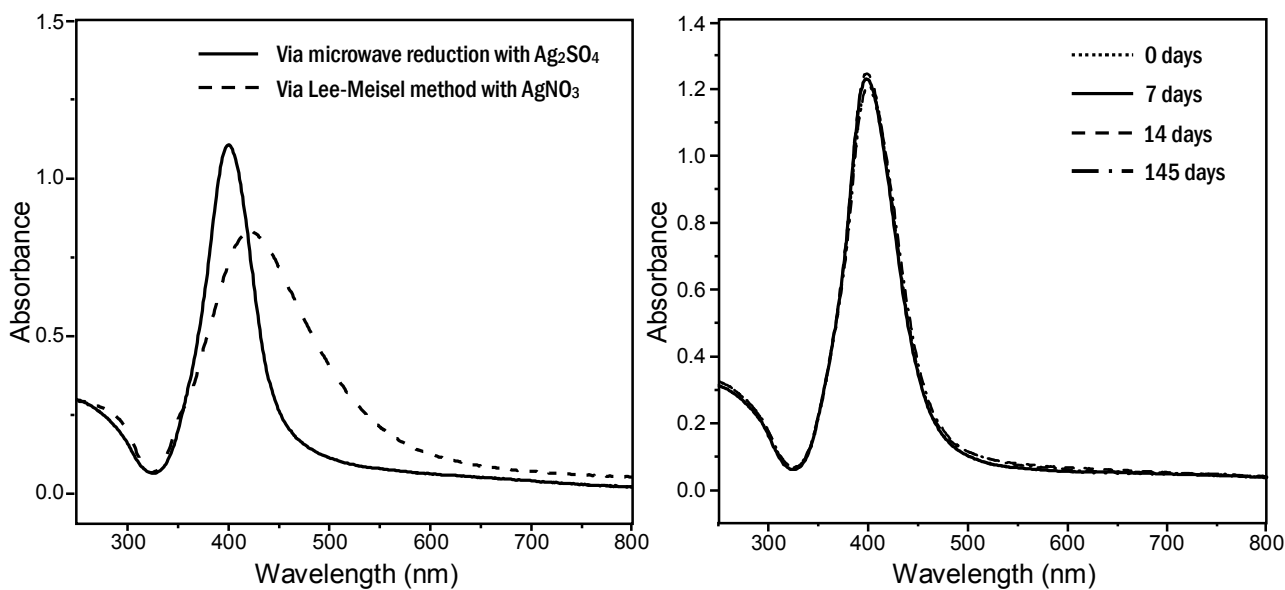


Figure 3. On the left, comparison between UV-vis spectra of Ag nanoparticles synthesized by microwave-assisted reduction of silver sulfate and according to the traditional Lee-Meisel procedure: a narrower absorption band, corresponding to a lower particle size distribution, is obtained when the first method is used. On the right, UV-vis measurements of Ag microwave nanoparticles taken 0, 7, 14 and 145 days after their synthesis, showing a very high stability for this colloid over the time.

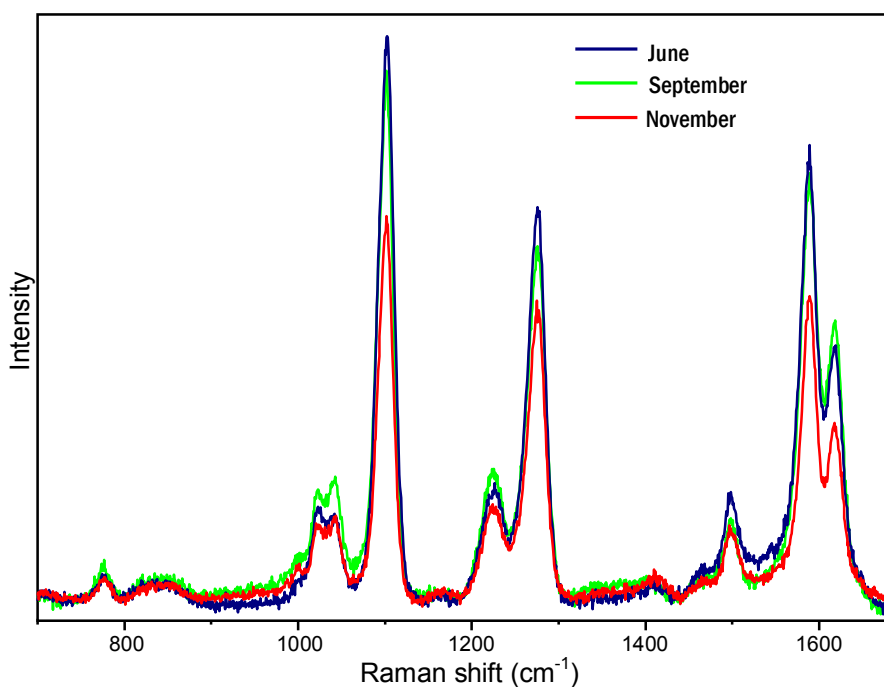


Figure 4. SERS spectra of 4-methylpyridine on Ag nanoparticles synthesized by microwave-assisted reduction of silver sulfate taken in June, September and November, using the same stock colloid. Spectra obtained from sequential measurements display comparable intensities, showing that a high stability and prolonged efficiency over time is associated with such nanoparticles.

As far as the sample preparation is concerned, reference solutions of pure dyes, namely alizarin, purpurin, carminic and laccaic acids, were daily prepared in ethanol at a concentration of 10^{-4} M, and aliquots of 10% NaOH and 6 M HNO₃ solutions were employed to adjust the pH. For SERS analysis, 0.2 μ L of the dye solution at a certain pH value were added to 0.8 μ L of the Ag colloid, followed by the addition of 0.1 μ L of a 0.5 M KNO₃ aqueous solution to induce aggregation of the nanoparticles. Reference madder and carmine lakes as well as all the art samples under investigation were analyzed upon deposition of 0.8 μ L of the Ag colloid and inducing the aggregation of the nanoparticles through the addition of 0.1 μ L of a 0.5 M KNO₃ aqueous solution (figure 5). SERS analyses were performed by focusing the laser beam onto the microaggregates which turned out to be visible inside the drop a few seconds after covering the sample with the Ag colloid. SERS spectra could be obtained immediately after the preparation of the sample and generally improved in quality as aggregation proceeded, before deteriorating when the liquid was fully evaporated.

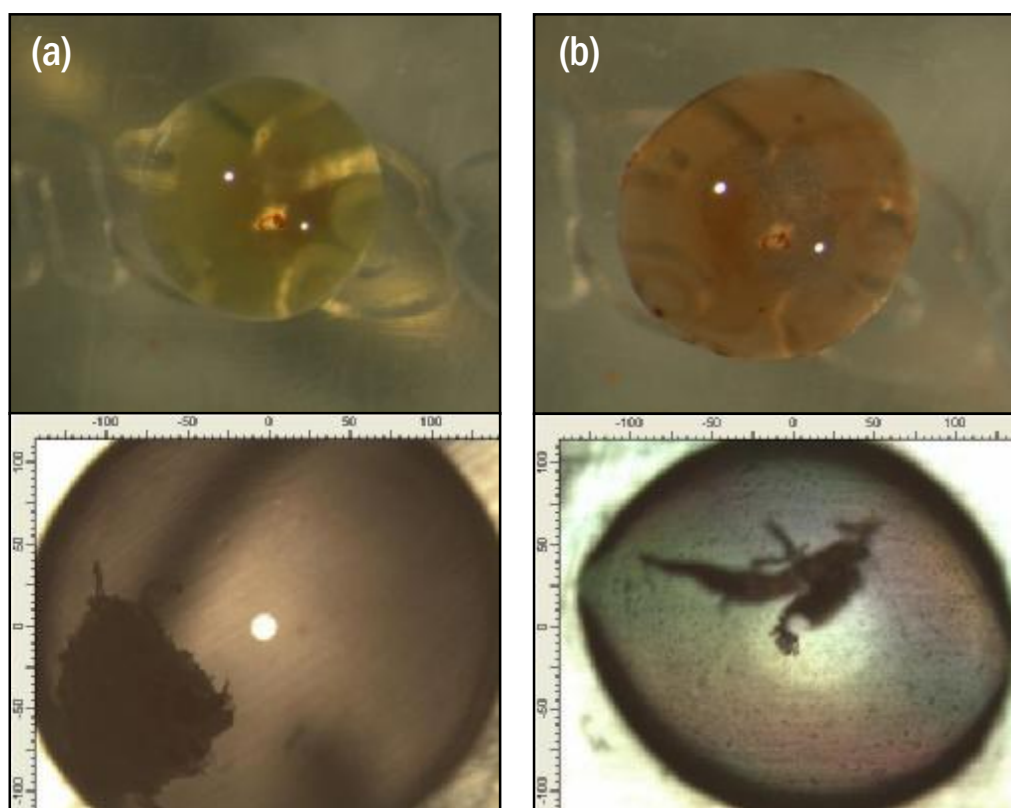


Figure 5. Drop of colloid covering a red-colored sample in the sample holder (a) before and (b) after the addition of 0.5 M KNO₃. As soon as the electrolyte is added, microaggregates of silver nanoparticles are formed into the drop itself, which visibly turns from yellow to orange color.

Instrumentation

SERS spectra were obtained in the dispersive mode using a Bruker Senterra Raman spectrometer equipped with an Olympus 20x long working distance microscope objective, a charge-coupled device (CCD) detector and a 1800 rulings/mm holographic grating providing a resolution of 3-5 cm^{-1} . The 488 nm radiation emitted by a Spectra Physics Model 2020 BeamLock Ar⁺ laser was employed as the excitation wavelength, with a power at the sample of about 0.5 mW. All the spectra were acquired collecting 1 scan with an integration time of 30 s.

Results and discussion

Analysis of reference dyes and HF hydrolysis optimization

First of all, some of the most common historical red dyes, namely alizarin, purpurin, carminic acid and laccaic acid, were commercially purchased and their SERS spectra were recorded at different pH values as a reference to be used for identification purposes. In particular, the molecular structures of alizarin, purpurin, carminic and laccaic acids are recalled in figure 6, while their SERS spectra are reported in figures 7 and 8.

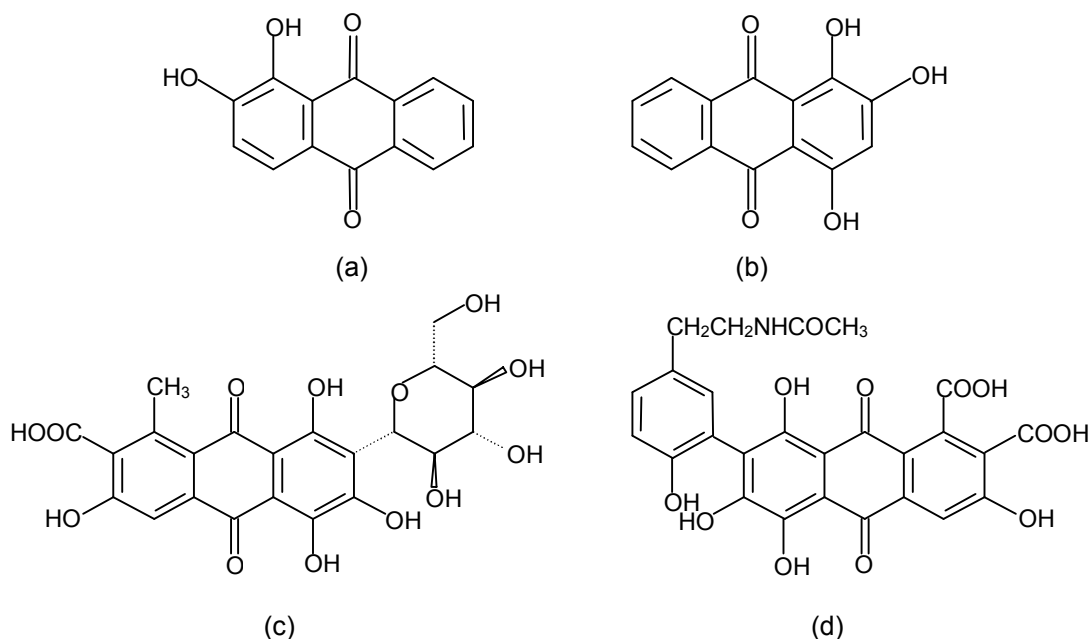


Figure 6. Molecular structure of (a) alizarin, (b) purpurin, (c) carminic acid and (d) laccaic acid.

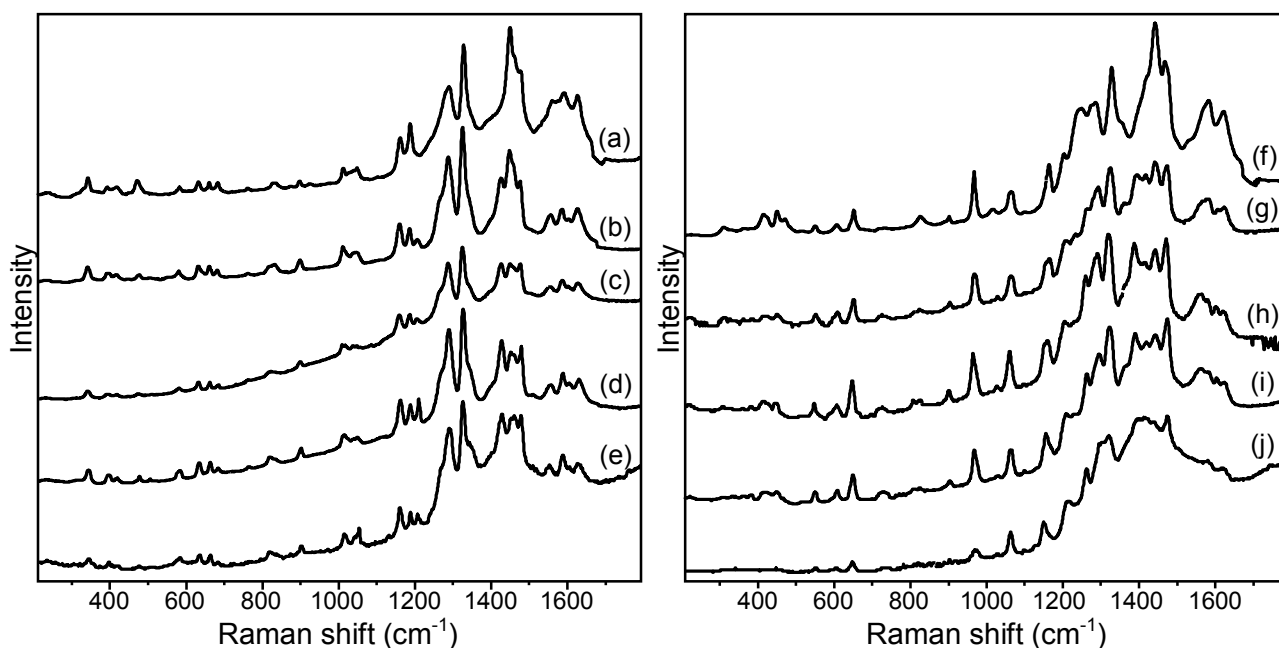


Figure 7. On the left, SERS spectra of a 10^{-4} M ethanolic solution of alizarin at (a) pH=2, (b) pH=4.5, (c) pH=7, (d) pH=9 and (e) pH=12. On the right, SERS spectra of a 10^{-4} M ethanolic solution of purpurin at (f) pH=2, (g) pH=4.5, (h) pH=7, (i) pH=9 and (j) pH=12.

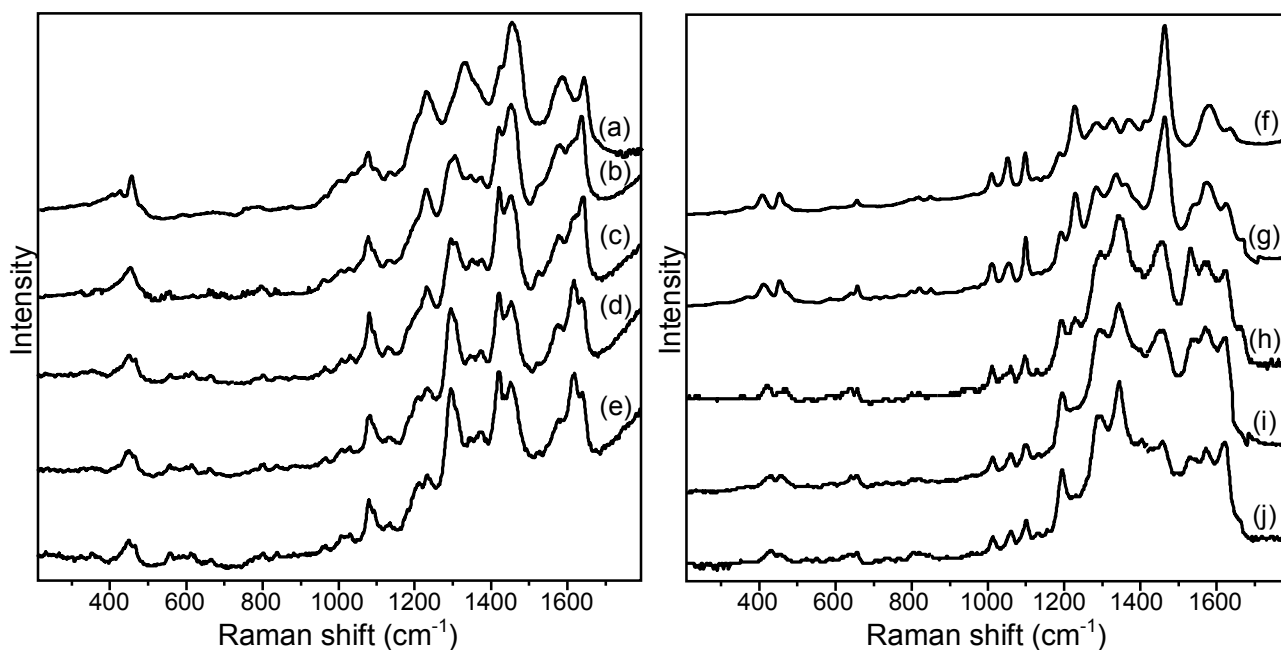


Figure 8. On the left, SERS spectra of a 10⁻⁴ M ethanolic solution of carminic acid at (a) pH=2, (b) pH=4.5, (c) pH=7, (d) pH=9 and (e) pH=12. On the right, SERS spectra of a 10⁻⁴ M ethanolic solution of laccaic acid at (f) pH=2, (g) pH=4.5, (h) pH=7, (i) pH=9 and (j) pH=12.

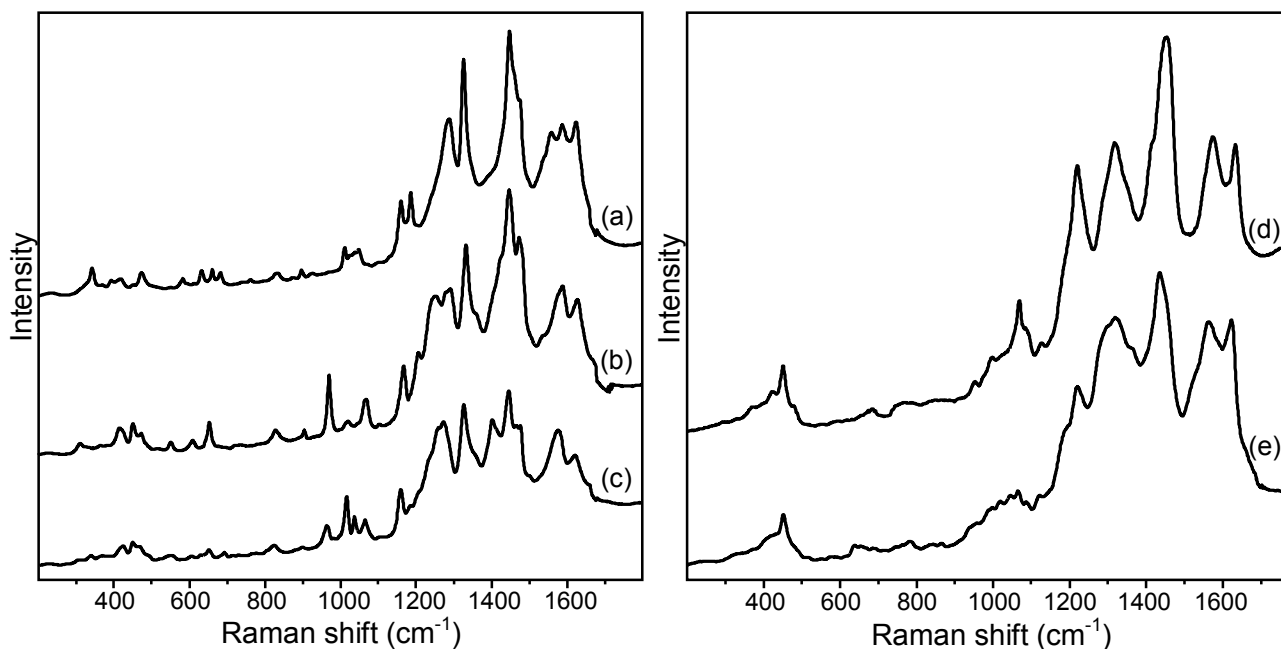


Figure 9. On the left, SERS spectra of (a) alizarin at pH=2 and (b) purpurin at pH=2 compared to (c) that of madder lake on Ag microwave colloid upon HF treatment. On the right, (d) SERS spectrum of carminic acid at pH=2 compared to (e) that of camine naccarat on Ag microwave colloid upon HF treatment.

Commercial madder lake and carmine naccarat purchased from Kremer Pigments were also investigated as a reference; as shown in figure 9, the analysis of these materials upon HF treatment gave rise, as expected, to bands that match well those of the main coloring molecules of these lakes, i.e. alizarin/purpurin and carminic acid, at pH=2. For these two commercial lake pigments, as well as in the case of art samples, as will be shortly discussed, SERS spectra recorded upon hydrolysis were found to result in spectral patterns that correspond perfectly to those obtained from the corresponding pure dyes at the lowest pH, fact that can be ascribed to the use of an acid, namely HF, for pretreating samples.

After collecting reference spectra from commercial pure dyes and lake pigments, the optimized HF hydrolysis procedure was applied to the analysis of several works of art and archaeological samples, and the results obtained are presented in the following. In detail, madder lake was identified in a tunic (figure 10), in a cap with feathers (figure 11), in a feathered bag (figure 12), in Lievens' oil painting *The card players* (figure 13), in Dove's watercolor *Silver ball, barge, and trees* (figure 14), in a Roman statue of Caligula (figure 15) and in a reliquary bust of Saint Barbara (figure 16), while carminic acid was only detected in a tasseled tunic (figure 17). Remarkably, the Asian colorant lac dye, imported to Europe only in the late 18th century according to the literature¹⁷⁻¹⁹ but an earliest use of which in this continent was recently documented for an Ottoman carpet dating to the late 16th - early 17th century³, was here detected in a Spanish crucifix dating to 1150-1200 (figure 18): therefore, this latter date can be henceforth acknowledged as the earliest historical occurrence of laccaic acid in European art.

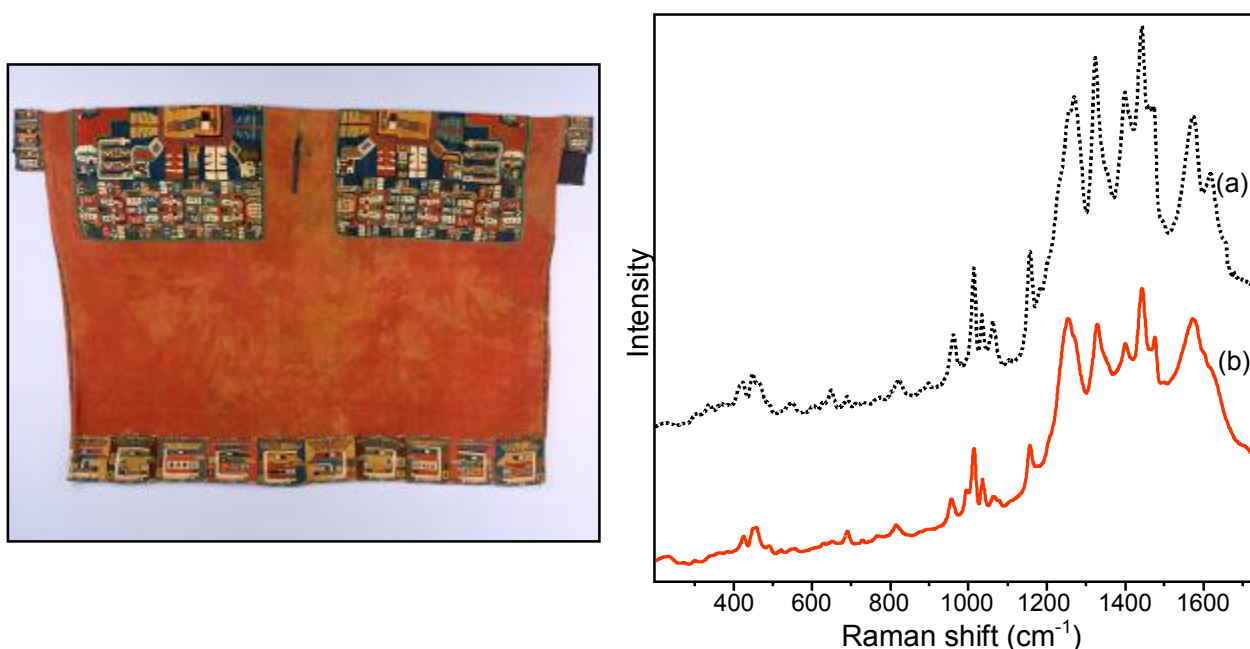


Figure 10. On the left, tunic from Peru, South highlands, Pucara, dating to ca.135–525. Camelid hair, plain weave and tapestry weave; 38 1/2 x 60 1/2 inches (98.1 x 153.7 cm). Private collection. On the right, (a) SERS spectrum of reference madder lake upon HF treatment compared to (b) that of a sample taken from the tunic upon HF treatment.

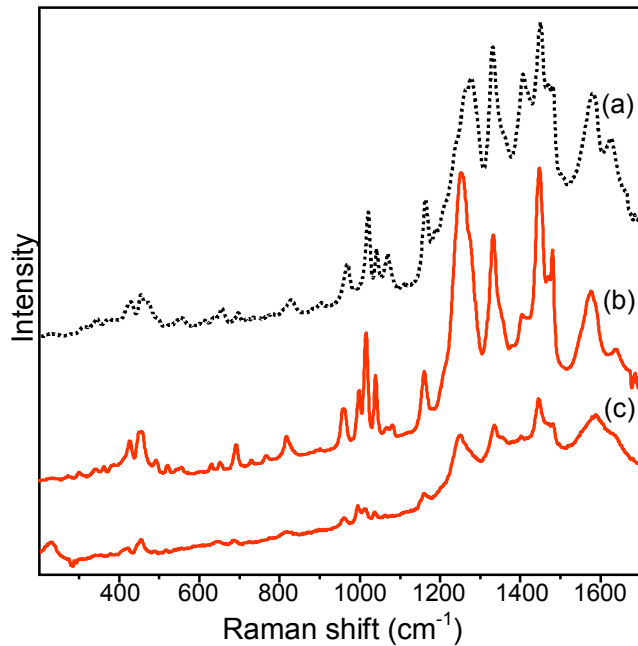


Figure 11. On the left, cap with feathers from Chile, dating to the 10th - 14th century. Wool and feathers; H. 4-1/8 inches. The Metropolitan Museum of Art, 1994.35.133. Bequest of Arthur M. Bullowa, 1993. On the right, (a) SERS spectrum of reference madder lake upon HF treatment compared to those of samples taken from (b) a red feather and (c) the red trim of the cap, both upon HF treatment.

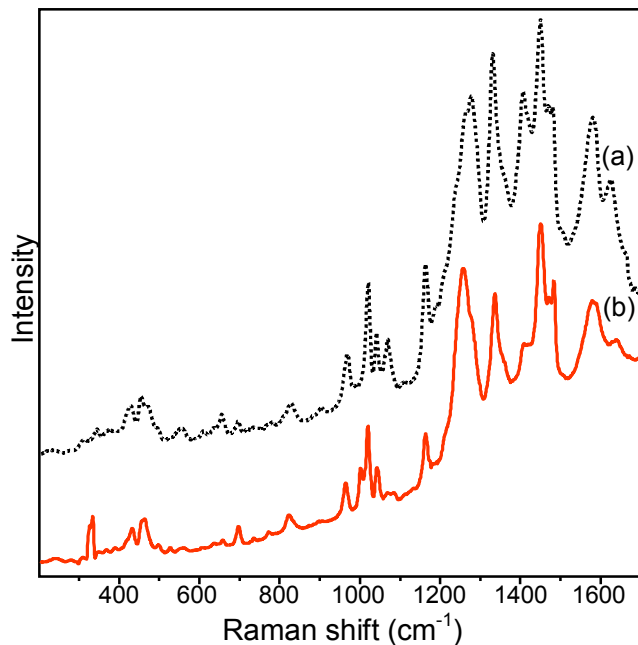


Figure 12. On the left, feathered bag from Peru, dating to the 15th - early 16th century. Cotton and feathers; H. 6 x W. 4 3/4 x D. 2 inches (15.2 x 12.1 x 5.1 cm). The Metropolitan Museum of Art, 1994.35.101. Bequest of Arthur M. Bullowa, 1993. On the right, (a) SERS spectrum of reference madder lake upon HF treatment compared to (b) that of a sample taken from a red feather of the bag upon HF treatment.

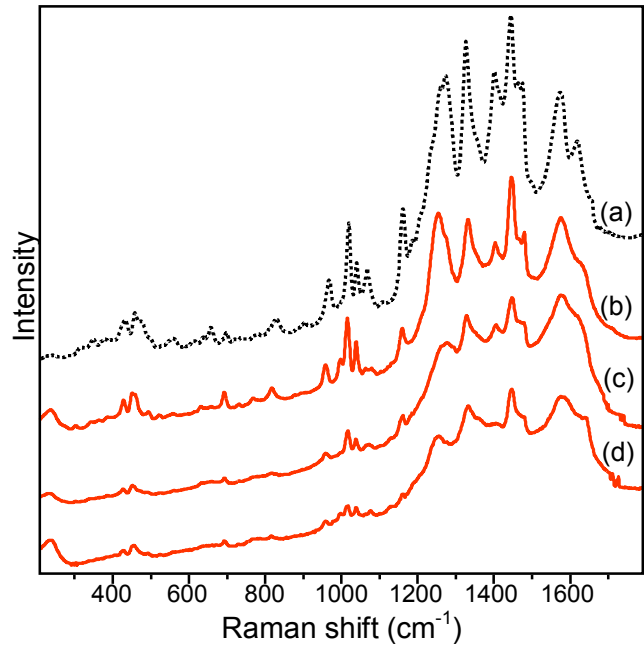


Figure 13. On the left, *The card players* by Jan Lievens, dating to ca. 1624. Oil on canvas; 99.1 x 108.6 cm. Private collection, New York. On the right, (a) SERS spectrum of reference madder lake upon HF treatment compared to (b), (c) and (d) those of samples taken from different areas of the painting upon HF treatment.

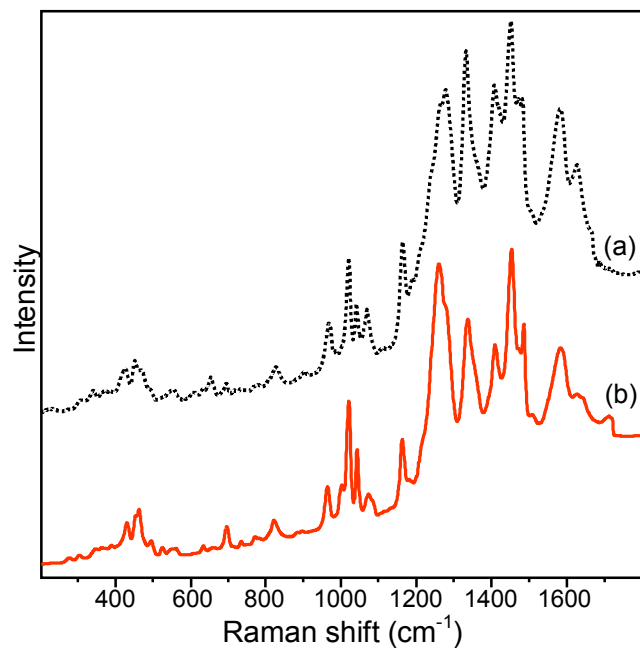
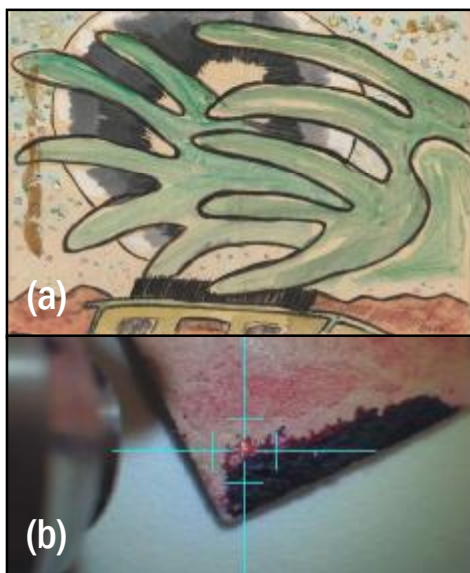


Figure 14. On the left, (a) *Silver ball, barge, and trees* by Arthur Dove, dating to 1930. Watercolor, gouache, ink and charcoal on paper; 4 7/8 x 6 7/8 inches (12.4 x 17.5 cm). The Metropolitan Museum of Art, 49.70.85. Alfred Stieglitz Collection, 1949. (b) Photograph of the sampled area. On the right, (a) SERS spectrum of reference madder lake upon HF treatment compared to (b) that of a sample taken from the watercolor upon HF treatment.

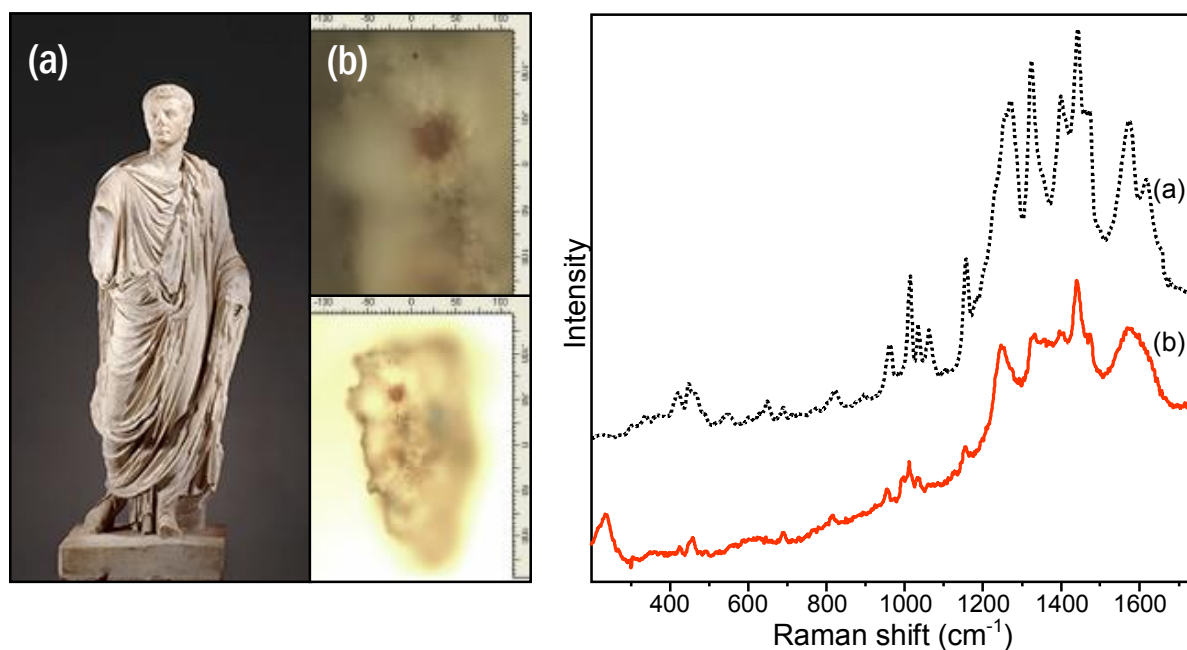


Figure 15. On the left, (a) Roman statue of Caligula dating to the 1st century. Marble; 80 x 26.5 x 19.5 inches (203.0 x 67.3 x 49.5 cm). Virginia Museum of Fine Arts, 71.20. Arthur and Margaret Glasgow Fund. (b) Photomicrographs of a ~30x30 μ m red spot from the sculpture taken using Olympus 50x and 20x microscope objectives. On the right, (a) SERS spectrum of reference madder lake upon HF treatment compared to (b) that of a red pigment sample found on the statue upon HF treatment.

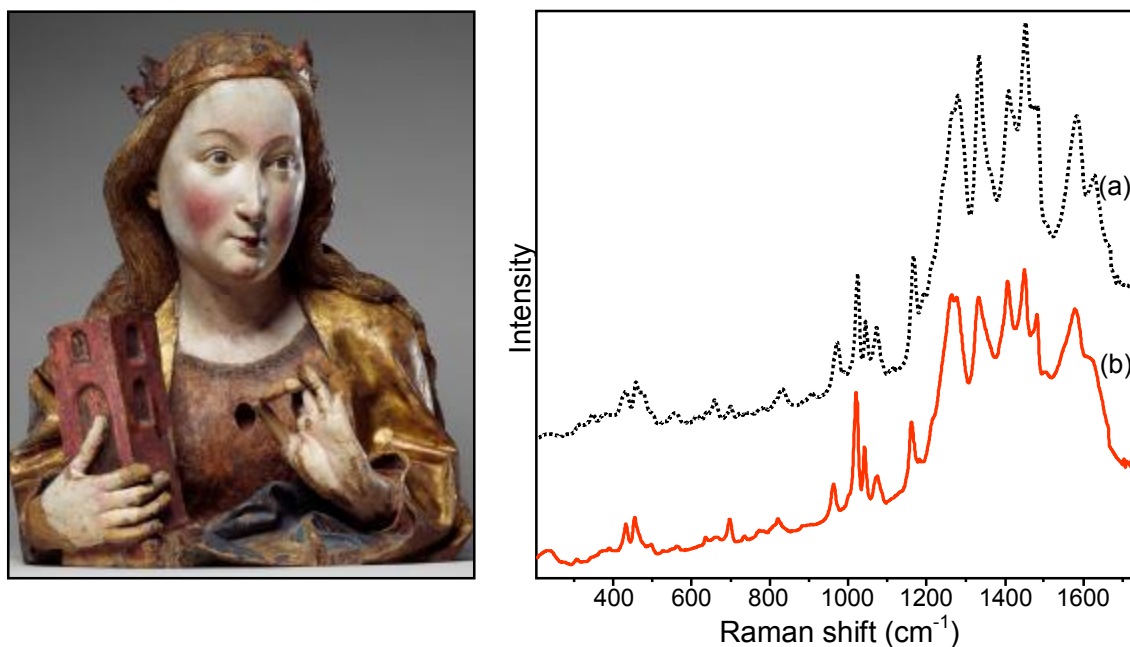


Figure 16. On the left, reliquary bust of Saint Barbara, made in the workshop of Nikolaus Gerhaert von Leiden in Germany, Strasbourg, and dating to ca. 1465. Ashwood with paint; 19 7/8 x 17 1/2 x 10 7/8 inches (50.5 x 44.5 x 27.6 cm). The Metropolitan Museum of Art, 17.190.1735. Gift of J. Pierpont Morgan, 1917. On the right, (a) SERS spectrum of reference madder lake upon HF treatment compared to (b) that of a sample taken from the bust upon HF treatment.

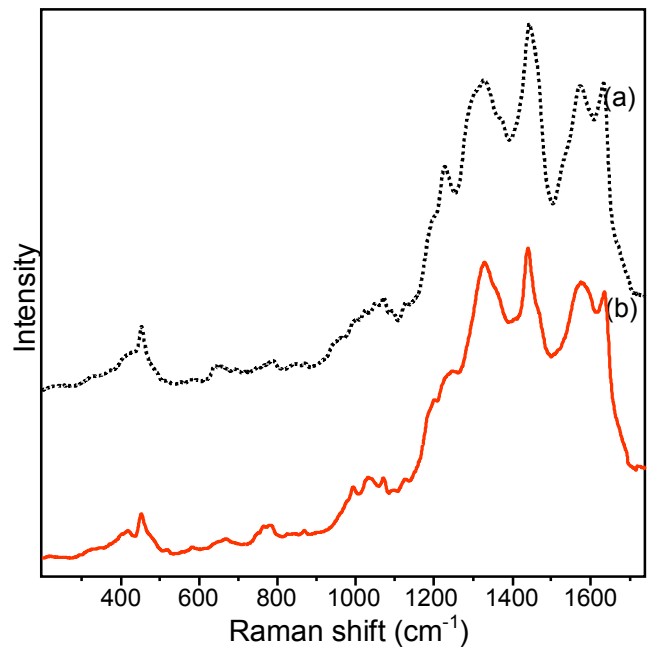


Figure 17. On the left, tasseled tunic from Peru, North coast, dating to 1100-1250. Camelid hair, cotton, tapestry weave and tassels; 21 x 51 inches (53.3 x 129.5 cm). The Metropolitan Museum of Art, L.2010.17. Lent by the Richard I. Levine Collection, 2010. On the right, (a) SERS spectrum of reference carminic acid at pH=2 compared to (b) that of a sample taken from the tasseled tunic.

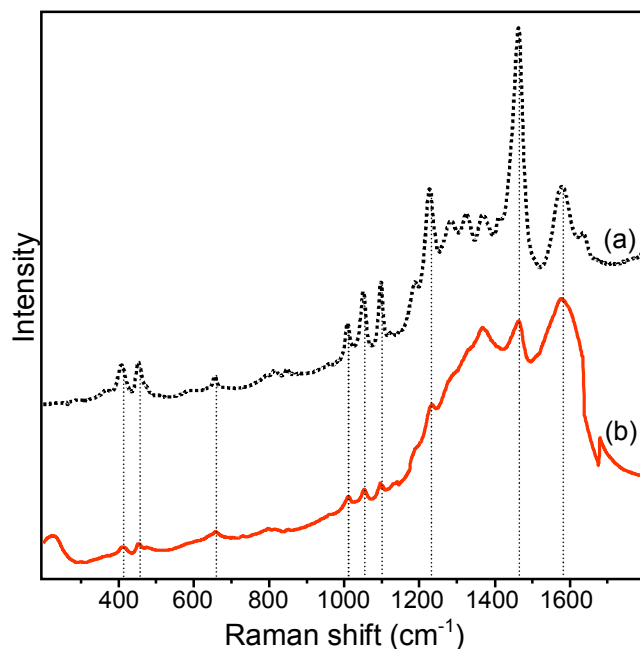


Figure 18. On the left, crucifix from Spain, Palencia, dating to ca. 1150-1200. Corpus: white oak and pine with polychromy, gilding, and applied stones; cross: red pine, polychromy; 102 1/2 x 81 3/4 inches (260.4 x 207.6 cm). The Metropolitan Museum of Art, 35.36a,b. Samuel D. Lee Fund, 1935. On the right, (a) SERS spectrum of reference laccaic acid at pH=2 compared to (b) that of a sample taken from the crucifix.

Comparison of SERS spectra with and without HF hydrolysis

In this paragraph, the results achieved from the comparative SERS analysis of commercial pure colorants and lake pigments, fibers from textiles dyed in the laboratory, as well as actual aged art samples are presented. Spectra acquired upon HF hydrolysis and without any pretreatment are here displayed without modifying their relative intensities, in order to allow an easy and effective evaluation of the results obtained from the use of these two different methodologies. Reference spectra of commercial pure dyes and lake pigments are also reported along with those collected with and without HF treatment from the art samples investigated for comparison purposes, i.e. to provide evidence of the colorants identified.

Madder and carmine commercial lakes

The comparison of the results obtained from the analysis of Kremer commercial lakes both with and without hydrolysis is a valuable way to appreciate the changes occurring in SERS spectra according to the form in which the dye molecules are present in the sample. In fact, several differences were observed between the spectra taken upon HF treatment and those obtained without hydrolysis for both madder and carmine lakes. This is consistent with the presence of their main constituents, namely alizarin/purpurin and carminic acid respectively, as free dyes upon hydrolysis or complexed with the inorganic components of the lake when the sample has not been treated.

For madder lake, the SERS spectral pattern arising upon HF treatment shows a good correspondence with those of both purpurin and alizarin solutions at pH=2. In detail, as also observed in Chapter 2, the contribution of purpurin is predominant and particularly evident in the spectrum of hydrolyzed madder lake for bands at 1620, 1576, 1466 cm^{-1} , as well as 1231 and 1201 cm^{-1} , appearing as shoulders, and, at lower wavenumbers, for signals at 1063, 962, 649, 606, 548, 448, 422 and 308 cm^{-1} . Also, a few bands exclusively due to alizarin are located at 1444, 1325 and 1157 cm^{-1} , while signals at 1445, 1326 and 1158 cm^{-1} are present in the SERS spectra of both hydrolyzed madder lake and the two pure dyes. On the other hand, the untreated pigment gave rise to a rather different spectral pattern, where bands at 1444, 1401 and 1015 cm^{-1} , quite strong upon HF treatment, disappear and are replaced by new signals at 1457, 1425 and 1359 cm^{-1} . Moreover, the band at 1620 cm^{-1} , which is fairly intense in the spectrum of the lake obtained upon hydrolysis, is present as a shoulder without treatment, while, on the contrary, the signal at 1475 cm^{-1} becomes relevant in the non-hydrolysis spectrum (figure 19).

It is interesting to notice that the band at 962 cm^{-1} , reported as a marker for mordanted alizarin by Brosseau *et al.*⁹ and attributed to the Al-O bending vibration characterizing the formation of the dye-mordant complex²⁰, is here observed only for the HF-treated sample (figure 19).

As far as carmine naccarat is concerned, the hydrolyzed lake is characterized by intense signals at 1632, 1574, 1446, 1325, 1223, 1069, 451 cm^{-1} , which correspond to the main bands of reference carminic acid solution at pH=2. A different spectral pattern was obtained for the pigment without hydrolysis, only displaying three major signals at 1638, 1464 and 1297 cm^{-1} . These wavenumbers are also reported by Oakley *et al.* as markers for untreated carmine lake¹¹, even though with different relative intensities possibly due to the use of a He-Ne laser emitting at 633 nm as the excitation source (figure 19).

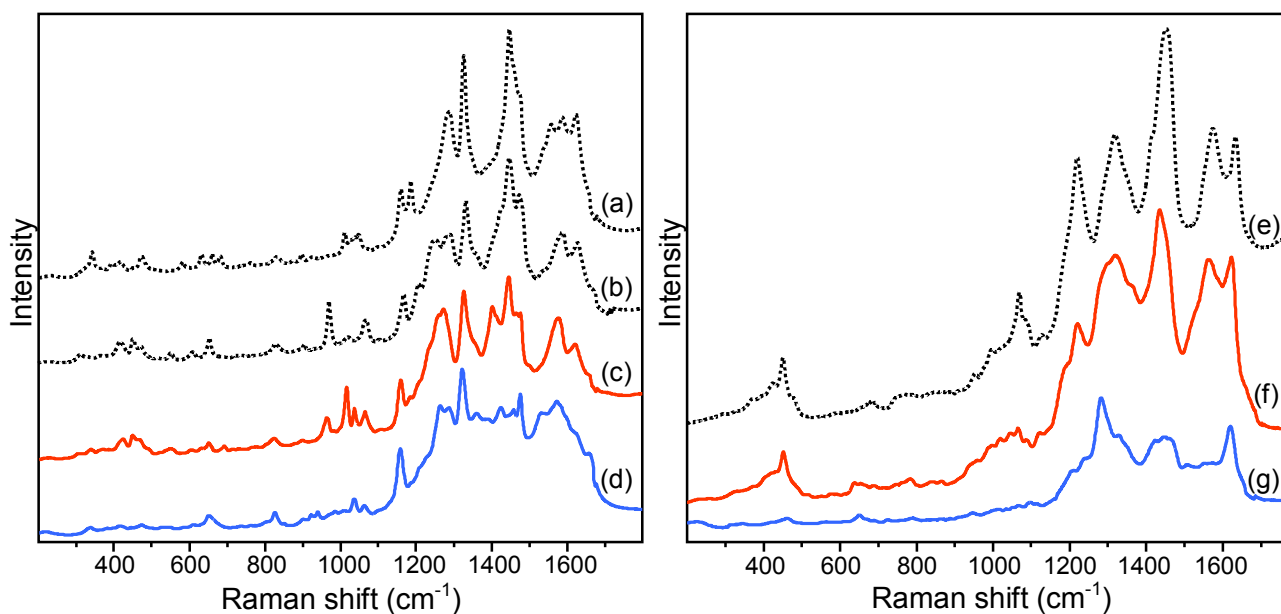


Figure 19. On the left, SERS spectra of (a) alizarin at pH=2 and (b) purpurin at pH=2 compared to those of madder lake (c) on Ag microwave colloid upon HF treatment and (d) on Ag microwave colloid without hydrolysis. On the right, (e) SERS spectrum of carminic acid at pH=2 compared to those of carmine naccarat (f) on Ag microwave colloid upon HF treatment and (g) on Ag microwave colloid without hydrolysis.

Winsor & Newton lakes

Five lakes on drawing paper, namely alizarin carmine, alizarin crimson, carmine, pink madder and purple madder (alizarin), have been examined as representative samples from a historical Winsor & Newton catalogue of watercolor pigments dating to 1887, which contains a wide collection of swatches showing the results obtainable with the firm's colors (figure 20).

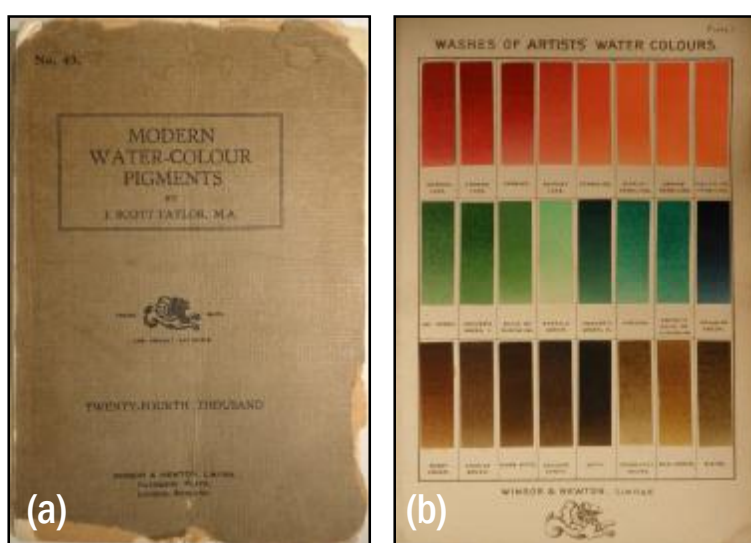


Figure 20. Original Winsor & Newton handbook of watercolor pigments dating to 1887, which contains a wide collection of swatches showing the results obtainable with the firm's colors: (a) cover and (b) selection of washes.

Neither for alizarin carmine nor for alizarin crimson a description is provided in the handbook concerning their chemical composition. Both lakes gave rise to excellent SERS spectra on microwave colloids upon HF treatment, showing a good correspondence with the spectral features of alizarin solution at pH=2. As expected, a few spectral shifts were observed in the spectra of the pigments as such in comparison to those taken upon hydrolysis: in detail, signals located at 1605, 1585 and 1430 cm^{-1} for the HF-treated samples are shifted to 1599, 1579 and 1424 cm^{-1} in the spectra of the untreated lakes. Also, a few changes were detected in terms of relative intensities of bands: for example, the signal at 1622 cm^{-1} , of medium intensity in the spectra obtained upon HF hydrolysis, appears as a shoulder in those of the untreated samples, while the band at 1474 cm^{-1} , which is just a shoulder for the hydrolyzed lakes, is fairly intense and more resolved for the pigments without any treatment. Also, two signals at 1207 and 1185 cm^{-1} , of weak and medium intensity respectively for the HF-treated samples, show reverse intensity ratios in the spectra of non-hydrolyzed lakes. Moreover, it is interesting to notice that, for untreated alizarin carmine, the use of a concentrated colloid did not result in higher enhancement factors in comparison to spectra obtained on regular nanoparticles (figure 21).

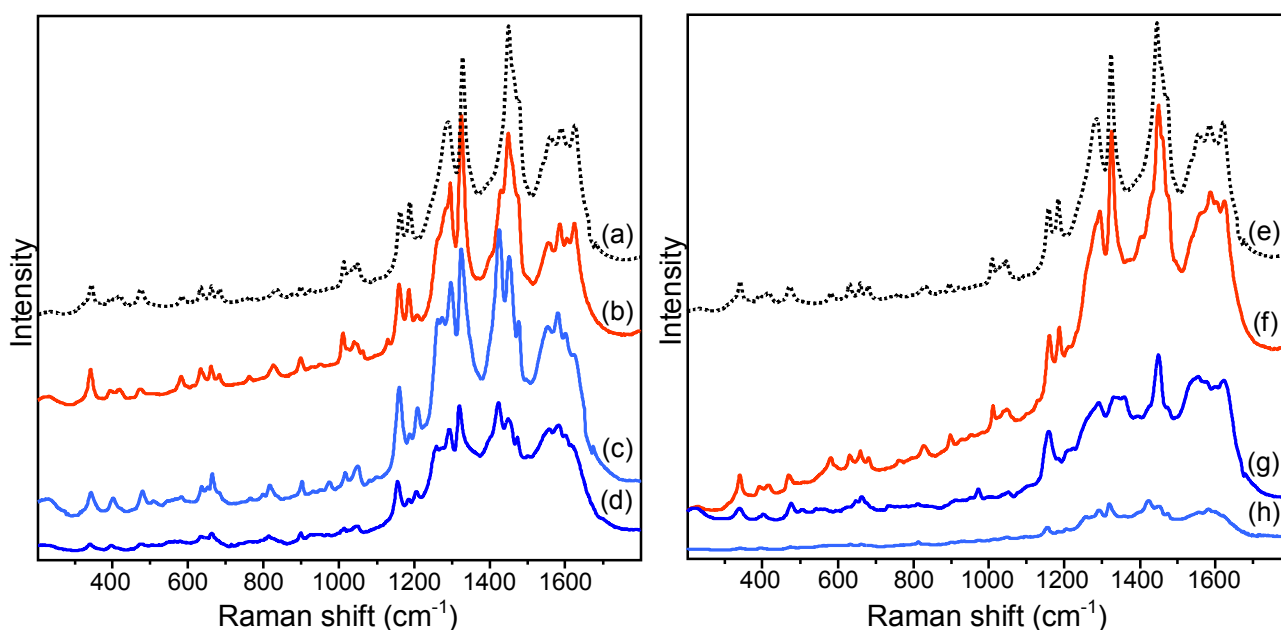


Figure 21. On the left, (a) SERS spectrum of reference alizarin at pH=2 compared to those of alizarin carmine from the Winsor & Newton catalogue (b) on Ag microwave colloid upon HF treatment, (c) on regular Ag microwave colloid without hydrolysis and (d) on 5x Ag microwave colloid without hydrolysis. On the right, (e) SERS spectrum of reference alizarin at pH=2 compared to those of alizarin crimson from the Winsor & Newton catalogue (f) on Ag microwave colloid upon HF treatment, (g) on 5x Ag microwave colloid without hydrolysis and (h) on regular Ag microwave colloid without hydrolysis.

The investigation of carmine, prepared by precipitating the coloring matter of cochineal with aluminous base according to the manufacturers, resulted in good SERS spectra on microwave colloids without hydrolysis, which match very well the spectral features of untreated carmine naccarat purchased by Kremer, the spectrum of which is reported in figure 19. Using the same laser power at the sample, i.e. 0.5 mW, questionable results were achieved from the analysis of such lake upon HF treatment: indeed, although some of the main spectral features of reference carminic acid are still recognizable in the spectrum at 1580, 1444, 1329, 1227, 1071 and 453 cm^{-1} , a significant broadening of signals is encountered despite the use of a low laser power (figure 22). This phenomenon could be possibly ascribed to a particular sensitivity of carminic acid to photodegradation depending to its chemical environment, as suggested in the literature^{21,22}.

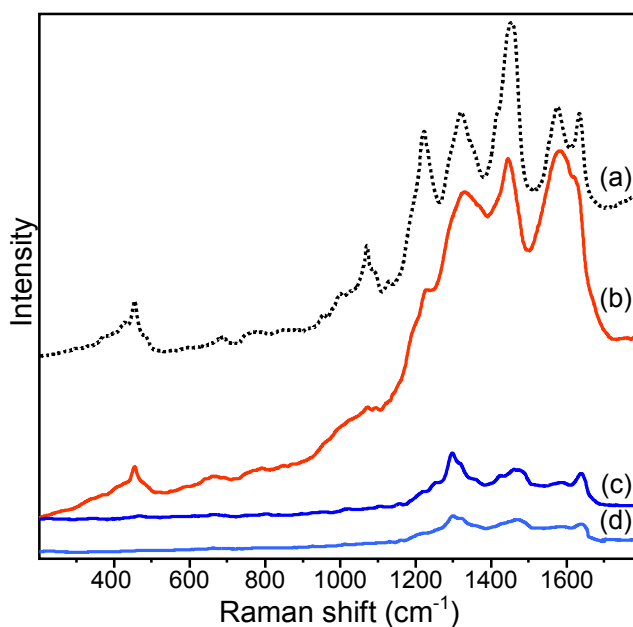


Figure 22. (a) SERS spectrum of reference carminic acid at pH=2 compared to those of carmine from the Winsor & Newton catalogue (b) on Ag microwave colloid upon HF treatment, (c) on 5x Ag microwave colloid without hydrolysis and (d) on regular Ag microwave colloid without hydrolysis.

Pink madder, alumina lake produced from madder roots according to Winsor & Newton, and purple madder (alizarin), for which a description is not provided by the manufacturers, gave rise to very good results on microwave nanoparticles especially upon HF treatment. Spectra collected with and without hydrolysis show a remarkable resemblance with those obtained from hydrolyzed madder lake and madder lake as such, respectively, even if minor differences in relative intensities were detected. However, it is worth highlighting that in both cases higher intensities as well as an improved resolution of the signals were obtained upon HF treatment (figure 23).

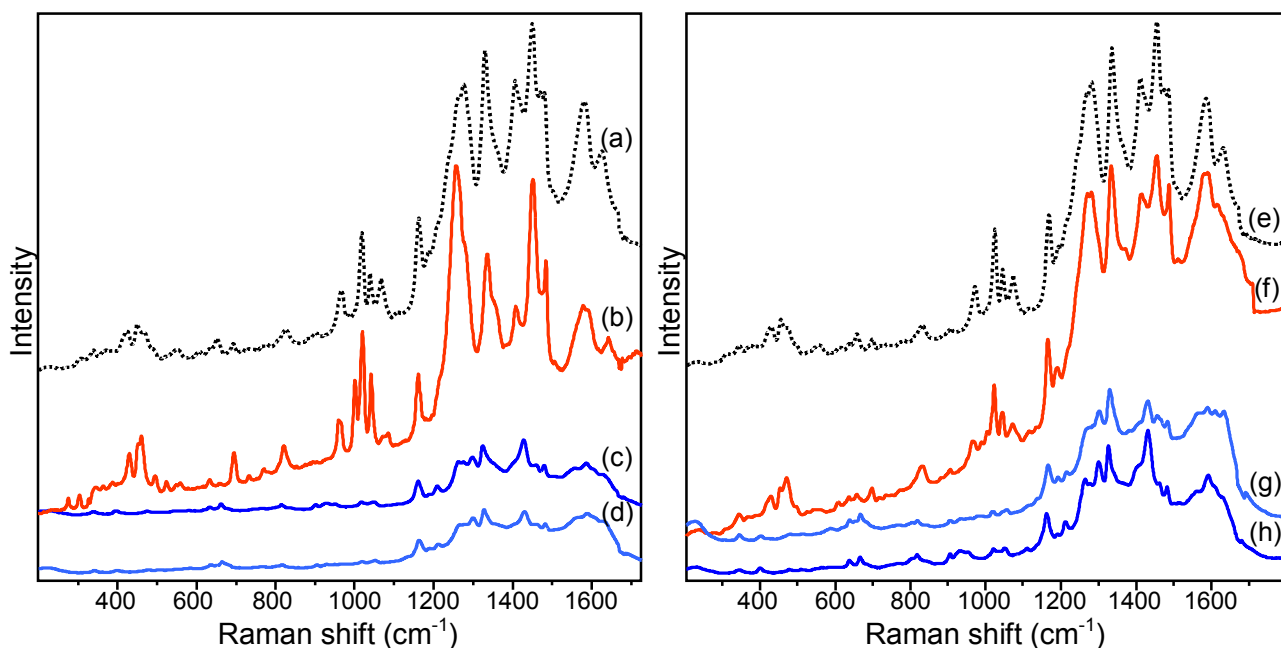


Figure 23. On the left, (a) SERS spectrum of reference madder lake upon HF treatment compared to those of pink madder from the Winsor & Newton catalogue (b) on Ag microwave colloid upon HF treatment, (c) on 5x Ag microwave colloid without hydrolysis and (d) on regular Ag microwave colloid without hydrolysis. On the right, (e) SERS spectrum of reference madder lake upon HF treatment compared to those of purple madder (alizarin) from the Winsor & Newton catalogue (f) on Ag microwave colloid upon HF treatment, (g) on regular Ag microwave colloid without hydrolysis and (h) on 5x Ag microwave colloid without hydrolysis.

Pink lake pigment from Corinth, Greece

The investigation of a pink lake pigment from Corinth, Greece, dating to the 2nd century B.C. is an effective example of the issues that might be encountered when applying different analytical methodologies to the analysis of very ancient samples. Indeed, the unknown pigment could only be identified using the HF hydrolysis procedure, which allowed us to obtain from a single particle an excellent SERS spectrum perfectly matching the spectral features of madder lake subjected to the same treatment. On the contrary, very poor spectra were obtained from the sample as such, displaying a significantly lower intensity and strongly dominated by the spurious bands due to the colloid (figure 24).

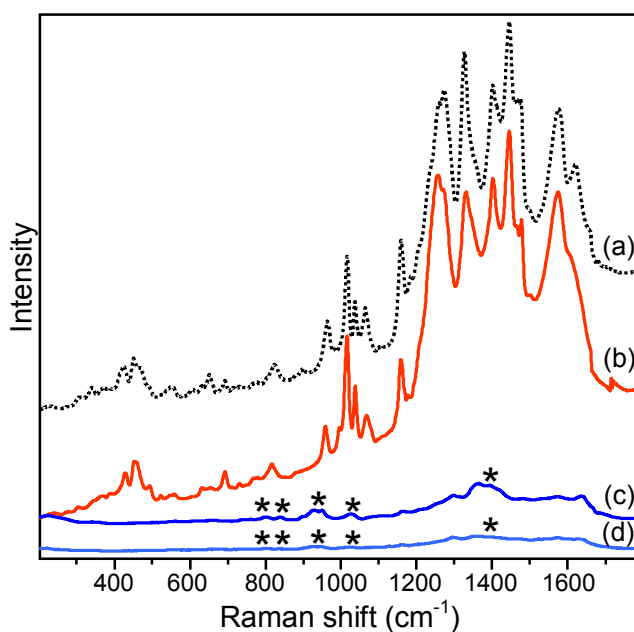


Figure 24. (a) SERS spectrum of reference madder lake upon HF treatment compared to those of a 2nd century B.C. pink pigment from Corinth, Greece, (b) on Ag microwave colloid upon HF treatment, (c) on 5x Ag microwave colloid without hydrolysis and (d) on regular Ag microwave colloid without hydrolysis. Spurious bands due to the colloid are marked with *.

Dyed textiles

Silk and wool fabrics dyed in the Department of Textile Conservation of the Metropolitan Museum of Art (figure 25) were also investigated by SERS upon HF hydrolysis and without pretreatment.

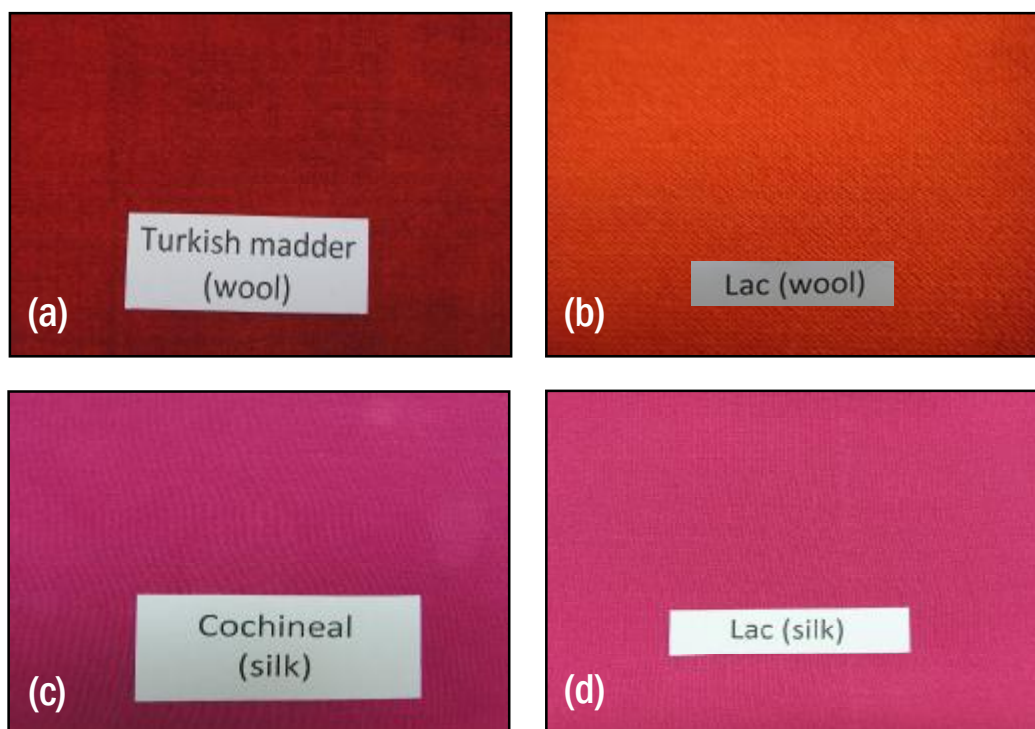


Figure 25. Fabrics dyed in the Department of Textile Conservation of the Metropolitan Museum of Art: (a) wool dyed with Turkish madder, (b) wool dyed with lac dye, (c) silk dyed with cochineal and (d) silk dyed with lac dye.

Satisfactory SERS spectra were taken from a single wool fiber dyed with Turkish madder using both the methodologies compared in this chapter. Results achieved with and without HF treatment are indeed consistent with those obtained from reference madder lake upon hydrolysis and as such, respectively. It is worth mentioning that, among the materials here investigated, this is the only case where the use of a concentrated colloid for the analysis of a sample without any preliminary treatment gave rise to a spectrum displaying a slightly higher intensity in comparison to that obtained upon hydrolysis. As far as wool dyed with lac dye is concerned, the HF treatment allowed us to acquire a high quality SERS spectrum with main features at 1583, 1461, 1366, 1324, 1283 and 1227 cm^{-1} , which turned out to be consistent with reference laccaic acid solution at $\text{pH}=2$. Good spectra, even if of lower intensity, were obtained without hydrolysis as well especially on 5x microwave colloids, with bands at 1604, 1585, 1563, 1428, 1364, 1320, 1291, 1256 and 1155 cm^{-1} (figure 26).

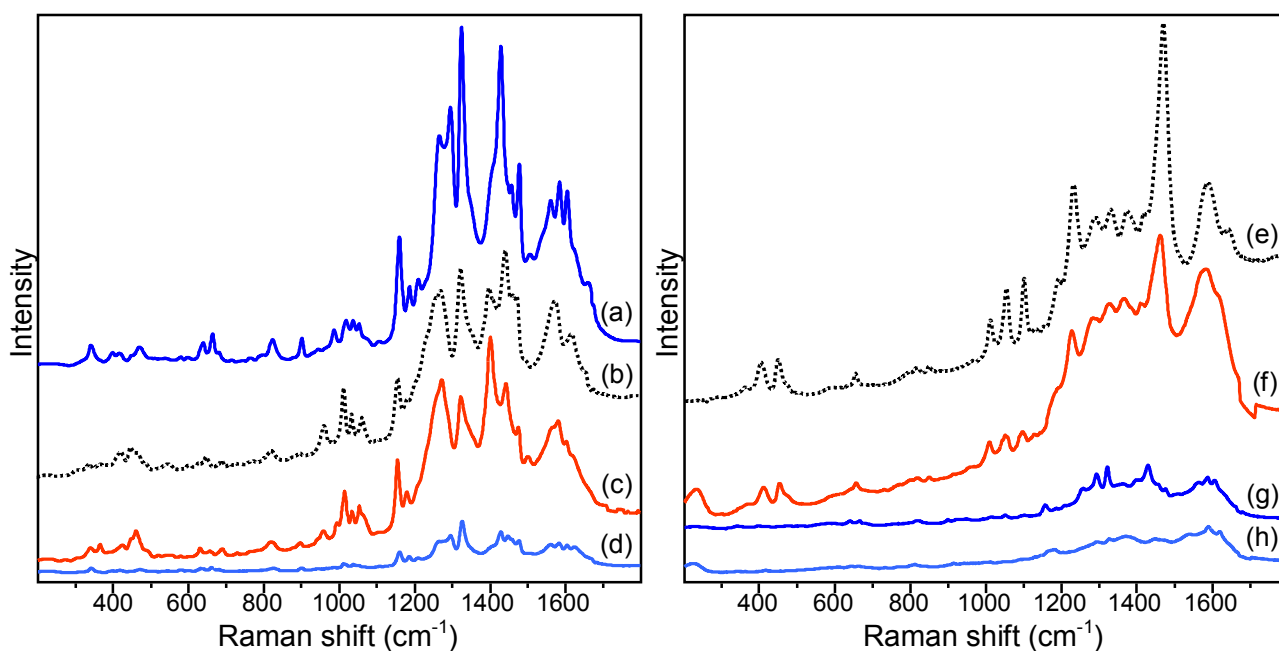


Figure 26. On the left, (b) SERS spectrum of reference madder lake upon HF treatment compared to those of Turkish madder on wool (a) on 5x Ag microwave colloid without hydrolysis, (c) on Ag microwave colloid upon HF treatment and (d) on regular Ag microwave colloid without hydrolysis. On the right, (e) SERS spectrum of laccaic acid at pH=2 compared to those of lac dye on wool (f) on Ag microwave colloid upon HF treatment, (g) on 5x Ag microwave colloid without hydrolysis and (h) on regular Ag microwave colloid without hydrolysis.

An interesting situation occurred for silk fabrics, the SERS spectra of which are characterized by a remarkable band broadening phenomenon when applying the HF hydrolysis procedure. In particular, some of the main spectral features of carminic acid were identified around 1576, 1444, 1339, 1071 and 453 cm^{-1} in the spectrum taken from a cochineal-dyed silk fiber upon HF treatment, even though, as already observed for Winsor & Newton carmine, the resolution of the signals was rather low. On the other hand, the typical signals of laccaic acid were not even detected in the spectrum of lac dye on silk after hydrolysis, as only two broad bands located around 1351 and 1575 cm^{-1} appeared in the spectrum. A slightly more detailed spectral pattern was obtained for untreated cochineal-dyed samples both on 5x and regular microwave colloids, which does not exactly correspond to the spectrum of carmine naccarat as such reported in figure 19 probably due to the different kind of substrate to which the organic colorant is bound. This spectrum shows a spectral shift from 1438 to 1418 cm^{-1} and a new band appearing at 1159 cm^{-1} with respect to spectra collected upon HF treatment. Non-hydrolysis experiments were particularly successful in the case of silk dyed with lac dye, for which a well resolved SERS spectrum was obtained with several sharp signals. This is consistent with the higher sensitivity to hydrolysis displayed by silk fibers compared with wool discussed in the literature: indeed, silk proteins released into solution are reported to be adsorbed onto the silver nanoparticles, causing interferences with dye adsorption²³ (figure 27).

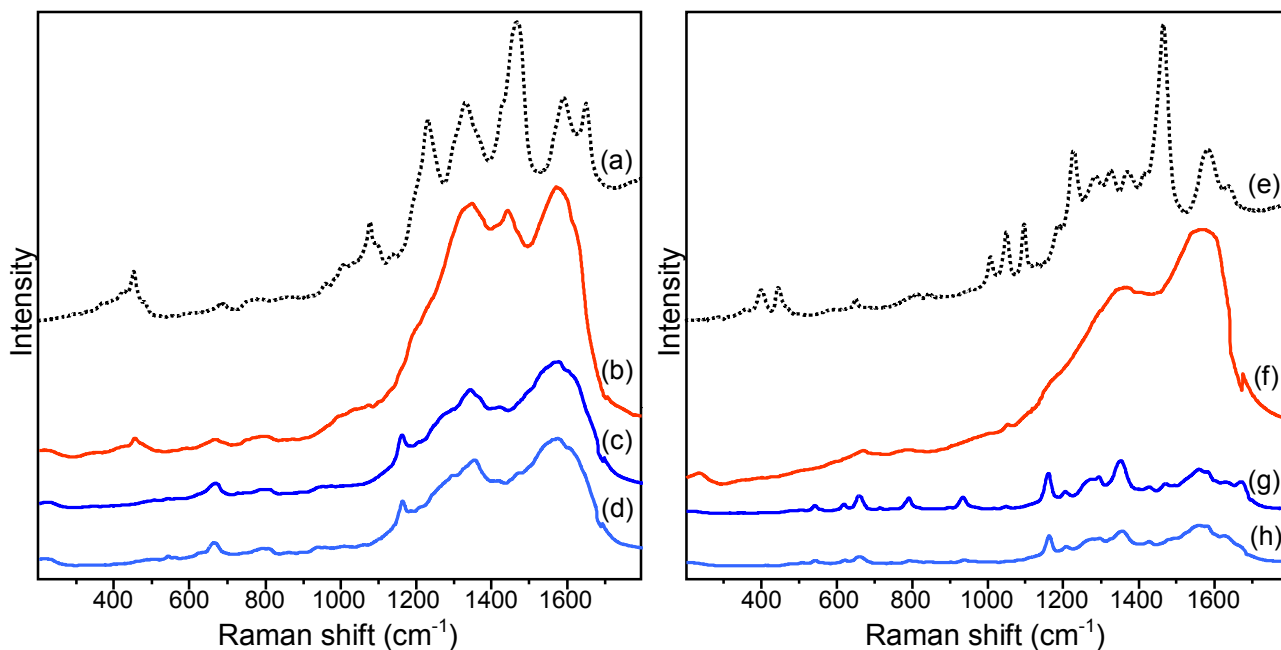


Figure 27. On the left, (a) SERS spectrum of reference carminic acid at pH=2 compared to those of cochineal on silk (b) on Ag microwave colloid upon HF treatment, (c) on 5x Ag microwave colloid without hydrolysis and (d) on regular Ag microwave colloid without hydrolysis. On the right, (e) SERS spectrum of laccaic acid at pH=2 compared to those of lac dye on silk (f) on Ag microwave colloid upon HF treatment, (g) on 5x Ag microwave colloid without hydrolysis and (h) on regular Ag microwave colloid without hydrolysis.

Cézanne's and Rembrandt's paintings

The HF hydrolysis and non-hydrolysis procedures were also compared when applied to the SERS analysis of samples taken from two of the greatest masterpieces in the history of oil painting: Cézanne's *The card players* (figure 28) and Rembrandt's *Aristotle with a bust of Homer* (figure 29).

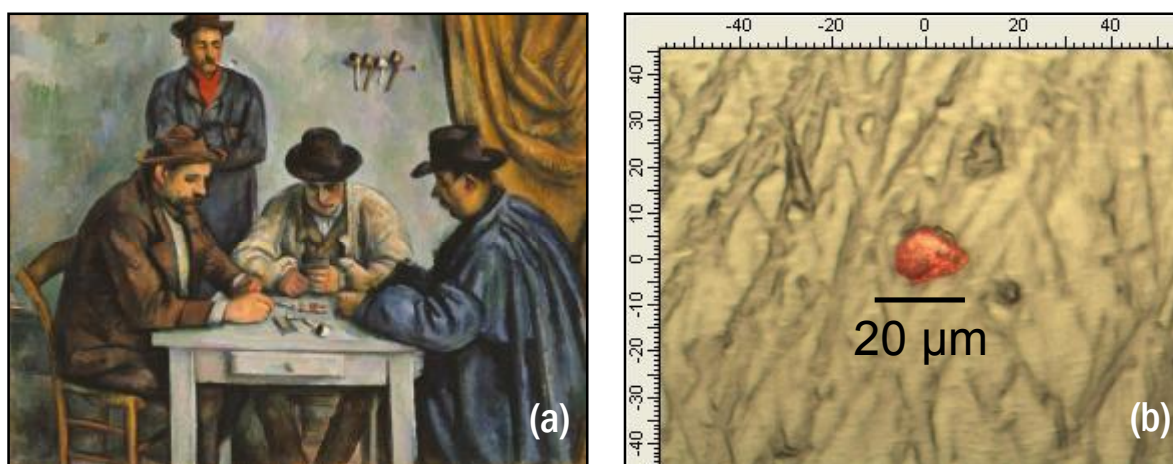


Figure 28. (a) *The card players* by Paul Cézanne, dating to 1890-1892. Oil on canvas; 25 3/4 x 32 1/4 inches (65.4 x 81.9 cm). The Metropolitan Museum of Art, 61.101.1. Bequest of Stephen C. Clark, 1960. (b) Photomicrograph of a ~20x20 μm sample from the painting taken by using an Olympus 50x microscope objective.

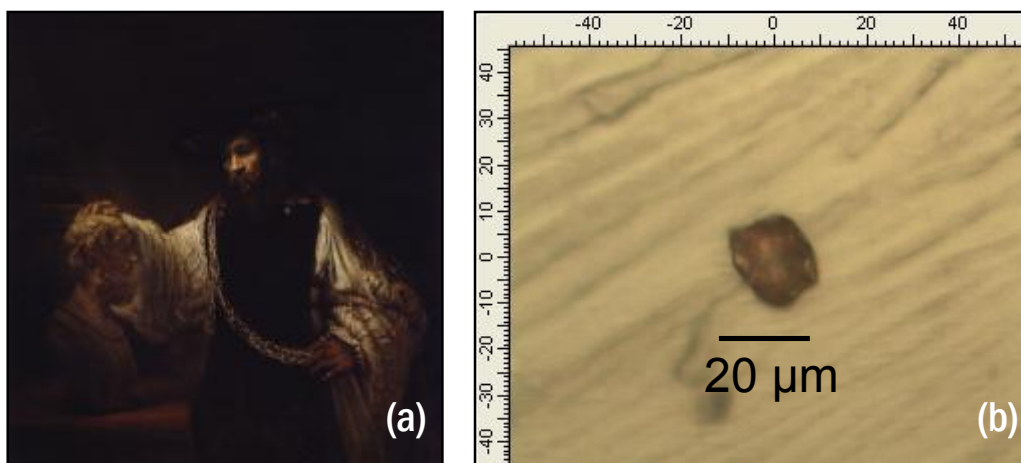


Figure 29. (a) *Aristotle with a bust of Homer* by Rembrandt, dating to 1653. Oil on canvas; 56 1/2 x 53 3/4 inches (143.5 x 136.5 cm). The Metropolitan Museum of Art, 61.198. Purchase, special contributions and funds given or bequeathed by friends of the Museum, 1961. (b) Photomicrograph of a $\sim 20 \times 20 \mu\text{m}$ sample from the painting taken by using an Olympus 50x microscope objective.

A red glaze sample of less than $20 \times 20 \mu\text{m}$ in size was taken from each painting (figures 28 and 29). The same microscopic fragment was analyzed first without hydrolysis using concentrated nanoparticles and, following removal of the colloid and a rinse with a drop of water, upon HF treatment. In both cases, the hydrolysis procedure allowed us to clearly identify the unknown colorants. Indeed, an excellent SERS spectrum was acquired upon HF treatment from the Cézanne's glaze, showing a remarkable correspondence with hydrolyzed madder lake purchased by Kremer. On the other hand, several spurious bands were detected in the spectrum collected from the sample as such due to the interference of citrate ions, even if signals at 1570 , 1474 , 1361 , 1273 and 1153 cm^{-1} are still recognizable and attributable to the presence of madder lake (figure 30). As far as the glaze taken from Rembrandt's painting is concerned, the HF treatment coupled with the use of 0.5 mW as a laser power gave rise to a SERS spectrum in which some of the key bands of carminic acid were detected; nevertheless, a considerable broadening of the signals, already encountered for other carmine-containing samples in the present work, was observed. The analysis of the same glaze sample with a lower laser power did not lead to any result; however, an improved spectrum of carminic acid, displaying a better resolution even if of lower intensity, could be obtained from a second sample of similar appearance and approximately the same size taken from Rembrandt's painting. In this case, the non-hydrolysis approach gave rise to a spectrum where signals of carmine lake were identified at 1637 , 1345 and 1294 cm^{-1} , even though the last two bands displayed reverse relative intensities in comparison to the same signals in the reference spectrum of untreated carmine naccarat shown in figure 19 (figure 30).

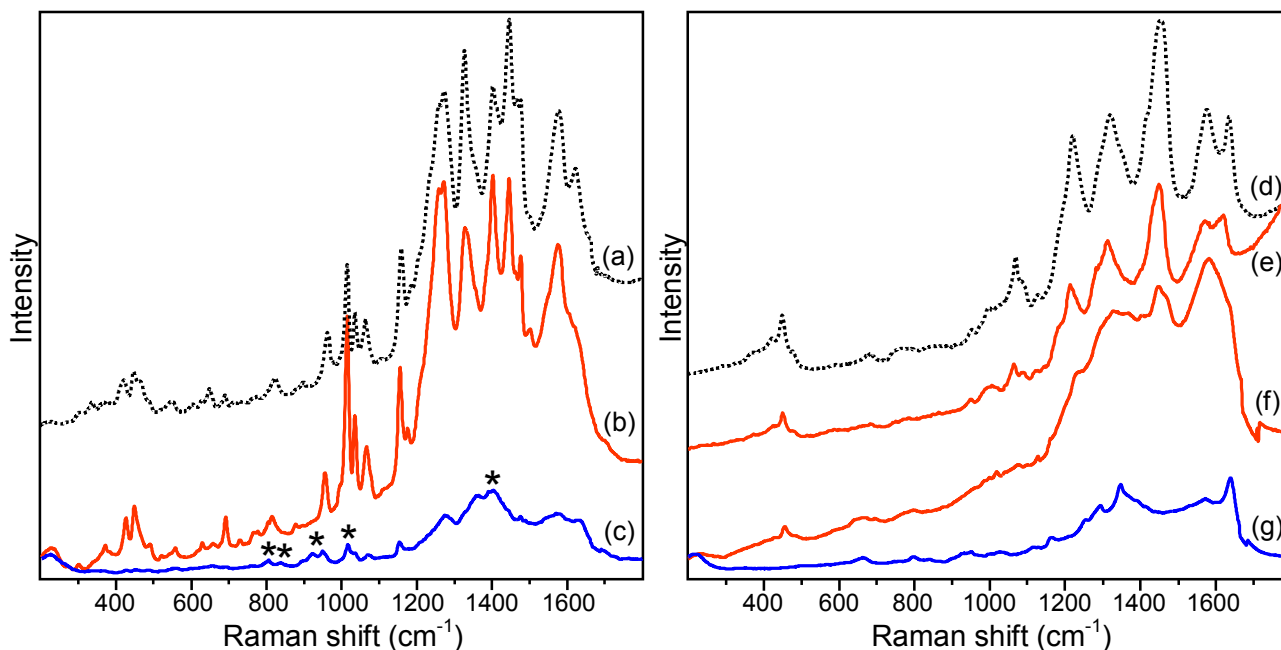


Figure 30. On the left, (a) SERS spectrum of reference madder lake upon HF treatment compared to those of a red glaze from Cézanne's *The card players* (b) on Ag microwave colloid upon HF treatment and (c) on 5x Ag microwave colloid without hydrolysis. Marked with * are spurious bands due to the colloid. On the right, (d) SERS spectrum of reference carminic acid at pH=2 compared to those of a red glaze from Rembrandt's *Aristotle with a bust of Homer* (e) and (f) on Ag microwave colloid upon HF treatment and (g) on 5x Ag microwave colloid without hydrolysis.

Nur al-Din room panel reproduction, mandolin and painted cloth

Carminic acid was found to be responsible for the reddish color of samples taken from a laboratory reproduction of a panel from the Nur al-Din room, the original version of which is on display at the Metropolitan Museum of Art (figure 31), and from an Italian mandolin made in Naples by Antonio Vinaccia (figure 32): SERS spectra obtained upon HF treatment, better resolved and of higher quality with respect to those acquired from the glazes as such, showed in both cases a good correspondence with the reference spectrum of carminic acid solution at pH=2 (figures 31 and 32). Spectra taken from both samples without hydrolysis match the spectral features of untreated carmine naccarat purchased by Kremer, the spectrum of which can be seen in figure 19 for comparison (figures 31 and 32). Such spectra generally display lower enhancement factors with respect to those obtained upon HF treatment, with the only exception of a sample taken from the Vinaccia mandolin, which gave rise, on 5x microwave colloids, to a SERS spectrum as intense as the one collected after hydrolysis (figure 32).

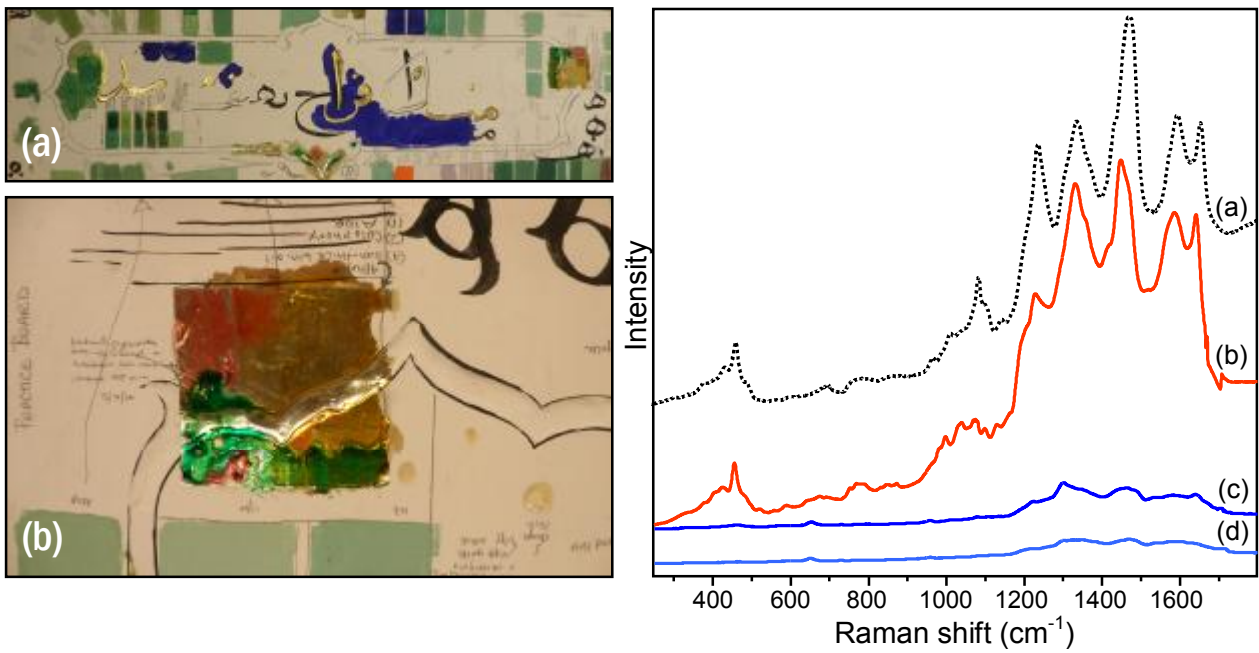


Figure 31. On the left, (a) laboratory reproduction of a panel from the Nur al-Din room at the Metropolitan Museum of Art and (b) detail of the red glazed area from which a sample was taken. On the right, (a) SERS spectrum of reference caminic acid at pH=2 compared to those of a red glaze sample from the Nur al-Din reproduction panel (b) on Ag microwave colloid upon HF treatment, (c) on 5x Ag microwave colloid without hydrolysis and (d) on regular Ag microwave colloid without hydrolysis.

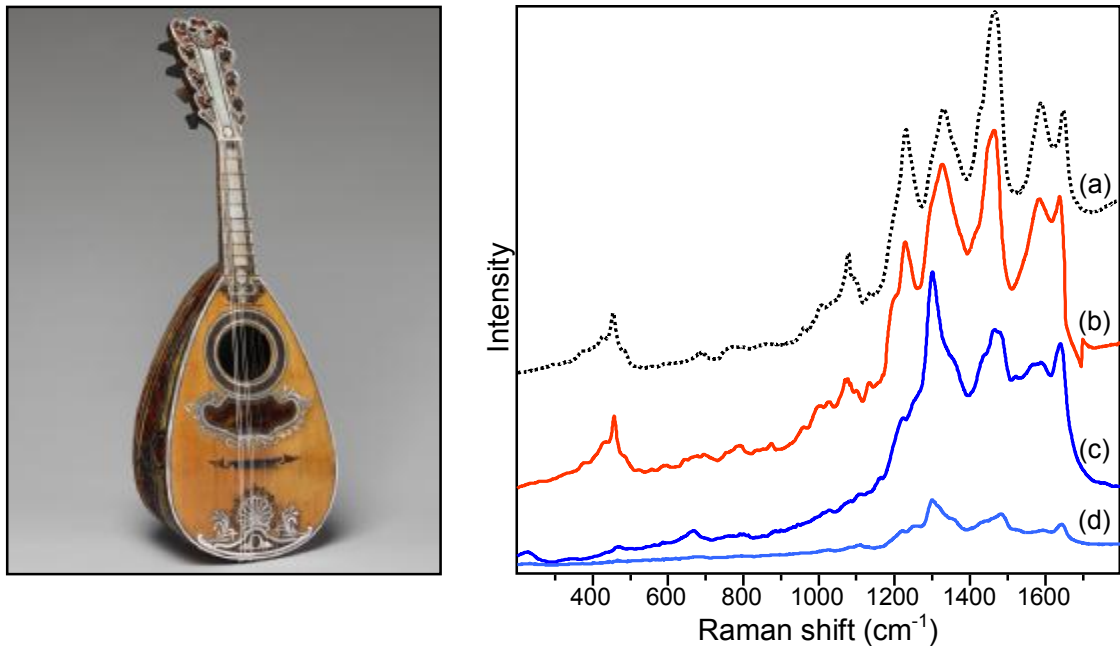


Figure 32. On the left, mandolin made in Naples, Italy, by Antonio Vinaccia and dating to 1781. Spruce, tortoiseshell, mother-of-pearl, gold alloy, ivory and various other materials; W. 7 1/2 x L. 23 inches (19.1 x 58.4 cm). The Metropolitan Museum of Art, 89.4.2140. On the right, (a) SERS spectrum of reference carminic acid at pH=2 compared to those of a red glaze sample from the Vinaccia mandolin (b) on Ag microwave colloid upon HF treatment, (c) on 5x Ag microwave colloid without hydrolysis and (d) on regular Ag microwave colloid without hydrolysis.

An excellent SERS spectrum was obtained from a glaze taken from the painted cloth depicting the celebration of the festival of cows upon HF treatment, showing a remarkable similarity with that of laccaic acid solution at pH=2; spectra of lower intensity and worse signal-to-noise ratio were collected without hydrolysis both on 5x and regular microwave colloids, with main features at 1661, 1582, 1466, 1341 and 1300 cm^{-1} (figure 33).

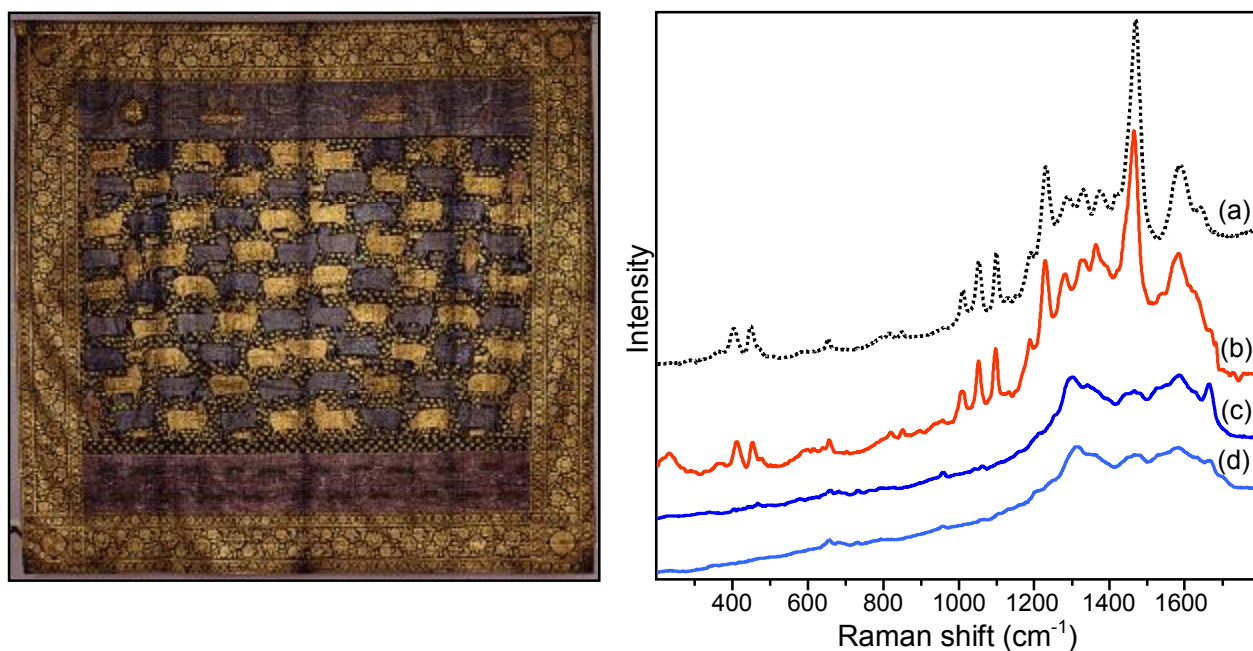


Figure 33. On the left, painted cloth depicting the celebration of the festival of cows, made in India and dating to the late 18th - early 19th century. Cotton, indigo-dyed ground with painted opaque watercolor, gold and silver; 97 5/8 x 103 1/8 inches (248 x 262 cm). The Metropolitan Museum of Art, 2003.177. Purchase, Friends of Asian Art Gifts, 2003. On the right, (a) SERS spectrum of reference laccaic acid at pH=2 compared to those of a red glaze sample from the painted cloth (b) on Ag microwave colloid upon HF treatment, (c) on 5x Ag microwave colloid without hydrolysis and (d) on regular Ag microwave colloid without hydrolysis.

Conclusions

Two SERS procedures for the detection of organic dyes in cultural heritage investigations, i.e. SERS on Ag nanoparticles upon HF hydrolysis and without any preliminary treatment, were compared when applied to the identification of colorants from a number of ancient samples and works of art representative of different cultures and covering a period of time of about 2000 years.

The experiments here conducted showed that spectra obtained without hydrolysis generally display lower intensity and worse signal-to-noise ratios in comparison to those taken upon HF treatment. Issues of reproducibility and variability of relative intensities of signals were sometimes encountered, even within the same measurement. Also, when dealing with very ancient samples, i.e. the pink pigment from Corinth, as well as for some glazes, as in the case of Cézanne's *The card players*, this methodology gave rise to spectra which turned out to be strongly affected by bands due to the colloid even when using nanoparticles of regular concentration. The non-hydrolysis approach was found to be particularly suitable for lac dye on silk, which produced very poor results upon HF treatment. The use of the HF hydrolysis procedure occasionally led to questionable results for carmine-containing samples: indeed, for Winsor & Newton carmine, silk dyed with cochineal and for one of the two samples taken from Rembrandt's *Aristotle with a bust of Homer*, significant phenomena of band broadening were encountered even if the laser power employed was rather low. When analyzing carmine-containing glazes or cochineal-dyed fabrics, the non-hydrolysis approach seemed to be a valid alternative, as it allowed us to obtain good SERS spectra from most samples.

Except for a few cases discussed above, the HF treatment has proven to be a very effective method, leading to achieve a reliable fingerprint for the great majority of samples examined within very short times of analysis. The introduction of an additional step in the analytical procedure, i.e. the HF hydrolysis, does not result in slower analysis when compared to the non-hydrolysis approach: in fact, well resolved and reproducible spectra with high enhancement factors were obtained in less than 30 minutes from sampling in all cases, while several minutes were needed just for nanoparticles aggregation when the HF step was not used.

In conclusion, because of the relative merits of both procedures and of their mutual compatibility, it is recommended to adopt a two-step procedure for analysis of unknown samples. By analyzing a sample first without the hydrolysis step and then removing the colloid and exposing the same sample to HF, the best and most consistent results for a variety of dyes and substrates are assured.

References

- [1] K. Chen, M. Leona, T. Vo-Dinh, *Sens. Rev.* **2007**; 27, 109.
- [2] K. L. Wustholz, C. L. Brosseau, F. Casadio, R. P. Van Duyne, *Phys. Chem. Chem. Phys.* **2009**; 11, 7350.
- [3] F. Casadio, M. Leona, J. R. Lombardi, R. Van Duyne, *Acc. Chem. Res.* **2010**; 43, 782.
- [4] P. C. Lee, D. Meisel, *J. Phys. Chem.* **1982**; 86, 3391.
- [5] M. V. Cañamares, J. V. Garcia-Ramos, J. D. Gómez-Varga, C. Domingo, S. Sanchez-Cortes, *Langmuir* **2007**; 23, 5210.
- [6] Z. Jurasekova, E. del Puerto, G. Bruno, J. V. Garcia-Ramos, S. Sanchez-Cortes, C. Domingo, *J. Raman Spectrosc.* **2010**; 41, 1165.
- [7] M. Leona, *Proceedings of the National Academy of Sciences* **2009**; 106, 14757.
- [8] E. Van Eslande, S. Lecomte, A.-S. Le Hô, *J. Raman Spectrosc.* **2008**; 39, 1001.
- [9] C. L. Brosseau, A. Gambardella, F. Casadio, C. M. Grzywacz, J. Wouters, R. P. Van Duyne, *Anal. Chem.* **2009**; 81, 3056.
- [10] C. L. Brosseau, A. Gambardella, F. Casadio, C. M. Grzywacz, J. Wouters, R. P. Van Duyne, *Anal. Chem.* **2009**; 81, 7443.
- [11] L. H. Oakley, S. A. Dinehart, S. A. Svoboda, K. L. Wustholz, *Anal. Chem.* **2011**; 83, 3986.
- [12] J. H. Hofenk de Graaff, *The Colourful Past - Origins, Chemistry and Identification of Natural Dyestuffs*, Archetype Publications, London, **2004**.
- [13] A. Casoli, M. E. Darcchio, L. Sarritzu, *I Coloranti nell'Arte*, Il Prato Casa Editrice, Padova, **2009**.
- [14] J. Wouters, *Stud. Conserv.* **1985**; 30, 119.
- [15] S. Bruni, V. Guglielmi, F. Pozzi, *J. Raman Spectrosc.* **2010**; 41, 175.
- [16] M. Leona, J. Stenger, E. Ferloni, *J. Raman Spectrosc.* **2006**; 37, 981.
- [17] M. V. Cañamares, M. Leona, *J. Raman Spectrosc.* **2007**; 38, 1259.
- [18] J. S. Mills, R. White, *The Organic Chemistry of Museum Objects*, Butterworths, London, **1994**, p. 121.
- [19] A. V. Whitney, R. P. Van Duyne, F. Casadio, *J. Raman Spectrosc.* **2006**; 37, 993.
- [20] A. M. Ahern, P. R. Schwartz, L. A. Shaffer, *Appl. Spectrosc.* **1992**; 46, 1412.
- [21] K. Jørgensen, L. H. Skibsted, *Food Chem.* **1991**; 40, 25.
- [22] G. Favaro, C. Miliani, A. Romani, M. Vagnini, *J. Chem. Soc., Perkin Trans.* **2002**; 2, 192.
- [23] D. Zhang, S. M. Ansar, K. Vangala, D. Jiang, *J. Raman Spectrosc.* **2010**; 41, 952.

Chapter 6

SERS and Raman study of watercolors from a historical Winsor & Newton handbook

Abstract

The Winsor & Newton company has been one of the main fine art products providers since its establishment in 1832, being responsible for the production of a wide assortment of materials ranging from oils and pigments to brushes and papers. All the items manufactured over the years have been indexed in what has become the most extensive historical archive of the 19th century. Scientific analysis of original Winsor & Newton handbooks represents a powerful resource which can offer insight into the world of artists' materials, allowing us to gain knowledge of the artist's choices and the techniques used through the identification of substances employed to obtain particular hues.

In this chapter, a number of organic dyes-containing tints on drawing paper were examined from a historical Winsor & Newton catalogue of watercolor pigments dating to 1887. An appropriate database was thus built, including both ordinary Raman and SERS spectra of a wide variety of shades. The comparison between the so obtained spectral patterns and reference spectra of pure colorants and lakes allowed us to divide the pigments into classes and to ascertain their main chemical components even when indications about their preparation procedure were not provided by the manufacturers.

Introduction

Founded in 1832, the Winsor & Newton company has always been one of the main art materials suppliers in the world, manufacturing a wide assortment of fine art products such as oils, alkyds, watercolors, acrylics, pastels, brushes, canvases and papers. Since the company was established, an extensive archive has been created, including bound records of processes and shopfloor accounts, as well as handwritten books of recipes and notes for making artists' pigments, oil colors, watercolors and a great variety of other art materials. The 19th century Winsor & Newton archive, which contains 87 manuscripts for an overall amount of 17,000 pages, is considered to be the most comprehensive and exhaustive historical collection of this kind dating back to the 1800s¹.

Winsor & Newton catalogues, with their collections of swatches showing the results obtainable with the firm's colors, are an important historical and scientific resource, which affords scholars a precious insight into the world of artists' materials. Information about the chemical composition of historical pigments can be of utmost importance for interpreting analytical data from actual paintings in technical studies or authentication efforts. As also pointed out in Chapter 1, understanding whether an artist decided to overlap a given set of colors to obtain a particular shade or if such mixture had been already created by the paint manufacturer is essential to expand our comprehension of the artist's choices, at the same time allowing us to shed new light on the techniques employed. Furthermore, chemical analysis applied to the study of original art products may also contribute to set up suitable conservation and restoration approaches, as paint defects as well as the deterioration degree of pigments in works of art can be deeply characterized and properly treated by examining actual recipes and preparation procedures for a certain material.

A few studies reported in the literature are dealing with the analysis of Winsor & Newton acrylic and alkyd paints, as well as watercolor pigment cakes by GC-MS, ATR-FTIR, MALDI-MS, ESI-MS, XRD and normal Raman spectroscopy²⁻⁵. More recently, a SERS characterization of four color washes from a Winsor & Newton catalogue was also performed in order to provide a reference for the identification of specific colorants in a watercolor by the American print-maker and painter Homer⁶; however, to the best of our knowledge, a complete Raman and SERS study of pigments from historical handbooks has never been carried out.

In this chapter, several color washes from an original Winsor & Newton catalogue entitled "A descriptive handbook of modern water-colour pigments", dating back to 1887, were examined, aiming to identify the organic colorants possibly contained in each shade, and the results obtained from such scientific study are presented. Figure 1 displays the six plates of the historical catalogue where pigments have been arranged by the manufacturers in order to bring out their color and emphasize the chromatic effect obtainable by their juxtaposition. An appropriate database of original art materials was here acquired, including ordinary Raman and SERS spectra of several pink, red, violet, brown and gray tints on drawing paper. Based on the observed spectral patterns, the pigments from the catalogue were subsequently divided into different categories and their chemical composition discussed in connection with the preparation procedures declared for each one of them by Winsor & Newton in the chapter of the handbook entitled "Section II. - Description of water-colour pigments". The results reported in the following may represent valuable reference data to be used for dating, as well as in authentication and identification studies.



Figure 1. Color washes on drawing paper from the original Winsor & Newton catalogue of watercolor pigments under investigation. Pigments are combined and arranged by the manufacturers onto six plates in order to bring out their color and emphasize the chromatic effect obtainable by their juxtaposition.

Experimental

Chemicals

Silver nitrate, sodium citrate, sulfuric acid, glucose and hydrofluoric acid were purchased from Fisher Scientific, alizarin, carminic acid, crystal violet, ethanol and potassium nitrate from Sigma-Aldrich, while madder lake, carmine naccarat (alumina lake of carminic acid) and indigo were obtained from Kremer Pigments. All the aqueous solutions used for the silver nanoparticle synthesis were prepared using 18 M Ω ultrapure water (Millipore Simplicity 185 water purification system).

Analytical methods: HF hydrolysis, Ag colloid synthesis and sample preparation

SERS analyses of Winsor & Newton pigments were carried out upon HF hydrolysis on silver nanoparticles.

HF hydrolysis, a step designed to increase the mobility of the dye molecules and maximize their adsorption on the colloid surface, was performed by exposing the samples to HF vapor in a closed microchamber for 5 minutes⁷, according to a procedure previously optimized and discussed in Chapter 5.

Silver colloids synthesized by microwave-supported glucose reduction of silver sulfate in the presence of sodium citrate as a capping agent⁸ were chosen as a metal substrate for SERS analyses; a detailed description of their synthesis is given in Chapter 5.

As far as the sample preparation is concerned, reference solutions of pure dyes, namely alizarin and carminic acid, were daily prepared in ethanol at a concentration of 10^{-4} M, and aliquots of 10% NaOH and 6 M HNO₃ solutions were employed to adjust the pH. For SERS analysis, 0.2 μ L of the dye solution were added to 0.8 μ L of the Ag colloid, followed by the addition of 0.1 μ L of a 0.5 M KNO₃ aqueous solution to induce aggregation of the nanoparticles. Reference madder and carmine lakes as well as all the pigments from the Winsor & Newton catalogue under investigation were analyzed upon deposition of 0.8 μ L of the Ag colloid on top of the treated samples, inducing the aggregation of the nanoparticles through the addition of 0.1 μ L of a 0.5 M KNO₃ aqueous solution. SERS analyses were performed by focusing the laser beam onto the microaggregates which turned out to be visible inside the drop a few seconds after covering the sample with the Ag colloid. SERS spectra could be obtained immediately after the preparation of the sample and generally improved in quality as aggregation proceeded, before deteriorating when the liquid was fully evaporated.

Instrumentation










Ordinary Raman experiments were performed in the dispersive mode using a Bruker Senterra Raman spectrometer equipped with an Olympus 100x long working distance microscope objective and a charge-coupled device (CCD) detector. A Spectra Physics Model 2020 BeamLock Ar⁺ laser and a continuous wave diode laser, emitting at 488 nm and 785 nm respectively, were used as the excitation sources, and two holographic gratings provided a spectral resolution of 3-5 cm^{-1} (1800 rulings/mm for the 488 nm laser, 1200 rulings/mm for the 785 nm laser). An output laser power of 0.25 or 2.5 mW for 488 nm excitation and 10 or 25 mW for 785 nm excitation, according to the Raman response of the different pigments, was employed for the analysis.

SERS spectra were recorded with the above mentioned Bruker Senterra Raman instrument, using a 20x long working distance microscope objective and excitation at 488 nm, as the average of 1 scan with an integration time of 30 s.

Results and discussion

Detailed results obtained from ordinary Raman and SERS analyses of pink, red, violet, brown and gray shades from the Winsor & Newton handbook of watercolor pigments under investigation are presented in this section. Spectra collected from a number of tints were compared with those of reference pure dyes and lakes, allowing us to group the examined pigments into different classes according to the outcomes of scientific investigations. It is worth pointing out that the chemical composition is declared by Winsor & Newton only for some of the color washes included in the catalogue, and the names given to each shade by the manufacturers are typically indicative of the color rather than the chemical constituents. Pigments studied are listed in table 1 along with their chemical composition indicated in the descriptive section of the Winsor & Newton handbook and with the results obtainable in terms of color.

Table 1. Detailed list of the color washes examined from the Winsor & Newton catalogue of watercolor pigments, shown along with their chemical composition declared by the manufacturers in the descriptive section of the handbook and with the results obtainable in terms of color.

| Pigment name | Composition declared by Winsor & Newton | Color |
|-----------------|---|---|
| Crimson lake | Similar to carmine. |  |
| Carmine lake | Aluminium or aluminium tin lake of cochineal. |  |
| Carmine | Prepared by precipitating the coloring matter of cochineal in combination with the smallest quantity of aluminous base. |  |
| Scarlet lake | Intimate combination of crimson lake with pale vermilion. |  |
| Warm sepia | Natural sepia (obtained from a secretion of the cuttle-fish, <i>Sepia officinalis</i>) warmed by mixing it with browns of a red hue. |  |
| Permanent brown | |  |
| Madder carmine | The strongest of a series of lakes, prepared by precipitating the coloring matter of the madder root in combination with alumina. |  |
| Madder lake | Synonym for rose madder. |  |
| Rose madder | Alumina lake obtained from madder roots. |  |

| | | |
|---------------------------|--|---|
| Rose madder (alizarin) | |  |
| Pink madder | Synonym for rose madder. |  |
| Rose madder pk shade | |  |
| Scarlet madder | |  |
| Rose dorè | |  |
| Brown madder | Lake prepared from the madder root. |  |
| Rubens' madder | Preparation of the madder root. |  |
| Dragons' blood | Originally a resin brought from the East Indies, now imitative pigment which is a semi-permanent substitute. |  |
| Alizarin scarlet | |  |
| Scarlet madder (alizarin) | |  |
| Alizarin carmine | |  |
| Alizarin crimson | |  |
| Ruby madder (alizarin) | |  |
| Burnt carmine | Obtained by partially charring carmine. |  |

| | | |
|---------------------------|---|---|
| Purple lake | Species of crimson lake with a purple cast. |  |
| Permanent mauve | |  |
| Permanent violet | |  |
| Mauve | Lake prepared from aniline. |  |
| Neutral tint | |  |
| Payne's gray | Similar to neutral tint. |  |
| Violet carmine | Prepared from the roots of <i>Anchusa Tinctoria</i> . |  |
| Indian purple | Prepared by precipitating the coloring matter of a decoction of cochineal on a base of oxide of copper. |  |
| Purple madder | Lake prepared from the madder plant. |  |
| Spectrum violet | |  |
| Purple madder (alizarin) | |  |
| Permanent crimson | |  |
| Madder carmine (alizarin) | |  |
| Spectrum red | |  |

Cochineal-based pigments

Among the classes of colorants here identified, a first group is composed of crimson lake, carmine lake, carmine, burnt carmine, purple lake and Indian purple, all ranging from dark red to purple shades. All these pigments are reported in the catalogue to have been prepared by precipitating the coloring matter of cochineal in combination with different amounts of inorganic substrates, such as aluminous base, tin or copper oxide. Consistently with the chemical composition declared by the manufacturers, SERS spectra obtained upon HF hydrolysis display the typical spectral pattern of the main coloring component of cochineal, i.e. carminic acid (structure shown in figure 2), which, after acid treatment, is reasonably detected as a free dye; in particular, signals at 1634, 1577, 1447, 1322, 1222 and, at lower wavenumbers, 1070 and 449 cm^{-1} show a remarkable correspondence with those of carminic acid at pH=2 (figure 3). Resonance Raman spectra acquired from these lakes using the 488 nm laser line as the excitation wavelength are all very similar and show common features at 1641, 1479, 1318 and 1109 cm^{-1} that match well the main Raman bands of carmine naccarat commercially purchased by Kremer Pigments (figure 3).

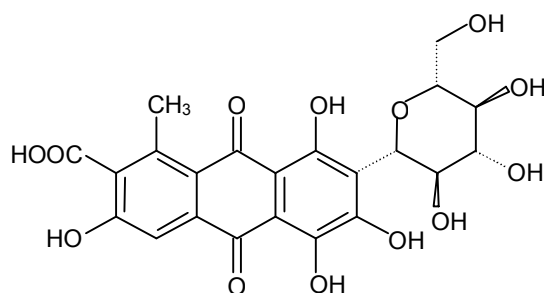


Figure 2. Molecular structure of carminic acid.

Particularly interesting is the case of dragons' blood. In fact, this name has been used since ancient times with reference to a red natural resin native of East Indies which was extracted from plants belonging to *Dracaena* and *Daemonorops* genera. However, as also pointed out by Burgio *et al.*², such dye was replaced in the 19th century by a more lightfast one due to its lack of permanence and its tendency to fade upon exposure to light. Dragons' blood is described in the Winsor & Newton handbook under investigation as an imitative colorant which is a semi-permanent substitute of the original one, even if more detailed information concerning its chemical composition was not provided by the company. Scientific analyses allowed us to number Winsor & Newton's dragons' blood among cochineal-based tints, as both its SERS and Raman spectra match well the spectral patterns observed for the other shades of this category (figure 3). In particular, the Raman spectrum obtained for this tint shows a remarkable similarity with that acquired by Burgio *et al.* from a dragons' blood pigment cake belonging to a 19th century Winsor & Newton watercolor box², suggesting an analogous composition for the two materials.

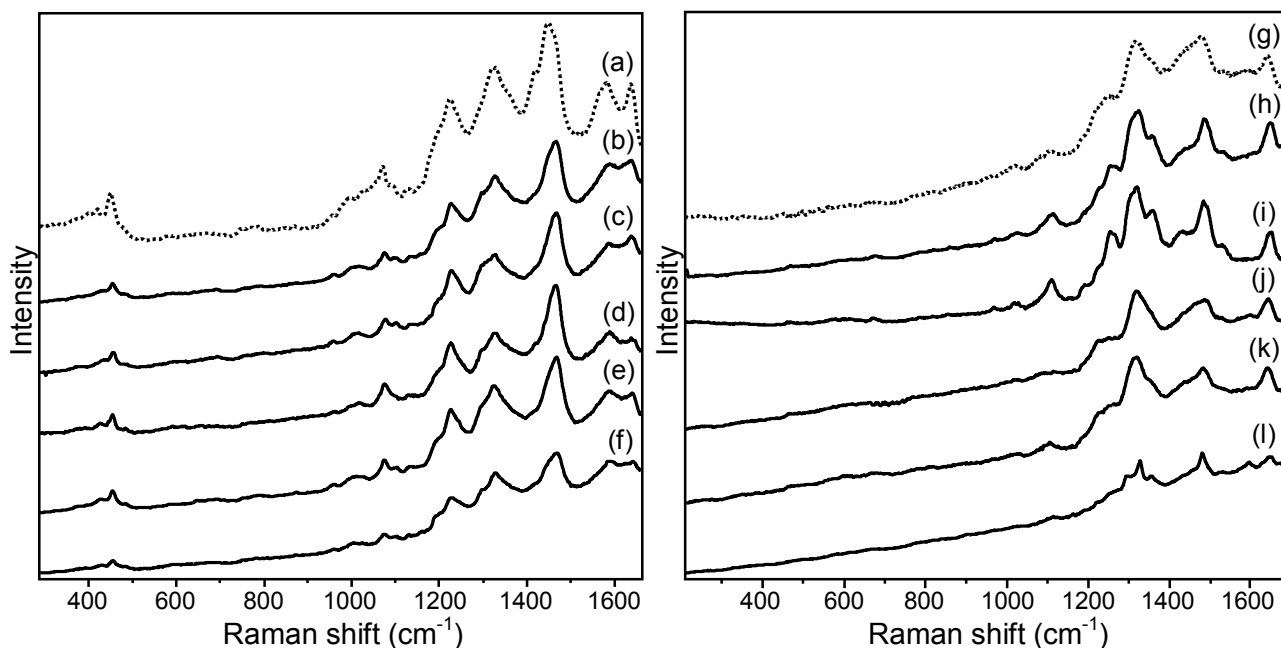


Figure 3. On the left, (a) SERS spectrum of reference carminic acid at pH=2 compared to examples of SERS spectra ($\lambda_{\text{exc}} = 488 \text{ nm}$) obtained from cochineal-based pigments: (b) crimson lake, (c) carmine, (d) burnt carmine, (e) purple lake and (f) dragons' blood. On the right, (g) Raman spectrum of reference carmine naccarat compared to examples of Raman spectra ($\lambda_{\text{exc}} = 488 \text{ nm}$) obtained from cochineal-based pigments: (h) crimson lake, (i) carmine, (j) burnt carmine, (k) purple lake and (l) dragons' blood.

Alizarin-based pigments

A second large group of lakes includes scarlet lake, rose madder (alizarin), alizarin scarlet, scarlet madder (alizarin), alizarin carmine, alizarin crimson, ruby madder (alizarin), purple madder (alizarin), permanent crimson and madder carmine (alizarin). SERS spectra taken from such samples upon HF treatment are in good agreement with that of alizarin at pH=2 (structure shown in figure 4), with bands at 1622, 1603, 1584, 1557, 1447, 1324 and 1292 cm^{-1} (figure 5). For all these dyes, resonance Raman spectra with common features at 1477, 1350, 1325 and 1288 cm^{-1} were obtained, matching well the two most intense signals at 1477 and 1325 cm^{-1} arising in the Raman spectra of both reference alizarin and madder lake (figure 5).

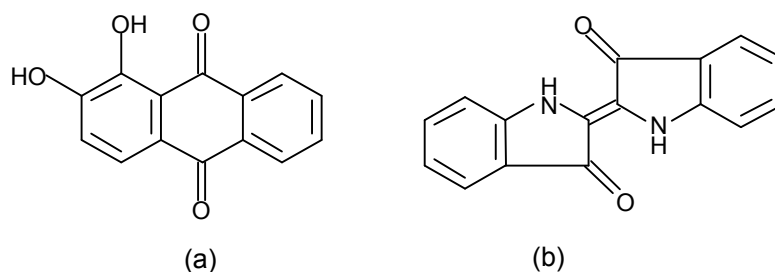


Figure 4. Molecular structures of (a) alizarin and (b) indigotin.

Among the pigments belonging to this category, scarlet lake is the only one for which indications about the main chemical constituents were provided by Winsor & Newton, according to whom such tint was obtained as an intimate combination of crimson lake with pale vermillion. However, it is interesting to notice how the composition declared is only partially consistent with the results arising from scientific analyses: indeed, even if the typical Raman signals of vermillion were identified at 253, 283 and 343 cm^{-1} using the 785 nm laser line as excitation wavelength, no trace of carminic acid was detected. Instead, SERS and Raman spectroscopy with excitation at 488 nm highlighted the presence of alizarin (figure 5).

A rather similar situation occurred for violet carmine: indeed, both the SERS and Raman spectral patterns observed for this lake match well those collected from the other colorants of the present family (figure 5) although, according to the manufacturers, such shade was prepared as a lake obtained from the roots of *Anchusa tinctoria*, a tinctorial plant from which alkanet, a completely different red dye with naphthoquinonic chromophores, is extracted.

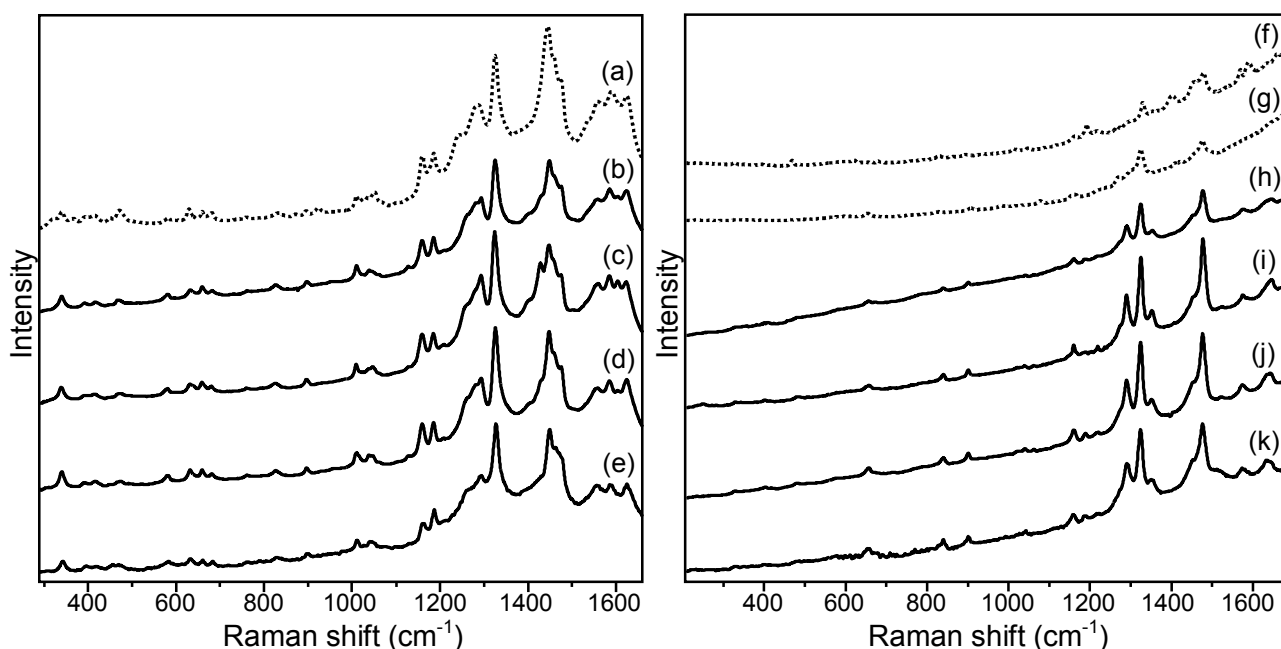


Figure 5. On the left, (a) SERS spectrum of reference alizarin at pH=2 compared to examples of SERS spectra ($\lambda_{\text{exc}} = 488 \text{ nm}$) obtained from alizarin-based pigments: (b) ruby madder (alizarin), (c) scarlet lake, (d) permanent crimson and (e) violet carmine. On the right, Raman spectra of (f) reference alizarin and (g) reference madder lake compared to examples of Raman spectra ($\lambda_{\text{exc}} = 488 \text{ nm}$) obtained from alizarin-based pigments: (h) ruby madder (alizarin), (i) scarlet lake, (j) permanent crimson and (k) violet carmine.

The typical bands of alizarin were identified in the SERS spectrum of neutral tint as well: this pigment has not been described in the catalogue from a chemical point of view, even if it is reported in the Colour Index to have been prepared as a mixture of Indian ink, which is composed of a variety of fine soot, and the inorganic pigment Prussian blue, with a very small proportion of madder lake. In accordance with what observed for the other lakes belonging to the present class, the Raman spectrum of neutral tint excited at 488 nm is dominated by the response of alizarin, the main chromophore of madder lake, thanks to the use of resonance conditions; unexpectedly, the characteristic signals of indigo (structure of its main component, indigotin, shown in figure 4)

turned out to be visible when a higher excitation wavelength, namely 785 nm, was employed, while no traces of Prussian blue were detected (figure 6).

A partly comparable situation was encountered for Payne's gray, which, according to what claimed by Winsor & Newton, was expected to have a composition similar to that of neutral tint and, even if more lilac in hue, to resemble its properties: indeed, even if for an HF-treated sample taken from this color wash SERS spectroscopy did not lead to any significant result, the typical Raman bands of alizarin and indigo were detected when exciting the sample at 488 and 785 nm, respectively.

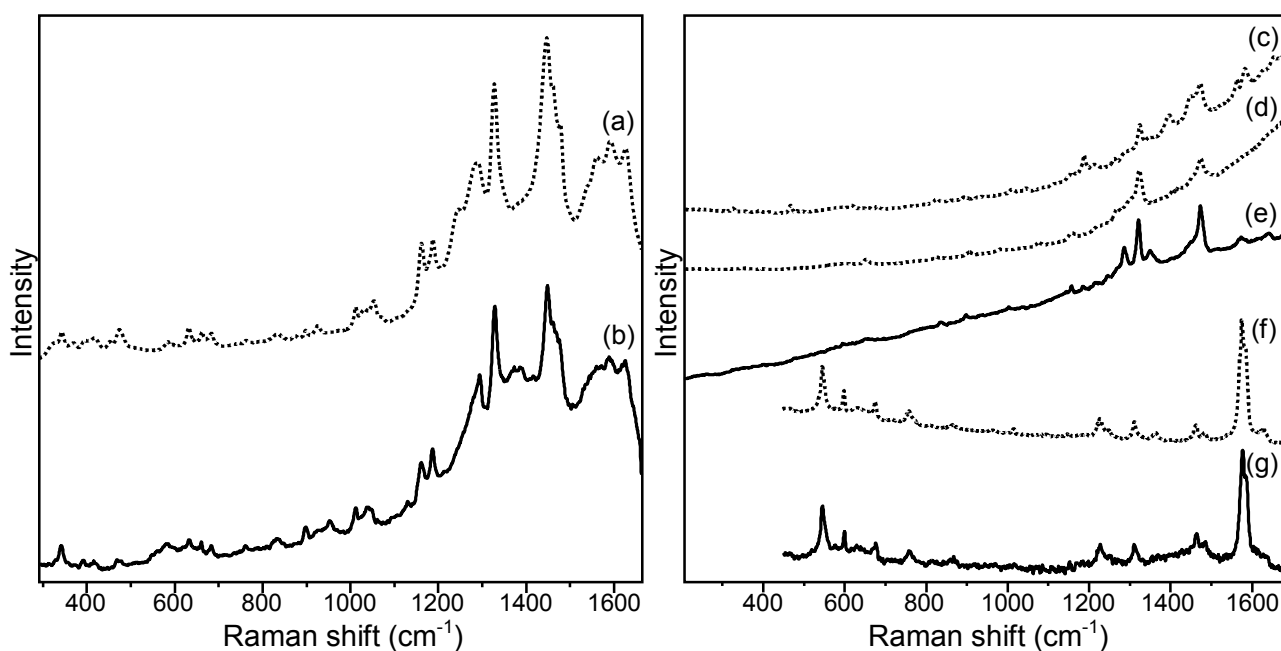


Figure 6. On the left, (a) SERS spectrum of reference alizarin at pH=2 compared to (b) that of neutral tint ($\lambda_{\text{exc}} = 488$ nm). On the right, Raman spectra of (c) reference alizarin and (d) reference madder lake compared to (e) that of neutral tint ($\lambda_{\text{exc}} = 488$ nm), and (f) Raman spectrum of reference indigo compared to (g) that of neutral tint ($\lambda_{\text{exc}} = 785$ nm).

Madder lake-based pigments

Another wide class of tints consists of madder carmine, madder lake, rose madder, pink madder, brown madder, Rubens' madder and purple madder. These pigments, all reported by Winsor & Newton to have been prepared by precipitating the coloring matter of madder roots mostly in combination with alumina, gave rise upon HF hydrolysis to high quality SERS spectra with intense signals at 1573, 1475, 1443, 1325, 1252 and 1156 cm^{-1} , well corresponding to those of madder lake commercially purchased by Kremer and subjected to the same kind of pretreatment (figure 7). In addition, lakes such as permanent brown, rose madder pk shade, scarlet madder and rose dorè, for which additional information regarding their composition was not provided either by the manufacturers or in the Colour Index, could also be included in the present category based on the outcomes of chemical investigations (figure 7). On the other hand, no results were achieved from the ordinary Raman study of the pigments belonging to the present class, as they were all characterized by a very strong fluorescence emission.

As clearly suggested by SERS spectroscopy, madder lake was used for warm sepia as well (figure 7). This dark brown pigment is described by Winsor & Newton as a mixture of a secretion of the cuttlefish, *Sepia officinalis*, with browns of a red hue, the composition of which was not better specified by the manufacturers but could be here ascertained by means of scientific analyses.

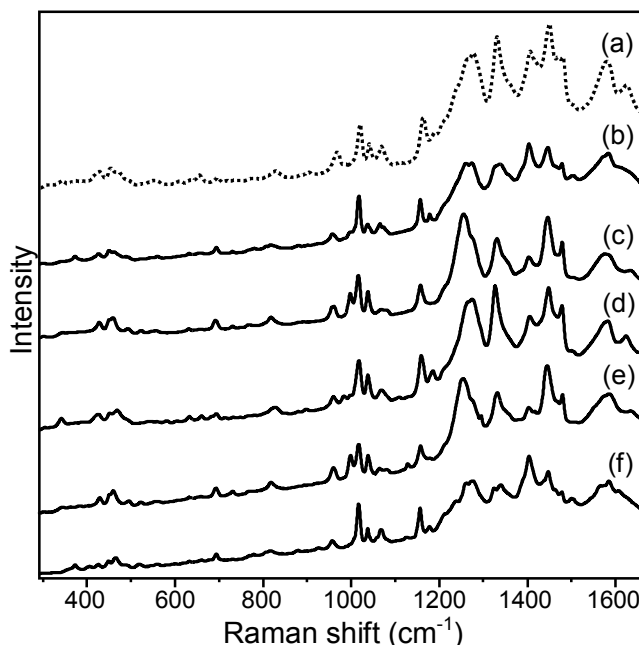


Figure 7. (a) SERS spectrum of reference madder lake upon HF treatment compared to examples of SERS spectra ($\lambda_{\text{exc}} = 488 \text{ nm}$) obtained from madder lake-based pigments: (b) rose dorè, (c) madder carmine, (d) Rubens' madder, (e) permanent brown and (f) warm sepia.

Synthetic pigments

Besides the pigments already numbered in the three wide classes previously discussed, which analyses showed to be based on insect and plant dyes such as cochineal and madder, good quality SERS and Raman spectra could also be obtained for a few violet and red tints of different composition belonging to the Winsor & Newton handbook of watercolor pigments here studied.

Mauve, described in the catalogue as a lake prepared from aniline, displayed very intense SERS signals at 1621, 1591, 1371, 1178, 912 and 807 cm⁻¹, well corresponding to the spectral pattern obtained for the reference synthetic dye crystal violet (figure 9, structure shown in figure 8). Surprisingly, a completely different spectrum was obtained from permanent mauve, violet pigment the main chemical constituents of which were not declared by the manufacturers. Indeed, although its trade name might suggest a similar composition to that of the previous tint, SERS signals essentially corresponding to those observed for alizarin solution were obtained in the present case, while the Raman spectrum recorded with the 785 nm line as exciting radiation exhibits characteristic spectral features that are very similar to those of permanent violet but remained unidentified.

The use of synthetic dyes was also highlighted in the case of spectrum red by Raman spectroscopy, using 488 and 785 nm laser lines for excitation: indeed, in both cases the observed spectral patterns essentially correspond to the Raman spectrum taken from the beta-naphthol pigment 1-(4-methyl-2-nitrophenylazo)-2-naphthol, commercially named Pigment Red 3 or Hansa Scarlet RNC (figure 9, structure shown in figure 8). It is important to remark that the detection of this colorant, first synthesized in the early 20th century, called the official release date of the catalogue under investigation into question. Further analyses and comparisons with other editions of Winsor & Newton handbooks will be undertaken in the next future to clarify the “mystery” and investigate the possible introduction of new colors.

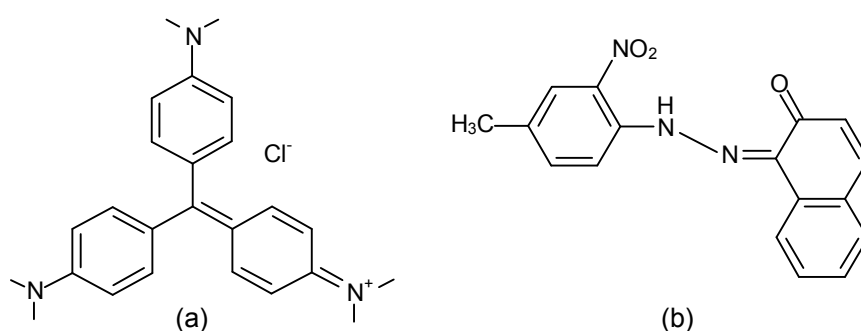


Figure 8. Molecular structures of (a) crystal violet and (b) Pigment Red 3 or Hansa Scarlet RNC.

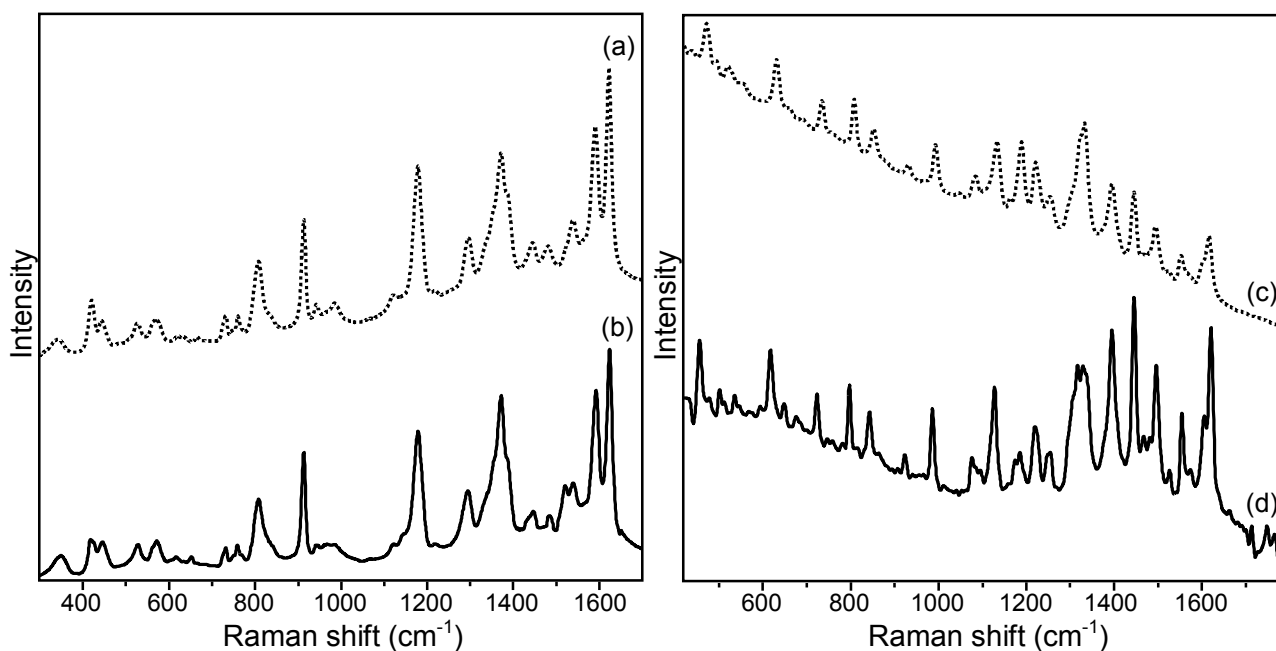


Figure 9. On the left, (a) SERS spectrum of reference crystal violet compared to (b) that of mauve ($\lambda_{exc} = 488$ nm). On the right, (c) Raman spectrum of reference Pigment Red 3, or Hansa Scarlet RNC, compared to (d) that of spectrum red ($\lambda_{exc} = 785$ nm).

Conclusions

In the present study, pink, red, violet, brown and gray tints on drawing paper from a historical Winsor & Newton handbook of watercolor pigments dating to 1887 were studied, aiming to identify the organic colorants contained in each of them. An appropriate database was thus built, including both ordinary Raman and SERS spectra for a wide number of shades. The so obtained spectral patterns were carefully examined, compared to reference spectra of pure colorants and lake pigments, divided into different groups and thus discussed.

Scientific analysis of Winsor & Newton color washes allowed us to deepen our knowledge about the variety of pigments in use during the modern age, and the results obtained will provide valuable reference data for dating, as well as in authentication and identification studies. While lakes prepared from plant and insect dyes, mainly madder and cochineal, are predominant among the colors offered by Winsor & Newton, some tints based on synthetic dyes were found as well, often accompanied by commentary on their poor light fastness. The present ordinary Raman and SERS study allowed us to formulate some hypotheses concerning the main constituents of those shades for which a description is not available in the handbook, such as dragons' blood and most of the alizarin-based pigments. In addition, we could correct erroneous indications provided by Winsor & Newton on some tints, as in the case of violet carmine. Moreover, the detection of the beta-naphthol pigment Hansa scarlet RNC, synthesized in the early 20th century, called the release date of the catalogue into question. Further analyses and comparisons with other editions of Winsor & Newton handbooks will be carried out in the next future to elucidate the matter at issue and investigate the possible introduction of new colors.

References

- [1] <http://www.winsornewton.com>.
- [2] L. Burgio, R. J. H. Clark, G. Martin, E. Pantos, M. A. Roberts, *NATO Science Series II: Mathematics, Physics and Chemistry* **2003**; 117, 61.
- [3] F. G. Hoogland, J. J. Boon, *Int. J. Mass Spectrom.* **2009**; 284, 72.
- [4] R. Ploeger, S. Musso, O. Chiantore, *Prog. Org. Coat.* **2009**; 65, 77.
- [5] V. Pintus, S. Wei, M. Schreiner, *Anal. Bioanal. Chem.* **2011**, DOI: 10.1007/s00216-011-5369-5.
- [6] C. L. Brosseau, F. Casadio, R. P. Van Duyne, *J. Raman Spectrosc.* **2011**; 42, 1305.
- [7] M. Leona, J. Stenger, E. Ferloni, *J. Raman Spectrosc.* **2006**; 37, 981.
- [8] M. Leona, *Proceedings of the National Academy of Sciences* **2009**; 106, 14757.

Chapter 7

TLC-SERS study of the main components of Syrian rue dye (*Peganum harmala*)

Abstract

Although greatly appreciated in the field of art conservation for its high sensitivity, SERS is not a separation technique and, therefore, it is not suitable for distinguishing different components in dye mixtures. To accomplish this task, coupling of TLC and SERS has been investigated in this chapter as a promising tool possibly allowing to reduce the amount of material, sophisticated equipment and time needed for HPLC analysis, overcoming at the same time the poor limit of detection of TLC as such. This technique has been here applied to the separation and identification of harmalol, harmaline and harmane, the main alkaloid constituents of Syrian rue, a historical colorant extracted from the seeds of *Peganum harmala*. In addition, FT-Raman, normal Raman and SERS spectra were acquired from Syrian rue seed extract and its commercial components, in order to provide valuable reference data to be used for identification purposes. Complementary HPLC analyses were also carried out to ascertain the real composition of the dye extract and verify the actual reliability of the results obtained from TLC-SERS investigations.

Introduction

As already pointed out several times throughout the present doctoral thesis, a lot of research for the identification of organic colorants has been carried out during the last few years by SERS, which has proven to be an extremely effective analytical tool because of its great sensitivity¹⁻³. Nevertheless, SERS is not a separation technique and therefore it does not allow to distinguish different components in a mixture. This is certainly one of the main limitations associated with SERS for dye analysis: in fact, organic colorants were prepared in ancient times from natural sources such as plants and insects, and the resulting extracts were obviously obtained as mixtures of several coloring compounds; moreover, particular hues could be only produced by overlapping different dyes, as it has been reported, for instance, in the scientific investigation of Kaitag textiles from Caucasus discussed in Chapter 4, where green shades were found to have been achieved as a mixture of blue and yellow colorants. In these cases, SERS analysis usually allows to detect only one of the chemical compounds contained in the dye mixture, i.e. the one that has the stronger affinity for the metal substrate; in the case of green embroideries of Kaitag textiles, for example, the SERS response of yellow constituents was always predominant compared to that of blue. The use of separation methods such as HPLC or LC-MS would be preferable for the characterization of colorants, but it is often precluded for the study of historical materials and works of art because sizable sample is required for the analysis. Hyphenated techniques such as HPLC-SERS or TLC-SERS could offer effective separation of different components of a mixture and provide valuable spectral information for each one of them to be used for identification purposes. In particular, TLC-SERS would allow to significantly reduce the amount of material, sophisticated equipment and time needed for HPLC analysis, overcoming at the same time the poor limit of detection of TLC as such. Coupling of TLC and SERS was first reported by Henzel in 1977⁴, and since then it has been successfully employed for the separation and detection of several analytes, including pharmaceuticals⁵⁻⁸. Although the great potential of this technique for the study of dye mixtures was recently highlighted by Brosseau⁹, Geiman¹⁰ and coworkers, its application to the field of art analysis has not yet become a well-established part of the conservation scientists' toolbox.



Figure 1. Flowers and seeds of the plant *Peganum harmala*. From the seeds the colorant Syrian rue can be extracted.

TLC-SERS was here investigated as a tool for the separation and identification of harmalol, harmaline and harmane, the main alkaloid components of the historical colorant Syrian rue, traditionally extracted from dry seeds of *Peganum harmala* (figure 1). This plant is native from the Eastern Mediterranean region east to India. Seeds and roots contain β -carboline alkaloids, mostly harmaline, harmalol, harmane, as well as harmine (figure 2). Reported to have been used as an incense and spice, it was also employed in traditional medicine and for ritual purposes. The vivid red dye which can be obtained from Syrian rue seeds is documented in the literature to have been used in Western Asia for dyeing carpets and, more in general, wool fabrics¹¹. Although the synthesis and Raman analysis of biologically active platinum(II) and palladium(II) complexes of harmaline, harmalol, harmine and harmane have been reported in the literature¹², to the best of our knowledge a complete vibrational study of the free molecules has never been carried out to date. Hence, a complete FT-Raman, normal Raman and SERS characterization of harmalol, harmaline and harmane, commercially available and thus purchased from Sigma-Aldrich, has been here performed in addition to TLC-SERS experiments, in order to provide valuable data which could be used as a reference in identification efforts. Furthermore, HPLC analyses of Syrian rue seed extract and the three alkaloid commercial standards were carried out for comparison, to ascertain the real chemical composition of the dye extract and evaluate the actual reliability of the results obtained from the TLC-SERS investigation of these materials.

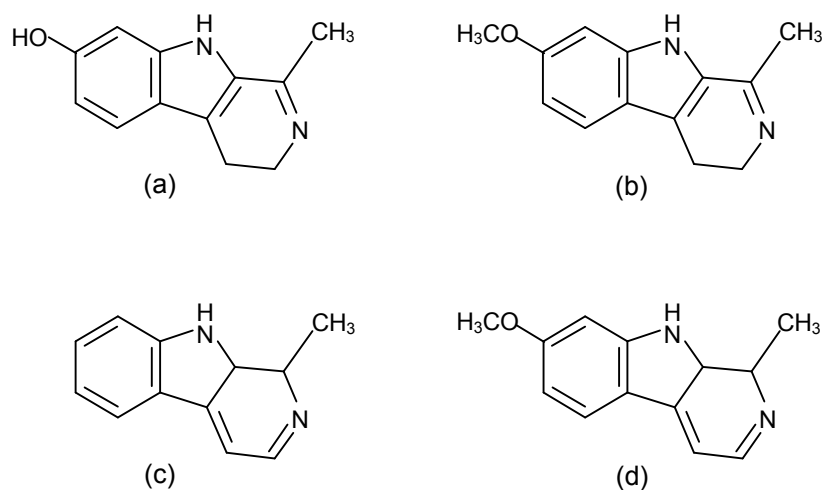


Figure 2. Molecular structures of the main alkaloid components of the historical dye Syrian rue, namely (a) harmalol, (b) harmaline, (c) harmane and (d) harmine.

Experimental

Chemicals

Silver nitrate, sodium citrate, sulfuric acid, glucose and hydrochloric acid were purchased from Fisher Scientific, while harmalol, harmaline, harmane, methanol, ethanol, potassium nitrate, chloroform and ammonia from Sigma-Aldrich. All the aqueous solutions used for dye extraction and the silver nanoparticle synthesis were prepared using 18 MΩ ultrapure water (Millipore Simplicity 185 water purification system).

Analytical methods: extraction procedure, Ag colloid synthesis and sample preparation

Syrian rue dye was extracted from *Peganum harmala* seeds in methanol and HCl:H₂O, heating the suspension on a hot plate at 60°C for 30 minutes. As SERS spectral patterns obtained from both extracts were the same, only Syrian rue dye extracted in methanol was then used for TLC-SERS experiments.

Silver colloids synthesized by microwave-supported glucose reduction of silver sulfate in the presence of sodium citrate as a capping agent¹³ were chosen as a metal substrate for SERS analyses; a detailed description of their synthesis is given in Chapter 5. A 5 times concentrated colloid was also prepared for TLC-SERS experiments by centrifuging the colloidal suspension and replacing 900 μL of the supernatant with 100 μL of ultrapure water.

As far as the sample preparation is concerned, reference solutions of Syrian rue commercial components, namely harmalol, harmaline and harmane, were prepared in ethanol at a concentration of 10⁻⁴ M. For SERS analysis, 0.2 μL of the analyte solution were added to 0.8 μL of the Ag colloid, followed by the addition of 0.1 μL of a 0.5 M KNO₃ aqueous solution to induce aggregation of the nanoparticles. SERS analyses were performed by focusing the laser beam onto the microaggregates which turned out to be visible inside the drop a few seconds after covering the sample with the Ag colloid. SERS spectra could be obtained immediately after the preparation of the sample and generally improved in quality as aggregation proceeded, before deteriorating when the liquid was fully evaporated.

TLC-SERS analytical method

The TLC-SERS analytical procedure adopted is shown in figure 3; experiments were conducted as explained in the following. First of all, the extract obtained from Syrian rue seeds as well as commercial harmalol, harmaline and harmane were eluted on a silica gel TLC plate in a glass developing chamber. The best developing solvent turned out to be 80:20:1.5 CHCl₃:CH₃OH:NH₃ 10%, which led to an optimal separation of the three reference alkaloids. SERS analyses were subsequently performed directly on the TLC plate by focusing the laser beam onto each spot, upon deposition of 0.8 μL of silver colloid and 0.1 μL of 0.5 M KNO₃ aqueous solution. Good quality SERS spectra could be obtained while the spots were still wet.

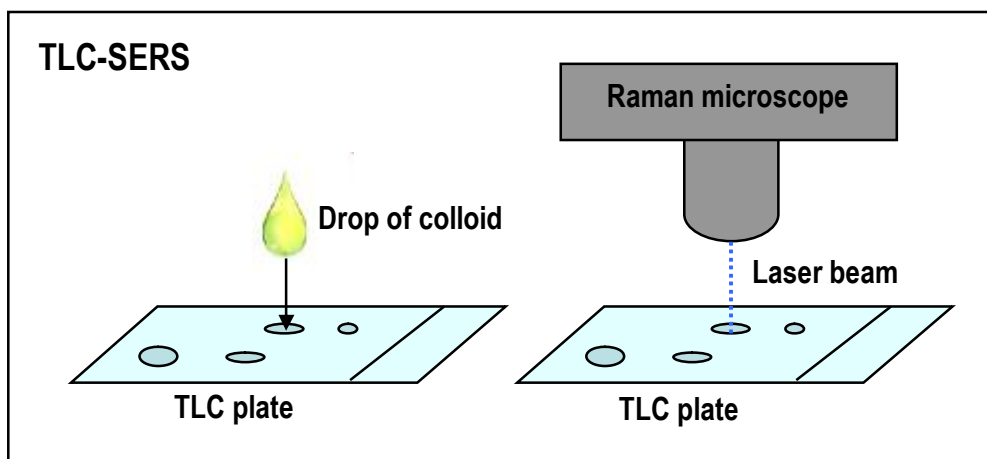


Figure 3. TLC-SERS analytical procedure: a drop of silver colloid and, subsequently, of aggregating agent are deposited onto each spot on the TLC plate; the SERS analysis is then carried out while the spots are still wet, by focusing the laser beam directly onto each one of them on the TLC plate.

Instrumentation

FT-Raman spectra were acquired with a Bruker RamII Vertex 70 spectrometer equipped with a liquid nitrogen-cooled Ge detector. The 1064 nm line provided by a Nd:YAG laser was used for excitation, together with a resolution of 4 cm^{-1} and a 180° geometry. The output laser power was 25 mW and the scans collected 128.

Normal Raman experiments were performed in the dispersive mode using a Bruker Senterra Raman spectrometer equipped with an Olympus 100x long working distance microscope objective and a charge-coupled device (CCD) detector. A Spectra Physics Model 2020 BeamLock Ar⁺ laser, a Melles Griot He-Ne laser and a continuous wave diode laser, emitting at 488 nm, 633 nm and 785 nm respectively, were used as the excitation sources, and two holographic gratings (1800 and 1200 rulings/mm) provided a spectral resolution of $3\text{-}5\text{ cm}^{-1}$. Raman analyses were carried out by collecting 1 scan with an integration time of 30 s, using an output laser power of 0.25 or 2.5 mW for 488 nm excitation, 2 or 5 mW for 633 nm excitation and 10 or 25 mW for 785 nm excitation, according to the Raman response of each compound.

SERS spectra of both reference commercial materials and TLC spots were recorded with the above mentioned Bruker Senterra Raman instrument, using a 20x long working distance microscope objective and excitation at 488 nm, as the average of 1 scan with an integration time of 30 s.

HPLC system consisted of a 1525 micro binary HPLC pump, 1500 series column heater, in-line degasser and a Rheodyne 7725i manual injector with 20 μL loop (Waters, Milford, MA, USA). A Waters Xterra RP18 reverse-phase column (3.5 μm , 2.1 mm I.D. x 150 mm) equipped with a Xterra RP18 guard column (3.5 μm , 2.1 mm I.D. x 10 mm) was used with a flow rate of 0.2 mL/min. A Direct-Connect universal column prefilter (2 μm , W. R. Grace & Co.-Conn., Augusta, GA, USA) was attached in front of the guard column. Column temperature was set at 40°C . The mobile phase was eluted in a gradient mode of (A) methanol and (B) 0.88% formic acid in deionized water. The solvent gradient was as follows: 90% B for 3 minutes, 90-60% B in 3-7 minutes in a linear slope, 60-0% B in 7-25 minutes in a linear slope, 0% B for 5 minutes. A 2996 photodiode array (PDA) detector was employed in order to obtain spectral information in the range 210-800 nm.

Results and discussion

FT-Raman spectra, normal Raman spectra at 488, 633 and 785 nm as well as SERS spectra on silver colloids at 488 nm excitation for the extract obtained from Syrian rue seeds and its alkaloid components, namely harmalol, harmaline and harmane, commercially purchased, are reported here for the first time. Like in Chapter 2, vibrational wavenumbers are displayed in tables along with their relative intensities.

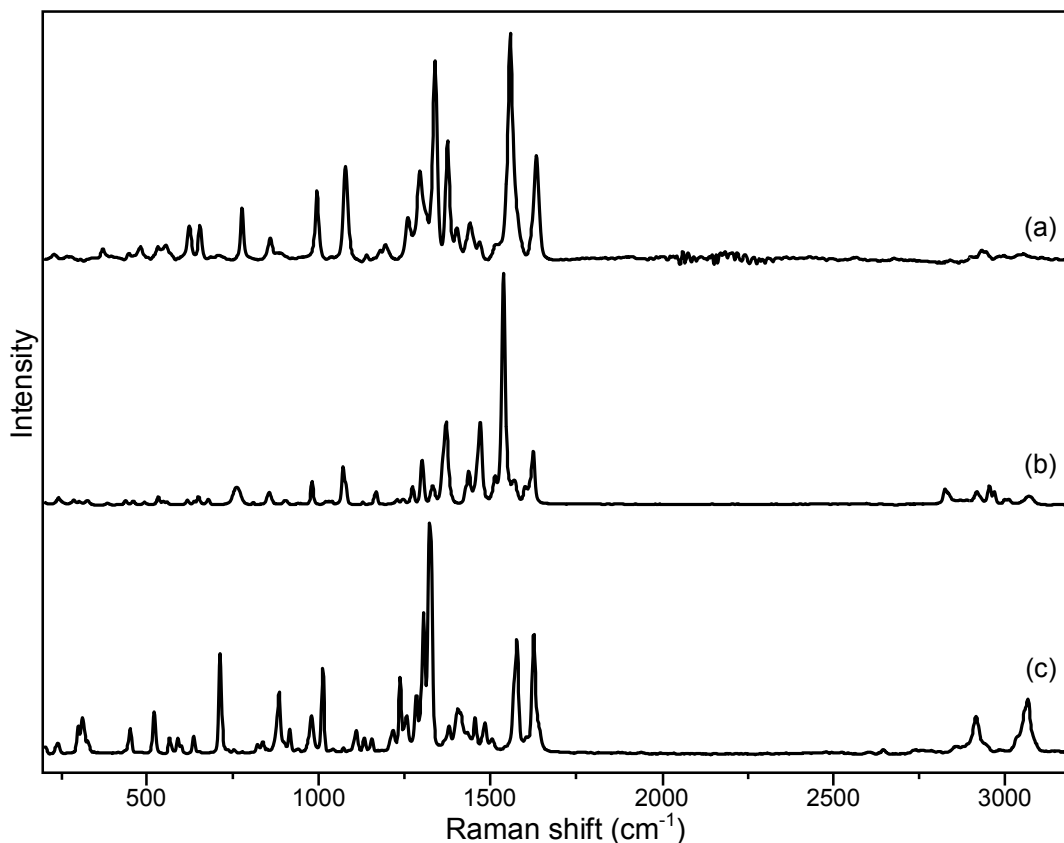


Figure 4. FT-Raman spectra of (a) harmalol, (b) harmaline and (c) harmane.

Table 1. Frequencies of FT-Raman spectra of harmalol, harmaline and harmane with relative intensities.

| Dyes | FT-Raman bands (cm ⁻¹) |
|---------------------------------------|---|
| Harmalol Fig. 4 - Spectrum (a) | 1634m, 1560vs, 1516 vw, 1469vw, 1442w, 1404w, 1376m, 1339s, 1295m, 1261w, 1195vw, 1179vw, 1141vw, 1079m, 995m, 860w, 776m, 655w, 624w, 555vw, 532vw, 503vw, 480vw, 446vw, 370vw |
| Harmaline Fig. 4 - Spectrum (b) | 1625m, 1602w, 1569w, 1539vs, 1514w, 1471m, 1438w, 1373m, 1333w, 1301m, 1274w, 1247vw, 1229vw, 1168w, 1129vw, 1071m, 1039vw, 981w, 903vw, 856w, 809vw, 762w, 679vw, 649vw, 618vw, 558vw, 549vw, 533vw, 492vw, 460vw, 439vw, 326vw, 286vw |
| Harmane Fig. 4 - Spectrum (c) | 1626s, 1604vw, 1577s, 1505vw, 1483w, 1456w, 1432vw, 1413sh, 1404w, 1379w, 1322vs, 1305s, 1284m, 1256w, 1237m, 1216w, 1154w, 1132w, 1109w, 1071vw, 1041vw, 1011s, 978w, 940vw, 914w, 884m, 851vw, 835vw, 821vw, 753vw, 734vw, 712s, 635w, 599sh, 589w, 565w, 519w, 450w, 327sh, 311w, 298w |

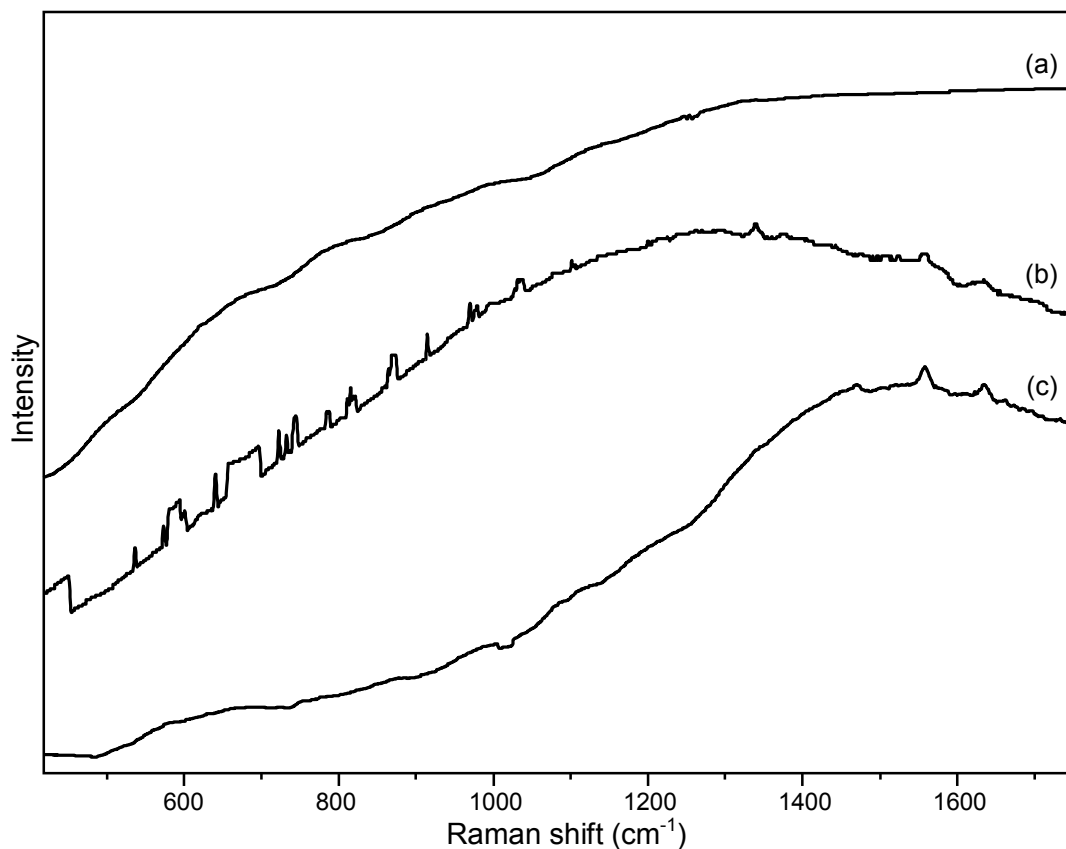


Figure 5. Normal Raman spectra of harmalol at excitation (a) 488 nm, (b) 633 nm and (c) 785 nm.

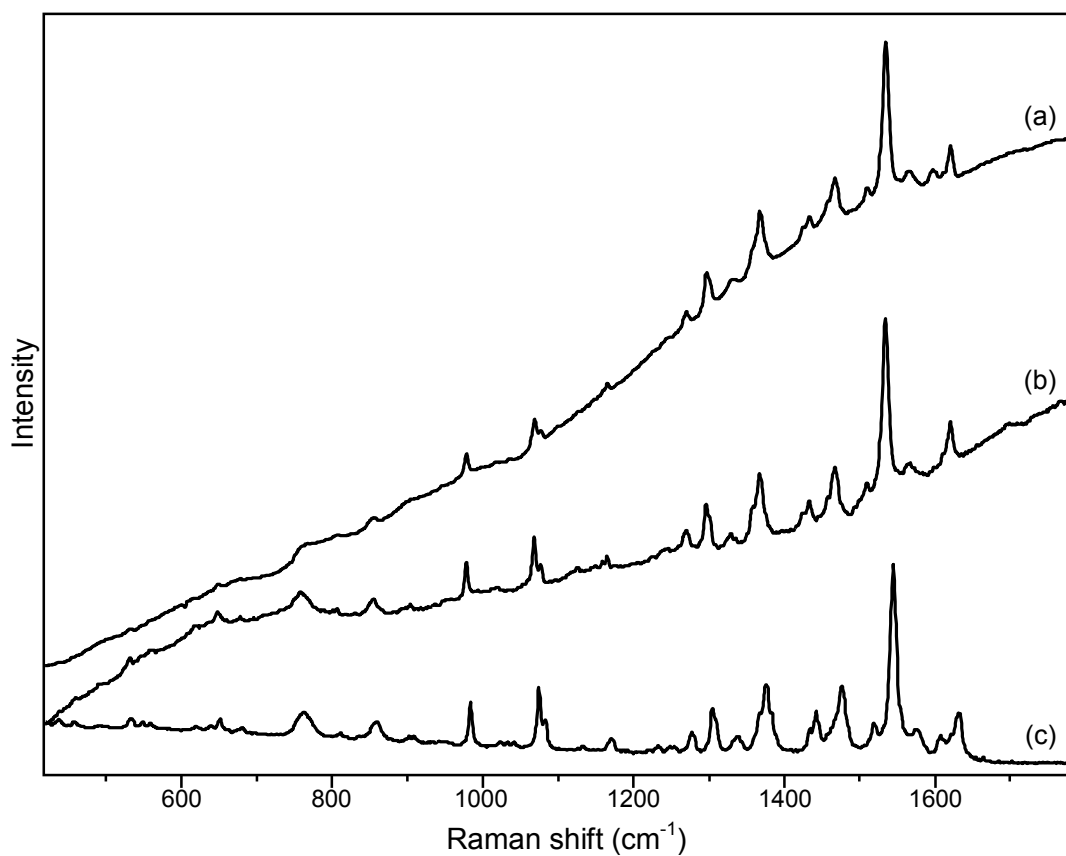


Figure 6. Normal Raman spectra of harmaline at excitation (a) 488 nm, (b) 633 nm and (c) 785 nm.

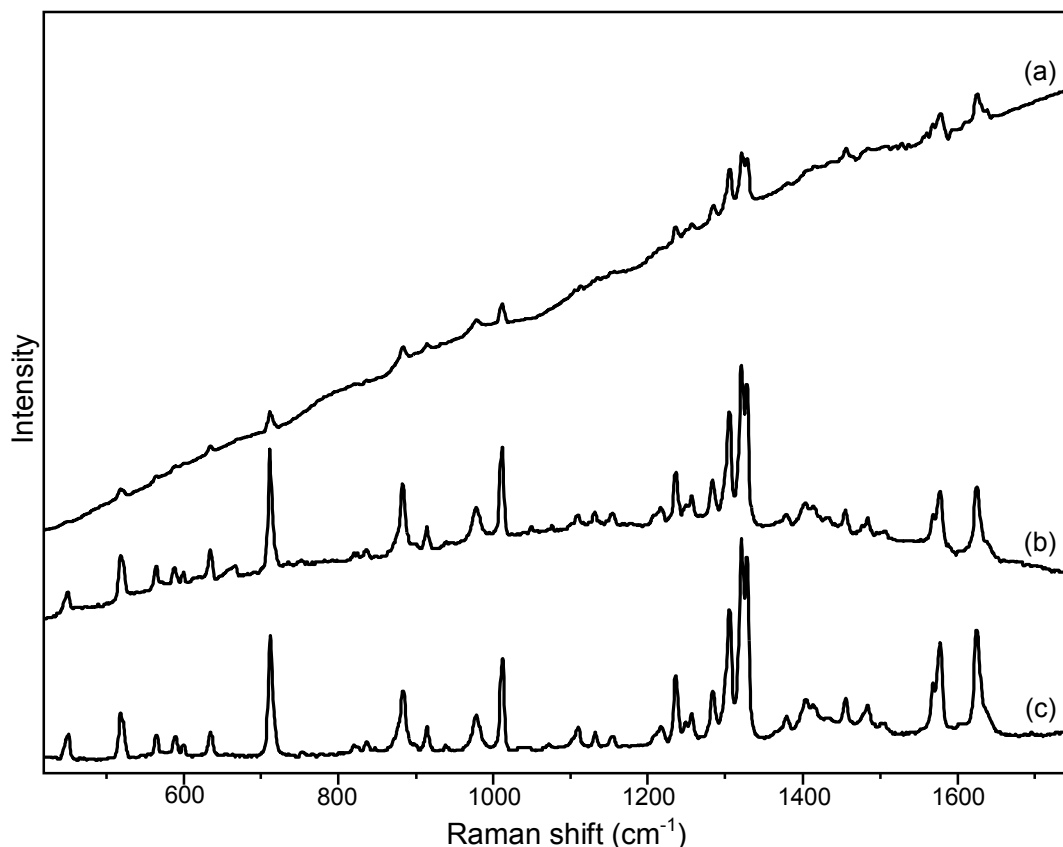


Figure 7. Normal Raman spectra of harmane at excitation (a) 488 nm, (b) 633 nm and (c) 785 nm.

Table 2. Frequencies of Raman spectra of harmaline and harmane at 488, 633 and 785 nm excitation with relative intensities.

| Dyes | Raman bands (cm ⁻¹) |
|--|---|
| Harmaline 488 nm Fig. 6 - Spectrum (a) | 1624w, 1615sh, 1601vw, 1569vw, 1538s, 1513vw, 1471m, 1461sh, 1437vw, 1428sh, 1370m, 1361sh, 1334vw, 1299w, 1272vw, 1167vw, 1129vw, 1078vw, 1070vw, 980vw |
| Harmaline 633 nm Fig. 6 - Spectrum (b) | 1624w, 1615sh, 1569vw, 1538s, 1513vw, 1471m, 1461sh, 1437vw, 1428sh, 1370m, 1361sh, 1339vw, 1332vw, 1304sh, 1299w, 1272vw, 1167vw, 1162sh, 1129vw, 1078vw, 1070w, 980w, 905vw, 856vw, 809vw, 759vw, 679vw, 649vw, 637vw, 618vw, 558vw, 548vw, 532vw, 491vw, 460vw |
| Harmaline 785 nm Fig. 6 - Spectrum (c) | 1624w, 1615sh, 1601vw, 1569vw, 1538s, 1512vw, 1471m, 1461sh, 1437w, 1428sh, 1377sh, 1371m, 1361sh, 1333vw, 1299w, 1272vw, 1249vw, 1244vw, 1228vw, 1167vw, 1129vw, 1078w, 1070m, 1038vw, 1029vw, 1019vw, 980w, 905vw, 899vw, 856vw, 809vw, 759w, 679vw, 649vw, 637vw, 618vw, 558vw, 548vw, 533vw, 491vw, 457vw |
| Harmane 488 nm Fig. 7 - Spectrum (a) | 1638sh, 1625m, 1577m, 1567sh, 1483vw, 1455vw, 1414vw, 1403vw, 1378vw, 1328m, 1321m, 1305m, 1283w, 1256vw, 1249vw, 1235w, 1012w, 977vw, 914vw, 883w, 835vw, 711w, 634vw, 600vw, 589vw, 564vw, 518vw, 450vw |
| Harmane 633 nm Fig. 7 - Spectrum (b) | 1638sh, 1625m, 1577m, 1567sh, 1507vw, 1483vw, 1455vw, 1432vw, 1413vw, 1403vw, 1378vw, 1328s, 1321vs, 1305s, 1283w, 1256w, 1249vw, 1235m, 1216vw, 1154vw, 1131vw, 1109vw, 1012s, 977w, 914w, 883m, 835vw, 825vw, 819vw, 752vw, 711s, 667vw, 634w, 600vw, 589vw, 564vw, 518w, 450vw |
| Harmane 785 nm Fig. 7 - Spectrum (c) | 1638sh, 1624m, 1577m, 1567sh, 1506vw, 1483vw, 1455vw, 1432vw, 1413vw, 1403vw, 1378vw, 1328s, 1321vs, 1305s, 1283w, 1256w, 1248vw, 1235m, 1216vw, 1208sh, 1154vw, 1131vw, 1109vw, 1071vw, 1012m, 977w, 914w, 883m, 836vw, 825vw, 819vw, 752vw, 711s, 634w, 600vw, 589w, 564w, 518w, 450w |

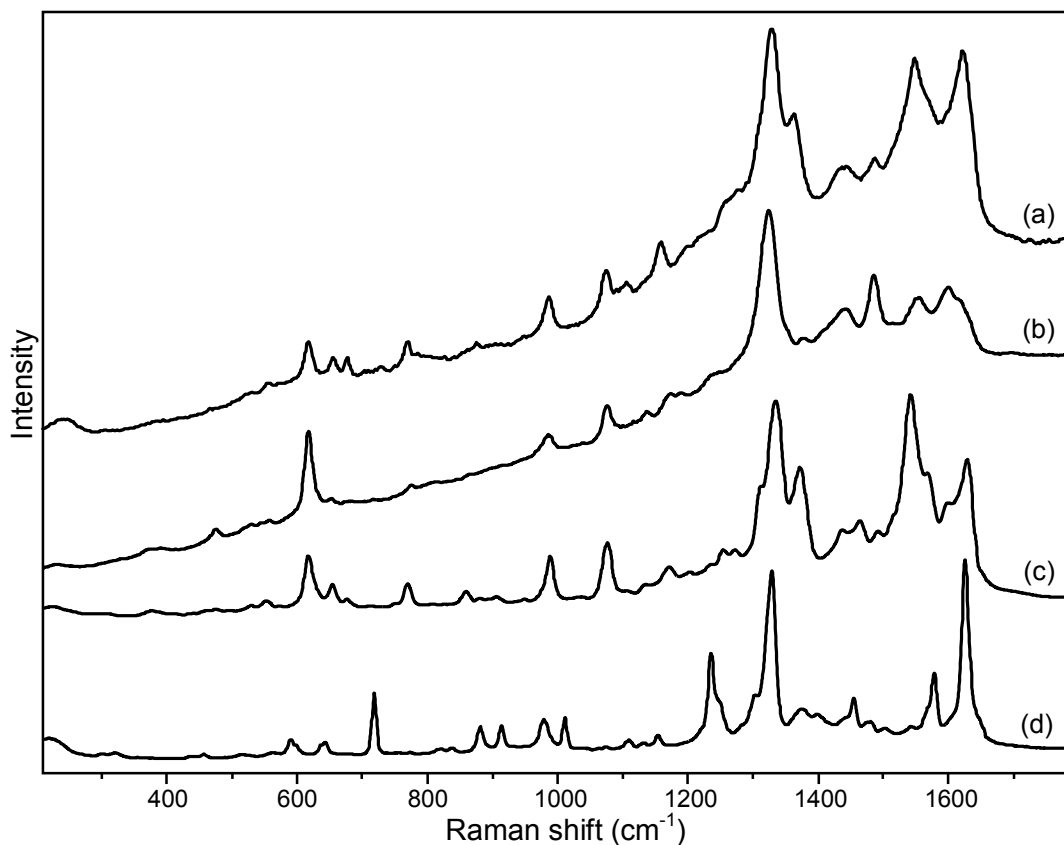


Figure 8. (a) SERS spectrum of Syrian rue seed extract compared to those of (b) hamalol, (c) harmaline and (d) harmane.

Table 3. Frequencies of SERS spectra of Syrian rue seed extract, harmalol, harmaline and harmane with relative intensities.

| Dyes | SERS bands (cm ⁻¹) |
|--|--|
| Syrian rue extract Fig. 8 - Spectrum (a) | 1627s, 1552s, 1491vw, 1444vw, 1367m, 1332s, 1159w, 1107vw, 1074w, 987w, 876vw, 767w, 675w, 653w, 615w, 551vw |
| Harmalol Fig. 8 - Spectrum (b) | 1619sh, 1602m, 1552w, 1485m, 1441w, 1378vw, 1324vs, 1170vw, 1138vw, 1074w, 986vw, 772vw, 653vw, 616m, 474vw |
| Harmaline Fig. 8 - Spectrum (c) | 1627s, 1599sh, 1568sh, 1541vs, 1491vw, 1463w, 1435w, 1370s, 1333vs, 1311sh, 1271vw, 1253vw, 1170vw, 1074m, 986m, 858vw, 768w, 675vw, 653w, 616m, 551vw |
| Harmane Fig. 8 - Spectrum (d) | 1626vs, 1579m, 1541vw, 1503vw, 1479vw, 1454w, 1399vw, 1374vw, 1328vs, 1303sh, 1248sh, 1235m, 1153vw, 1131vw, 1109vw, 1010w, 979w, 912w, 880w, 718m, 642vw, 589vw |

Raman spectra of harmalol, harmaline and harmane were collected by the use of four different excitation wavelengths. In detail, all the FT-Raman spectra acquired with excitation at 1064 nm (figure 4; the corresponding wavenumbers with relative intensities are listed in table 1) display excellent signal intensity and signal-to-noise ratios, and exhibit distinctive bands which could be used as a fingerprint for each one of the three alkaloid compounds. While harmalol was found to be characterized by a significant fluorescence emission when analyzed in the dispersive mode regardless of the laser line employed for excitation (figure 5), good quality Raman spectra were instead obtained for harmaline and harmane especially when using the 785 nm laser (figures 6 and 7; the corresponding wavenumbers with relative intensities are listed in table 2). However, moving to lower excitation wavelengths, namely 633 and 488 nm, an increasing fluorescence emission was encountered for these two molecules as well, even though a detailed spectral pattern with many Raman lines could be observed in these cases over the fluorescent background anyway.

Excellent results were obtained by SERS, which provided remarkable signal enhancements and fluorescence suppression, allowing us to collect a high quality spectrum even for harmalol (figure 8; the corresponding wavenumbers with relative intensities are listed in table 3). A good SERS spectrum could also be acquired for Syrian rue seed extract which, at first glance, appeared to have many features shared with those of harmaline and harmalol. In particular, lines at low wavenumbers, namely 1074, 987, 767, 615 cm^{-1} , are common to both the dye extract and the two reference molecules; overall, the specific contribution of harmaline is predominant and was found to be particularly evident for bands located at 1627, 1491, 1367, 1332, 675 and 653 cm^{-1} (figure 8; the corresponding wavenumbers with relative intensities are listed in table 3).

Results obtained from TLC analysis are shown in figure 9. The extract of Syrian rue seeds was eluted along with the three reference alkaloids on a silica gel plate, where it separated into three spots, marked in the figure as spot 1, 2 and 3. The retention factors calculated for each of these spots were then compared with those of the commercial standards, allowing us to preliminarily classify components 1, 2 and 3 from Syrian rue extract as harmalol, harmaline and harmane. This hypothesis was further supported by the color of the fluorescence emission detected for each spot when examining the TLC plate under UV light; in fact, harmalol, harmaline and harmane were respectively characterized by yellow, light blue and violet emissions, which were found to match perfectly the color of the fluorescence emission of spot 1, 2 and 3 from the dye extract. Incidentally, the visual inspection of the developed TLC plate also revealed the presence of a small quantity of harmaline in the commercial standard of harmalol purchased from Sigma-Aldrich.

SERS spectra of the separated spots were recorded by using the dispersive Raman system with a 488 nm laser, focusing directly on the TLC plate. Spectra were collected from spot 1, 2 and 3 from Syrian rue extract and the three alkaloid standards both on regular and 5 times concentrated silver colloids, in order to evaluate the actual necessity of using a higher concentration of nanoparticles to obtain better signals and superior enhancements from the spots on the TLC silica gel support. A comparison between SERS spectra acquired from spot 1, 2 and 3 of Syrian rue extract and those of reference alkaloids from the TLC plate is presented in figures 10, 11 and 12. No background subtraction, normalization or other spectral manipulations were performed, in order to allow a direct comparison of the results obtained.

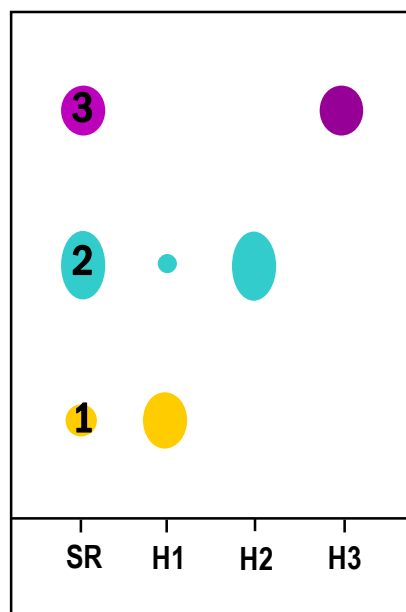


Figure 9. Results of TLC analysis of Syrian rue seed extract (SR), eluted along with its main commercial components, harmalol (H1), harmaline (H2) and harmane (H3).

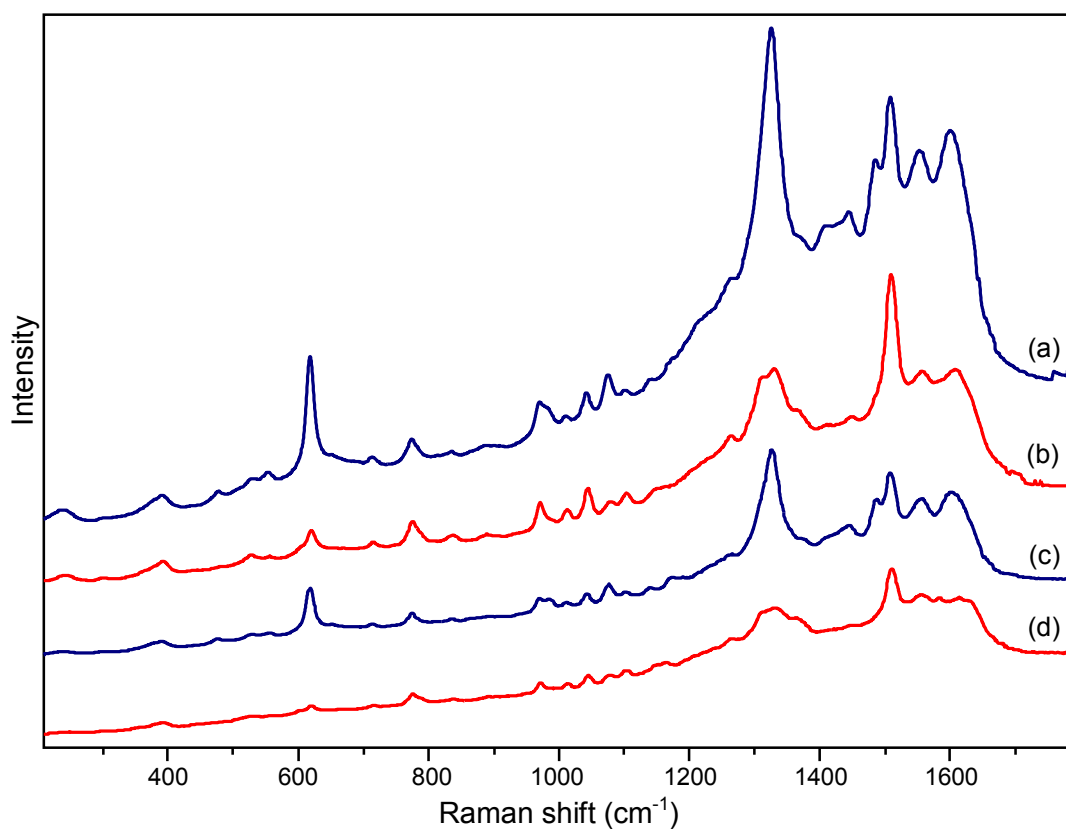


Figure 10. SERS spectra of (a) harmalol H1 eluted on TLC plate and (b) component 1 eluted on TLC plate from Syrian rue seed extract on concentrated nanoparticles, and (c) harmalol H1 eluted on TLC plate and (d) component 1 eluted on TLC plate from Syrian rue seed extract on regular nanoparticles.

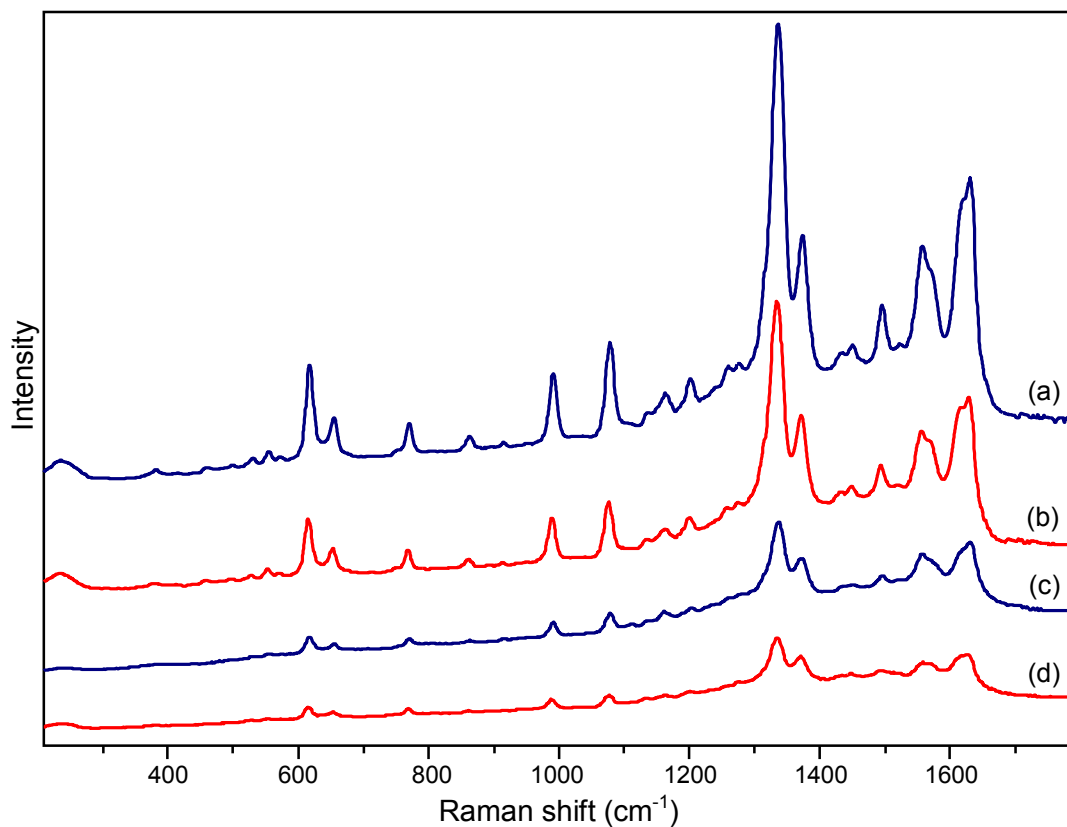


Figure 11. SERS spectra of (a) harmaline H2 eluted on TLC plate and (b) component 2 eluted on TLC plate from Syrian rue seed extract on concentrated nanoparticles, and (c) harmaline H2 eluted on TLC plate and (d) component 2 eluted on TLC plate from Syrian rue seed extract on regular nanoparticles.

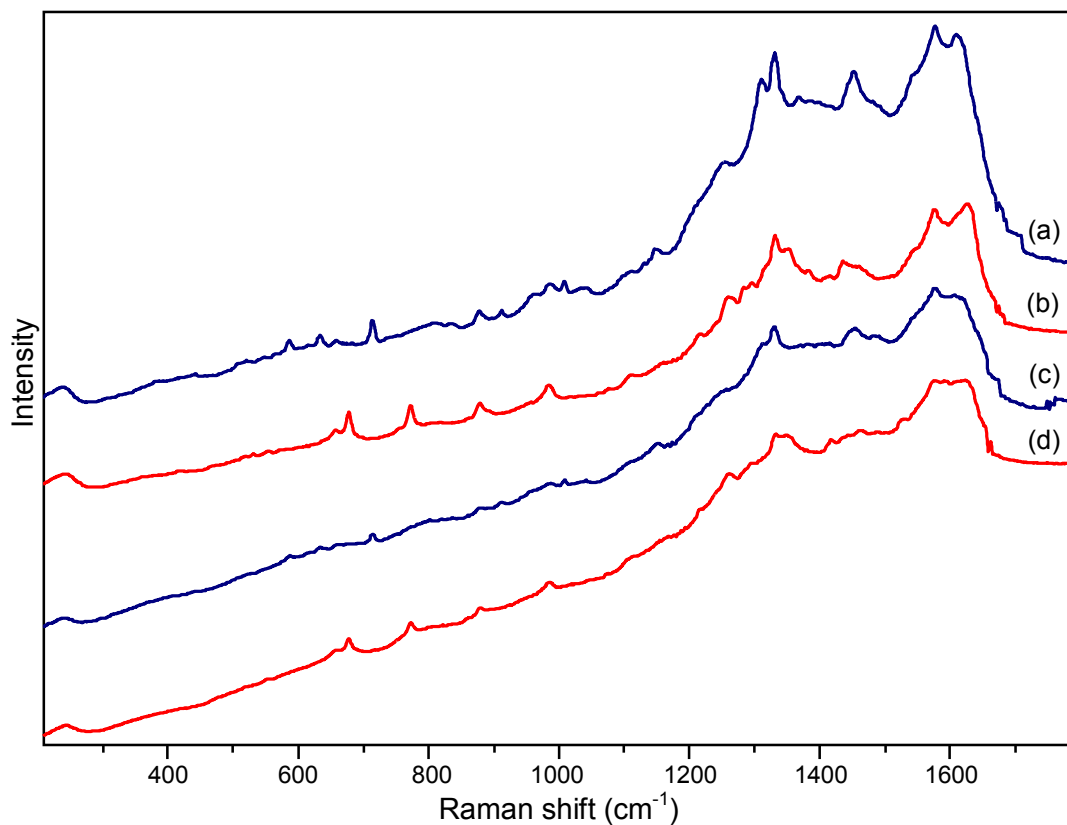


Figure 12. SERS spectra of (a) harmane H3 eluted on TLC plate and (b) component 3 eluted on TLC plate from Syrian rue seed extract on concentrated nanoparticles, and (c) harmane H3 eluted on TLC plate and (d) component 3 eluted on TLC plate from Syrian rue seed extract on regular nanoparticles.

First of all, a few differences could be observed between the SERS spectra of harmalol, harmaline and harmane solutions (figure 8), analyzed according to the regular SERS procedure, and those of the three molecules taken from the TLC plate (figures 10, 11 and 12), probably due to the interaction of these organic compounds with the silica gel substrate. Adsorption-induced spectral distortions include shifts in wavenumber, variation of the relative intensity of certain bands, as well as, in the case of harmane, a significant decrease of the signal resolution and of the overall spectral quality.

Due to the differences detected in the SERS spectra of alkaloid solutions compared to those of the molecules adsorbed on the silica gel plate, identification of the compounds contained in the extract of Syrian rue seeds was carried out by direct comparison of spot 1, 2 and 3 with the three standards eluted on the TLC plate.

In particular, the SERS spectra of spot 1 and 2 from Syrian rue seed extract showed an excellent correspondence with those of reference harmalol and harmaline obtained from the TLC plate, respectively (figures 10 and 11); this observation allowed us to positively validate the classification of components 1 and 2 in Syrian rue extract as harmalol and harmaline. Different was the case of component 3, the SERS spectra of which were found to be analogous but not completely consistent with those of harmane; in fact, clear spectral differences could be detected especially at low wavenumbers, where signals located at 1006, 985, 959, 911, 877, 713, 658, 632 and 586 cm^{-1} for reference harmane are replaced by bands at 985, 877, 771, 677 and 657 cm^{-1} in the spectrum of spot 3. However, based on the overall similarity of such spectral patterns, component 3 of Syrian rue extract was suggested to be harmine, which is in fact reported in the literature to be one of the main components of this dye besides harmalol, harmaline and harmane¹¹. Indeed, as shown in figure 2, the molecular structure of harmine is closely related to that of harmane and the two compounds are therefore expected to give similar SERS responses on silver colloids; moreover, these two molecules are co-eluted in the solvent here used according to the literature¹¹. This hypothesis is still to be verified, due to the commercial unavailability of harmine standard at the time when the work here presented has been carried out.

SERS measurements on regular and 5 times concentrated nanoparticles taken from the TLC plate led to the acquisition of reproducible spectral patterns in all cases; although spectra collected on concentrated colloids obviously displayed improved enhancements and spectral resolution, their use was not strictly necessary to provide identification, as experiments on nanoparticles of regular concentration also gave rise to good quality spectra, which were themselves sufficient to detect and classify the unknown analytes under investigation.

HPLC analyses of the extract obtained from Syrian rue seeds and its three alkaloid components commercially purchased were also carried out for comparison, and the chromatograms and visible spectra thus recorded are displayed in figures 13 and 14. In detail, two compounds detected in the chromatogram of Syrian rue extract, marked in figure 13 as peak 1 and 2, could be recognized as harmalol and harmaline on the basis of their retention times, 7.9 and 11.3 minutes, and their absorption maxima in the visible region of the spectrum, namely 259/370 and 259/375 nm; a third component of the plant extract found at 12.3 minutes and showing absorption maxima at 247/320 nm, marked in figure 13 as peak 4, did not correspond to reference harmane and remained therefore unidentified. In conclusion, HPLC analyses confirmed all the results obtained by means of TLC-SERS, i.e. that the extract obtained from Syrian rue seeds is composed of a high amount of harmaline together with smaller quantities of harmalol and that the commercial standard of harmalol purchased from Sigma-Aldrich also contains small amounts of harmaline, thus proving the real effectiveness of the TLC-SERS methodology here presented.

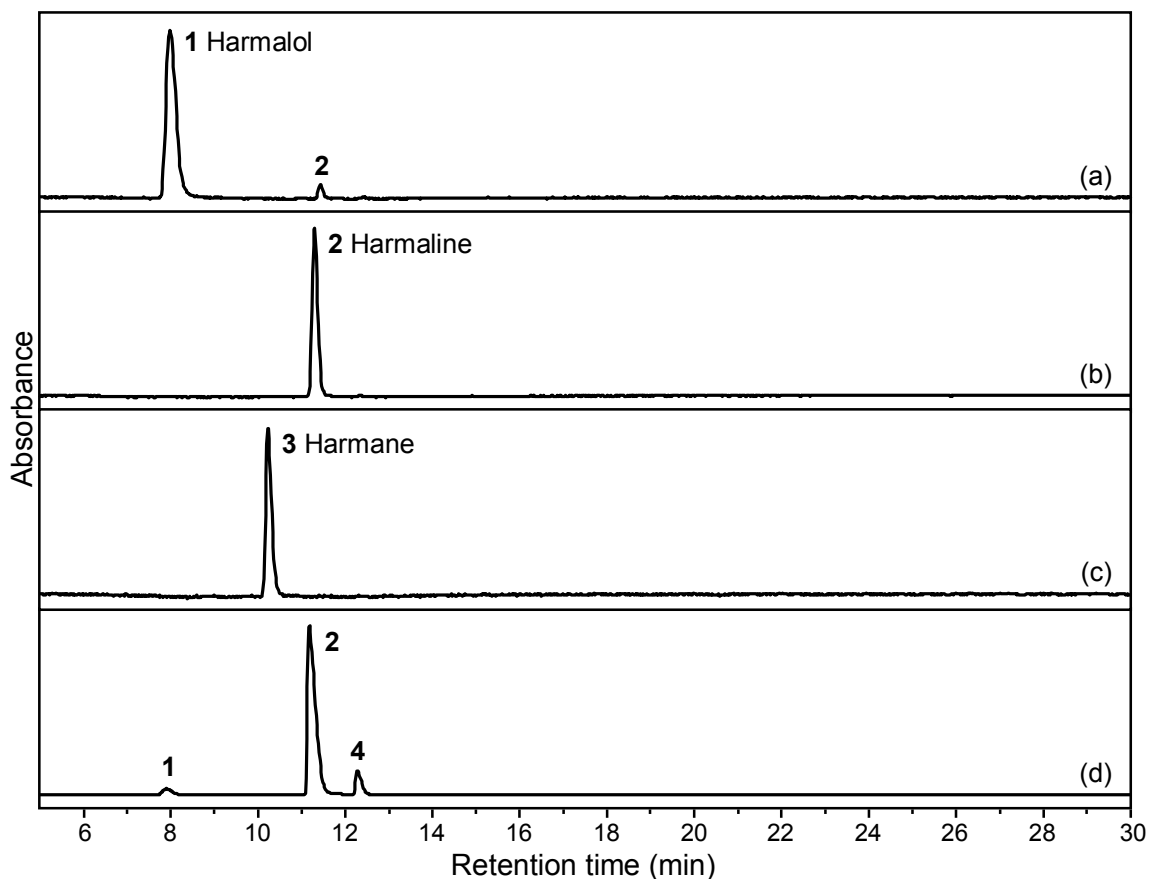


Figure 13. HPLC chromatograms of (a) commercial harmalol, (b) commercial harmaline and (c) commercial harmane compared to (d) that of Syrian rue seed extract. Based on retention times and visible spectra of the components, such extract turns out to contain (1) harmalol, (2) harmaline and (4) a third unknown compound which does not correspond to harmane.

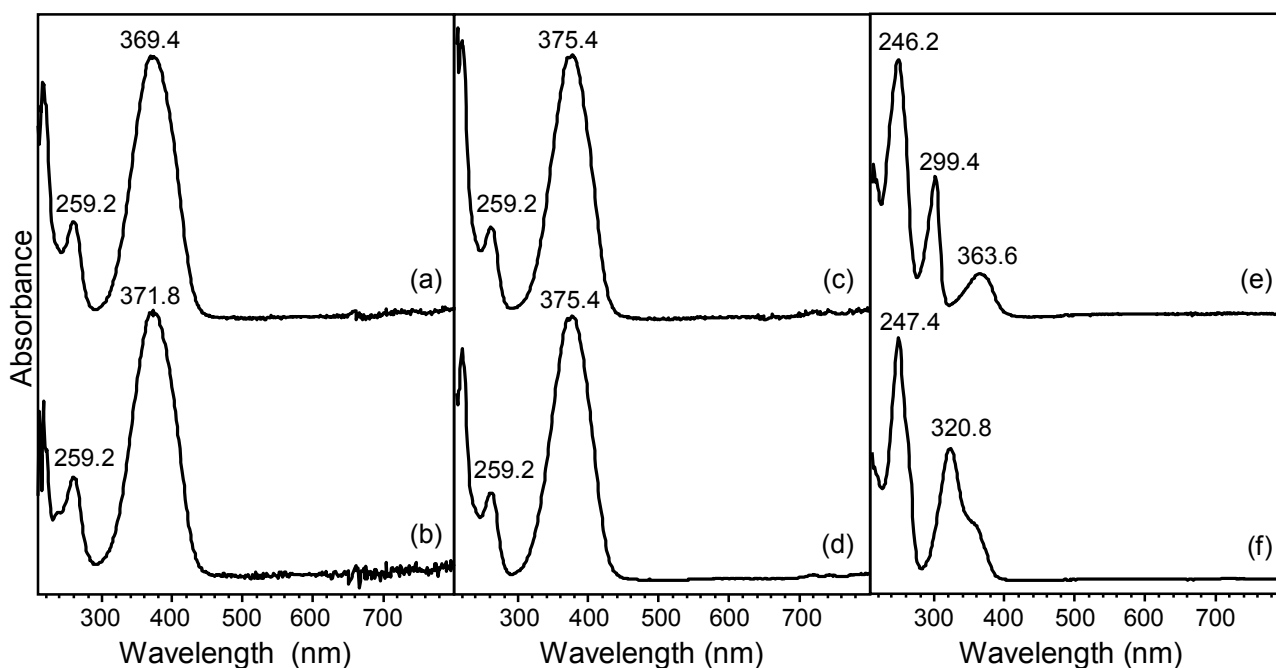


Figure 14. UV-vis spectra of (a) commercial harmalol compared to (b) compound 1 in Syrian rue seed extract, (c) commercial harmaline compared to (d) compound 2 in Syrian rue seed extract, and (e) commercial harmane compared to (f) compound 4 in Syrian rue seed extract.

Conclusions

TLC-SERS was explored as a promising tool for the separation and identification of the main alkaloid constituents of a historical dye named Syrian rue, which was preliminarily extracted from *Peganum harmala* seeds. According to the results obtained by using this hyphenated technique, Syrian rue extract contains harmaline and harmalol, while a third component, co-eluted with harmine on the TLC plate, led to SERS spectra similar to those of such molecule even though not identical, and was therefore suggested to be harmine. Indeed, due to their closely related structures, these two compounds are expected to give rise to similar spectra and, moreover, they are reported in the literature to be co-eluted in the solvents here used. HPLC analyses confirmed the results achieved by TLC-SERS, showing how the method here presented could be massively exploited for the effective separation and detection of different components in dye mixtures. In addition, a complete spectral characterization of Syrian rue extract and its commercial components was provided in this chapter, including FT-Raman spectra, Raman spectra acquired at $\lambda_{\text{exc}} = 488, 633, 785$ nm and SERS spectra recorded at $\lambda_{\text{exc}} = 488$ nm that could be used as reference data in identification studies.

Acknowledgements

Nobuko Shibayama (The Metropolitan Museum of Art, Department of Scientific Research) is acknowledged for carrying out HPLC analyses of Syrian rue seed extract and its components commercially purchased.

References

- [1] K. Chen, M. Leona, T. Vo-Dinh, *Sens. Rev.* **2007**; 27, 109.
- [2] K. L. Wustholz, C. L. Brosseau, F. Casadio, R. P. Van Duyne, *Phys. Chem. Chem. Phys.* **2009**; 11, 7350.
- [3] F. Casadio, M. Leona, J. R. Lombardi, R. Van Duyne, *Acc. Chem. Res.* **2010**; 43, 782.
- [4] U. B. Henzel, *Journal of Chromatography Library*, (Eds: A. Zlatkis, R. E. Kaiser), Elsevier, Amsterdam, **1977**, Vol. 9, Chapter 8.
- [5] E. Koglin, *J. Mol. Struct.* **1988**; 173, 369.
- [6] J. P. Caudin, A. Beljebbar, G. D. Sockalingum, J. F. Angiboust, M. Manfait, *Spectrochim. Acta Part A* **1995**; 51, 1977.
- [7] K. István, G. Keresztury, A. Szèp, *Spectrochim. Acta Part A* **2003**; 59, 1709.
- [8] Y. Wang, J. Z. Zhang, X. Y. Ma, *Spectrosc. Spectral Anal.* **2004**; 24, 1373.
- [9] C. L. Brosseau, A. Gambardella, F. Casadio, C. M. Grzywacz, J. Wouters, R. P. Van Duyne, *Anal. Chem.* **2009**; 81, 3056.
- [10] I. Geiman, M. Leona, J. R. Lombardi, *J. Forens. Sci.* **2009**; 54, 947.
- [11] H. Schweppe, *Handbuch der naturfarbstoffe*, Landsberg/Lech, Germany, **1993**.
- [12] T. A. K. Al-Allaf, M. T. Ayoub, L. J. Rashan, *J. Inorg. Biochem.* **1990**; 38, 47.
- [13] M. Leona, *Proceedings of the National Academy of Sciences* **2009**; 106, 14757.

Chapter 8

Raman and DFT study of monobromoindigo

Abstract

Monobromoindigo is a component of Tyrian purple, a purple-red natural colorant extracted from various species of sea snails, which was possibly first produced by the ancient Phoenicians and has been employed as a symbol of royalty and power by several civilizations over the centuries. While other constituents of Tyrian purple have been comprehensively investigated by Raman spectroscopy in the past years, monobromoindigo, a molecule that has been correlated with a specific snail species, *Hexaplex trunculus*, also known as *Murex trunculus*, has never been studied using a combined approach based on quantum mechanical density functional theory (DFT) calculations. A complete Raman spectral characterization of monobromoindigo is thus provided in this chapter, including experimental spectra recorded at 488 and 785 nm, which were compared to those collected from indigo in the same conditions. Moreover, theoretical Raman spectra for both molecules were obtained using DFT calculations, and a detailed assignment of the Raman lines is here presented.

Introduction

Monobromoindigo is an organic molecule of natural origin obtained from a Mediterranean mollusk, and is of great interest as a component of Tyrian purple, a dye that has since ancient times been of political, economic, religious, psychological and artistic importance. Tyrian purple, also called royal purple, has been the subject of very extensive research, and an exhaustive compilation of references is available in the literature¹.

Monobromoindigo is a flat molecule, almost planar, and aromatic (figure 1). It shares with indigo and dibromoindigo molecules a similar framework structure, even though monobromoindigo, with one bromine attached at the 6' position, differs from the former which has no bromine atom attached, and from the latter, which has two bromines attached at the 6 and 6' positions.

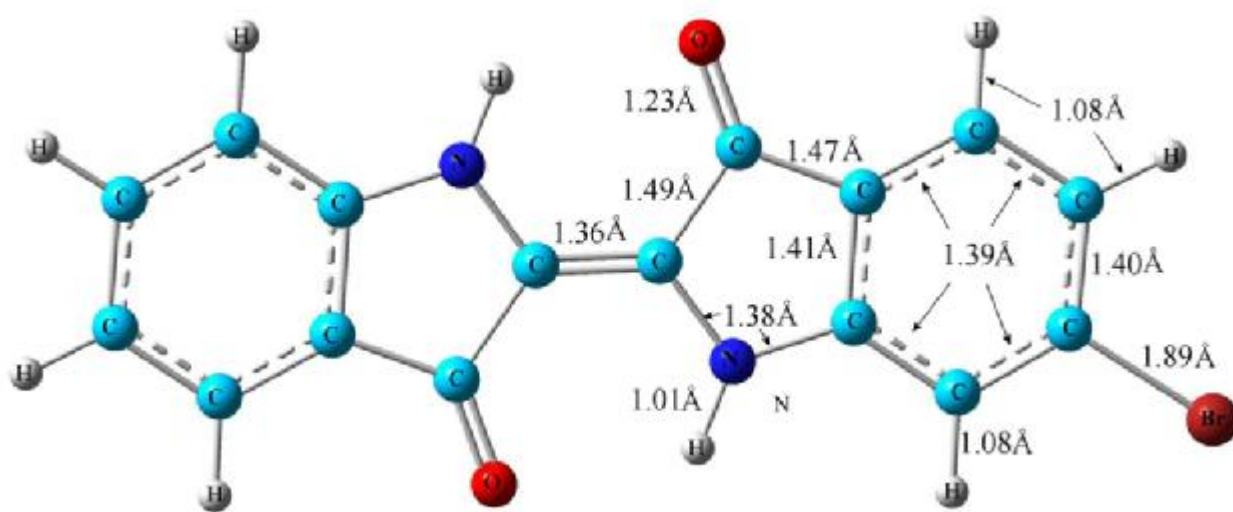


Figure 1. Molecular structure of monobromoindigo with bond lengths calculated by DFT after geometry optimization.

In the Mediterranean basin, Tyrian purple was obtained from the hypobranchial gland of certain related species of snails. The glands, when pressed, exude a white liquid which upon exposure to air and sunlight quickly oxidizes, passing through a succession of yellow and green colors and finally turning purple. Such change of color is quite dramatic and gave rise to the myth attributing its discovery to Hercules, who observed that the mouth of his dog turned purple upon biting a snail as they strolled along the seashore. Aristotle is quoted as saying the value of such purple dye is beyond that of gold, and this seems plausible when it is realized some 10,000 snails need collecting to deliver about a gram of the purple matter. Nero decreed that only he could wear the purple, perhaps lending impulse to the historical name of this colorant, royal purple; its manufacture was in fact state controlled. Archeological finds of “mountains” of snail shells at production sites along the Mediterranean coast attest to the vast scale of ancient manufacture. The use of Tyrian purple was not limited to textile dyeing: indeed, Koren identified by HPLC 6,6'-dibromoindigo, 6,6'-dibromoindirubin and, importantly, 6-monobromoindigo in a stone jar belonging to the Achaemenid king Darius I (figure 2), in which this material was used to paint the entire external surface in a fresco-type technique².

Tyrian purple can be obtained from mollusks found widely across the world, and it always contains a number of compounds including monobromoindigo³. Work by Koren proved that monobromoindigo is a marker for the *Hexaplex Trunculus* snail² (figure 2), highlighting the importance of monobromoindigo identification for proper sourcing of the pigment: that is, if a large amount of monobromoindigo is present in the pigment, then that means that the snail used was *H. Trunculus*. As stated by Koren, “The common denominator for all *H. trunculus* snails studied so far is the existence of significant levels of monobromoindigo”².

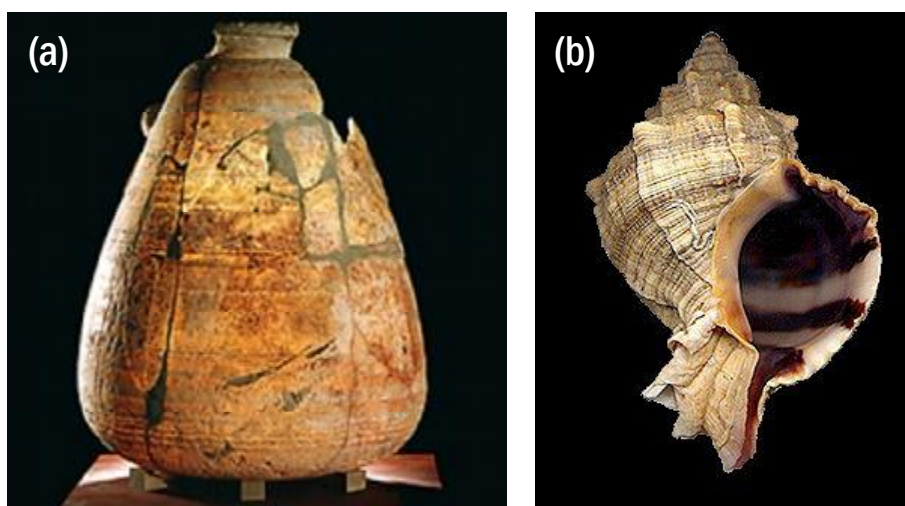


Figure 2. (a) Traces of the snail-purple dye on an alabaster jar from the Achaemenid period, 486 B.C. The object resides in the Bible Lands Museum of Jerusalem. A hieroglyphic inscription translates as “King of Upper and Lower Egypt, lord of the two lands, Darius...”. (b) *Hexaplex trunculus* sea snail, from which monobromoindigo-containing Tyrian purple can be extracted.

Monobromoindigo has been studied chromatographically and spectrometrically³⁻⁷, and colorimetrically⁵; its Raman spectrum was first reported in 1999⁵. Although monobromoindigo is closely related to indigo and dibromoindigo, it has not been investigated as completely as these substances and, in particular, an exhaustive Raman spectral study of the molecule, including spectral assignments by comparison with density functional theory (DFT) calculations, has never been carried out.

Because of its importance as an historical dye, its general characterization was here undertaken and, more specifically, the Raman spectrum of the molecule is reported in this chapter. Raman spectroscopy has proven in this case to be both a quick and accurate method of chemical analysis; it is in fact a non-destructive technique and requires a sample size which is almost miniscule. Besides, the Raman spectrum is one of the most important properties of a colorant as, for example, it can provide definitive analytical identification of a dye, at least when fluorescence does not interfere with the measurement.

Raman spectra of monobromoindigo were here recorded at different excitation wavelengths and compared in detail to those of indigo acquired in the same experimental conditions. Although the spectra of the two molecules are surprisingly similar, given the relatively large mass of bromine attached to the indigo framework, their important differences could be identified and are here presented. In addition, it has been possible to make a detailed assignment of the Raman spectral lines by comparison to the quantum mechanical prediction of the spectra using DFT. This part of the work has been carried out in collaboration with the Center for

Computational Materials Science, Naval Research Laboratory (Washington DC, USA) and the City College of the City University of New York (CUNY). A close proximity was found between the calculated and experimental spectra, which lends confidence to the spectral assignments that have been made and, importantly, the similarity and differences between experimental monobromoindigo and indigo spectra are reflected in the DFT calculations carried out for both molecules and could be therefore explained.

Experimental and theoretical methods

Chemicals

6-Monobromoindigo was synthesized in the laboratory. Its precursor, 6-bromoisatin, was obtained from TCI America, while phosphorus pentachloride, chlorobenzene, 3-acetoxyindole, ethanol and ethyl benzoate were purchased from Alfa Aesar. Reference indigo was obtained from Kremer Pigments.

Synthesis of monobromoindigo

6-Monobromoindigo was prepared by Olga Lavinda and Keith Ramig of Baruch College (CUNY, New York, USA) according to a recipe published in the literature⁵, and the reaction mechanism is shown in figure 3.

1 g of 6-bromoisatin and 1 g of PCl_5 were heated in 30 mL of chlorobenzene under nitrogen gas at 98-102°C for 4 hours. After cooling, 716 mg of 3-acetoxyindole were added to the solution, which was then allowed to stand overnight. The mixture was diluted with 30 mL of ethanol and then filtered. The residue was washed with 30 mL of ethanol twice and recrystallized from 100 mL of ethyl benzoate. The yield was 40%. The purity of the product was ascertained by ^1H , ^{19}F and ^{13}C NMR using its trifluoroacetyl derivative⁹. HPLC analysis showed approximately 93% purity for the so obtained monobromoindigo.

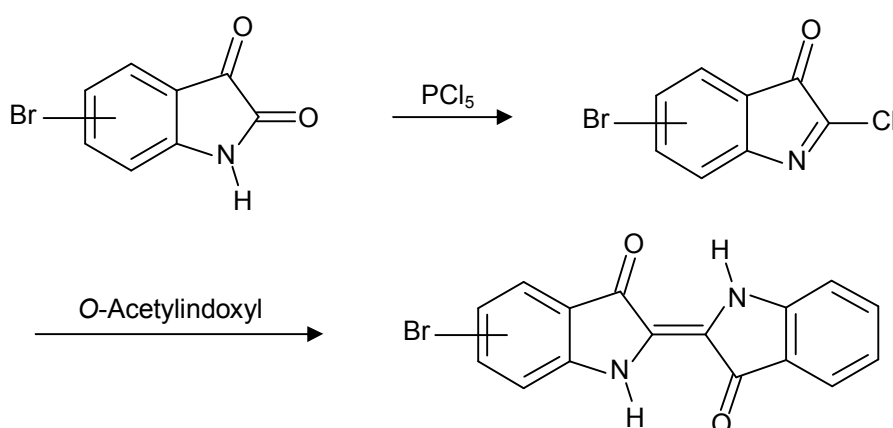


Figure 3. Synthesis of monobromoindigo starting from its precursor, bromoisatin (see reference 5).

Instrumentation

Experimental Raman spectra from indigo and monobromoindigo were acquired in the dispersive mode using a Bruker Senterra Raman apparatus, excitation at 785 nm and 488 nm, an Olympus 100x long working distance microscope objective, a charge-coupled device (CCD) detector and holographic gratings providing a resolution of 3-5 cm^{-1} (1200 rulings/mm for the 785 nm line, 1800 rulings/mm for the 488 nm line). For analyses at 785 nm, a continuous wave diode laser was employed as the excitation source. Measurements were taken collecting 1 scan with an integration time of 30 s, and the lowest output laser power available within the equipment in these experimental conditions, namely 1 mW, was selected in order to avoid sample damages. Measurements at 488 nm were performed using a Spectra Physics Model 2020 BeamLock Ar⁺ laser, with an output power of 0.25 mW. In this latter case, the spectra were obtained as the result of 1 scan with an integration time of 1000 s, in order to improve the signal-to-noise ratio.

The UV-visible absorption spectrum of monobromoindigo was collected with a Varian Cary 50 spectrophotometer, using a quartz cuvette with a path length of 1.0 mm. The sample, insoluble in water and most organic solvents, was dissolved in dimethylsulfoxide (DMSO) in an ultrasonic bath for the analysis.

Density functional theory (DFT) calculations

DFT calculations were performed by Lulu Huang of Center for Computational Materials Science, Naval Research Laboratory (Washington DC, USA), while the detailed assignments of the observed Raman lines was led by professor John Lombardi of City College (CUNY, New York, USA).

The theoretical Raman spectrum of monobromoindigo was obtained using the computer program GAUSSIAN09 (G09)⁸. This software provides Raman intensities by calculating polarizability derivatives with respect to nuclear Cartesian coordinates and then converting these to derivatives with respect to mass-weighted normal coordinates at a stationary point of the geometry⁹⁻¹³.

The results of DFT calculations performed for monobromoindigo include geometry optimization, vibration frequencies and Raman activity. The initial geometry for optimization is obtained from the crystal coordinates of the molecule. The use of the Becke, three-parameter, Lee-Yang-Parr (B3LYP) exchange correlation functional^{14,15} with orbital basis functions 6-31G(2d,2p)^{16,17} gave rise to a true minimum geometry for monobromoindigo. According to the specification of these basis functions, (2d,2p) designates polarization functions having two sets of d functions for heavy atoms and two sets of p functions for hydrogen atoms¹⁸. A schematic representation of the molecular geometry of a single isolated molecule of monobromoindigo is shown in figure 1. The total energy at the optimized geometry of the molecule is -3447.006 a.u., value which is lower than that of the starting geometry by 0.158 a.u. (about 99 kcal/mol). The molecular point group is C₁, and has a calculated dipole moment equal to 2.10 Debye. A total of 84 vibrational frequencies (3N-6) have been calculated with the same quantum method (B3LYP) and basis functions (6-31G(2d,2p)) mentioned earlier. The most relevant experimental wavenumbers are listed in table 1 and shown along with the normal mode numbers arising from DFT calculations.

Table 1. Wavenumbers of experimental Raman spectra obtained for monobromoindigo and indigo are shown along with the normal mode numbers calculated by DFT and compared to literature data (see references 20 and 22). “Oop” and “Ip” refer to out-of-plane and in-plane vibrations. The signal marked with (*) for monobromoindigo was observed only with 488 nm excitation.

| Description of normal modes | MBI experimental | MBI DFT | Indigo experimental | Indigo DFT | References | |
|-----------------------------|------------------|---------|---------------------|------------|------------|---------|
| | Wavenumber | Mode # | Wavenumber | Mode # | Wavenumber | Mode # |
| OC-C-CH stretch (Br) | 267 | 13 | | | | |
| C=O stretch (Br) | 304 | 14 | 302 | 12 | | |
| C-Br stretch | 364 | 15 | | | | |
| | 466 | | | | | |
| CH, NH oop rock | 516 | 22 | | | | |
| CH, CO rock | 554 | 23 | 545 | 20 | 544 | 26 |
| CC-C-C-CN stretch | | | 599 | 25 | 598 | 51 |
| C-C-C, CC-CO-CC stretch | 619 | 25 | | | | |
| CH, CO ip rock | 682 | 29 | 675 | 26 | 674 | 24 |
| HN-CC-CO stretch | 716 | 31 | | | | |
| C-NH-C=C-NH-C ip bend | 760 | 34 | 756 | 32 | 758 | 23 |
| C-C stretch, C-N stretch | 868 | 41 | 866 | 37 | 868 | 22 |
| C-C stretch, C-N stretch | 894 | 42 | | | | |
| CH oop rock | 940(*) | 46 | | | | |
| C-C-C stretch-Benzene ring | 1011 | 47 | | | | |
| CO-C=C-CO oop stretch | | | 1014 | 47 | 1015 | 20 |
| C-C-C stretch-Benzene ring | 1046 | 48 | | | | |
| CH, CO ip rock | 1125 | 50 | 1149 | 53 | 1147 | 18 |
| CH ip rock | 1219 | 57 | 1224 | 56 | 1224 | 16 |
| CH ip rock | 1244 | 60 | 1246 | 59 | 1248 | 15 |
| NH-C=C-NH rock | 1308 | 62 | 1309 | 61 | 1310 | 14 |
| NH-C=C-NH rock | 1337 | 63 | | | | |
| CH ip rock | 1362 | 65 | 1362 | 62 | 1365 | 13 |
| C-C-C str-Benzene-Br-ring | 1441 | 66 | | | | |
| C-C-C str-Benzene-Br-ring | 1461 | 67 | 1460 | 65 | 1460 | 11 |
| CH oop rock | | | 1481 | 66 | 1482 | 10 |
| C=C stretch | 1580 | 71 | 1572 | 70 | 1582 | 8 and 9 |
| C=O ip stretch | 1625 | 73 | 1625 | 72 | 1625 | 7 |
| C=C stretch, C=O ip stretch | 1700 | 75 | 1700 | 74 | 1701 | 6 |

Results and discussion

In figure 4 the absorption spectrum of a 10^{-4} M solution of monobromoindigo in DMSO is displayed, showing a prominent maximum at 616 nm. Such value is close to the absorption maximum of indigo¹⁹, which is observed at 604 nm in chloroform and 619 nm in DMSO. This band is assigned to the lowest lying π - π^* transition, and the same assignment is likely in monobromoindigo.

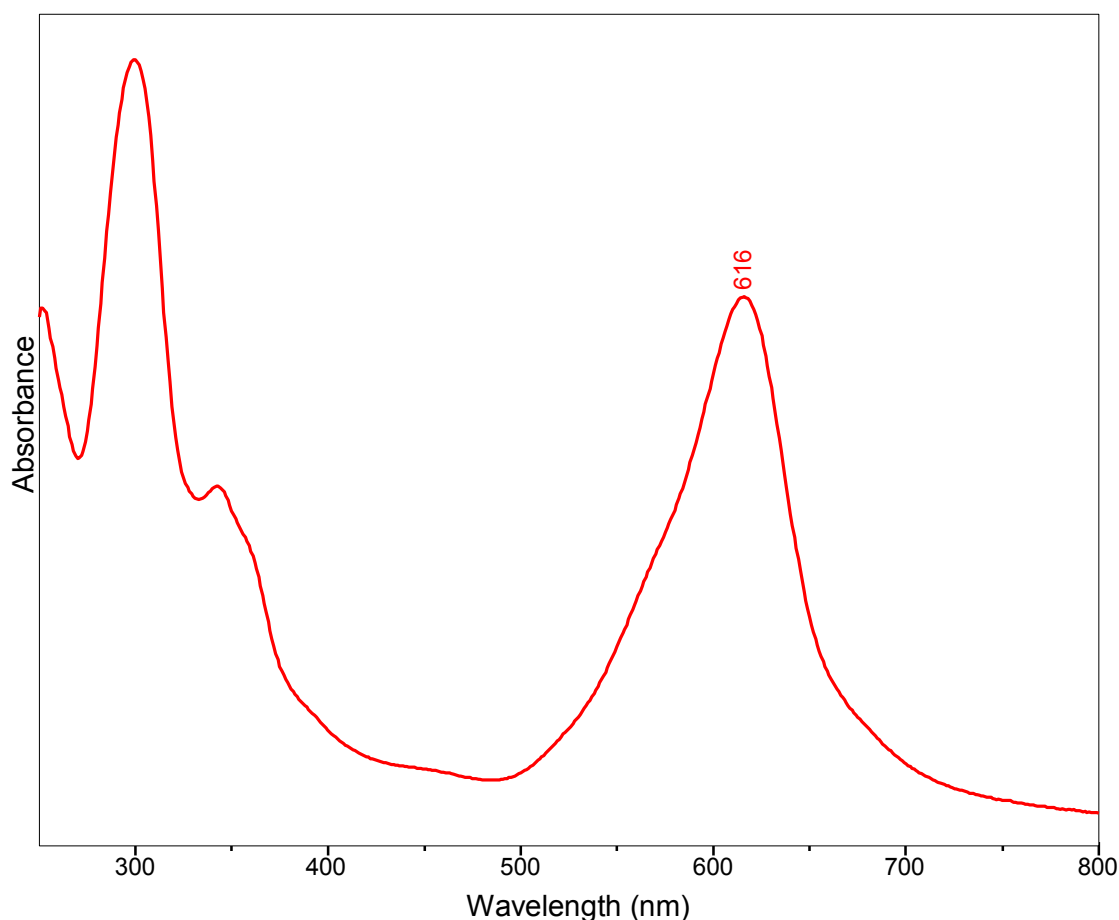


Figure 4. UV-vis spectrum of monobromoindigo in DMSO, showing an absorption maximum at 616 nm. This spectrum may be compared with that of indigo in the same solvent (see reference 19), for which the absorption maximum is at 619 nm. In both cases, the band is assigned to the lowest lying π - π^* transition.

The Raman spectrum of monobromoindigo acquired at 785 nm in the range of wavenumbers 300-1900 cm^{-1} is shown in figure 5, where it is compared to that of indigo recorded in the same conditions. The measured wavenumbers are listed in table 1. The spectra of the two molecules are remarkably similar, being both dominated by a single line around 1580 cm^{-1} with two much weaker signals at higher wavenumbers, namely 1625 and 1700 cm^{-1} . In indigo these bands have been assigned to C=O stretching modes²⁰, while the very intense line is assigned to the C=C stretch of the central bond. The remaining lines are moderate to weak in

intensity and are found to lower wavenumbers. At first glance, the spectra of the two molecules are indistinguishable; however, a closer inspection reveals several important differences. It is important to note that, since indigo has C_{2h} symmetry, the normal modes belonging to A_u or B_u irreducible representations will be forbidden in the Raman spectrum, while the lower symmetry of monobromoindigo will result in less stringent selection rules, and more lines might be expected to be detected in the Raman spectrum. This is exactly as observed, as can be noticed by inspection of both figure 5 and table 1.

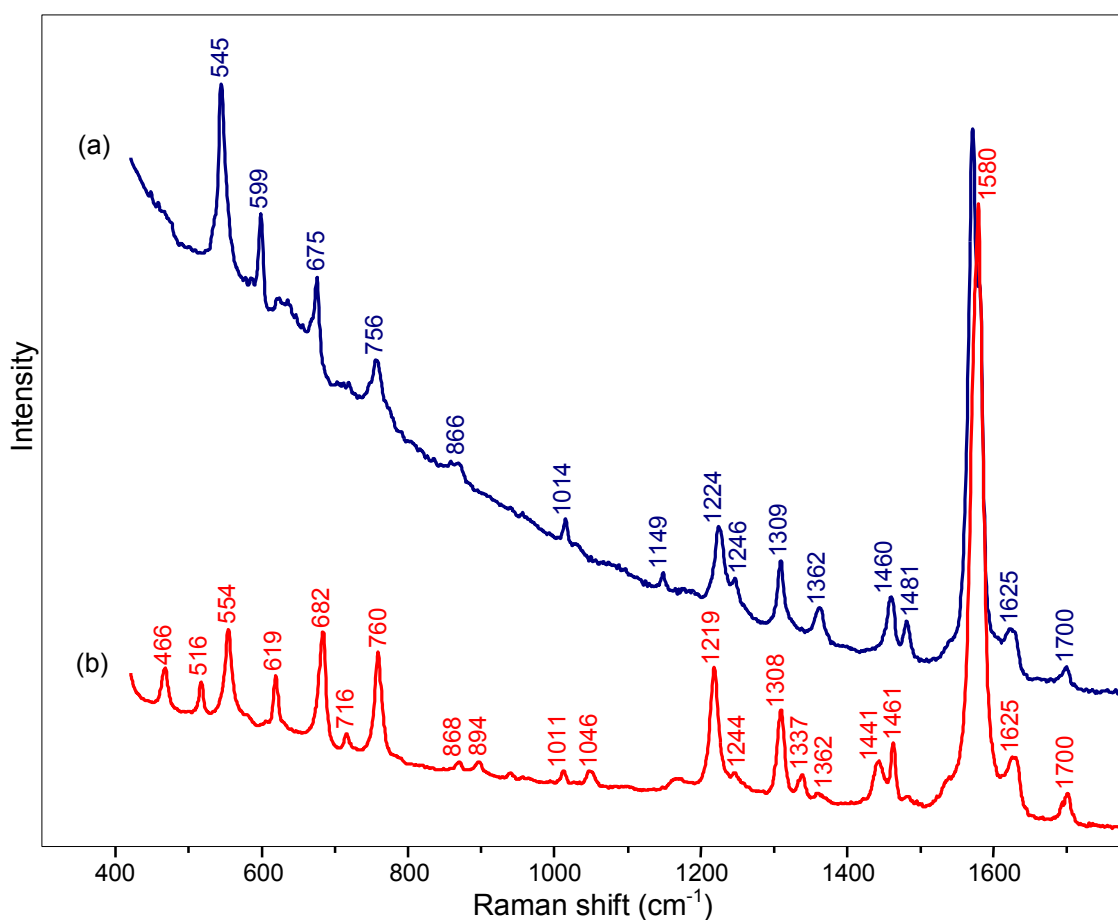


Figure 5. Comparison of experimental Raman spectra of (a) indigo and (b) monobromoindigo acquired at excitation 785 nm.

To assign the spectral lines in detail, the results of DFT calculations are displayed along with the experimental spectrum of monobromoindigo in figure 6. In order to obtain a good match, the wavenumber scale of the calculation has been multiplied by a scaling factor of 0.958, as this practice was found to give excellent results in previous works reported in the literature²¹. With the exception of the relative intensities of several lines and small shifts, especially at lower wavenumbers, almost an exact correspondence of the spectral features was achieved.

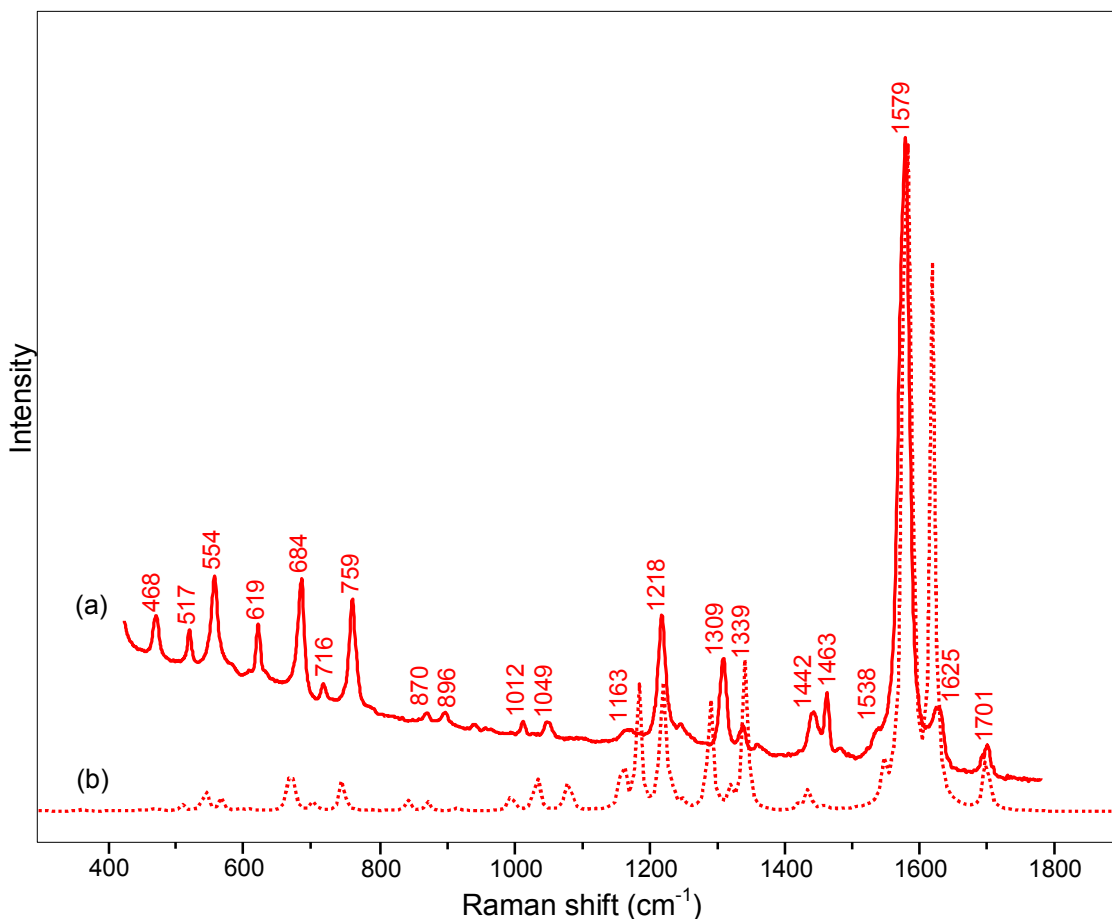


Figure 6. (a) Experimental Raman spectrum of monobromoindigo compared to (b) that calculated by DFT at excitation 785 nm. The wavenumber scale of the DFT results were shifted by a factor of 0.958 to obtain the best fit.

However, due to the strong similarity of the monobromoindigo and indigo experimental spectra shown in figure 5, a comparison of the DFT of the two molecules was undertaken as well, in order to ensure that the small spectral differences could be reproduced and therefore explained by the theoretical calculations. DFT calculations on indigo have been performed to the same level of theory as that of monobromoindigo, and the calculated Raman spectra are displayed in figure 7 for the region 300-1900 cm^{-1} . As in the experimental spectra, a few differences can be detected, but most of them are in the low wavenumber region. Some of the main differences as well as similarities have been highlighted by inserting the measured wavenumbers for the spectral lines. It should be pointed out that, in this figure, the wavenumber scale has not been shifted by a scaling factor, so that these numbers are not directly comparable to those of figure 5, but they must be multiplied by 0.958 for direct comparison.

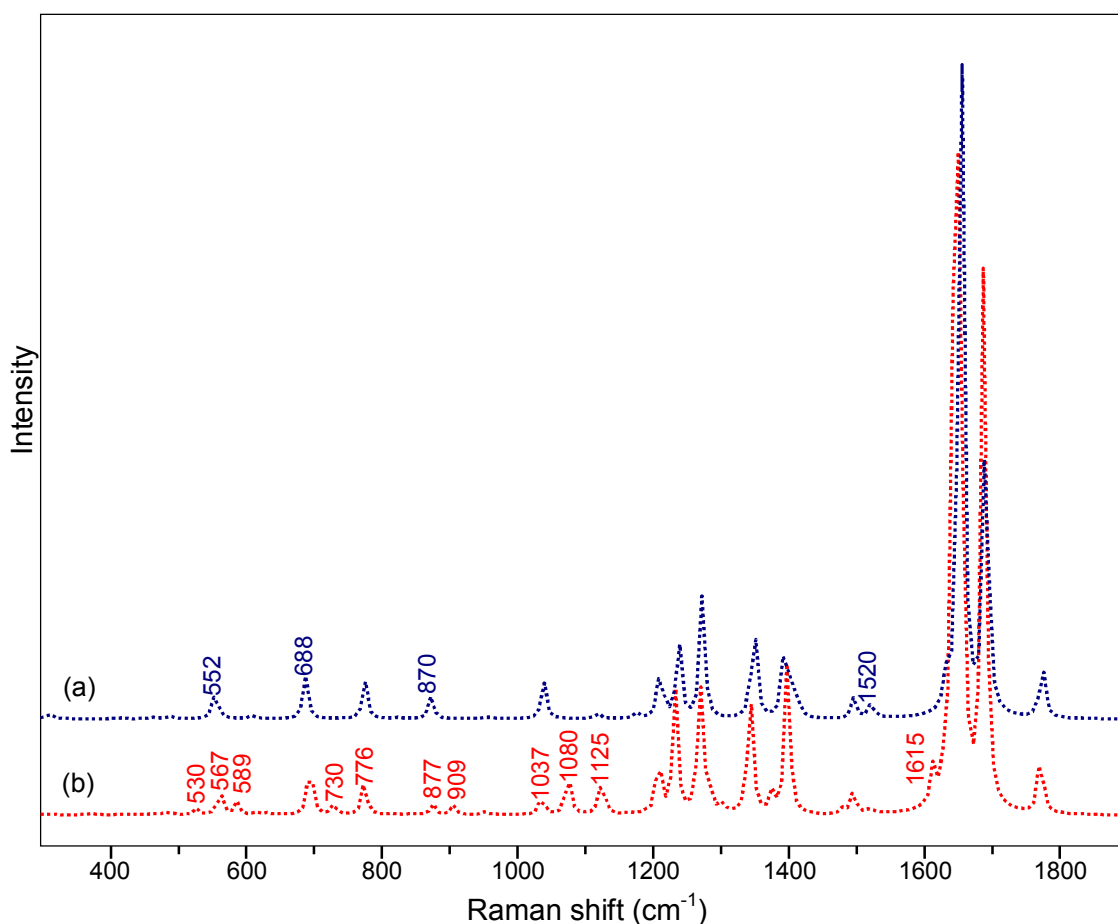


Figure 7. Comparison of unshifted DFT calculations for (a) indigo and (b) monobromoindigo.

In order to compare the differences between the two molecules and ensure that the calculated differences match the experimental ones, a comparison for the region 400-1200 cm^{-1} , where most of the dissimilarities lie, is also displayed in figure 8. The top two spectra are DFT calculations for indigo and monobromoindigo, while the lower traces are the experimental Raman spectra of both species. To aid in inspection, arrows were drawn connecting the lines for which there is an observable difference between the two spectra and, for convenience, the measured wavenumbers of the observed spectra were added. It can easily be seen that both sets of signals are characterized by the same differences. For example, the 1046 cm^{-1} line appears in monobromoindigo in both sets, with no counterpart in the indigo spectra, and the same can be said of the 894, 716, 619, 576, and 516 cm^{-1} lines. For indigo, on the other hand, lines at 1149 and 599 cm^{-1} have no monobromoindigo counterpart. All the remaining bands are common to both spectra, even though with slight shifts, for both calculation and experiment. As expected from the symmetry lowering of monobromoindigo with respect to indigo, there are more new lines for the former than for the latter.

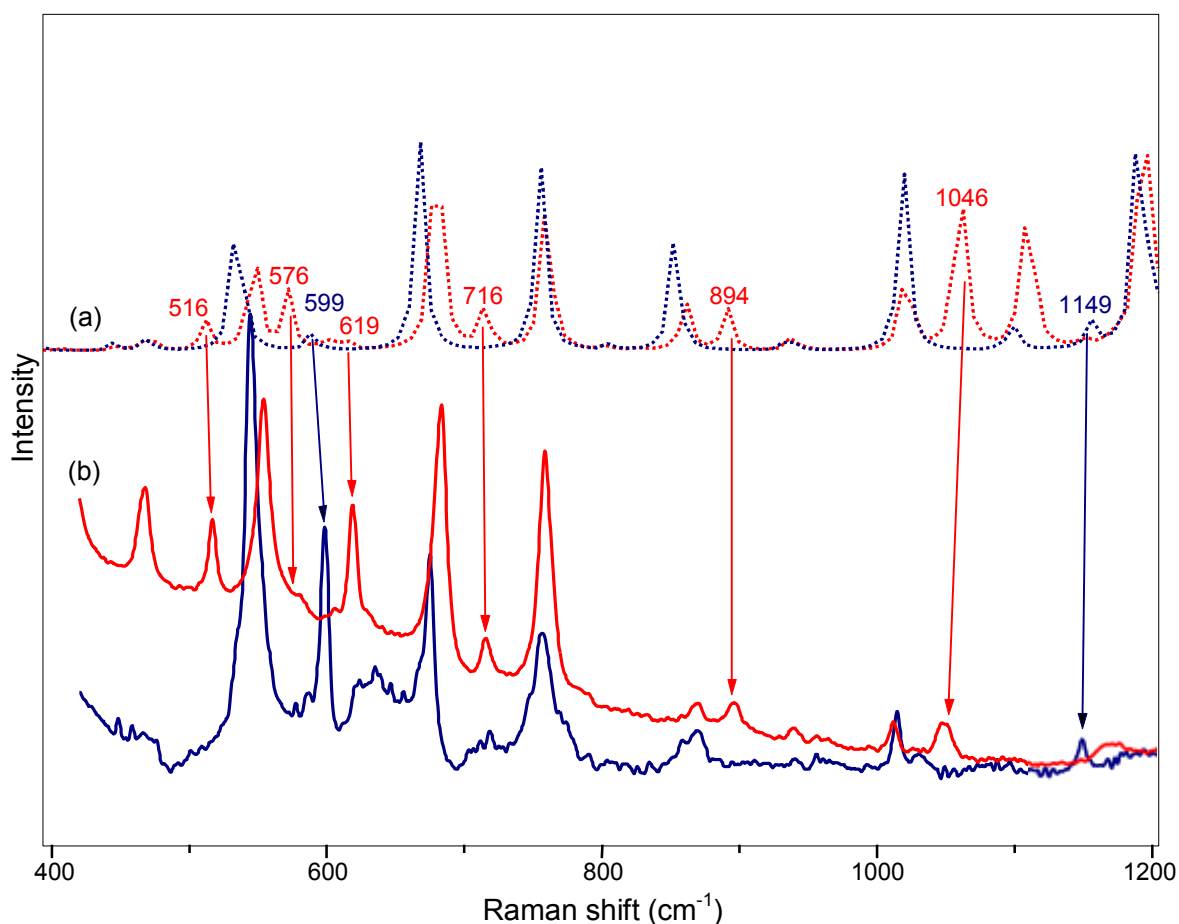


Figure 8. Detailed comparison of (a) theoretical spectra calculated by DFT and (b) experimental Raman spectra for monobromoindigo (red) and indigo (blue). The fluorescence background shown in figure 5 has been subtracted. The arrows highlight the correspondences between calculation and observation for those lines not common to the spectrum of both monobromoindigo and indigo.

All the spectral measurements on indigo and monobromoindigo have been summarized in table 1, with comparison to the recent work by Tomkinson *et al.*²⁰ in which the Raman spectrum of indigo is reassessed using DFT. Wavenumbers of the experimental Raman spectra here collected are nearly identical to theirs and the DFT calculation here performed is also in complete agreement with their work.

As far as the mode numbering is concerned, Tomkinson *et al.*²⁰ correctly use the Wilson numbering convention, that has been included in table 1. However, for DFT calculations, especially for a molecule with low symmetry, the Wilson notation is of little net benefit. In the table, the DFT designation has been instead used for mode numbering for monobromoindigo and indigo. This is not usually of much value, since in DFT these numberings are just in order of ascending wavenumber; worse yet, they may differ with use of a different basis set since the energy ordering may change, thus making comparisons difficult. In fact it is best to rely, as it has been done here, on a visual comparison of the normal modes displayed in GaussView to assign which normal modes of monobromoindigo and indigo are the same. This must be accomplished to prevent misassignment due to a possible coincidence in energy or DFT mode numbering; this is the case, for example, of mode number 47 for monobromoindigo and indigo: they have almost the same wavenumber but, on visual inspection, they are very different normal modes. Thus, the only value of including the numbering in this table

is as a guide to the calculated mode to which we are referring, so that anyone can reproduce the results presented in this chapter. The verbal descriptions of the normal modes in the first column of table 1 were obtained from visual inspection of the GaussView output. Where possible, the lines which were especially sensitive to Br substitution were identified. The band at 364 cm^{-1} is attributed directly to the C-Br stretch, and the assignments of a work by Karapanayiotis *et al.*²² on the 6,6'-dihalogen analogues of indigo have been used for comparison as well.

In figure 9 a comparison of the Raman spectra of monobromoindigo at two different excitation wavelengths, i.e. 785 nm and 488 nm, is shown. It is interesting to notice that these two wavelengths lie on either side of the optical resonance of such molecule at 616 nm (figure 4). The most important differences are highlighted by arrows. Several lines between 1200 and 1400 cm^{-1} change somewhat in intensity, and these are assigned as CH in-plane rocking motions. In addition, the two lines above 1600 cm^{-1} , classified as C=O stretch modes, increase drastically in intensity when excitation at 488 nm is employed. The line at 940 cm^{-1} in the spectrum acquired at 488 nm does not appear at all in the 785 nm trace, and is assigned to a CH out-of-plane rock. This assignment is to mode number 46 of the scaled DFT calculation, which predicts a very low Raman activity, which is consistent with its extreme weakness at 785 nm, but not with the relative intensity observed when using an excitation wavelength of 488 nm.

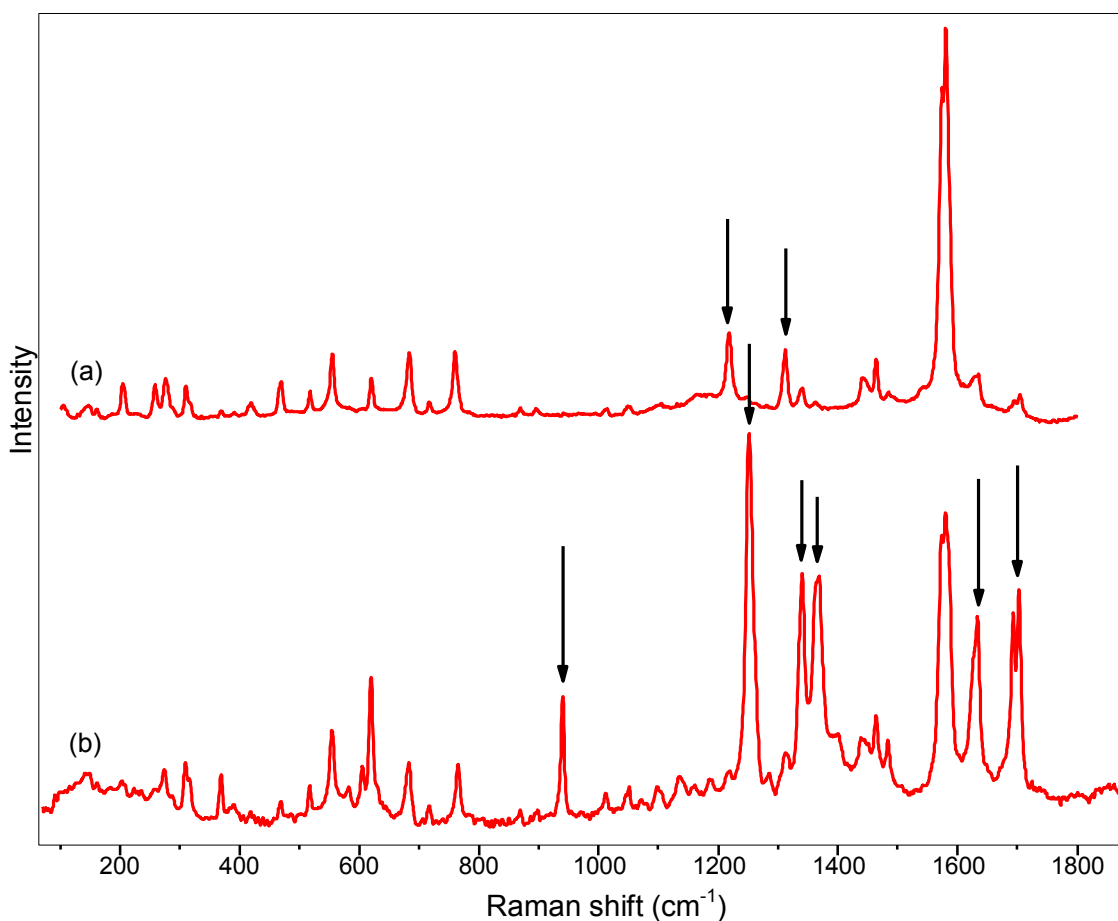


Figure 9. Comparison of experimental Raman spectra of monobromoindigo acquired at excitation (a) 785 nm and (b) 488 nm. The most important differences are highlighted by arrows.

Conclusions

In the present chapter, the results obtained from an extensive Raman spectral study of monobromoindigo are presented, which complete the data that have been published thus far in the literature concerning the characterization of the historical dye Tyrian purple and its chemical components. In particular, experimental Raman spectra of the molecule were taken at two different excitation wavelengths, namely 488 and 785 nm, and the spectral patterns were subsequently discussed based on the spectral assignments obtained by DFT calculations. Moreover, the Raman spectrum of monobromoindigo at 785 nm was compared with that of indigo acquired in the same experimental conditions. Even though at first glance these two spectra looked identical, a more careful inspection revealed several dissimilarities due to the different symmetry of the two molecular structures. The differences between the experimental spectra of monobromoindigo and indigo were confirmed and explained by DFT calculations, and spectral assignments were carried out and discussed in detail for each of the two molecules.

From the analytical point of view, the present study showed that Raman spectroscopy is a powerful technique which can be used to obtain a quick and specific fingerprint from molecules with similar structures and differentiate between them. It is worth pointing out that the analysis requires a microscopic amount of compound and is carried out in a completely non-invasive way, which is essential when dealing with samples of historical and artistic interest.

We should further note that, in actual artifacts, Tyrian purple is a mixture of several compounds including the two studied here. Since the spectra observed differ mostly in the weaker bands, it is possible that the practical applications for identification of monobromoindigo will be limited. However, the differences are clear, since the lines involved are distinct and well-isolated from the surroundings, so there remains a reasonable possibility that both compounds can be identified in a mixture. Indeed, if sufficient sample for chromatographic analysis is not available, Raman spectroscopy may allow an identification of the purple dye by detecting the presence of monobromoindigo.

Acknowledgements

This work has been promoted by professor Lou Massa and Hiroko Ajiki of Hunter College (CUNY, New York, USA). Monobromoindigo was synthesized by Olga Lavinda and Keith Ramig of Baruch College (CUNY, New York, USA) and analyzed with HLPC by Zvi Koren of Shenkar College (Ramat Gan, Israel). DFT calculations were performed by Lulu Huang of Center for Computational Materials Science, Naval Research Laboratory (Washington DC, USA), while the Raman lines were assigned by professor John Lombardi of City College (CUNY, New York, USA).

References

- [1] C. J. Cooksey, *Dyes Hist. Archaeol.* **1994**; *12*, 57.
- [2] Z. C. Koren, *Microchim. Acta* **2008**; *162*, 381.
- [3] C. J. Cooksey, *Molecules* **2001**; *6*, 736.
- [4] J. Wouters, A. Verhecken, *J. Soc. Dyers Colour.* **1991**; *107*, 266.
- [5] R. J. H. Clark, C. J. Cooksey, *New J. Chem.* **1999**; *3*, 323.
- [6] Z. C. Koren, *Dyes Hist. Archaeol.* **2008**; *21*, 26.
- [7] W. Nowik, R. Marcinowska, K. Kusyk, D. Cardon, M. Trojanowicz, *J. Chromatogr. A* **2011**; *1218*, 1244.
- [8] M. J. Frisch, G. W. Trucks, H. B. Schlegel, G. E. Scuseria, M. A. Robb, J. R. Cheeseman, G. Scalmani, V. Barone, B. Mennucci, G. A. Petersson, H. Nakatsuji, M. Caricato, X. Li, H. P. Hratchian, A. F. Izmaylov, J. Bloino, G. Zheng, J. L. Sonnenberg, M. Hada, M. Ehara, K. Toyota, R. Fukuda, J. Hasegawa, M. Ishida, T. Nakajima, Y. Honda, O. Kitao, H. Nakai, T. Vreven, J. A. Montgomery, Jr., J. E. Peralta, F. Ogliaro, M. Bearpark, J. J. Heyd, E. Brothers, K. N. Kudin, V. N. Staroverov, R. Kobayashi, J. Normand, K. Raghavachari, A. Rendell, J. C. Burant, S. S. Iyengar, J. Tomasi, M. Cossi, N. Rega, J. M. Millam, M. Klene, J. E. Knox, J. B. Cross, V. Bakken, C. Adamo, J. Jaramillo, R. Gomperts, R. E. Stratmann, O. Yazyev, A. J. Austin, R. Cammi, C. Pomelli, J. W. Ochterski, R. L. Martin, K. Morokuma, V. G. Zakrzewski, G. A. Voth, P. Salvador, J. J. Dannenberg, S. Dapprich, A. D. Daniels, Ö. Farkas, J. B. Foresman, J. V. Ortiz, J. Cioslowski, D. J. Fox, *Gaussian 09, Revision A.1*, Gaussian, Inc., Wallingford CT, **2009**.
- [9] A. Frisch, M. J. Frisch, F. R. Clemente, G. W. Trucks, *Gaussian 09 User's Reference*, **2009**, 105–107.
- [10] E. B. Wilson, J. C. Decius, P. C. Cross, *Molecular Vibrations*, McGraw-Hill, New York, **1955**.
- [11] J. W. Ochterski, *Vibrational Analysis in Gaussian*, Gaussian, Inc., **1999**.
- [12] S. A. Perera, R. J. Bartlett, *Chem. Phys. Lett.* **1999**; *314*, 381.
- [13] M. J. Frisch, Y. Yamaguchi, J. F. Gaw, H. F. Schaefer, *J. Chem. Phys.* **1986**; *84*, 531.
- [14] A. D. Becke, *J. Chem. Phys.* **1993**; *98*, 5648.
- [15] B. Miehlich, A. Savin, H. Stoll, H. Preuss, *Chem. Phys. Lett.* **1989**; *157*, 200.
- [16] A. D. McLean, G. S. Chandler, *J. Chem. Phys.* **1980**; *72*, 5639.
- [17] T. Clark, J. Chandrasekhar, G. W. Spitznagel, P. V. R. Schleyer, *J. Comput. Chem.* **1983**; *4*, 294.
- [18] M. J. Frisch, J. A. Pople, J. S. Binkley, *J. Chem. Phys.* **1984**; *80*, 3265.
- [19] A. Amat, F. Rosi, C. Miliani, A. Sgamellotti, S. Fantacci, *J. Mol. Struct.* **2011**; *993*, 43.
- [20] J. Tomkinson, M. Bacci, M. Picollo, D. Colognesi, *Vibr. Spectrosc.* **2009**; *50*, 268.
- [21] T. Teslova, C. Corredor, R. Livingstone, T. Spataru, R. Birke, J. R. Lombardi, M. V. Canameres, M. Leona, *J. Raman Spectrosc.* **2007**; *38*, 802. C. Corredor, T. Teslova, Z. Chen, J. Zhang, M. V. Cañameres, J. R. Lombardi, *Vibr. Spectrosc.* **2009**; *49*, 190. J. Chang, M. V. Cañameres, M. Aydin, W. Vetter, M. Schreiner, W. Xu, J. R. Lombardi, *J. Raman Spectrosc.* **2009**; *40*, 1557.
- [22] T. Karapanayiotis, S. E. Jorge Villar, R. D. Bowen, H. G. M. Edwards, *Analyst* **2004**; *129*, 613.

Conclusions

This doctoral thesis work aimed to improve and validate pre-existing analytical methods as well as to develop innovative and effective procedures for the identification of organic colorants of artistic and archaeological interest, with special focus being dedicated to SERS. This technique has been recently appreciated for its great sensitivity, which enables to detect and identify trace compounds, and for its ability to suppress the fluorescence that typically characterizes organic dyes, thus making their identification impossible to be accomplished by means of normal Raman spectroscopy. However, on the other hand, SERS poses a whole set of challenges, as only a small number of molecules have been studied so far and the necessity of searchable databases of reference materials is still to be fulfilled; moreover, SERS is not a separation technique, and therefore it often suffers from spectral interferences due to the presence of impurities or matrix components. The present research was thus intended to compensate for some of the main lacks of this promising analytical tool and, in this context, has allowed to achieve several goals:

- development and optimization of a SERS analytical procedure based on the use of Ag nanoparticles synthesized according to the Lee-Meisel method and aggregated by 1.8 M NaClO₄, and validation of other techniques, such as HPLC and GC-MS, as auxiliary tools which play a key role in providing preliminary and complementary information concerning the samples under investigation;
- acquisition of a wide number of SERS spectra from commercial colorants and pure chromophores, and construction of an extensive spectral database which integrates data previously published in the literature;
- validation of the SERS analytical procedure developed on real samples - identification of a yellow dye in ancient threads from the Libyan Sahara and characterization of dyestuffs in Kaitag textiles from Daghestan;
- optimization of a non-extractive HF hydrolysis procedure as a step designed to increase the mobility of the dye molecules and maximize their adsorption on the colloid surface, and its validation on microscopic samples taken from several works of art and archaeological materials - SERS identification of colorants in ancient textiles, cloth accessories, sculptures, watercolors and oil paintings;
- comparative study of HF hydrolysis and non-hydrolysis methodologies for SERS analysis, evaluation of their relative merits and drawbacks, and development of a two-step procedure for the investigation of organic dyes in works of art - SERS characterization of archaeological and modern lake pigments and identification of colorants in fabrics, musical instruments and oil paintings;
- normal Raman and SERS investigation of several color washes from a historical Winsor & Newton catalogue of watercolor pigments dating to 1887 and acquisition of a spectral database of original art materials to be used for dating as well as in authentication and identification studies;
- investigation of TLC-SERS as a tool for the separation and ultrasensitive identification of dye mixtures and its application to the analysis of the historical colorant Syrian rue and its main alkaloid components;
- Raman study of monobromoindigo, a component of the historical colorant Tyrian purple, including experimental spectra acquired at different excitation wavelengths, comparison with spectra obtained from indigo in the same conditions and detailed spectral assignment performed by means of DFT calculations.

Publications

S. Bruni, V. Guglielmi, F. Pozzi, "Surface-enhanced Raman spectroscopy (SERS) on silver colloids for the identification of ancient textile dyes: Tyrian purple and madder", *Journal of Raman Spectroscopy* **2010**; *41*, 175-180.

S. Bruni, E. De Luca, V. Guglielmi, G. Poldi, F. Pozzi, "Colour in Kaitags. A new scientific approach to detecting dyes in textiles", in C. Scaramuzza, *Kaitag. Arte per la vita*, ed. Silvana Editoriale, Cinisello Balsamo, **2010**, pp. 120-147.

S. Bruni, V. Guglielmi, F. Pozzi, A. M. Mercuri, "Surface-enhanced Raman spectroscopy (SERS) on silver colloids for the identification of ancient textile dyes. Part II: pomegranate and sumac", *Journal of Raman Spectroscopy* **2011**; *42*, 465-473.

S. Bruni, V. Guglielmi, F. Pozzi, "Historical organic dyes: a surface-enhanced Raman spectral (SERS) database on Ag Lee-Meisel colloids aggregated by NaClO₄", *Journal of Raman Spectroscopy* **2011**; *42*, 1267-1281.

S. Bruni, E. De Luca, V. Guglielmi, F. Pozzi, "Identification of natural dyes on laboratory-dyed wool and ancient wool, silk, and cotton fibers using attenuated total reflection (ATR) Fourier transform infrared (FT-IR) spectroscopy and Fourier transform Raman spectroscopy", *Applied Spectroscopy* **2011**; *65*, 1017-1023.

H. Ajiki, F. Pozzi, L. Huang, L. Massa, M. Leona, J. R. Lombardi, "Raman spectrum of monobromoindigo", *Journal of Raman Spectroscopy* **2011**; in press, DOI: 10.1002/jrs.3066.

S. Bruni, E. De Luca, V. Guglielmi, G. Poldi, F. Pozzi, "Multi-technique characterization of dyestuffs in ancient Kaitag textiles from Caucasus", *Archaeological and Anthropological Sciences* **2011**; submitted.